METER SCALE CYCLES IN THE EOCENE ÇAYRAZ FORMATION (HAYMANA BASIN) AND RESPONSE OF FORAMINIFERS TO CYCLICITY

A THESIS SUBMITTED TO
THE GRADUATE SCHOOL OF NATURAL AND APPLIED SCIENCES
OF
MIDDLE EAST TECHNICAL UNIVERSITY

BY

BEDİA GEYİKÇİOĞLU ERBAŞ

IN PARTIAL FULFILLMENT OF THE REQUIREMENTS FOR THE
DEGREE OF
MASTER OF SCIENCE
IN
GEOLOGICAL ENGINEERING

NOVEMBER 2008

Approval of thesis:

METER SCALE CYCLES IN THE EOCENE ÇAYRAZ FORMATION (HAYMANA BASIN) AND RESPONSE OF FORAMINIFERS TO CYCLICITY

submitted by **BEDİA GEYİKÇİOĞLU ERBAŞ** in partial fulfillment of the requirements for the degree of **Master of Science in Geological Engineering Department, Middle East Technical University** by,

Prof. Dr. Canan Özgen _____
Dean, Graduate School of **Natural and Applied Sciences**

Prof. Dr. M. Zeki Çamur _____
Head of Department, **Geological Engineering**

Prof. Dr. Demir Altıner _____
Supervisor, **Geological Engineering Dept., METU**

Examining Committee Members:

Prof. Dr. Asuman Türkmenoğlu _____
Geological Engineering Dept., METU

Prof. Dr. Demir Altıner _____
Supervisor, Geological Engineering Dept., METU

Assis. Prof. Dr. İsmail Ömer Yılmaz _____
Geological Engineering Dept., METU

Assoc. Prof. Dr. Bora Rojay _____
Geological Engineering Dept., METU

Dr. Zühtü Batı _____
Research Center, TPAO

Date: _____

I hereby declare that all information in this document has been obtained and presented in accordance with academic rules and ethical conduct. I also declare that, as required by these rules and conduct, I have fully cited and referenced all material and results that are not original to this work.

Name, Last Name: Bedia Geyikçioğlu Erbaş

Signature :

ABSTRACT

METER SCALE CYCLES IN THE EOCENE
ÇAYRAZ FORMATION (HAYMANA BASIN) AND RESPONSE OF
FORAMINIFERS TO CYCLICITY

Erbaş Geyikçioğlu, Bedia

M.Sc. Department of Geological Engineering

Supervisor: Assoc. Prof. Dr. Demir Altıner

November 2008, 181 pages

The aim of this study is to investigate the nature of the meter-scale cycles in the Çayraz Formation of the Middle Eocene age and to study the response of foraminifera to the sedimentary cyclicity. In order to perform this study, two stratigraphic sections, which are 44,55 m and 25,95 m in thickness, were measured on a regularly bedded succession mainly composed of carbonates and siliciclastics in the Çayraz Formation of the Haymana Basin.

In this study, detailed microfacies analyses were carried out in the studied sections and 10 different microfacies types were identified strictly based on the biofacies in order to define meter scale cyclic sedimentation.

Based on the detailed microfacies analysis and the distribution of the vertical facies relationships a composite depositional model is suggested. According to this model, three major facies associations were distinguished, from deepest to shallowest, as: shallow open marine, shoal and lagoon.

Studied sections are composed of meter-scale cycles of both upward shoaling or deepening in character and based on the stacking pattern of meter-scale cycles two systems tracts were identified along the measured sections. Section 1 is represented by highstand systems tract (HST) and section 2 is represented by lowstand systems tract (TST).

In this study, the responses of benthic foraminiferal groups to the sedimentary cyclicity have been documented by quantitative and statistical analysis to understand the shallowing upward cycles, which are fundamental stratigraphic units, in the Çayraz Formation of Middle Eocene age. Among foraminifera, particularly the forms like *Nummulites, Assilina* and *Discocyclina* are excellent in order to detect cyclic variations of facies. These studies lead to understand shoaling-upward character of the meter-scale cycles, which are the building blocks of the Çayraz Formation.

Keywords: Çayraz Formation, Haymana Basin, Eocene, Benthic foraminifera, Meter-scale Cycles,

ÖZ

EOSEN YAŞLI ÇAYRAZ FORMASYONU' NDA (HAYMANA HAVZASI) METRE ÖLÇEKLİ SEDİMANTER DEVİRLER VE FORAMİNİFERLERİN DEVİRSELLİĞE TEPKİLERİ

Erbaş Geyikçioğlu, Bedia
Yüksek Lisans, Jeoloji Mühendisliği Bölümü
Tez Yöneticisi: Prof. Dr. Demir Altıner
Kasım 2008, 181 sayfa

Bu çalışmanın amacı orta Eosen yaşlı Çayraz Formasyonu'ndaki metre ölçekli devirleri ve foraminiferlerin sedimanter devirlere olan tepkisini araştırmaktır. Bu çalışmayı gerçekleştirebilmek için Haymana Havzasıdaki Çayraz formasyonu'ndan 44,55 m ve 25,95 m kalınlığında çoğunlukla karbonat ve silisiklastik kayalardan oluşan iki stratigrafik kesit ölçülmüştür.

Bu çalışmada metre ölçekli devirleri tanımlayabilmek için detaylı microfasiyes analizleri yapılmış ve istiflerin biofasiyes özellikleri kullanılarak 10 farklı tipte mikrofasiyes tanımlanmıştır.

Detaylı mikrofasiyes analizleri ve dikey fasiyes ilişkileri baz alınarak bir kompozit depolanma modeli önerilmiştir. Bu modele göre derinden sığa doğru sığ açık deniz, sığ ve lagün olmak üzere üç ana fasiyes ayırt edilmiştir.

Kesitler üste doğru sığlaşan veya derinleşen metre ölçekli devirlerden oluşmaktadır.Bu devirlerin sıralanma ve paketlenme düzenlerine gore ölçülen kesitlerde iki tip systems tracts tanımlanmıştır. Birinci kesit high stand systems tract (HST) ve ikinci kesit transgressive systems tract (TST) olarak tanımlanmıştır.

Bu çalışmada, Orta Eosen yaşlı Çayraz Formasyonu içerisindeki temel

stratigrafi birimleri olan üste doğru sığlaşan devirleri anlamak için kantitatif ve istatiksel analizlerle bentik foraminifer gruplarının sedimanter devirlere karşı tepkileri ortaya konulmuştur. Foraminiferler arasından özellikle *Nummulites*, *Assilina* ve *Discocyclina* gibi formlar fasiyeslerin devirsellik değişimlerini bulmak için çok mükemmeldir. Bu çalışmalar Çayraz Formasyonu'nun yapı taşları olan, üste doğru sığlaşan karakterdeki metre ölçekli devirleri anlamamızı sağlamıştır.

Anahtar kelimeler: Çayraz Formasyonu, Haymana Havzası, Eosen, Bentik Foraminifera, Metre Ölçekli Sedimanter Devirler.

To my family …

ACKNOWLEDGEMENTS

First of all, I am greatly indebted to my supervisor Prof. Dr. Demir ALTINER for his valuable guidance advice, encouragement and constructive criticism during the preparation of this thesis.

I would like to thank my sponsor Turkish Petroleum Corporation (TPAO) for their permission and support during completion of this thesis.

I would like to express my gratitude to Assoc. Prof. Dr. Sevinç ÖZKAN-ALTINER for her attention, and I am grateful to her for valuable recommendations and encouragements during my studies.

I would like to thank to Dr. Zühtü Batı for his help and encouragements.

I am most grateful to all my friends for their friendships and endless encouragements. Especially, I would like to thank Ayşe ATAKUL, Selen ESMERAY and all the college of Turkish Petroleum Corporation Research Center for their encouragements.

I would like to thank to Mr. Orhan KARAMAN for the preparation of thin sections.

Finally (at last but does not mean the least), I would like to express my grateful appreciation to my family and my husband for their supports, patience and encouragements during my studies.

TABLE OF CONTENTS

LIST OF TABLES

LIST OF FIGURES

homoclinal carbonate ramp (Flügel, 2004).

Figure 15. Classification of carbonate rocks according to depositional texture (Dunham 1962).

Figure 16. Photomicrographs of mudstone to wackestone with small benthic foraminifera (MF 1) (S: small benthic foraminifera), (1: ÇBG 20, 2: ÇBG 21).

Figure 17. Photomicrographs of benthic foraminiferal wackestone (MF 2) (B: benthic foraminifera), (1: HBG 10, 2: HBG 11, 3: HBG 11).

Figure 18. Photomicrographs of bioclastic, alveolinid, nummulitid packstone with abundant small and large benthic foraminifera (MF3) (N: *Nummulites* sp., A: *Alveolina* s.l. S: small bethic foraminifera), (1: ÇBG 27, 2:ÇBG 28, 3:ÇBG29, 4:ÇBG30).

Figure 19. Photomicrographs of bioclastic, alveolinid, nummulitid wacke to packstone with abundant small and large benthic foraminifera (MF 4) (N: *Nummulites* s.p., A: *Alveolina* s.l. , S: small bethic foraminifera), (1: HBG 1, 2: HBG 2, 3: HBG 3).

Figure 20. Photomicrographs of bioclastic, alveolinid, nummulitid wackestone with abundant small and large benthic foraminifera (MF) (N: *Nummulites* sp., A: *Alveolina* s.l., S: small bethic foraminifera), (1: HBG 5, 2: HBG 6, 3: HBG 12, 4: HBG 13).

Figure 21. Photomicrographs of Bioclastic, assilinid, nummulitid wacke to packstone with abundant small and large benthic foraminifera (MF 6) (N: *Nummulites* sp., A: *Alveolina* s.l., As: *Assilina* sp., S: small bethic foraminifera), (1: HBG 7, 2: HBG 8, 3: HBG 9, 4: HBG 15).

Figure 22. Photomicrographs of bioclastic, nummulitid packstone with abundant small and large benthic foraminifera (MF 7) (N: *Nummulites* sp., S: small bethic foraminifera), (1: HBG 4, 2: HBG 4).

Figure 23. Photomicrographs of bioclastic, assilinid, nummulitid packstone (MF 8) (N: *Nummulites* sp., As: *Assilina* sp.) (1: HBG 16, 2: HBG 18, 3: HBG 20, 4: HBG 26, 5: HBG 30, 6: HBG 31).

Figure 24. Photomicrographs of bioclastic, discocyclinid, nummulitid packstone (MF 9) (N: *Nummulites*, D: *Discocyclina)*, (1: ÇBG 6, 2: ÇBG 11, 3:ÇBG 14, 4: ÇBG 16, 5: ÇBG 17, 6: ÇBG 24).

Figure 25. Photomicrographs of bioclastic, discocyclinid, nummulitid packstone with red algae (MF 7) (N: *Nummulites*, D: *Discocyclina*, R: Red algae), (1: ÇBG 1, 2: ÇBG 2, 3: ÇBG 8, 4: ÇBG 13, 5: ÇBG 9, 6: ÇBG 19).

CHAPTER 1

INTRODUCTION

1.1. Purpose and Scope

Cyclic development in earth history has been a primary interest in geology and stratigraphy since their beginning and there has been a growing amount of interest in biotic responces to cyclicity (Weber *et al*., 2001). Sedimentary cycles have been recognized in the field for centuries (e.g, Steno, 1669/1916, de Maillet, 1748, Suess, 1888 etc.) and it has been sugggested that sea-level rise and fall were the main cause of the cyclicity in sedimentary rocks. The aim of this study is to investigate the nature of the shallowing upward meter-scale cycles and to study the response of foraminifera to the cyclicity. Therefore, in this study, the responses of benthic foraminiferal groups to the sedimentary cyclicity have been documented to understand the shallowing upward cycles, which are fundamental stratigraphic units, in the Çayraz Formation of Middle Eocene age. Shallowing upward cycles named as parasequences are the building blocks of the sequence stratigraphy.

The biotas including benthic foraminifera are influenced by global and local factors such as, ecology (e.g. temperature, water chemistry and tropic resources), geology (e.g. sea level, plate tectonics) and phylogeny (e.g. radiation, extinction). Variation of these parameters affects the biotic composition and the abundance of biota in the depositional sequences (Chaproniere, 1975; Hottinger, 1983, 1997; Reiss and Hottinger, 1984; Hallock and Glenn, 1986).

The Eocene Çayraz Formation represents the youngest marine formation of the Haymana Basin. It is composed of two shelf systems (SS), within each of the two SS, two orders of coarsening-upward and shallowing-upward

sequences are recognized (Çiner *et al*, 1993). Peritidal carbonate-dominated or mixed carbonate–siliciclastic successions frequently display shallowing-upward cycles at meter-scale. In this study, meter scale shallowing upward cycles have been studied based on their lithologic variations in the field and detailed microfacies analysis in the laboratory. Microfacies studies aim the recognition of overall patterns that reflect the history of carbonate rocks, by means of examination of their sedimentological and paleontological characteristics.

The cyclic nature of shallow-water carbonate-dominated successions can be revealed by examination of sedimentary structures, the biotic composition, microfacies and textures at centimeter- (microstratigraphy), decimeter- or meter-scale. Careful examination of these microstratigraphic data helps to better understand the nature of the meter scale cycles.

1.2. Geographic Setting

The study area is located in central Anatolia at approximately 70 km southwest of the Ankara, in the Çayraz Formation of the Haymana Basin, (Figure 1). It is situated in 1:25.000 scale topographic map of Ankara J29-a1 quadrant and zone of 36. According to the GPS recordings, section 1 starts at coordinates 460535 E – 4370349 N and finishes at 460594 E – 4370320 N and section 2 starts at coordinates 459686 E – 4369827 N and finishes at 459766 E-4369942N

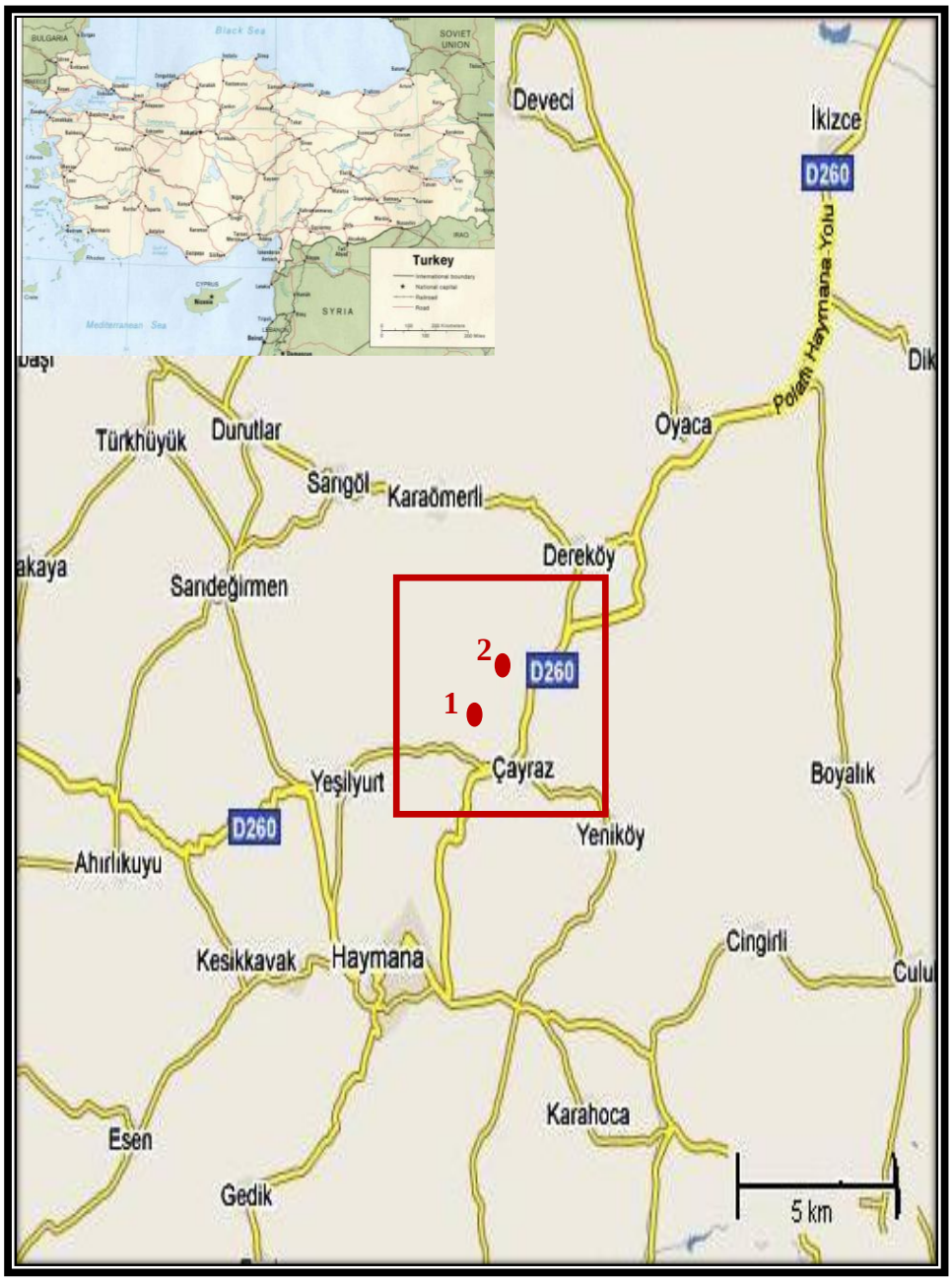

Figure 1. Location map of the study area and locations of the measured sections.

1.3. Method of Study

This study consisted of field and laboratory works. In the field study, two stratigraphic sections, which are 44,55 m and 25,95 m in thickness, were measured on a regularly bedded succession of the Çayraz Formation, mainly composed of carbonates and siliciclastics. 31 and 30 samples were collected from the section 1 and 2, respectively. Nearly each bed and also, thicker beds were sampled both from their bottom and top. Meter-scale shallowing upward cycles have been determined based on the lithological facies description in the field and detailed microfacies analysis in the laboratory.

In the field study, the microfacies and faunal content of each sample were examined by using a hand-lense for detecting and controlling facies changes and cyclicity.

In the laboratory study, detailed microfacies and micropaleontological studies were carried out. In order to carry out these petrographic and micropaleontological analysis, thin sections were prepared from each sample. In addition, micropaleontological and petrographic studies were carried out by taking photographs from every thin section. The discrimination of the facies-types is based on the petrographic analysis and the microfacies descriptions have been determined according to the standard microfacies models of Flügel (2004) and Wilson (1975) and ten types of microfacies have been determined.

Benthic foraminifera have been studied to understand the shoaling-upward character of meter-scale cycles, which are the building blocks of the Çayraz Formation. In order to perform this study, benthic foraminiferal taxa were classified into twenty one different groups, which are *Nummulites* sp., *Discocyclina* sp., *Assilina* sp., *Operculina* sp., *Alveolina* sp., *Sphaerogypsina* sp., miliolid, *Pygro* sp., *Triloculina* sp., *Spiroloculina* sp, *Coskinolina* sp., *Orbitolite*s sp., *Lockhartia* sp., biserialy to uniserialy coiled forms, *Medocia?* sp., *Valvulina* sp., *Textularia* sp., *Valvulina* sp. or *Textularia* sp., *Rotalia* sp., Verneulinidae and others (unidentified textularid, miliolid and rotalid forms).

After classifying benthic foraminifera, quantitative analyses were carried out for understanding foraminifera responses to environmental variations caused by sea-level oscillations and the nature of shallowing upward cycles. Quantitative analyses of benthic foraminifera were carried out in 4 cm^2 area of each thin section and benthic foraminiferal taxa, usually at genus level, were counted in each sample to find out the abundance and diversity of these benthic foraminiferal groups. Approximately 200 to 300 specimens were counted in most of the thin sections. Total and relative abundances of each biota have been used to understand the character and response to sedimentary cyclicity of the Middle Eocene Çayraz Formation. Because the Palaeogene was a time of particular abundance and radiation of the miliolid and larger hyaline foraminifera they occurred in rock-forming quantities in the samples. Due to their well-defined palaeoecological requirements, they represent valuable facies indicators (Rasser *et al*., 2005).

Furthermore, bulk mineralogical analyses were done to determine the clay content of the samples.

1.4. Previous Work

Geological studies related with the Haymana Basin began with the stratigraphic obsevations in the region. First geological studies in the Haymana Basin were carried out by Chaput (1932, 1935a, b, 1936). In his studies, Chaput recognized the presence of Upper Cretaceous-Eocene successions in the Haymana Basin and concluded that the basin was folded in the Tertiary. After the studies of Chaput, Lokman and Lahn (1946), Lahn (1949) and Egeran and Lahn (1951) continued to study the stratigraphy of the region and it was aimed to understand the structural evolution of the Haymana Basin in their studies. These researchers recognized the Senonian flysch, marl and limestones with *Cyclolites* in the Maastrichtian and limestones with algae in the Cretaceous-Paleocene boundary beds in the Haymana Basin. In addition, they mentioned the presence of limestones with *Nummulites* and *Assilina* above the

Paleocene flysch. In 1950's Erol (1954, 1961) continued to study the tectonic and geological evolution of the basin.

First lithostratigraphic definitions of the rocks in the basin were given in early 1960's, in the petroleum research reports of Rigo de Righi and Cortesini (1959), Reckamp and Özbey (1960), Schmidt (1960). These reports and the study of Akarsu (1971) are used for the following Haymana Basin stratigraphic studies (Sirel, 1975; Ünalan *et al*., 1976).

According to the studies of Ünalan *et al*., (1976) the deposition in the Haymana Basin ranges from Upper Cretaceous (Maastrichtian) to Lower Tertiary and the thickness of the Upper Cretaceous -Lower Tertiary deposits measures about 5800 m. At the base of these deposits there are Temirözü, Mollaresul and Dereköy Formations. The formations, starting from Maastrichtian are as follows, the Haymana Formation is composed of flysch facies, whereas the Beyobası Formation consists of coral sandstones and conglomerates. The Çaldağ Formation of Paleocene age is represented by algal limestones. In the north, west and south of the region, this unit shows interfingers with the red colored deposits of the Kartal Formation, and in the southeast of the region wedges out in the Yeşilyurt Formation which contains limestone blocks. The Thanetian Kırkkavak Formation is represented by algal limestones and black marls. The Ilgınlıkdere Formation (Ilerdian) is in flysch facies while the overlying Eskipolatlı Formation (Ilerdian to Cuisian) consists of marls with sandstone lenses and limestones. The Middle Eocene Çayraz Formation consists of sandy limestones with abundant *Nummulites.* This unit is the lateral equivalent of the Beldede Formation (conglomerates, marls, limestones) in the north and west, and of the Yamak Formation, which is in flysch facies, in the southeast of the region. Neogene unconformably overlies all these formations. Deposition was continuous with the exception of a local unconformity between Çayraz and Eskipolatlı Formations in the north of Haymana. Interpretation of the facies studies shows the presence of a semicircle-shaped shelf near Haymana and Çaldağ and Çayraz Formations were deposited on this shelf. Behind the shelf partly continental units, Kartal,

and Beldede, and in front of the shelf flysch units, Haymana, Yeşilyurt, and Yamak were deposited. Throughout Late Cretaceous – Early Tertiary times, the Haymana Basin is believed to be joined with the Salt Lake basin toward the southeast, and flysch deposits are accumulated in this part of the region. This shows that the northern and western parts of the region were filled with sediments and were uplifted afterwards (Arıkan, 1975 and Ünalan *et al*., 1976).

Paleontological studies in the Haymana Basin began with Dağer *et al*. (1963) and continued with benthic, planktonic and nannoplankton studies of the other researchers. Dizer (1964, 1968) carried out the details of the Eocene by studying of *Nummulites* and *Alveolina* type foraminifers. Based on the systematic description of *Nummulites, Assilina* and *Alveolina* species by Sirel and Gündüz (1976) the biostratigraphy of Paleocene-Eocene age units were identified. After the the study of Sirel (1976), Toker (1979) studied nannoplanktons in the formations of Campanian- Lutetian age. With the assistance of this study the compatibility of nannoplankton zones with the planktonic foraminifera zones were described and proved. Upper Cretaceous units of the basin were studied based on planktonic and benthonic foraminifers by Özcan and Özkan–Altıner, (1999, 1997), Özkan–Altıner and Özcan (1999). Other paleontologic stratigraphic investigations were carried out by Meriç and Görür (1979-1980), Sirel (1999), Özcan *et al.* (2001, 2002 and 2007).

The presence of oil saturated deep channels in the turbidite-bearing Haymana Formation had been thought to be oil saturated for a long time and therefore Gez (1957) and Druitt and Reckamp (1959), Schmidt (1960), Reckamp and Özbey (1960), Akarsu (1971), Arıkan (1975) and Ünalan and Yüksel (1985) studided Haymana region to discover the petroleum potential of the region. After these studies a sedimentological study of the oil-saturated sandstones of the Haymana region were performed by Şenalp and Gökçen (1978). They interpreted these oil – saturated turbidite facies as channel fill sediments deposited in the lower part of the submarine fans which gradually merge into the abbysal plain. Along with this petrographic work, they also studied the bottom sedimentary structures like flute casts and groove marks,

and interpreted the depositional environment as a deep marine basin fill deposit. Recent works related with oil exploration in the Haymana Basin was carried out by Grove *et al*. (2000) and Acar *et al.* (2007). Grove *et al*. (2000) work included that the Haymana Formation constitutes one of the three primary exploration targets in the Haymana-Polatlı Basin. It consists of flysch sediments that contain potentially important turbidite sand units deposited in submarine fans. Oil-impregnated turbidite sands of the Haymana Formation crop out in the eastern portion of the basin, on the Çaldağ Anticline, and point to a potential play for submarine fan traps in the subsurface. Acar *et al*. (2007) studied the source rock character and depositional environment and the thermal maturity, assessed from Spore Colour Index and Tmax, indicates that late Campanian-Maastrichtian Haymana Formation in the Salt Lake Basin range from diagenetic to over mature with respect to oil generation and may produce gas and oil. As a result, all studies made a good understanding of the evolution of the Haymana Basin and suggested careful sedimentological studies of turbidite formations which are essential in finding more proximal parts of the basin where the oil is likely to be accumulated.

The tectonic evolution of the Haymana Basin which developed on a forearc accretionary wedge in Central Anatolia has been studied by many researchers (Şengör and Yılmaz, 1981; Görür *et al.*, 1984; Koçyiğit *et al.*, 1988; Koçyiğit, 1991). According to these studies, the Haymana Basin was considered to be developed within a continental and oceanic collision regime along the northern branch of the Neo–Tethys (Izmir-Ankara Suture Zone). Due to the existence of Tertiary calcalkaline volcanism (Galata volcanism), and the presence of ophiolitic basement in the basin, the Haymana Basin was thought to be developed in an accretionary wedge which was active from the Late Cretaceous to the Late Eocene. Arc activity in the Sakarya continent during the Paleocene suggests that subduction was towards the north (Fourquin, 1975; Şengör and Yılmaz, 1981). As stated by Koçyiğit (1991), the Haymana Basin is a highly deformed sedimentary fill, which is more than 5000 m thick in the center of the basin and largely of turbiditic origin.

The sequence stratigraphic and sedimentological studies, in the Lutetian Beldede, Çayraz and Yamak formations of the Haymana Basin have been performed by Çiner *et al.* (1993, 1993, 1996). Çiner *et al.* (1993) studied the Middle Eocene Beldede Braid-Delta Complex and applied sequence stratigraphic concepts in order to interpret the depositional environments and controlling factors exerting on the development of sequences. They divided Beldede Braid-Delta complex into elementary units and elementary sequences. In addition to this, they studied the cyclicity in the Middle Eocene Yamak turbidite complex of the Haymana Basin (Çiner *et al.*, 1996). Yamak turbidite complex represents a prograding submarine fan and was subdivided into three depositional sequences, each consisting of a turbidite system with sandstone and conglomeratic sandstone beds alternating with mudstones. Each turbidite system has been subdivided into basic sequences which are composed of several basic units. Depositional sequences in this complex have been interpreted to correspond to third – order sea-level cycles of tectonic origin. Çiner *et al.* (1993) also studied the cyclicity in the Middle Eocene Çayraz Formation mainly made up of carbonates, which represents the youngest marine Formation of the Haymana Basin. The aim of their study was to describe coarsening-upward and shallowing-upward nummulite-bearing carbonate cycles of different magnitudes and the sequence stratigraphic frame of their study area. In addition, Çiner (1996) studied the distribution of small scale sedimentary cycles throughout some selected basins (Haymana and Sivas basins) in Central Anatolia in order to present the characteristics of small-scale cyclicities observed in different parts of basins and determined their autocyclic or allocyclic origin. High order cyclicities in the Haymana Basin probably have been controlled by tectonic processes (Çiner *et al.*, 1993).

Outside of Turkey, there are quite a number of studies carried out on sedimentary cyclicity. Sedimentary cycles have been recognized for centuries (e.g, Steno, 1699, de Maillet, 1748, Suess, 1888 etc.), and it has been sugggested that sea-level rise and fall was the main cause of the cyclicity in sedimentary rocks. In the twentieth century, geologists (e.g., Lemoine, 1911;

Graubau, 1936, Burollet, 1956, Sloss, 1962, etc.) have recognized the composite effect of tectonic and sea-level variations on the sedimentary cyclicity. Later, the advent of the plate tecnotic paradigm provided the foundation for the concepts of eustasy and relative sea level changes which are the basis of seismic stratigraphy, which was introduced in 1977. Later the eustatic curve (Haq *et al.*, 1987) depicts the global mean sea-level variations during the Mesozoic and Cenozoic and composed of varies eustatic curves with cycles of different periods or time duration. In shallow-water carbonate depositional settings, shallowing-upward meter scale cycles usually correspond to parasequences which are bounded by marine flooding surfaces as originally defined by Van Wagoner *et al.* (1988), and are interpreted as building blocks of larger sequences (Wright, 1986; Grotzinger, 1986; Hardie *et al.*, 1986; Osleger and Read, 1992; Tucker *et al.*, 1993; Catuneanu, 2006; Catuneanu, 2008). However, shallowing-upward meter-scale cycles are also interpreted as small-scale sequences (Strasser *et al.*, 1999). These cycles can be considered as the reflection of climatic changes (Milankovitch cycles) controlled by the Earth's orbital parameters (eg., Einsele *et al.*, 1991).

Under the light of all these previous studies, this study has been undertaken in order to investigate the nature of the shoaling upward meter-scale cycles, which are fundamental stratigraphic units, in the Çayraz Formation of Eocene age and to understand the responses of benthic foraminiferal groups to the sedimentary cyclicity.

1.5. Geological Setting

The Haymana Basin, 70 km SW of Ankara, developed within a continental collision regime along the northern branch of the Neo-Tethys (Izmir-Ankara suture zone; Figure 2).

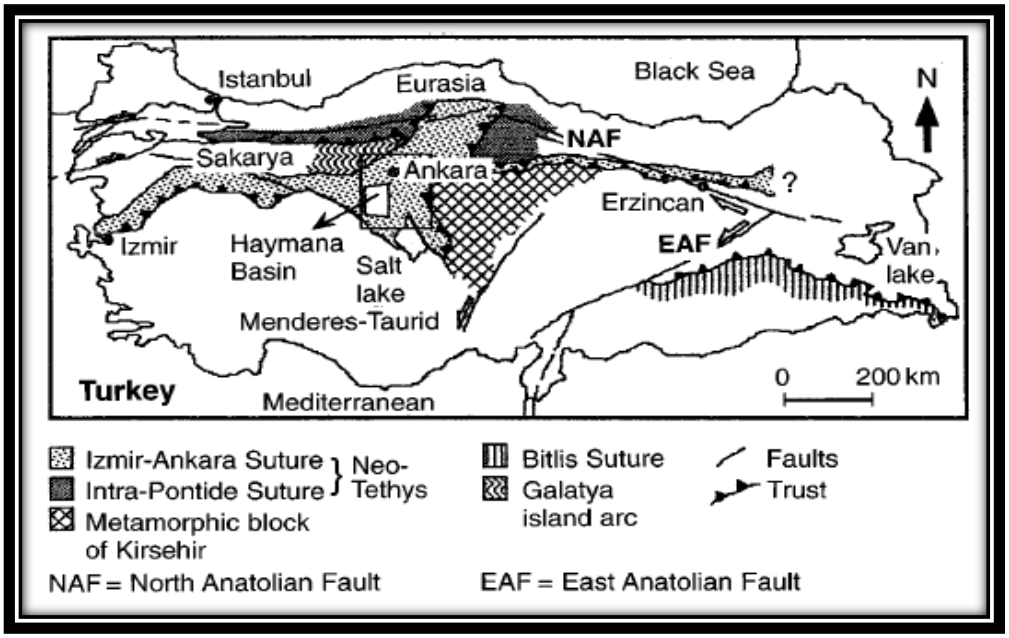

Figure 2. Main structural features of Turkey and location of the Haymana Basin (Çiner *et al*, 1993).

The Sakarya continent to the N–NW, the metamorphic block of Kirsehir to the east, and the Gondwana continent to the south, surrounded the basin (Görür *et al.* 1984). Because of the existence of Tertiary calcalkaline volcanism (Galata volcanics), and the presence of ophiolitic basement in the basin, many authors (Sengör and Yilmaz 1981; Görür *et al.* 1998; Koçyiğit *et al.* 1988; Koçyiğit 1991) suggested that the Haymana Basin developed on a fore-arc accretionary wedge (cf. Dickinson and Selly, 1979). This wedge was active from the Late Cretaceous to Late Eocene and formed on the oceanic crust of the northern branch of Neo-Tethys (Izmir – Ankara Suture Zone) by the convergence and collision of the Eurasian continent to the north, and the intervening Sakarya continent (Fourquin, 1975; Şengör and Yılmaz, 1981; Görür *et al.*, 1984, 1998; Koçyiğit *et al.*, 1988; Koçyiğit 1991) (Figures 2, 3). According to the arc activity in the Sakarya continent during the Paleocene suggested that subduction was towards the north (Fourquin, 1975; Şengör and Yılmaz, 1981).

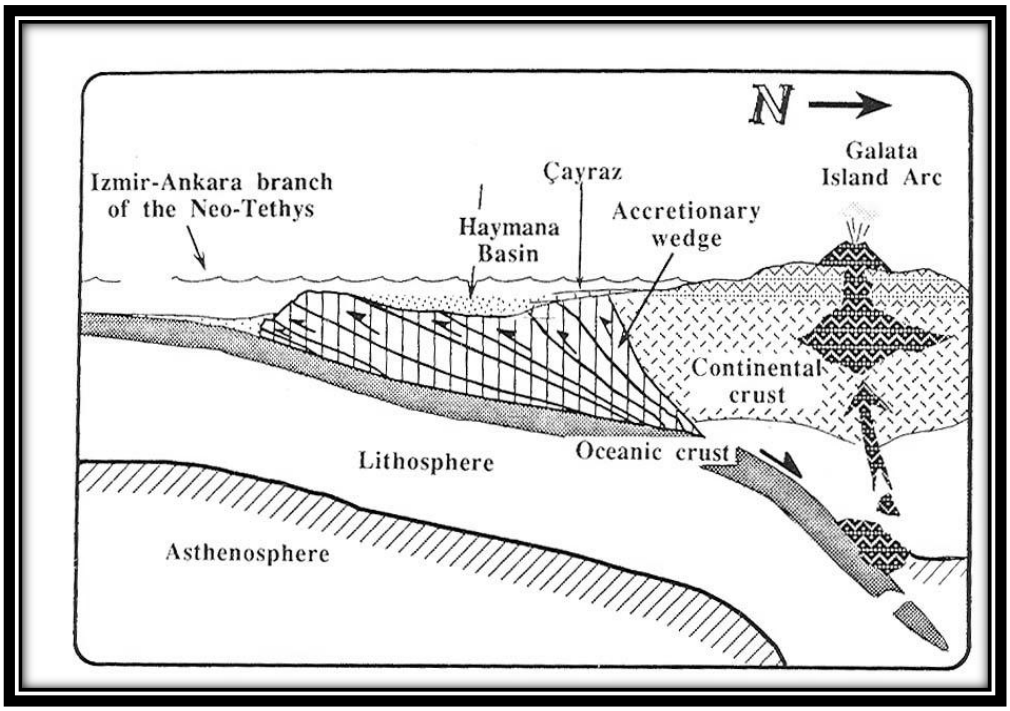

Figure 3. Schematic cross section (not to scale) showing the structural setting of the Haymana Basin during the Campanian to the Lutetian time interval (Çiner *et al*, 1993).

The basement of the Haymana Basin, in which the cumulative thickness of the Upper Cretaceous - Tertiary deposits reaches thousands of meters, is composed of the Jurassic – Lower Cretaceous carbonate cover of the Sakarya Continent (Şengör & Yılmaz 1981), the Karakaya Complex (Metamorphic Basement) forming a part of the pre - Jurassic basement of the Sakarya Continent (Şengör *et al.*, 1981), and the Ankara Mélange (Bailey and McCallien, 1953; Norman, 1973; Ünalan *et al.*, 1976; Görür and Derman, 1978; Norman *et al.*, 1980). Above this basement, mostly above an unconformity and according to the references given above, are deposited as turbidites which consist dominantly of sandstone – shale intercalations with frequent conglomerates, olistostromes and debris-flow deposits forming the Haymana Formation of Late Cretaceous age. During Paleocene, deposition of

continental red clastics of the Kartal Formation and reefal limestones of the Çaldağ Formation characterized the basin edges whereas the relatively deeper water shale-limestone intercalations of the Kırkkavak Formation were laid down in the interior of the basin. The Palaeocene age Kartal Formation contain clasts of ophiolites, radiolarian cherts, and limestones (Görür and Derman 1978). In Early to Middle Eocene, the Haymana Basin was characterized by a shallow transgressive sea in which widespread sandy and nummulite bearing limestones were deposited on the shelf, but deep marine sedimentation continued to the SE, within the basin interior (Ünalan *et al.*, 1976; Koçyiğit and Lünel, 1987).

Around the basin margins, deep-sea deposits change laterally and vertically into highly fossiliferous shallow marine sandstones, shales and limestones with *Hippurites* sp., *Orbitoides* sp., *Cyclolites* sp. with various gastropods and lamellibranches. Because of extensive tectonic deformation, it is not possible to trace the passage from turbiditic strata into shelf and continental outcrops (Çiner, 1992).

The Early and Middle Eocene witnessed the deposition of thick turbidite successions in the central part of the basin, which occupied larger area than its Paleocene predecessor. Eocene turbidites of the Haymana Basin constitute the Eski Polatlı Formation and contain clasts of serpentinite, dunite, peridotite, diabase, basalt, radiolarian chert and glaucophane schist, derived from the ophiolitic mélanges of the Karakaya Complex and the Ankara Mélange, as well as micaschists and amphibolites from the ophiolitic mélange and the Sakarya basement, and rhyolitic lava flows from the Sakarya magmatic arc (Şengör & Yılmaz 1981).

The Paleocene to Middle Eocene part of the basin is represented by the abundance and diversity of nummulitids and partly alveolinids. Towards the end of the Middle Eocene, the turbiditic depositional areas of the Haymana Basin began to decrease because these turbiditic depositions passed vertically and laterally into shallow marine nummulitic limestones of the Çayraz

Formation and the continental clastic sediments of the Kartal Formation. All these formations were terminated by the arrival of a slice of Ophiolitic Mélange (Ankara Mélange) and the Miocene-Pliocene age Cihanbeyli Formation, which consists of conglomerates, sandstones, marls, evaporaites, and tuffs, deposited unconformably above the mélange nappe and the underlying formations.

Under this general geologic context, our study area is located in the Haymana Basin and the measured sections of the Çayraz Formation are located nearly in the northwest of the Çayraz town. Stratigraphic details of this formation will be given in the following chapter (Chapter 2).

CHAPTER 2

STRATIGRAPHY

2.1. Lithostratigraphy

The Haymana Basin, like many other central Anatolian basins, is characterized by Upper Cretaceous–Middle Eocene clastic turbidite sediments at its center, passing into platform carbonates and continental red beds towards the margins (Yüksel 1970; Görür 1981; Çiner 1992) (Figure 4). The thickness of the Upper Cretaceous - Lower Tertiary deposits is 5800 m in the region. Deposition in the basin was continuous with the exception of a local unconformity between Çayraz and Eskipolatlı Formations in the north of Haymana.

The lower boundary of the Haymana basin deposits has been disputable for a long time and it has been modified in the M.Sc. thesis by Afgan Hüseyinov (2007) based on the study of Yüksel (1970). According to this study, the successions under the Haymana Formation consists of three formations, namely Kocatepe, Seyran and Çaltepe Formations. The Haymana Formation which contains shale and sandstone interclanations with frequent conglomerates and debris flow deposits, rests on the Kocatepe Formation which is represented by reddish to pinkish limestones comprising a breccioid level in the lowest part. The Kocatepe Formation overlies the Seyran Formation unconformably comprising limestones, shales and breccias (Yüksel, 1970) and the Seyran Formation overlies in turn unconformably the thick bedded limestones of the Çaltepe Formation which is probably a block embedded within the matrix of the ophiolitic melange (Figure 5). Ophiolitic

Mélange of Cretaceous age has tectonic contact with metamorphics or Karakaya Comlex in the region.

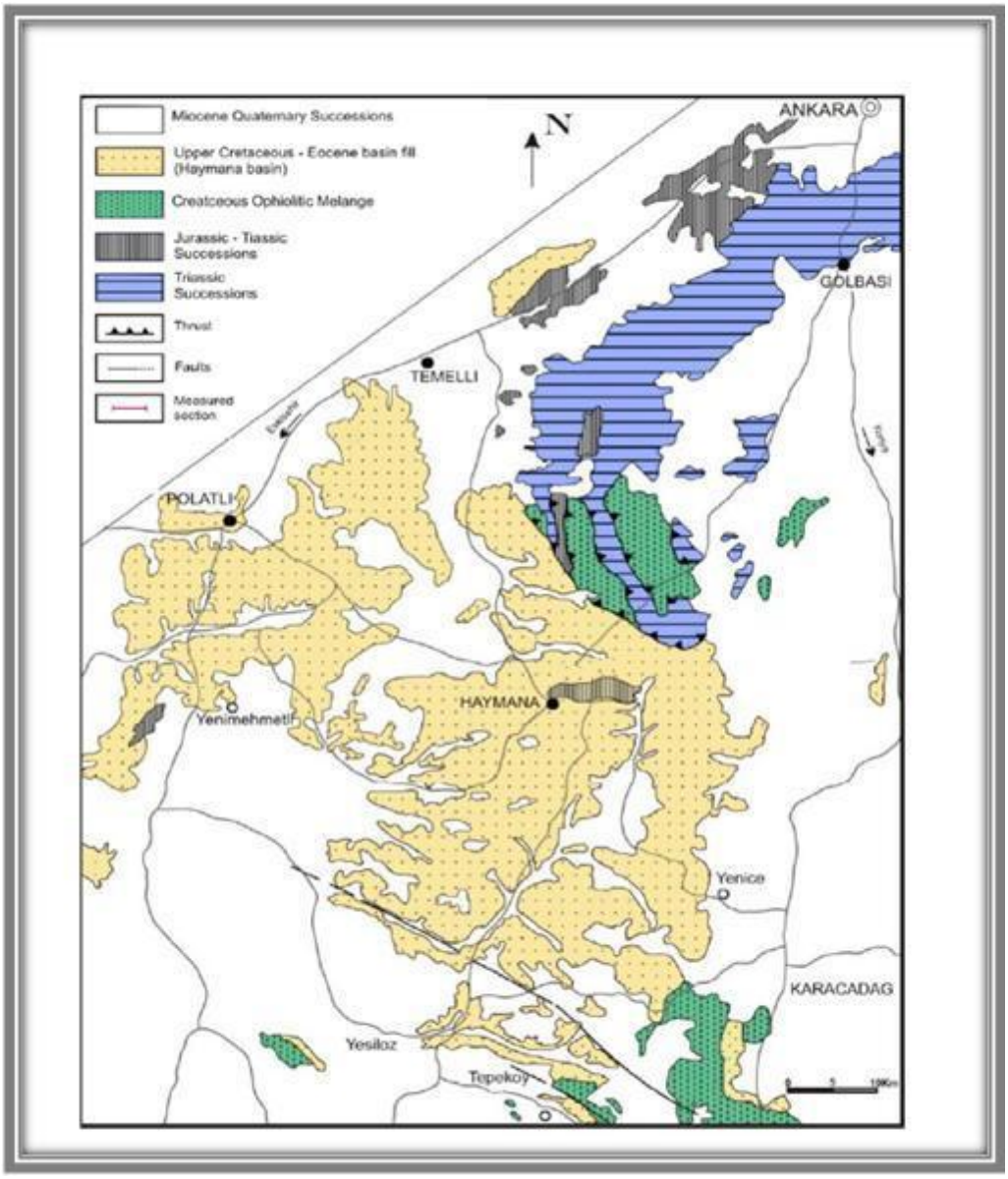

Figure 4. General geological map of the Haymana Basin (Map has been prepared under the supervison of Prof. D. Altıner based on 1/500000 scale Geologic Map of the General Directorate of Mineral Research and Exploration).

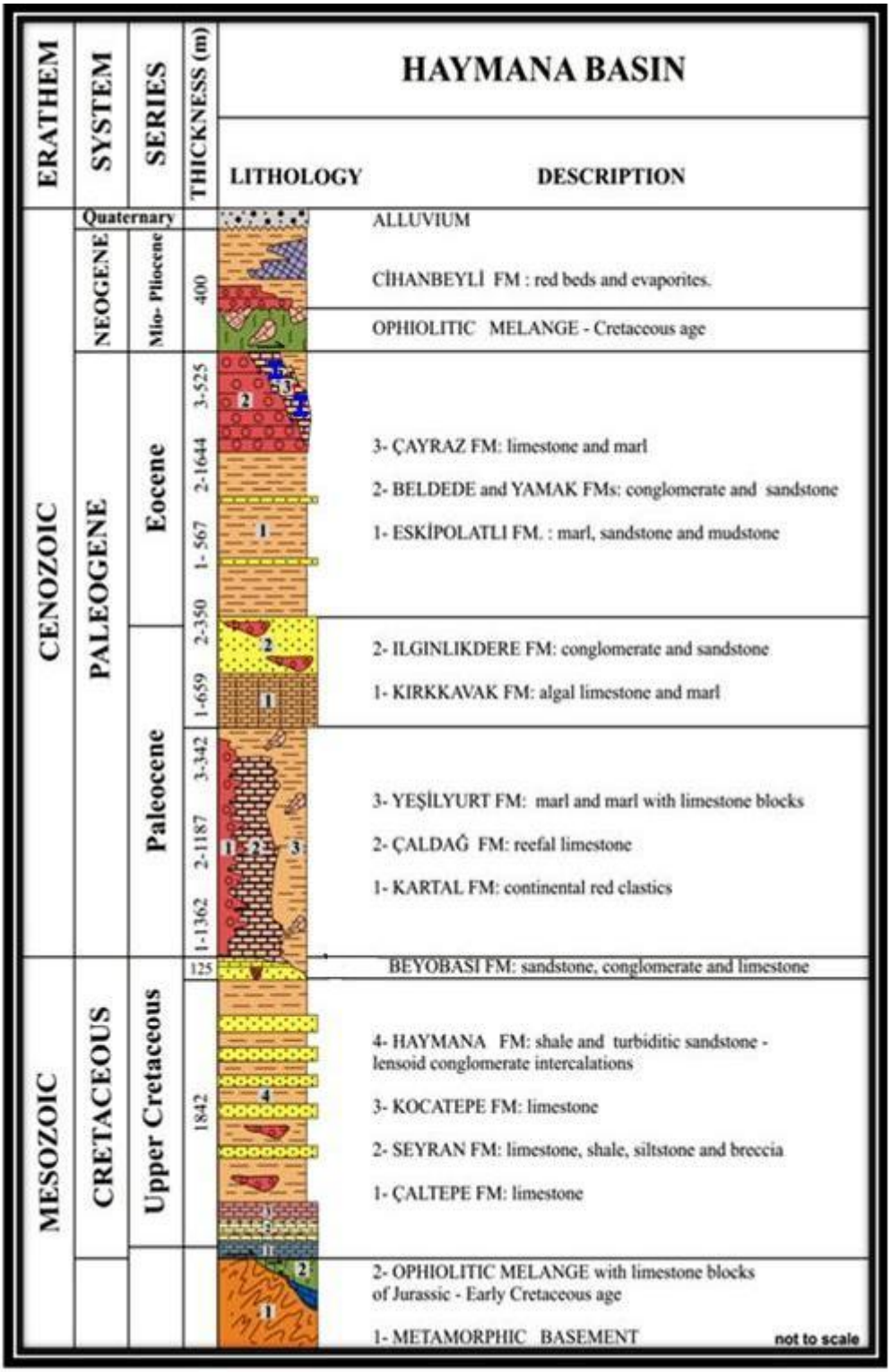

Figure 5. Generalized columnar section of the Haymana basin (modified from Yüksel, 1970 and Ünalan *et al.*, 1976 under the supervison of Prof. D. Altıner) and measured sections within the Çayraz Formation.

The upper boundary of the Haymana Formation is with the Beyobası Formation which consists of limestone, sandstones and conglomerates. The overlying formations are the Çaldağ Formation which is represented by reefal limestones and the red colored Kartal Formation and the Yeşilyurt Formation which is composed of marl and marl with limestone blocks. The Thanetian Kırkkavak Formation is represented by algal limestones and black marls. The rest of the Tertiary deposits of the basin are the Ilgınlıkdere Formation (Ilerdian) comprising conglomarate and sandstone, the overlying Eskipolatli Formation (Ilerdian to Cuisian) consisting of marls with sandstone lenses and mudstones and the Middle Eocene Çayraz Formation represented by limestones with abundant *Nummulites* and marl. This formation is the lateral equivalent of the Beldede Formation which is composed of conglomerates, marls and limestones in the north and west, and of the Yamak Formation, which is composed of sandstones, in the southeast of the region. All these formations were terminated by the arrival of a slice of Ophiolitic Mélange (Ankara Mélange). Among these formations of the Haymana Basin, this study has been dealed with the Çayraz Formation in order to investigate the nature of the shoaling upward meter-scale cycles and the response of foraminifera to the cyclicity.

2.1.1. Çayraz Formation

The Çayraz Formation is defined by Schmidt (1960) and is located nearly Çayraz Village north of the Haymana town (Figure 6). The type section of the formation is west of the Çayraz Village. In the type section, the formation is reperesented by limestones with *Nummulites* and *Alveolina* with marly intercalations, containing abundant large *Nummulites* and *Assilina* at its base, and sandstones and marls with *Nummulites* at its top. The formation comformably overlies the Eskipolatlı Formation except the local unconformity in the northwest of the Yeşilyurt and is terminated by Ophiolitic Mélange. This formation is the lateral equivalent of the Beldede Formation in the north and west, and of the Yamak Formation in the southeast of the region.

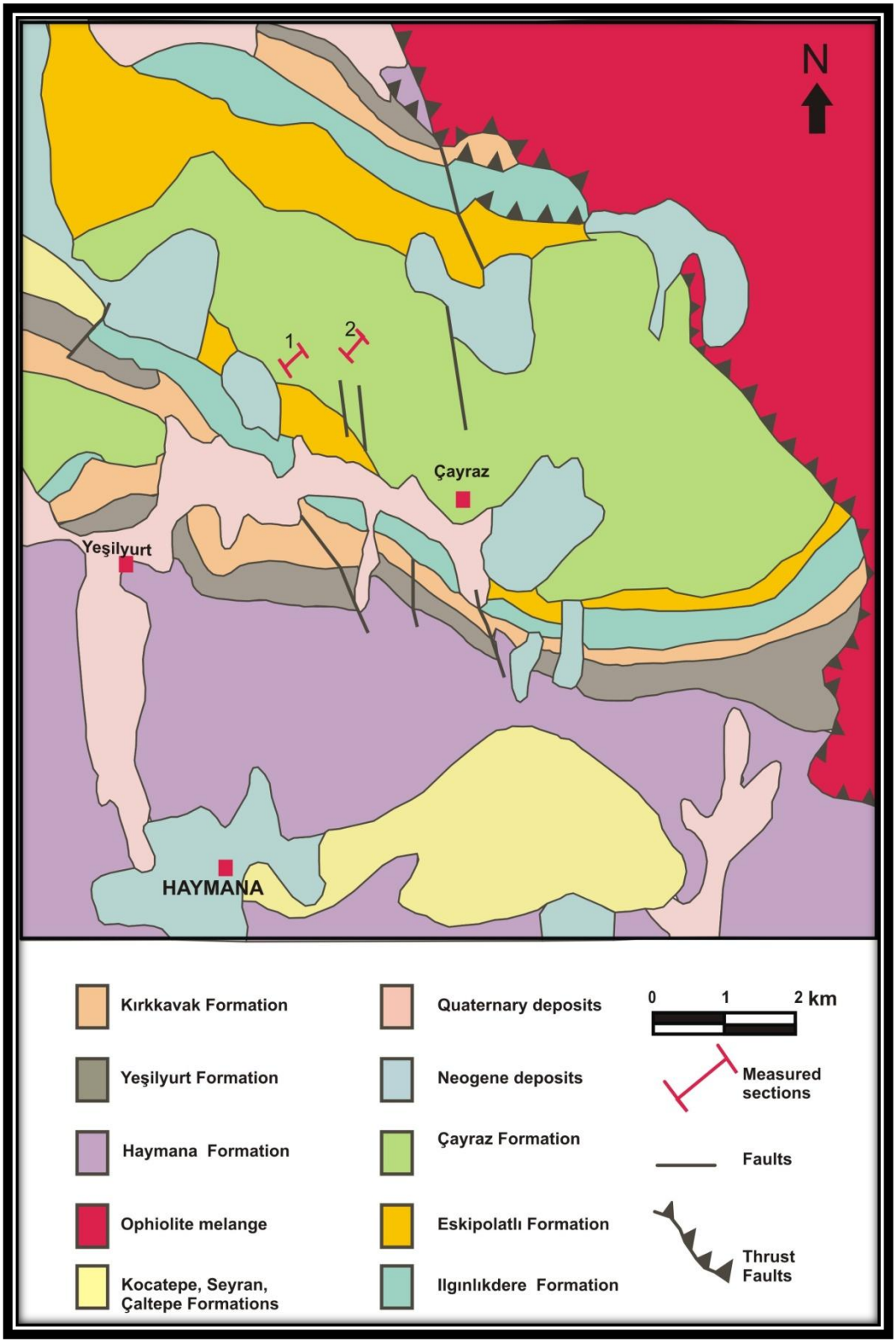

Figure 6. Geological map and subdivision of the Çayraz region and location of measured sections (Section 1and 2) (Modified from Çiner *et al*.,1993).

The thickness of the formation is 525 m. The age of the formation is given Cuisian-Lutetian. By using *Alveolina canavari* Checchia and Rispoli, *Alveolina bayburtensis* Sirel, *Alveolina çayrazensis* Dizer the age of the lower part is given as Cuisian and by using *Nummulites laevigatus* Bruguiere, *Nummulites lehneri* Schaub, *Nummulites helveticus* Kaufmann, *Assilina spira* de Roissy, *Assilina exponensis* Sowerby the age of the upper part of the formation is given as Lutetian (Sirel and Gündüz, 1976).

Furthermore, the age of the formation has also been studied by Özcan (2007) based on orthophragmines (*Discocyclina fortisi* cf. *cairazensis D. spliti polatliensis* Özcan, *D. senegalensis*, *Nemkovella evae karitensis* Özcan, and *Orbitoclypeus varians ankaraensis* Özcan and *D. trabayensis* cf. *Trabayensis* and a Late Ypresian- Middle Lutetian has been assigned to the formation.

The depositional environment of the formation is decribed as shallow water based on the lithological and paleontological data. According to Çiner (1993), Çayraz Formation represents a shelf environment upon which laterally extensive nummulitic banks developed.

The measured sections (Figure 5) section 1 and section 2 were located northwest of the Çayraz region within the Çayraz Formation, whose map is illustrated in Figure 6. In this map, the geology and formation subdivision of the Çayraz region were shown. In the southern part of the region, Upper Cretaceous–Middle Eocene formations of the Haymana Basin were overlied tectonically on the cretaceous basement. In the nourthern part of the region, the Ophiolitic Mélange has a tectonic contact (thrust fault) with all the underlying formations.

Çiner 1993 defined two shelf systems by the association of basic sequences that form the nummulite-bearing carbonate packages and the underlying nearly nummulite-free mudstones. The measured sections (Figure 7) are within the two shelf systems, lower and upper shelf systems (Figure 8) of the formation. Section 1 is measured in the uppermost part of the lower shelf system and section 2 is measured within the upper shelf system (Figure 8).

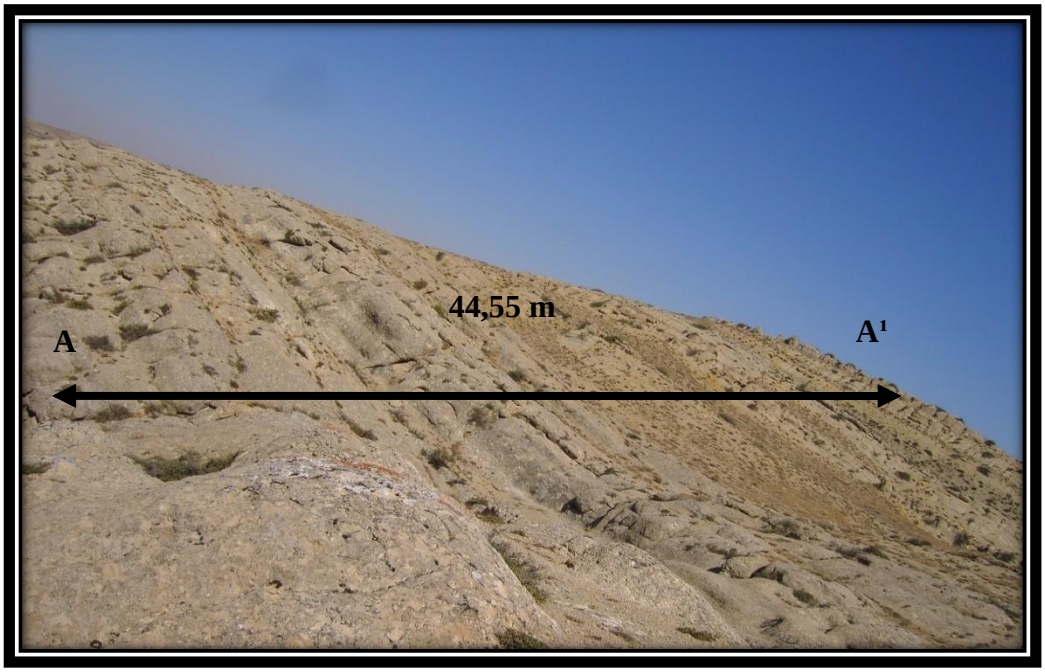

A

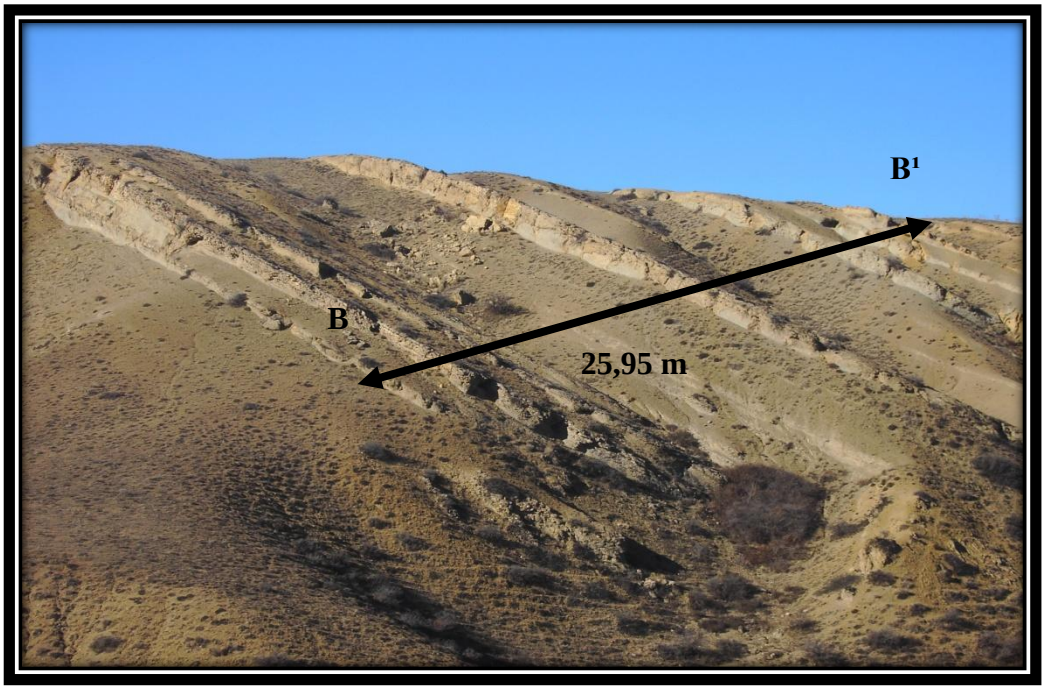

B

Figure 7. Measured sections in the Çayraz Formation, A- A¹: section 1;

B-B¹: section 2.

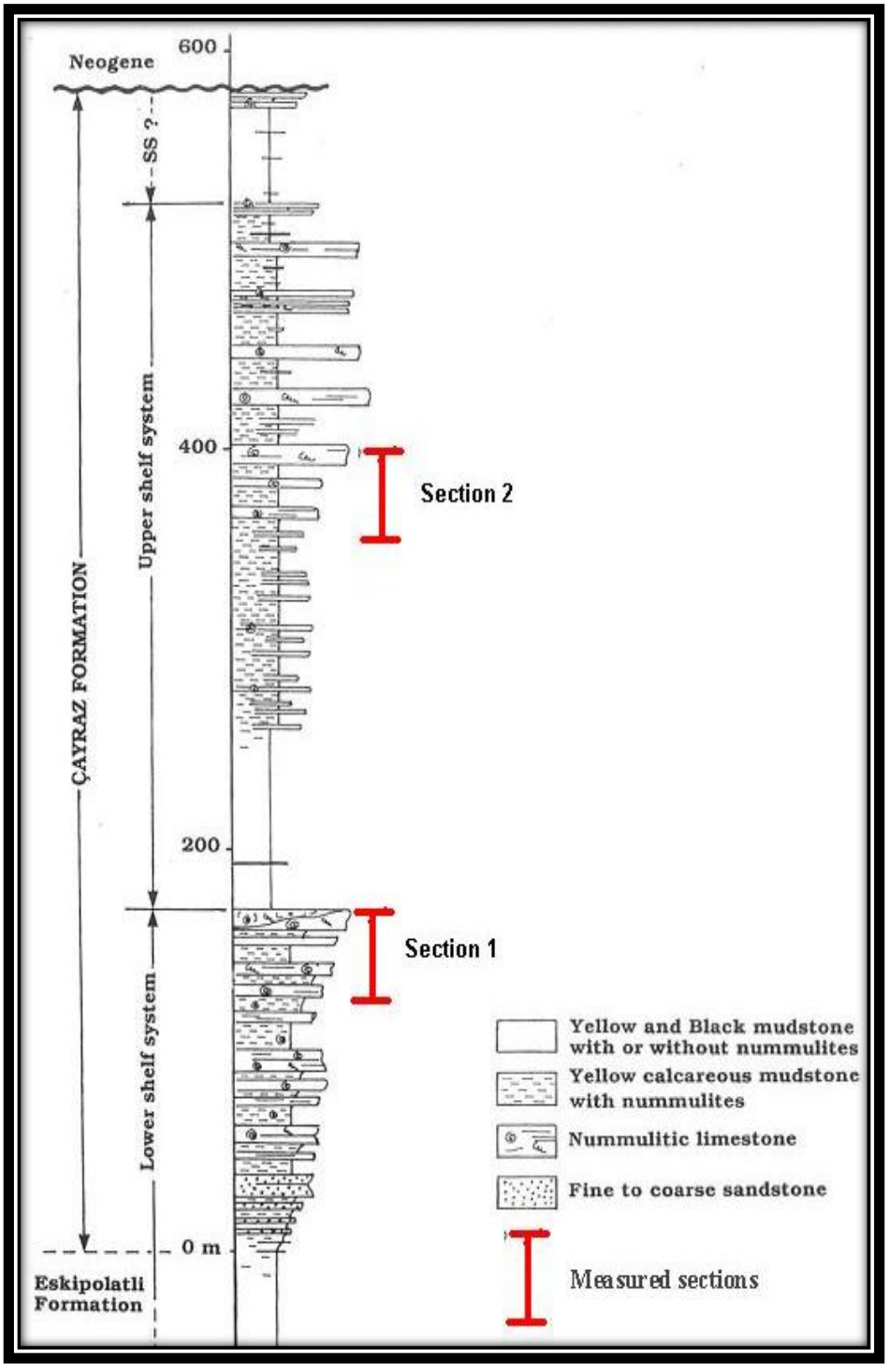

Figure 8. Subdivision of the Çayraz Formation into lower and upper shelf systems (Modified from Çiner *et al*., 1993) and location of measured sections.

Section 1 (Figure 9) is composed of thirty samples and the thickness of the section is 44,55 m. The section begins with limestones with *Nummulites* and *Discocyclina* (ÇBG 1) (Figure 10 A) and continues with the same lithology until the sample ÇBG 3. Lithology of the section 1 changes to clayey limestone with *Nummulites* and *Discocyclina* with the samples ÇBG 4 and ÇBG 5 and the lithology of the section changes again to limestone with *Nummulites* and *Discocyclina* (samples ÇBG 6-9). Clayey limestones with *Nummulites* and *Discocyclina* continues along the middle part of the section (samples ÇBG 10 (Figure 10 B), 12-18) with exception of the level ÇBG 11. Lithology of the ÇBG 11 is the greenish marl-clayey limestone with *Nummulites.* Middle part of the section is represented by a prominent limestone level (ÇBG 19-21). Upward in the section begins the clayey limestone level with *Nummulites* and *Discocyclina* (ÇBG 22-23) and continues with the greenish marl-clayey limestone with *Nummulites* (ÇBG 24-26) and finishes with the clayey limestone with *Nummulites* and *Discocyclina* (ÇBG 27-28) (Figure 1O C) and the limestone with *Nummulites* and *Alveolina* (ÇBG 29-30).

Section 2 (Figure 11), which is composed of thirty one samples and 25,95 m thick, starts in the lower part with the limestone with *Nummulites* (samples HBG 1, 5, 7-8) (Figure 12 A) and the limestone with *Nummulites* and *Alveolina* alternations (samples HBG 2-4, 6, 9). Then lithology of the section changes into the brownish marl-clayey limestone with *Nummulites* (sample HBG 10-12) (Figure 12 B) and continues with the greenish marl-clayey limestone with *Nummulites* (sample HBG 13). It passes upward into the limestone with *Nummulites* (sample HBG 15-17) and limestones with *Nummulites* and *Alveolina* (sample HBG 14). Towards the upper parts of the section the brownish marl-clayey limestone with *Nummulites* (samples HBG 18-20, 22-24, 27, 29) are intercalated with the limestone with *Nummulites* (samples HBG 21, 25- 26, 28) and the section finally terminates with the thick limestone with *Nummulites* (sample HBG 30-31).

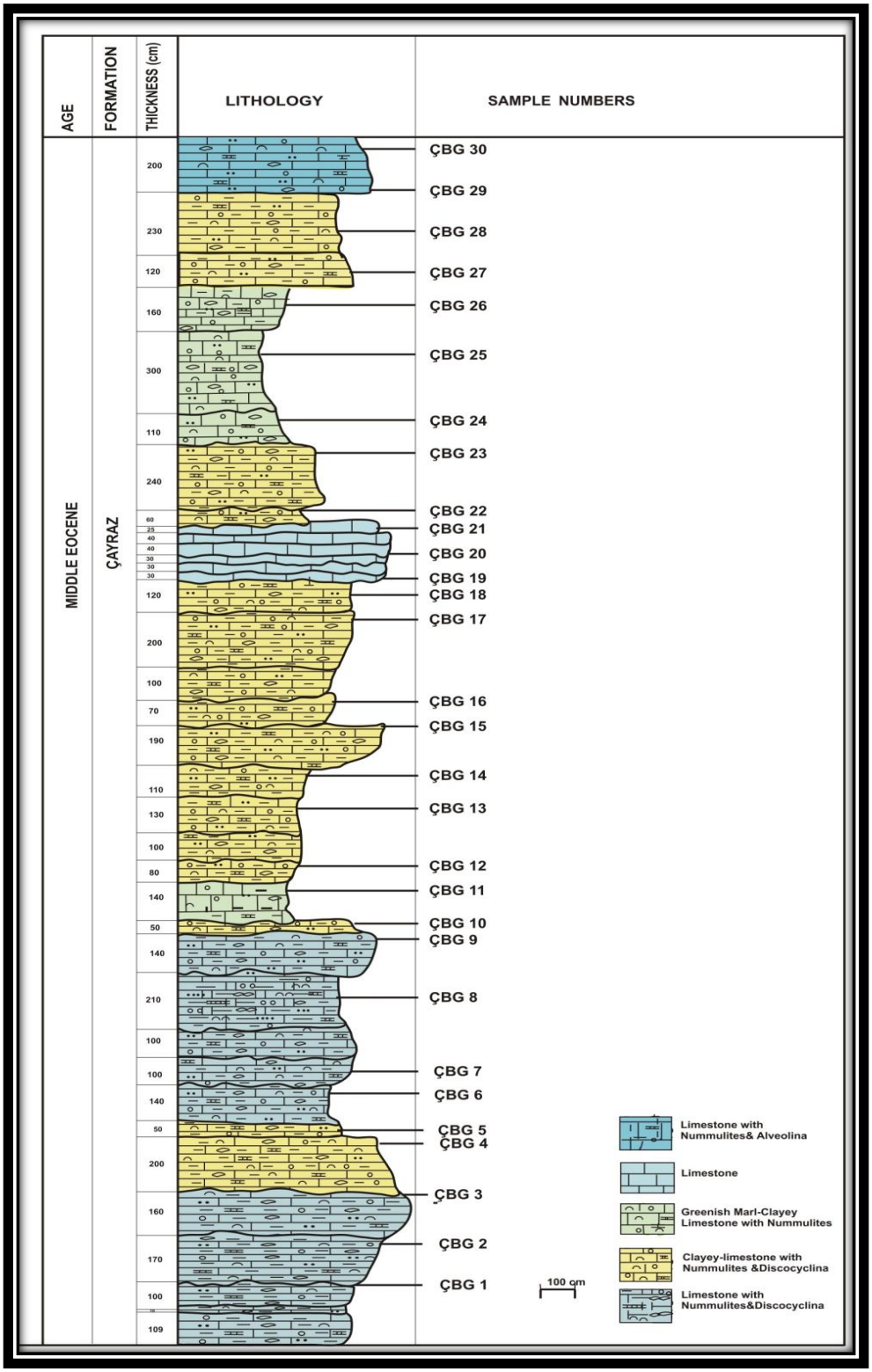

Figure 9. Lithostratigraphy of the measured section 1.

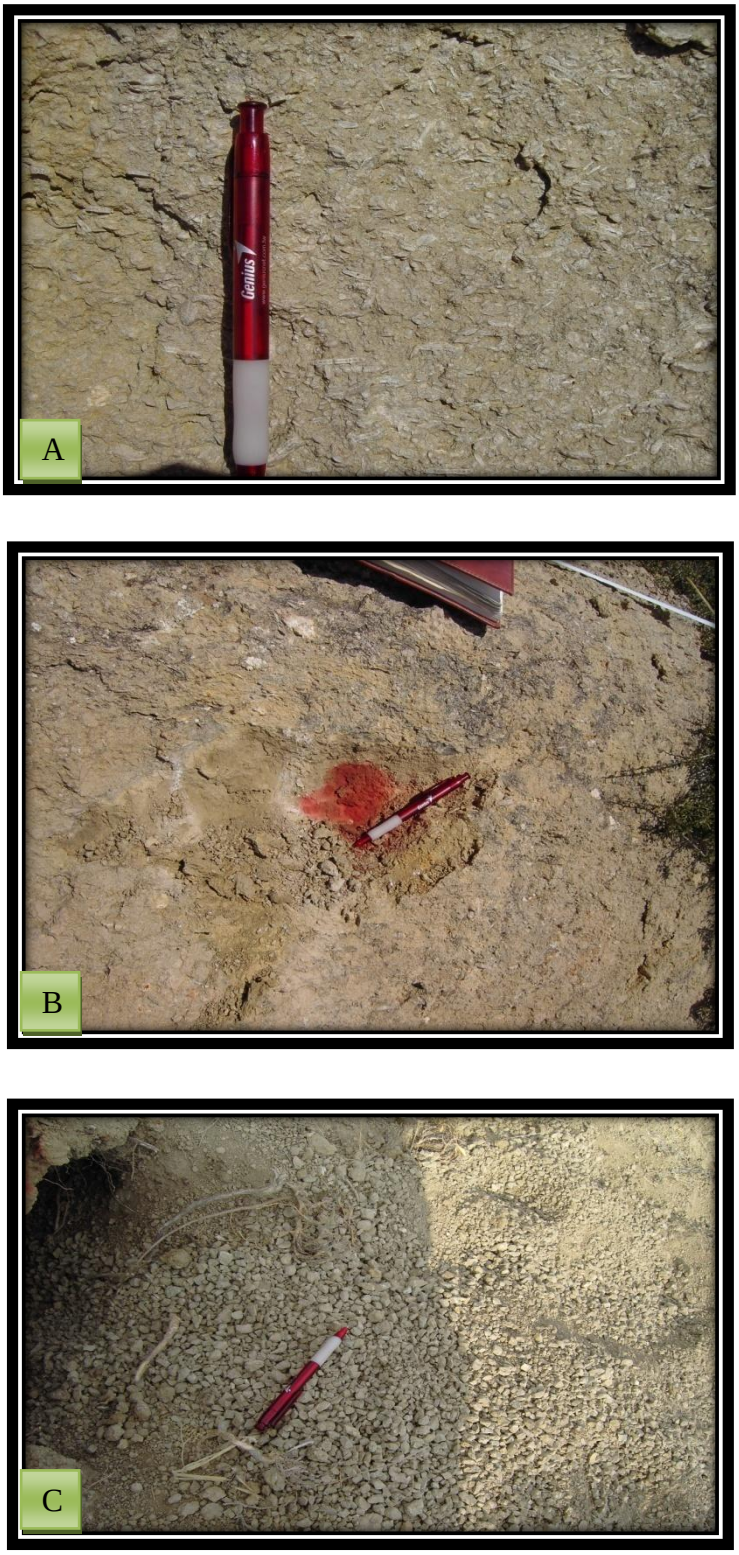

Figure 10. Field photograph of the rock units along the measured section 1, A: limestone with *Nummulites* and *Discocyclina* (ÇBG 1); B, C: clayey limestone with *Nummulites* and *Discocyclina* (ÇBG 10, ÇBG 27).

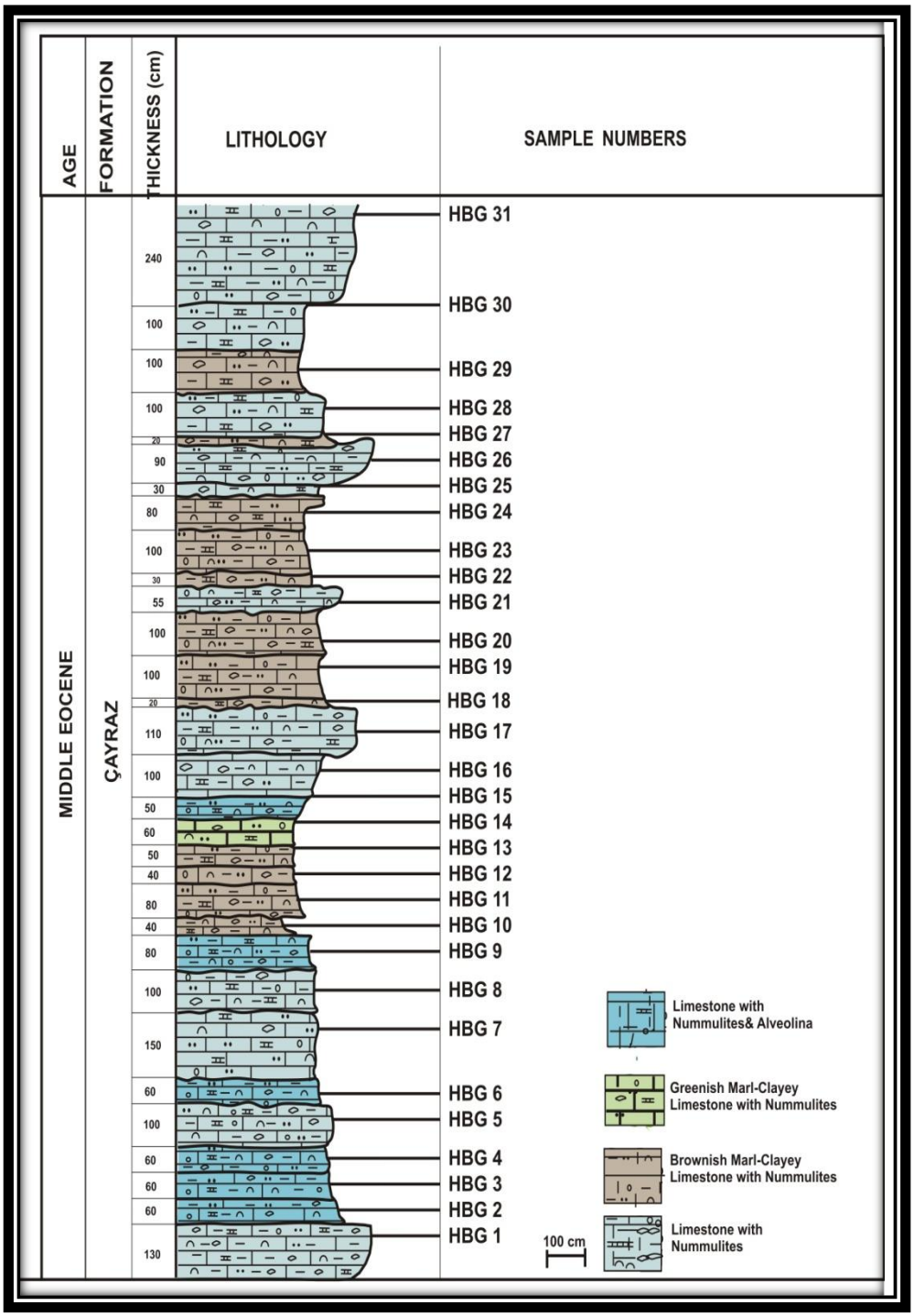

Figure 11. Lithostratigraphy of the measured section 2.

Figure 12. Field photograph of the rock units along the measured section 2, A: Limestone with *Nummulites*, which also consists of *Assilina* (sample HBG 1), B: brownish marl-clayey limestone with *Nummulites* (HBG 10).

In the studied sections, in order to verify the gross lithological attributions a set of analyses have been carried out. To determine particularly the clay content of the some rock samples bulk (whole rock) mineralogical analysis (XRD) have been carried out in TPAO Research Center XRD Laboratory. The results of the analyses are given in the table 1 (see for details appendix A). These analyses have meant to us that some levels identified as marls in visual inspection by us are actually not marls but clayey limestones.

Sample Number		Bulk Minerlogy XRD Results (% Volume)				
	Lithology	Calcite	Quartz	Dolomite	Clay+Mica	Feldspars
ÇBG-3	Limestone	97	3	_	_	_
ÇBG-4	Clayey Limestone	90	3	_	7	_
ÇBG-10	Clayey Limestone	97	2	_	1	_
ÇBG-11	Clayey Limestone	70	7	_	20	3
ÇBG-22	Clayey Limestone	97	2	_	1	_
ÇBG-24	Clayey Limestone	84	3	_	10	3
HBG-10	Clayey Limestone	53	10	_	33	4
HBG-17	Limestone	90	3	_	7	_
HBG-18	Clayey Limestone	90	3	_	7	_
HBG-22	Clayey Limestone	72	4	6	18	_

Table 1. Results of the bulk (whole rock) analysis by XRD (X-ray diffraction) (TPAO Research Center XRD Laboratory).

CHAPTER 3

METER SCALE CYCLES

3.1. Sequence Stratigraphy and Its Historical Background

Modern sequence stratigraphy is a direct outgrowth of the concept of unconformity bound stratigraphic units as mentioned by Sloss (1963), with some very important variations. In simplest terms, Sloss (1963) defined sequence stratigraphy as a tool to identify major unconformity-bound packages for the purpose of correlation across large areas of the craton, which is now called as second order sequences.

The second major evolutionary step in the conceptual evolution to modern sequence stratigraphy was seismic stratigraphy. Seismic stratigraphy is a geologic approach to the stratigraphic interpretation of seismic data (Vail and Mitchum, 1977). Seismic sequence analysis is based on the depositional sequences, which are defined as a stratigraphic unit composed of a relatively conformable succession of genetically related strata and bounded at its top and base by unconformities or their correlative conformities (Mitchum *et al.*, 1977). The seismic stratigraphic analysis method together with the global cycle chart was published by Vail *et al.* (1977). This seismic chronostratigraphy led to third key development, which was concept of sequence stratigraphy.

The transition from seismic stratigraphy to sequence stratigraphy represents a major conceptual jump. Focus shifted from global mapping of unconformity-bound packages to the interpretaion of the internal reflector patterns of stratigraphic sequences, which came to be viewed as genetically significant depositional sequences. The definition of depositional sequence was modified by Vail *et al.* (1984, 1987), Posamentier and Vail (1988), to include

systems tracts. A system tract is associated with a segment of the eustatic curve and its timing in any given basin will depend on local subsidence and sediment supply. A sequence is now defined as a relatively conformable succession of genetically related strata bounded at its top and base by unconformities and their correlative conformities. It is composed of a succession of systems tracts and it is interpreted to be deposited between eustatic fall inflection points.

Sequence stratigraphic analysis, integrated with other stratigraphic techniques, biostratigraphy, magnetostratigraphy, and radiometric data was used by Haq *et al.* (1987) to build sea-level cycle charts.

Much as parasequences are the building blocks of siliciclastic sequence stratigraphy (Van Wagoner *et al.* 1990), the high-frequency cycle, or cycle of this study, forms the building block of modern carbonate stratigraphic analysis (James 1979; Pratt *et al.*1992; Koershner and Read 1989; Grotzinger 1986; Goldhammer *et al.* 1990, 1991; Borer and Harris 1991; Crevello 1991). Sarg (1988) was the first to discuss specifically the issue of sequence stratigraphy in carbonate systems. He intepreted changes in carbonate productivity, as well as platform or bank growth and the resultant facies distribution, as the result of short-term eustatic fluctuations superimposed on longer term changes. Schlager (1992, 1993) added another perspective to the sequence stratigraphic models in carbonate settings, pointing out many previously underevaluated aspects of the carbonate environments. Handford and Loucks (1993) more recently have addressed in great detail sequence stratigraphy in carbonate settings, also stressing very much the role of sea-level changes as a control on geometries and stratal patterns.

In sequence straigraphic terms, depositional sequences can be correlated worldwide, because sequence stratigraphy is a global correlation model. Therefore, this method is a powerful tool in modern stratigraphic studies and it integrates many aspects of stratigraphy including seismic stratigraphy, lithostratigraphy, cyclostratigraphy, event-stratigraphy, and biostratigraphy into a single stratigraphic framework.

This study documents a detailed study of meter scale shallowing upward cyclic sedimentation in the shallow water environment. Shallowing upward cycles are named as parasequences and they are the building blocks of the sequence stratigraphy.

3.2. Meter Scale Cycles

Sedimentary cycle is defined as a sequence of related process and conditions, repeated in the same order, that is recorded in a sedimentary deposit and cyclicity is described by the stratal repetition of physical and chemical characters of sedimentary rocks, such as, lithofacies and biofacies (Yang *et al.*, 1998). This stratal regularity is the basis for establishing a high resolution cyclostratigraphy (Yang *et al.*, 1998).

Peritidal carbonate-dominated or mixed carbonate–siliciclastic successions frequently display shallowing-upward cycles at meter-scale. Meter scale depositional cycles are fundamental stratigraphic units. Vertically stacked shallowing-upward deposits are either bounded by marine flooding surfaces through transgressive events or by subaerial exposure surfaces which represent sea-level fall. In shallow-water carbonate depositional settings, shallowing-upward meter-scale cycles usually correspond to parasequences which are bounded by marine flooding surfaces as originally defined by Van Wagoner *et al.* (1988), and are interpreted as building blocks of larger sequences (Wright, 1986; Grotzinger, 1986; Hardie *et al.*, 1986; Osleger and Read, 1992; Tucker *et al.*, 1993). However, shallowing-upward meter-scale cycles are also interpreted as small-scale sequences (Strasser *et al.*, 1999). These cycles can be considered as the reflection of climatic changes (Milankovitch cycles) controlled by the Earth's orbital parameters (Einsele *et al.*, 1991). The parasequence is a relatively conformable succession of bed or bedsets bounded by marine flooding surfaces and their correlative surfaces (Van Wagoner *et al.*, 1988). Most parasequences are asymmetrical shallowing-upward sedimentary cycles.

The shallowing-upward succession indicates that accommodation space is being filled more rapidly than it is being created.

In order to define meter-scale cyclic sedimentation in this study firstly detailed vertical lithofacies association have been carried out and documented in the field and secondly microfacies analyses have been performed in the laboratory based on thin section analyses.

3.3. Microfacies Types

Microfacies determination is largely descriptive and microfacies types should be defined by microfacies criteria whose existence and abundance indicate the specific depositional settings (Flügel, 2004). Each lithofacies indicates a specific hydrodynamic environment. Microfacies types of carbonate rocks are not restricted to specific time intervals. Therefore, Wilson (1975) introduced the term standard microfacies types (SMF types) which can describe major depositional and biological controls and suggested major depositional settings. Wilson (1975) constituted a standard facies model that describes 10 standard facies zones (FZ) of a rimmed tropical carbonate platform. The standart FZ describe idealized facies belts from open marine deep basins across a slope, a platform marginal rim which characterized by reefs or/and sand shoals zone, and an inner platform to the coast. In addition, Flügel (2004) classified 26 standard microfacies types (SMF) for rimmed carbonate platforms (Figure 13). These SMF types are described according to grain types, matrix types, depositional fabrics, fossils and depositional texture types. Flügel (2004) also described 30 microfacies types for carbonate ramps as ramp microfacies types (RMF) (Figure 14). Because common microfacies types show the environmental conditions controlling depositional patterns and the distribution of organisms, the assemblage of characteristics standard microfacies types can be used as a key for specific facies belts, SMF types in the rimmed carbonate model and RMF types in the cabonate model. Distribution SMF types in the FZ are given in figure 13 (SMF 1- 4, 12 in the

deep sea represented (FZ 1); SMF 1-2, 8-10, 12-13 in the deep shelf (FZ 2), SMF 2-4, 12 in the toe of slope(FZ 3); SMF 5-6, 12-13, 16 in the slope (FZ 4); SMF 7,11-14, 16 in the platform (FZ 5); SMF 11-13, 15 platform margin (FZ 6); SMF 8-10,12-13, 15-18, 20 in open marine (FZ 7); SMF 12, 15-24 in restricted environment (FZ8); SMF 15-16, 19-21, 23, 25 in evaporitic or brakish environment (FZ9); SMF 26 in the meteorically affected environment (FZ 10).

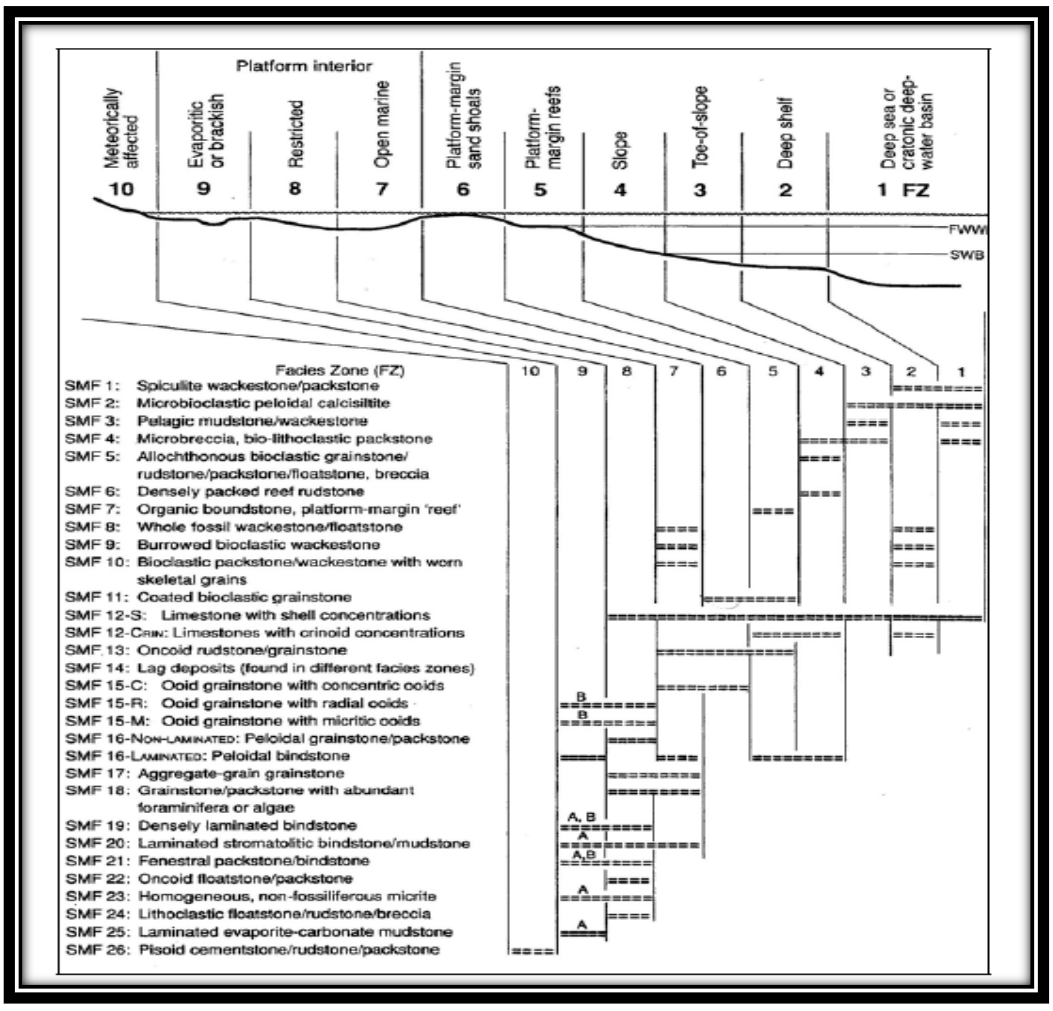

Figure 13. Distribution of Standard Microfacies (SMF) types in the Facies Zones (FZ) of the rimmed carbonate platform model (Flügel, 2004).

Distribution of RMF types start from the deeper outer ramp zones (RMF 1-6), and continues with mid-ramp (RMF 7-12) and inner ramp (RMF 13-18), and ended with lagoonal environment (RMF 19-25) and carbonate sand shoals and banks (RMF 26-30) (Figure 14).

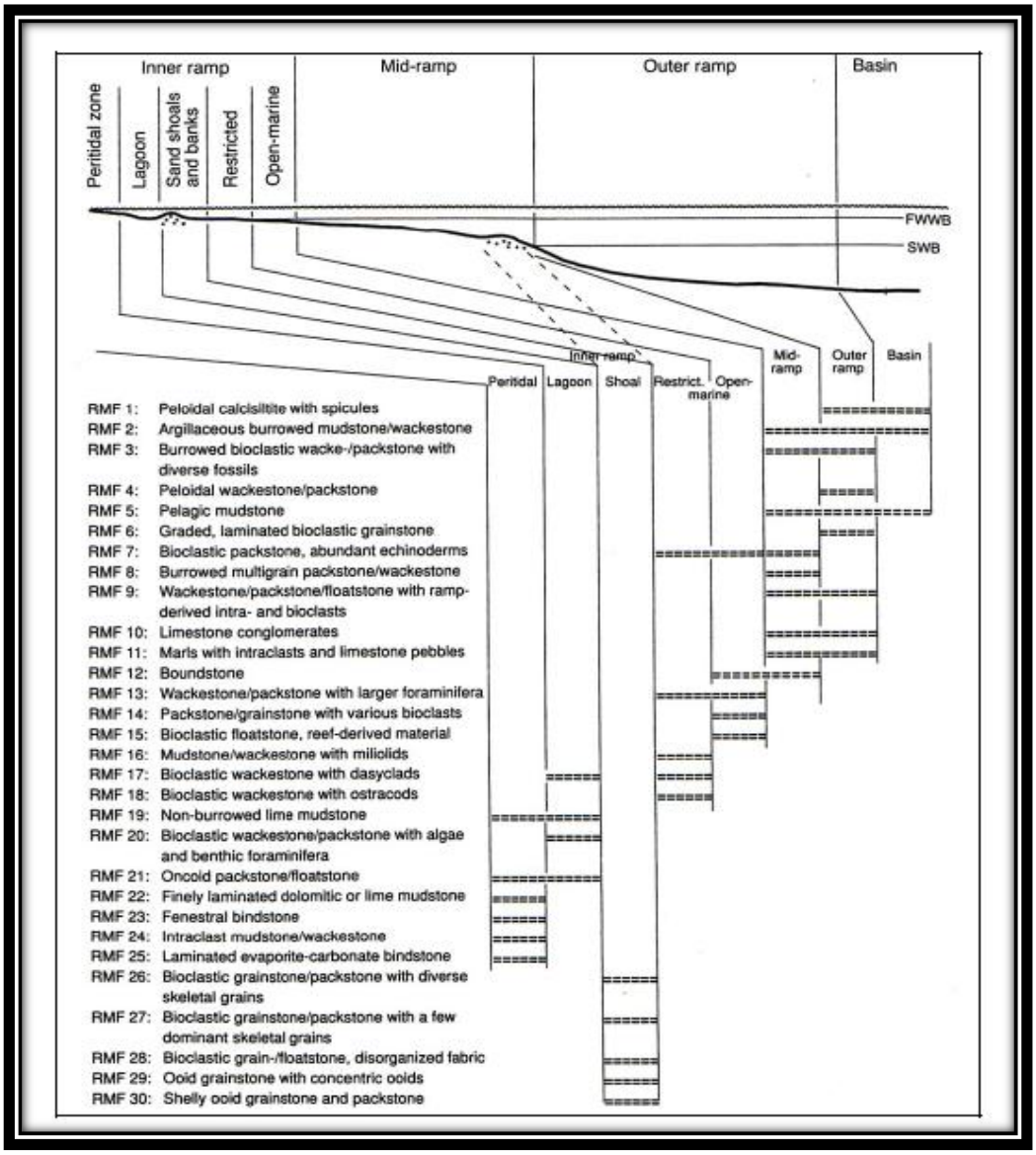

Figure 14. Generalized distribution of microfacies types in different parts of a homoclinal carbonate ramp (Flügel, 2004).

The most widely used microfacies classifications are those of Dunham (1962) and Folk (1959, 1962). Dunham's classification can equally well be applied in the field, in investigations of cores, and in laboratory studies. Folk's classification is more restricted to laboratory studies based on thin sections or peels. Therefore, in this study, the microfacies classification is made according to the Dunham Classification (1962) (Figure 15) and 10 different microfacies in the measured sections are determined by the analysis of matrix and grains, textural features, fossil content, petrographic and energy index classification, and standard microfacies zone. The most important components of the studied carbonate sedimentary samples are larger foraminifera, alveolinids, nummulitids, assilinids and discocyclinids. The Palaeogene was a time of particular abundance and radiation of these miliolid and larger hyaline foraminifera and, especially during the Eocene, they occurred in rock-forming quantities. Due to their well-defined palaeoecological requirements, they represent valuable facies indicators (Rasser *et al.* 2005). Major microfacies types distinguished in the study which were defined strictly based on the biofacies, are mudstone to wackestone with small benthic foraminifera (MF 1); benthic foraminiferal wackestone (MF 2); bioclastic, alveolinid, nummulitid packstone with abundant small and large benthic foraminifera (MF 3); bioclastic, alveolinid, nummulitid wacke- to packstone with abundant small and large benthic foraminifera (MF 4); bioclastic, alveolinid, nummulitid wackestone with abundant small and large benthic foraminifera (MF 5); bioclastic, assilinid, nummulitid wacke- to packstone with abundant small and large benthic foraminifera (MF 6); bioclastic nummulitid packstone with abundant small and large benthic foraminifera (MF 7); bioclastic, assilinid, nummulitid packstone (MF 8); bioclastic, discocyclinid, nummulitid packstone (MF 9); bioclastic, discocyclinid, nummulitid packstone with red algae (MF 10).

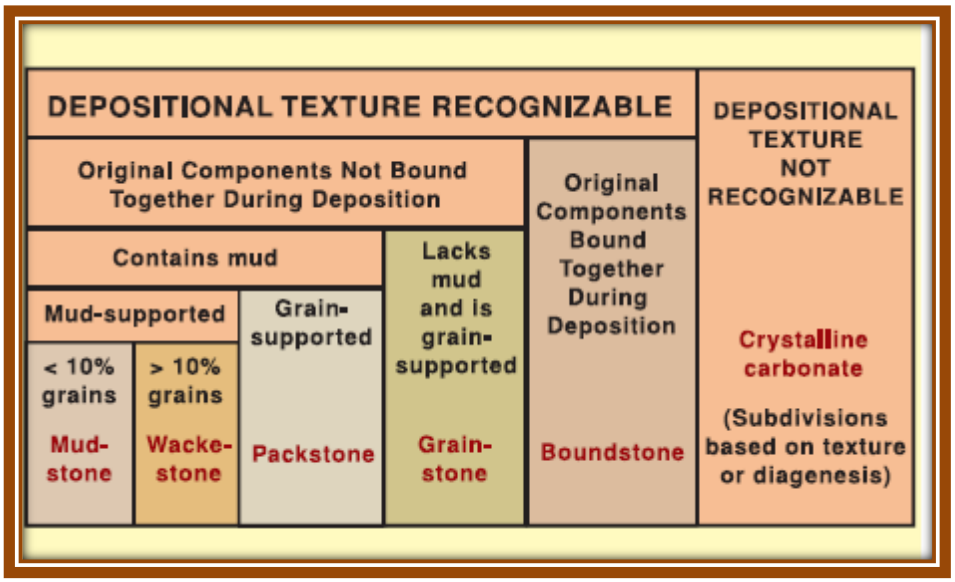

Figure 15. Classification of carbonate rocks according to depositional texture (Dunham 1962).

3.3.1. Mudstone to wackestone with small benthic foraminifera (MF 1)

This facies is poorly fossilifereous and composed of mainly micrite, algae and small benthic foraminifera (10-15%). This type of microfacies is deposited in very shallow marine environment (Figure 16). The presence of mud matrix in this microfacies shows that, for the most part, deposition was in a low to moderate energy environment (Wray 1977). A lack of larger benthic foraminifera and high abundance but low diversity of small benthic foraminifera may be indicative of lagoonal setting.

3.3.2. Benthic foraminiferal wackestone (MF 2)

This facies is composed of mainly micrite and green algae. It contains few fossils (15-20%) which indicates that this facies is deposited in a lagoonal environment (Figure 17). The presence of the green algae suggests a very shallow marine setting (Wray 1977). Because this type of microfacies occurs in low energy, lagoonal setting, this facies corresponds to RMF 20 of Flügel

(2004), which is defined as bioclastic wackestone/packstone with algae and benthic foraminifera and distributed in lagoonal setting.

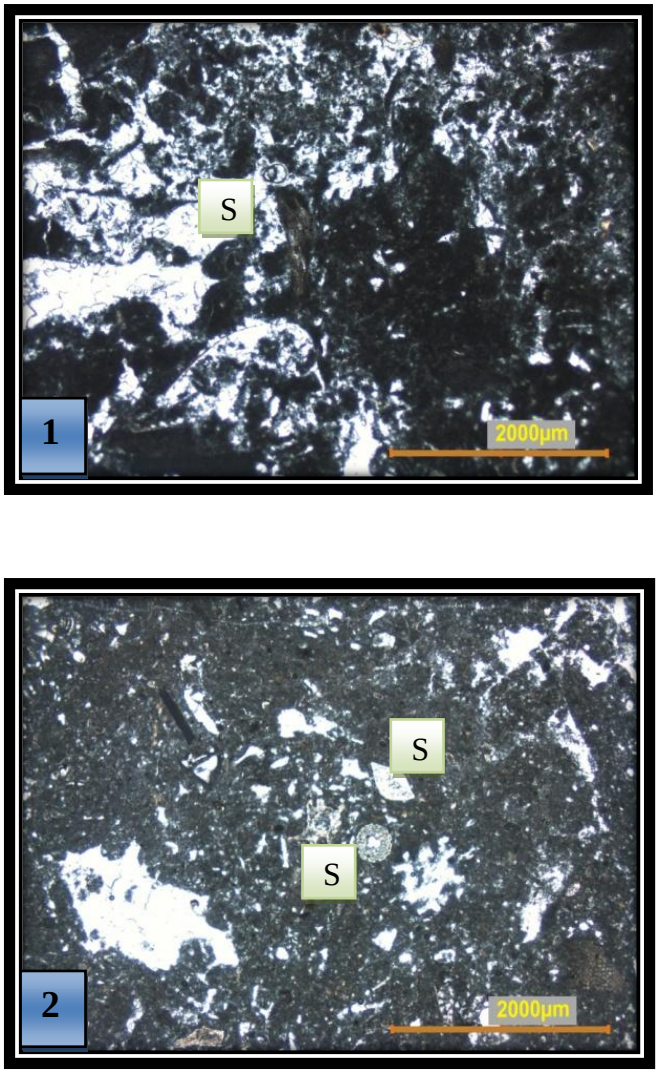

Figure 16. Photomicrographs of mudstone to wackestone with small benthic foraminifera (MF 1) (S: small benthic foraminifera), (1: ÇBG 20, 2: ÇBG 21).

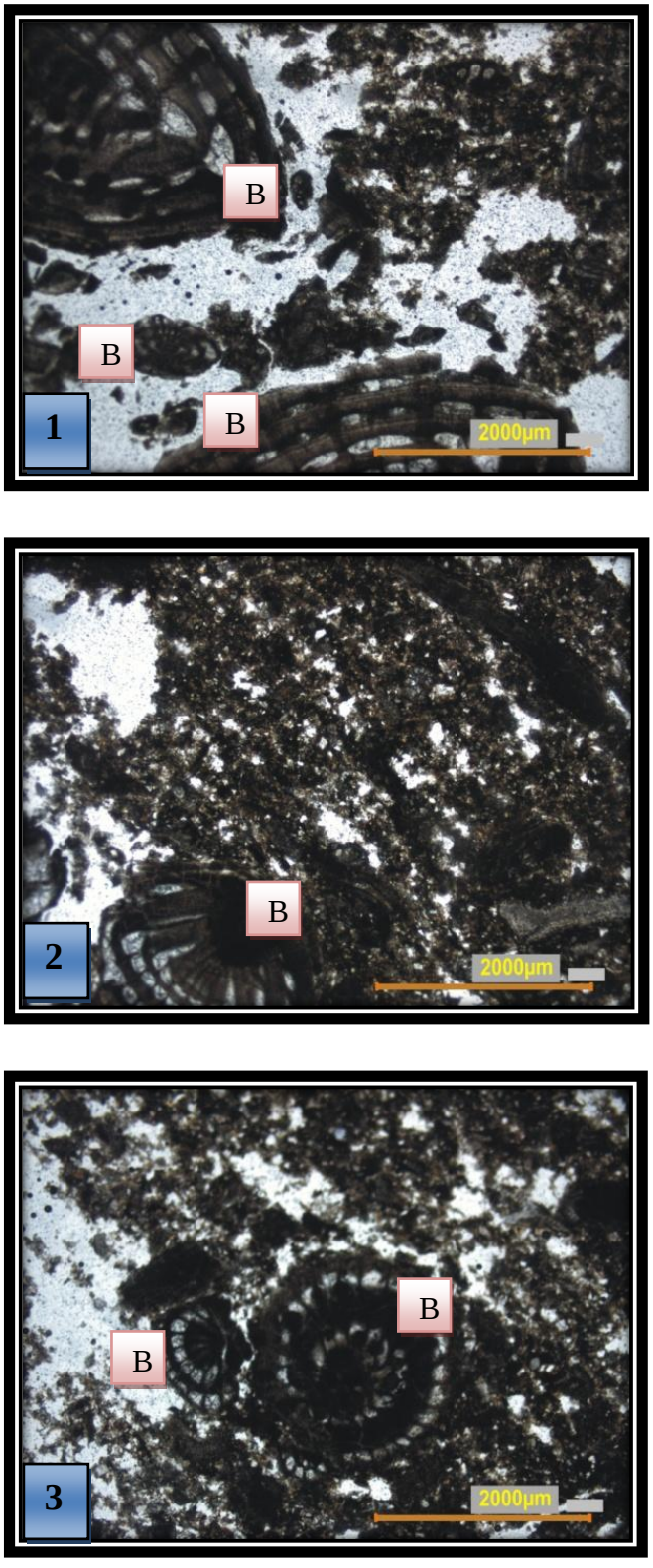

Figure 17: Photomicrographs of benthic foraminiferal wackestone (MF 2) (B: benthic foraminifera), (1: HBG 10, 2: HBG 11, 3: HBG 11).

3.3.3. Bioclastic, alveolinid, nummulitid packstone with abundant small and large benthic foraminifera (MF 3)

The main feature of this microfacies is the dominance of *Alveolina* s.l. (2-20%) and *Nummulites (*29-49%). Other minor biogenic components include miliolids, *Spiroloculina*, *Coskinolina*, *Rotalia* and valvulinids and textularids. The presence of miliolids and *Coskinolina* suggest a very shallow marine setting (Figure 18). Generally porcellaneous larger foraminifera and miliolids have lived in the lagoon environment (Leutenegger, 1984). In addition mud matrix support this.

3.3.4. Bioclastic, alveolinid, nummulitid wacke to packstone with abundant small and large benthic foraminifera (MF 4)

The most dominant components of this bioclastic microfacies are larger benthic foraminifera, *Alveolina* s.l. (7-9%) and *Nummulites* (26-39%) , bioclast and small benthic foraminifera, miliolid (1-9%), *Pygro* (6-10%), *Spiroloculina* (4-11%) (Figure 19). Other components are *Orbitolites* , *Lockhartia* and *Rotalia*.

The presence of miliolid, *Orbitolites*, *Alveolina* indicates shallow marine depositional settings. In more proximal settings, nummulithoclasts are less abundant in the matrix of restricted/lagoonal muddy facies dominated by *Orbitolites, Alveolina*, and miliolids (Middle Eocene Dernah Formation, NE Cyrenaica; Jorry 2004). In Spain (Scheibner *et al.* 2007) and in France (Rasser *et al.* 2005) *Alveolina*-dominated assemblages have been considered as thriving in inner platform, influenced by silicoclastic input. Smaller rotaliids including *Lockhartia* are locally relatively common in the *Alveolina* and *Nummulites* facies (Racey, 2001). *Nummulites* are more often associated with *Alveolina* and occur in shallower inner platform/shelf/ramp settings.

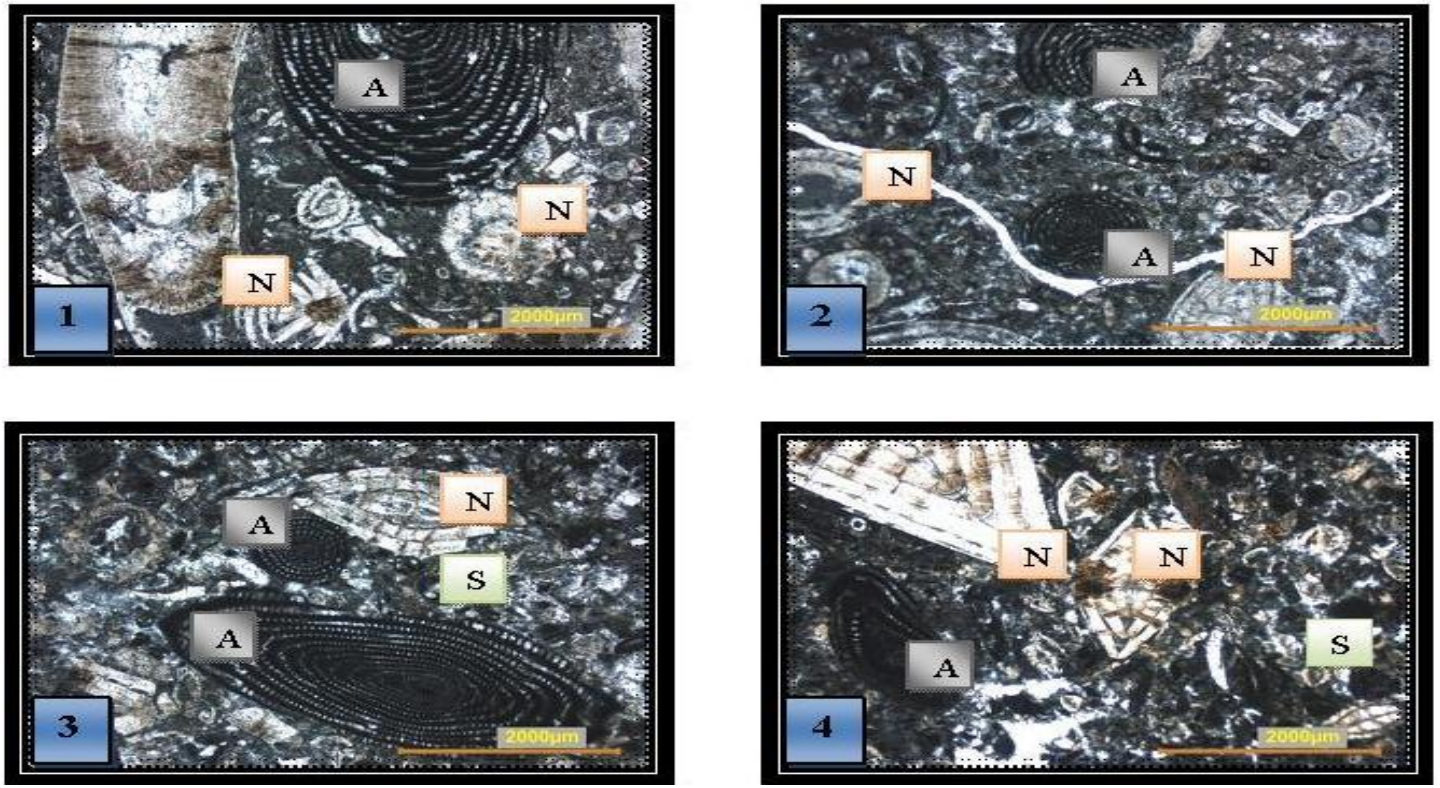

Figure 18. Photomicrographs of bioclastic, alveolinid, nummulitid packstone with abundant small and large benthic foraminifera (MF 3) (N: Nummulites sp., A: Alveolina s.l. S: small bethic foraminifera), (1: ÇBG 27, 2: ÇBG 28, 3: ÇBG 29, 4: ÇBG 30).

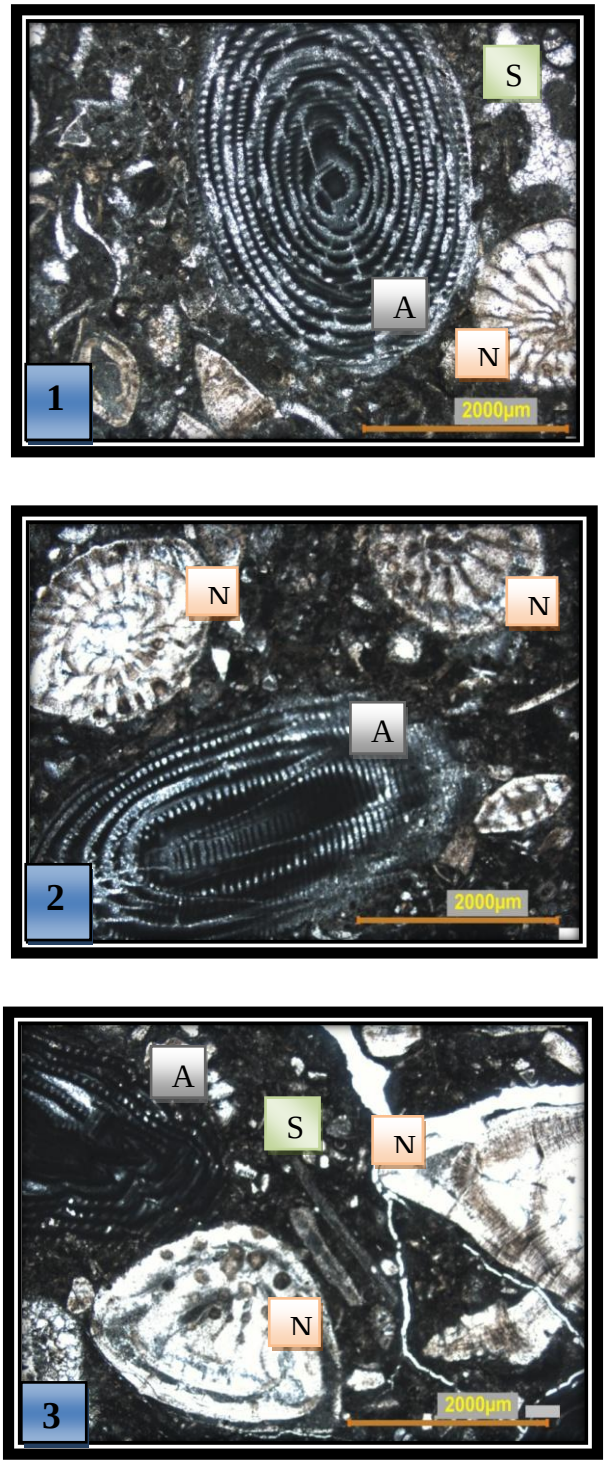

Figure 19. Photomicrographs of bioclastic, alveolinid, nummulitid wacke to packstone with abundant small and large benthic foraminifera (MF 4) (N: *Nummulites* s.p., A: *Alveolina* s.l. , S: small bethic foraminifera), (1: HBG 1, 2: HBG 2, 3: HBG 3).

3.3.5. Bioclastic, alveolinid, nummulitid wackestone with abundant small and large benthic foraminifera (MF 5)

This facies contains abundant small and large benthic foraminifera (Figure 20). The main components of this facies are *Nummulites* (20-35%), Alveolina s.l. (2-4%). Other components are *Assilina*, *Sphaerogypsina*, Miliolids, *Pygro*, *Spiroloculina* and *Rotalia*.

Inner ramp/ platform/ shelf settings are characterized by alveolinid-dominated microfacies types, middle ramp/ in platform/ shelf margin setting are dominated by nummulitids (Racey, 2001). Therefore this facies is deposited in between this setting.

3.3.6. Bioclastic, assilinid, nummulitid wacke to packstone with abundant small and large benthic foraminifera (MF 6)

The constituent of this microfacies are *Nummulites* (25-50%) and *Assilina* (9-24%) (Figure 21). *Alveolina* and *Orbitolites* are also present. Other abundant small and large benthic foraminifers are *Sphaerogypsina*, *Pygro*, *Triloculina*, *Spiroloculina*, *Lockartia*, *Rotalia* and miliolids. Textularids are very rare.

Alveolinids have been described from the Eocene of Oman, associated with *Nummulites* and *Assilina* as living on protected, inner ramp setting with sparsely vegetated sand substrates close to seagrass beds (Beavington-Penney *et al*., 2006). This facies corresponds to RMF 13 of Flügel (2004) which is defined as wackestone/packstone with larger foraminifera and distributed in inner ramp setting.

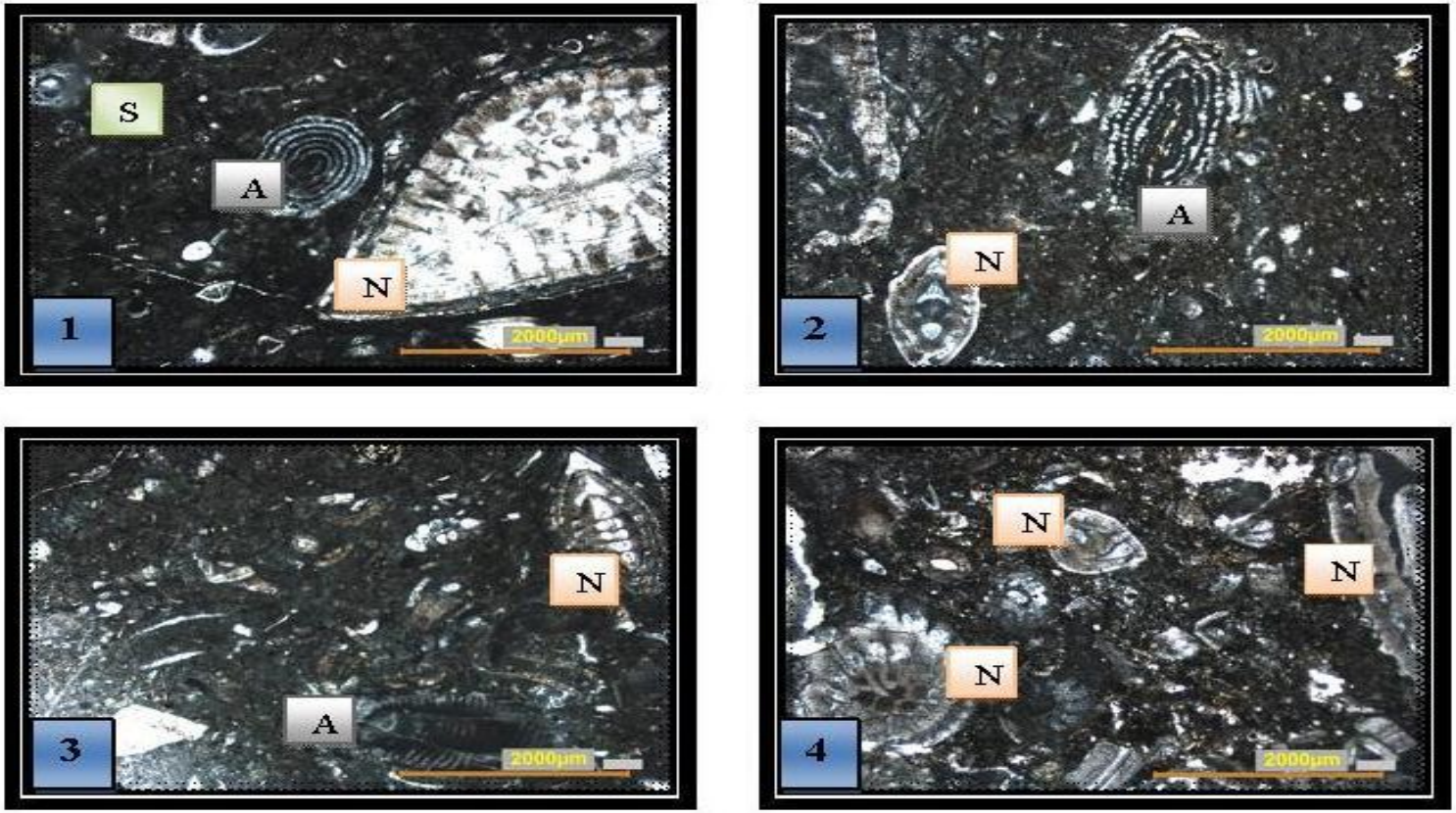

Figure 20. Photomicrographs of bioclastic, alveolinid, nummulitid wackestone with abundant small and large benthic foraminifera (MF 5) (N: *Nummulites* sp., A: *Alveolina* s.l., S: small bethic foraminifera), (1: HBG 5, 2: HBG 6, 3: HBG 12, 4: HBG 13).

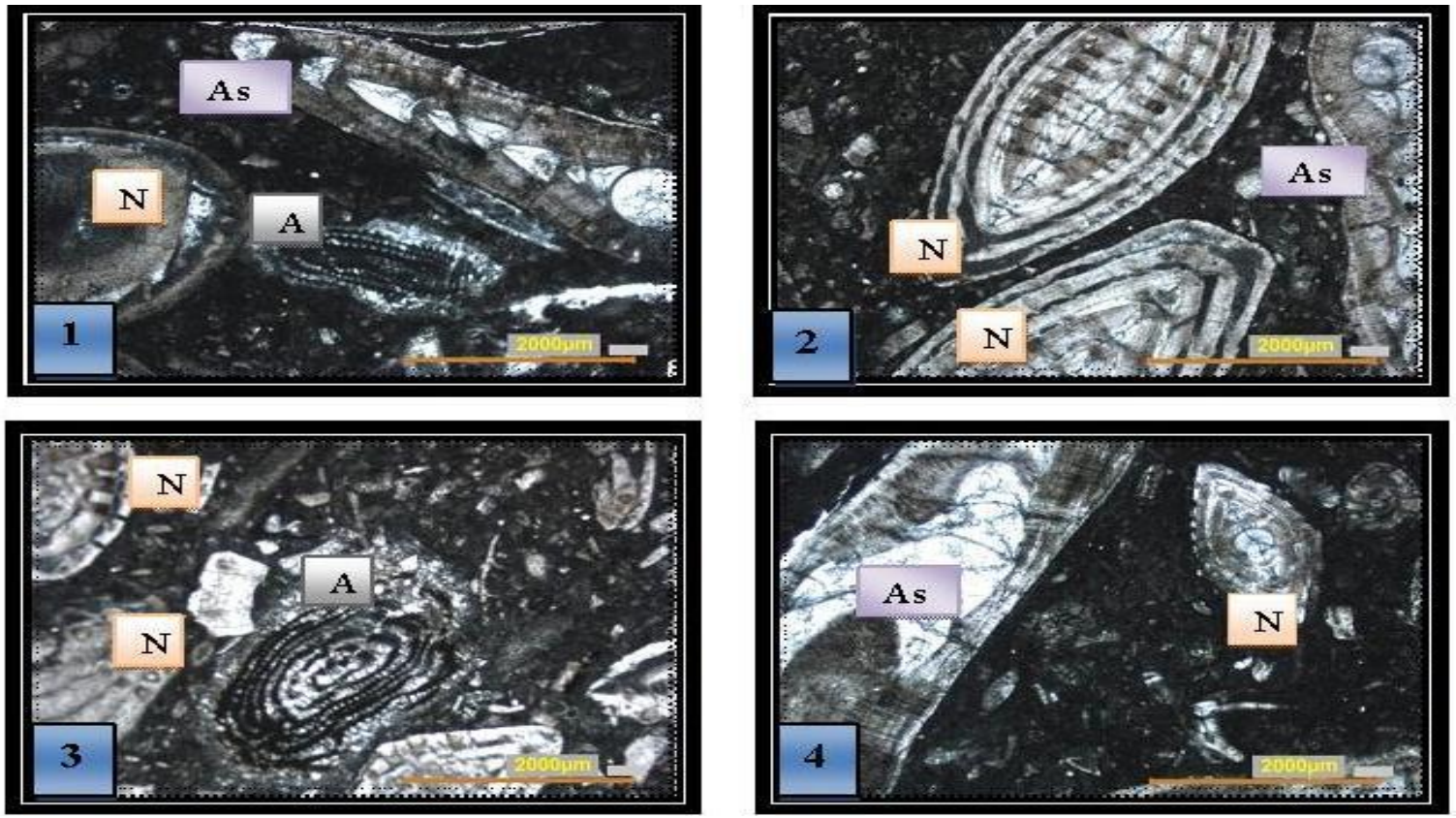

Figure 21. Photomicrographs of Bioclastic, assilinid, nummulitid wacke to packstone with abundant small and large benthic foraminifera (MF 6) (N: *Nummulites* sp., A: *Alveolina* s.l., As: *Assilina* sp., S: small bethic foraminifera), (1: HBG 7, 2: HBG 8, 3: HBG 9, 4: HBG 15).

3.3.7. Bioclastic, nummulitid packstone with abundant small and large benthic foraminifera (MF 7)

This microfacies is dominated by *Nummulites* (50-63%), and subordinate *Rotalia* (10-14%). Additional constituents are *Assilina* (1-3%), Miliolids (1-2%), *Pygro* (2-4%), *Spiroloculina* (1-2%), *Lockartia 1*-(2%) and other small and large benthic foraminifera (Figure 22). *Alveolina* s.l. is not present in this microfacies.

Various depositional models for *Nummulites* dominant facies have been proposed, and most of them described *Nummulites* accumulations as banks, bars or low-relief banks, sometimes related to palaeo highs. *Nummulites* accumulations or "banks" commonly occur in platform or shelf-margin settings and mid to outer ramp settings (Racey, 1988, 1995). This facies corresponds to SMF 10 of Flügel (2004) which is defined as bioclastic packestone/wackestone with worn skeletal grains.

3.3.8. Bioclastic, assilinid, nummulitid packstone (MF 8)

This type of microfacies is dominated by *Nummulites* and *Assilina*. The amounts of *Nummulites* and *Assilina* are very high, *Nummulites* (53% to 80%) and *Assilina* (13% to 40%) (Figure 21). The other component is bioclast. Dense packing of *Nummulites* and *Assilina* is characteristic feature of this microfacies.

Large, flat *Assilina* sp. has been interpreted as forms that lived in deep, oligophotic water (Racey, 1994; Luterbacher, 1998; Geel, 2000), and also in much shallower, open marine, high-energy settings (Ghose 1977; Gilham and Bristow 1998). Although the genus *Assilina* is now extinct, living nummulitids with similar large, flat tests (e.g. *Cycloclypeus carpenteri* and *Heterocyclina turberculata*) have been collected from water depths up to 150 m (Reiss and Hottinger, 1984; Hohenegger, 2000). This facies also corresponds to SMF 10

of Flügel (2004) which is defined as bioclastic packestone/wackestone with worn skeletal grains. But the difference of this microfacies from MF 7 is dense packing of *Nummulites* and *Assilina* and the absence of other small and larger benthic foraminmifera.

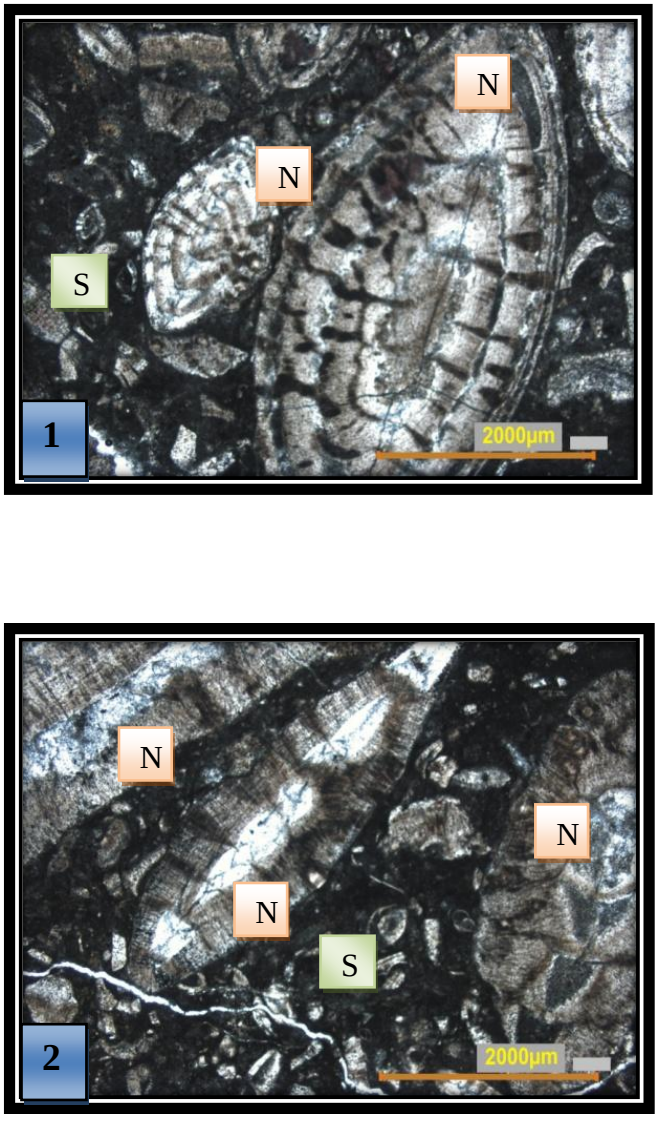

Figure 22. Photomicrographs of bioclastic, nummulitid packstone with abundant small and large benthic foraminifera (MF 7) (N: *Nummulites* sp., S: small bethic foraminifera), (1: HBG 4, 2: HBG 4).

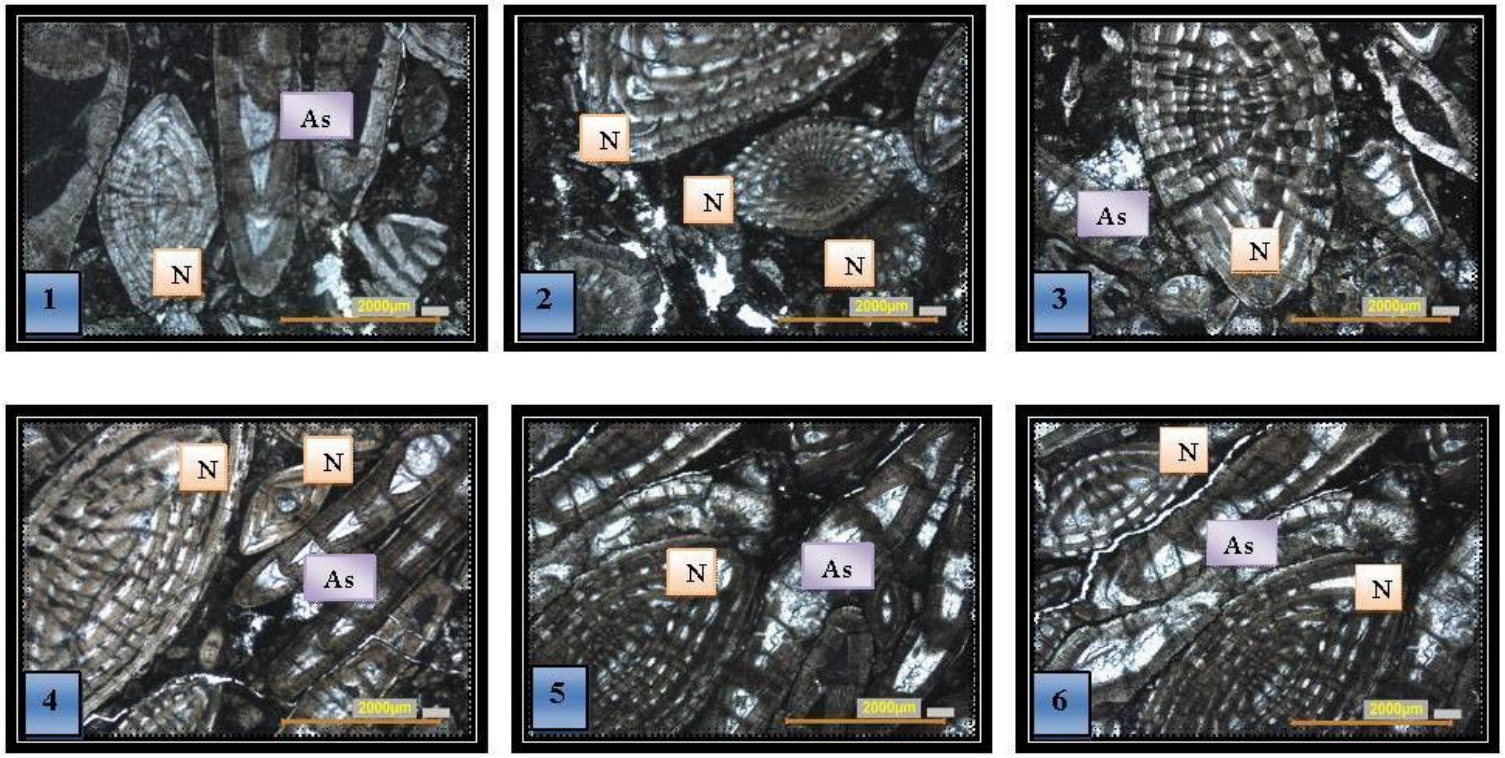

Figure 23. Photomicrographs of bioclastic, assilinid, nummulitid packstone (MF 8) (N: *Nummulites* sp., As: *Assilina* sp.) (1: HBG 16, 2: HBG 18, 3: HBG 20, 4: HBG 26, 5: HBG 30, 6: HBG 31).

3.3.9. Bioclastic, discocyclinid, nummulitid packstone (MF 9)

Bioclastic, discocyclinid, nummulitid packstone facies dominated by *Discocyclina* (10-24%) and *Nummulites* (40-60%). Other component are *Assilina* (10-20%) and *Operculina (4-20%)*. Calcareous red algae is not present in this microfacies (Figure 24).

The elongated *Assilina* and *Discocyclina* indicate the relatively deep water (50–80 m) on more open parts of the ramp (Racey, 1994).

3.3.10. Bioclastic, discocyclinid, nummulitid packstone with red algae (MF 10)

This microfacies is mainly composed of larger benthic foraminifera and calcareous red algae. Larger benthic foraminifera in this microfacies are characterized by *Nummulites* (50-70%), *Discocyclina* (10-25%), *Operculina* (2-20%), and *Assilina* (10-15%) (Figure 25).

Large *Nummulites* tend to be associated with large and flat *Assilina* and *Discocyclina* in “deeper” more outer platform/shelf/ramp settings (50-80 m water depth) and deeper “fore-bank” facies, dominated by perforate-walled foraminifera (assilinids, discocyclinids and operculinids) and calcareous red algae (Racey, 2001).

This type of microfacies corresponds to the SMF 18 of Flügel (2004), which is defined as packstone with abundant foraminifera and algae and distributed in open marine setting.

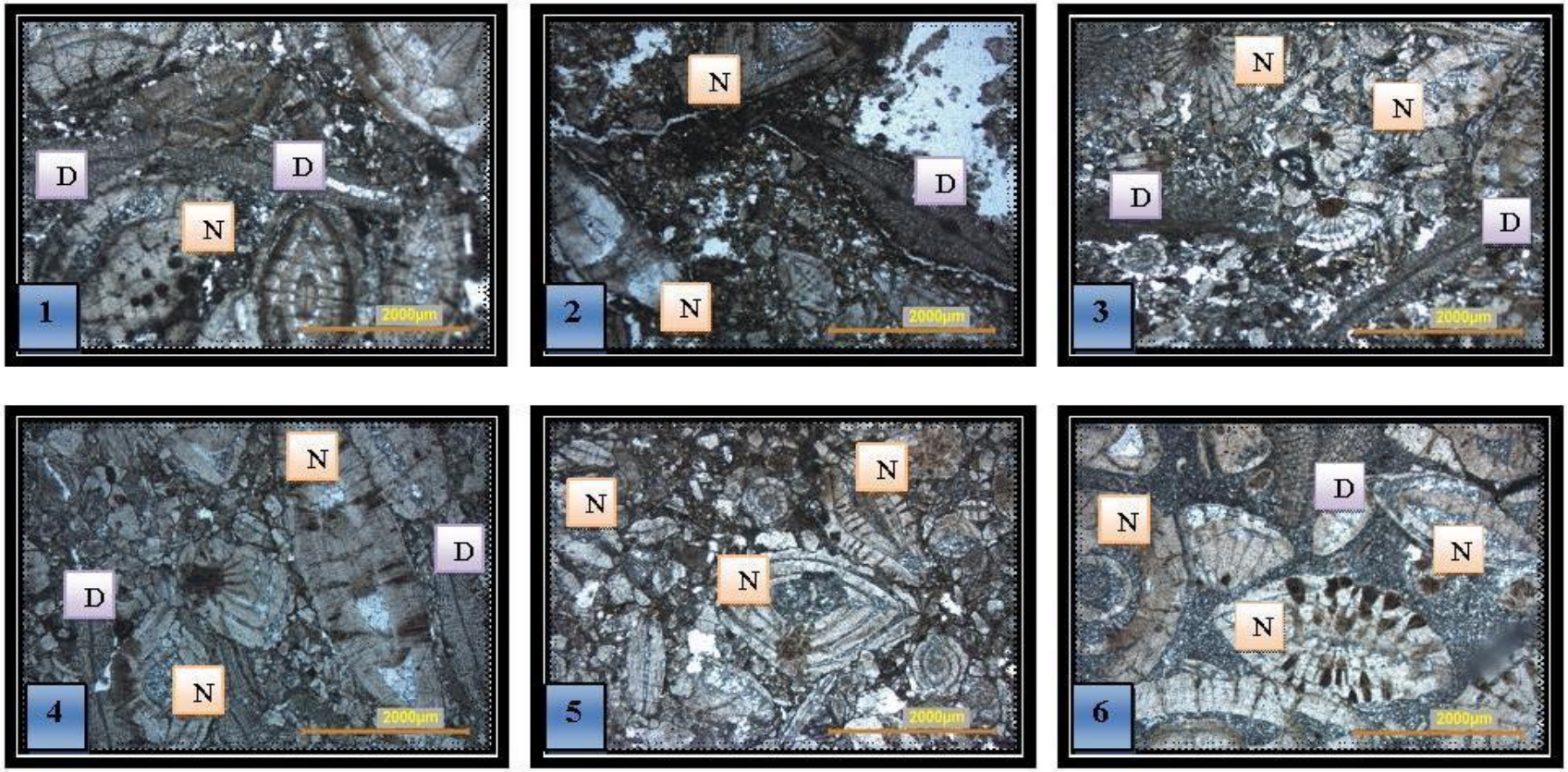

Figure 24. Photomicrographs of bioclastic, discocyclinid, nummulitid packstone (MF 9) (N: *Nummulites*, D: *Discocyclina)*, (1: ÇBG 6, 2: ÇBG 11, 3:ÇBG 14, 4: ÇBG 16, 5: ÇBG 17, 6: ÇBG 24).

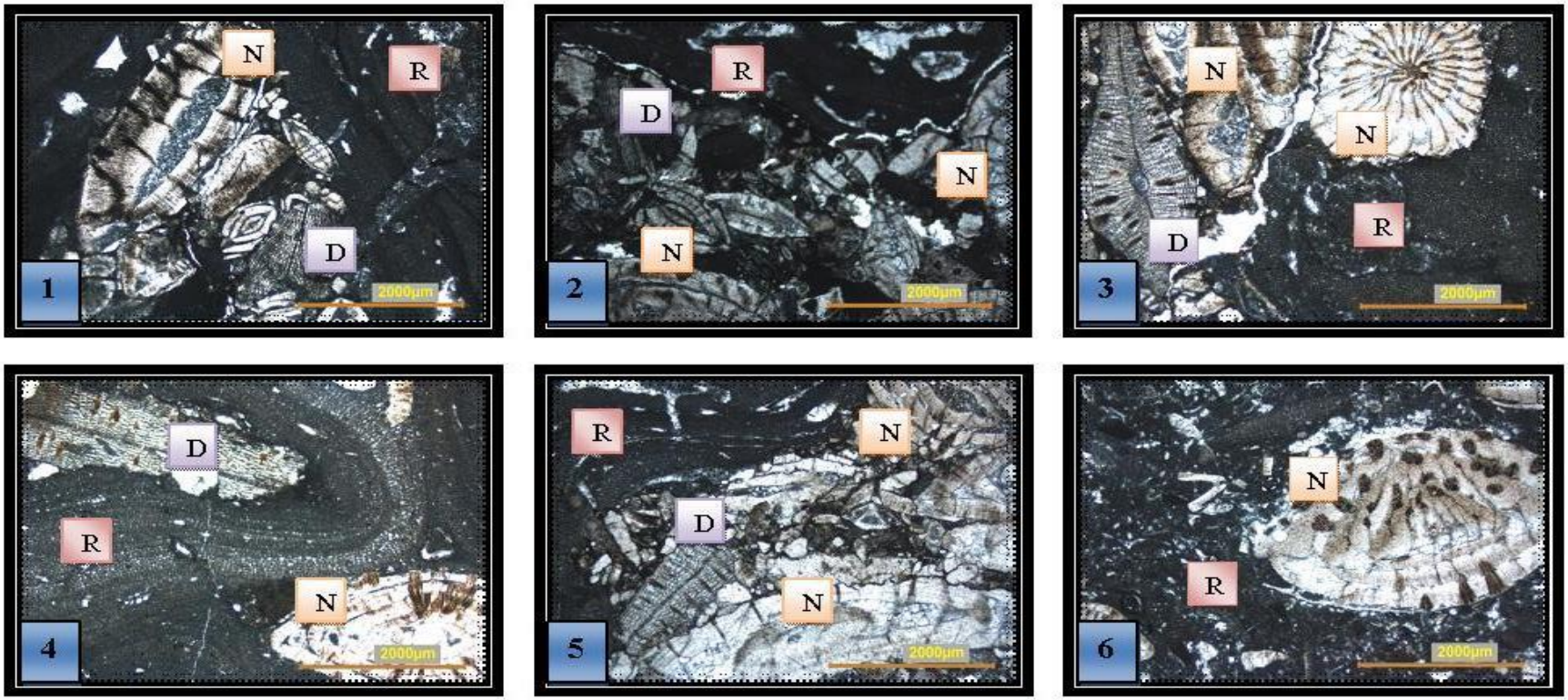

Figure 25. Photomicrographs of bioclastic, discocyclinid, nummulitid packstone with red algae (MF10) (N: *Nummulites*, D: *Discocyclina*, R: Red algae), (1: ÇBG 1, 2: ÇBG 2, 3: ÇBG 8, 4: ÇBG 13, 5: ÇBG 9, 6: ÇBG 19).

3.4. Depositional Environment

During the Early Cenozoic, following the demise of the end Cretaceous rudist-coral assemblage, nummulitid (*Nummulites*, *Assilina* and *Operculina*), orthophragminid (*Discocyclina*) and alveolinid (*Alveolina*) larger benthic foraminifera (LBF) thrived on shallow, oligotrophic, Circum-Tethyan carbonate platforms (Buxton and Pedley 1989). LBF were the most common constituents of Tertiary shallow water carbonates. Especially Eocene LBF were used extensively as a tool for reconstructing paleoenvironments due to their great diversity and abundance in the photic zone of tropical and subtropical settings (Hottinger 1997,1998).

Racey (1988, 1995) studied Middle Eocene *Nummulites* accumulations in Oman, and identified a low-amplitude *Nummulites* bank complex in a mid-ramp setting. Buxton and Pedley (1989) concluded that *Nummulites* deposits in the Tethyan Tertiary were generally associated with ramps, and interpreted them to have been deposited in shallow-water, shoaling, inner ramp environments analogous to the coralgal patch reef belt.

Racey (2001) summarized the complex relationships among LBF typical of Early Cenozoic carbonate platforms, concluding that *Nummulites* occupied a broad range of open-marine environments on both ramps and shelves, and was generally absent from more restricted waters. Large flat *Nummulites* tend to be associated with similarly shaped *Assilina* and *Discocyclina* in relatively deep-water environments, whilst smaller, lenticular *Nummulites* occur in shallower, inner ramp/shelf settings, often coexisting with *Alveolina*; ‘banks’ of medium- to large-sized, lenticular- to globular-shaped *Nummulites* tend to occupy intermediate environments.

From the literature it is difficult to formulate a general model for the distribution of *Nummulites* since different authors tend to use different terminologies for describing such accumulations (reefs, banks, shoals) or else they emphasise different aspects of *Nummulites* morphology. In general large flat *Nummulites* tend to be associated with large flat *Assilina* and *Discocyclina*

in “deeper” more outer platform/shelf/ramp settings (50-80 m water depth) whereas small and medium sized lenticular *Nummulites* are more often associated with *Alveolina* and occur in shallower inner platform/shelf/ramp settings. “Banks” of more robust medium to large sized lenticular to globular shaped *Nummulites* tend to occupy a position intermediate between these two extremes.

Based on the detailed microfacies analysis, previously published standard microfacies belts of Wilson (1975) and Flügel (2004) and biofacies distribution of the Early-Middle Eocene foraminifera (Sartorio and Verturini, 1988) (Figure 26) which indicates the idealized foraminiferal environmental distribution in early-middle Eocene by classifying foraminifera into 5 groups: *Coskinolina* and miliolids distributed in the inner shelf platform, *Alveolina* distributed in the inner shelf platform near edge *Nummulites* distributed in the edge, Planktonic and benthic foraminifera distributed in the slope and planktonic foraminifera distributed in the basin, summary of the key faunal associations on idealized carbonate ramps during the Eocene (after Racey 1994) (Figure 27) which summarizes foraminifera distribution during the Eocene on idealized carbonate ramp from shallowest to deepest part of the ramp such as Textularids, miliolids and orbitolites distributed in the shallowest part and *Discocyclina* and *Assilina* distributed in the deepest part of the ramp and *Nummulites*, *Alveolina* and *Assilina* distributed in between, depositional model for the platform carbonates of the Tale-Zang Formation at the type section and Kialo section, Zagros Basin, SW Iran (Figure 28) that also assert an depositional environmental model for Eocene platform carbonates by using microfacies (*Assilina* wackestone, *Nummulites Alveolina* packstone…) and foraminifera (*Assilina*, *Orbitolites*, *Alveolina*…), and the basis of the distribution of the microfacies and vertical facies relationships a composite depositional model is suggested (Figure 29).

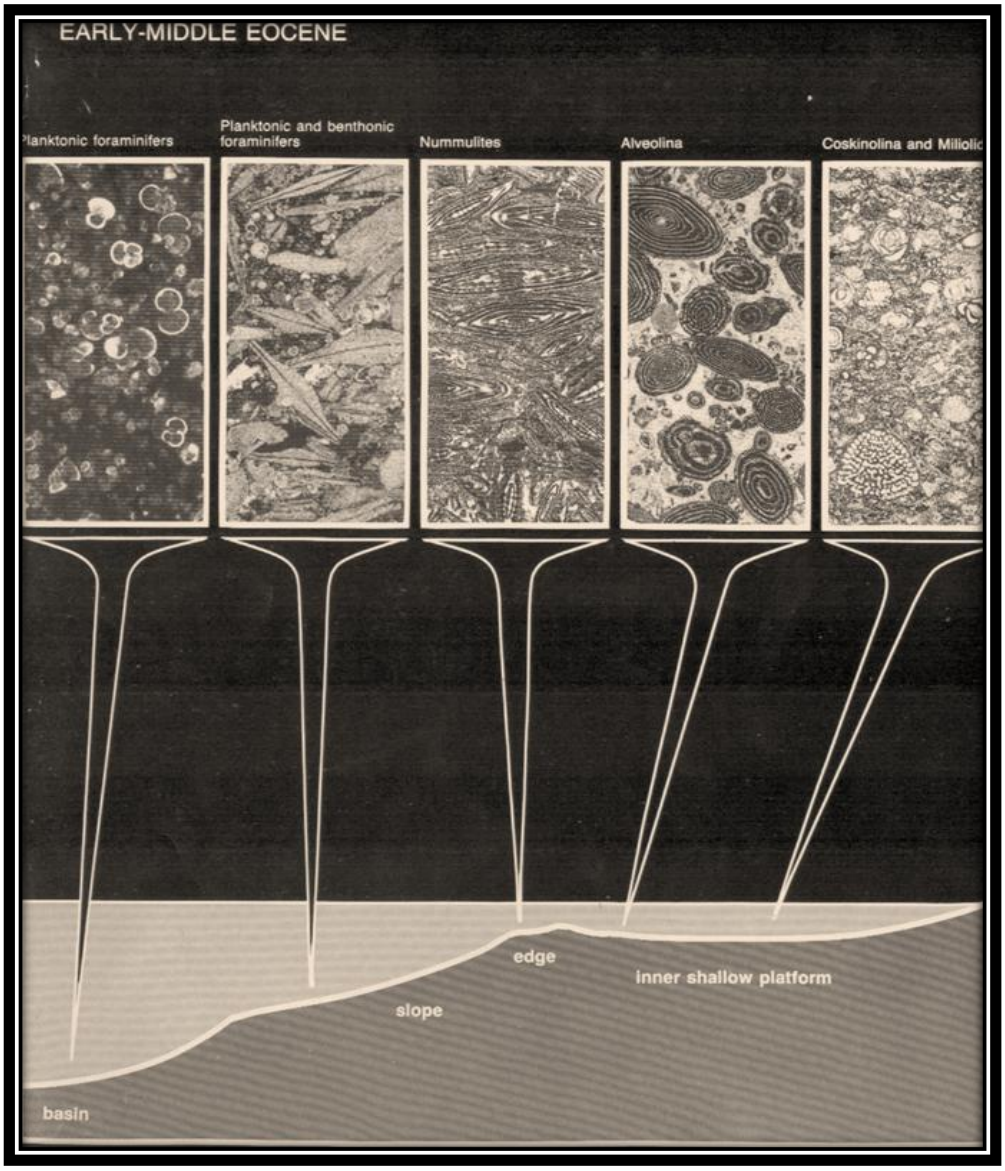

Figure 26. Microfacies distribution of the Early-Middle Eocene foraminifera (Sartorio and Verturini, 1988).

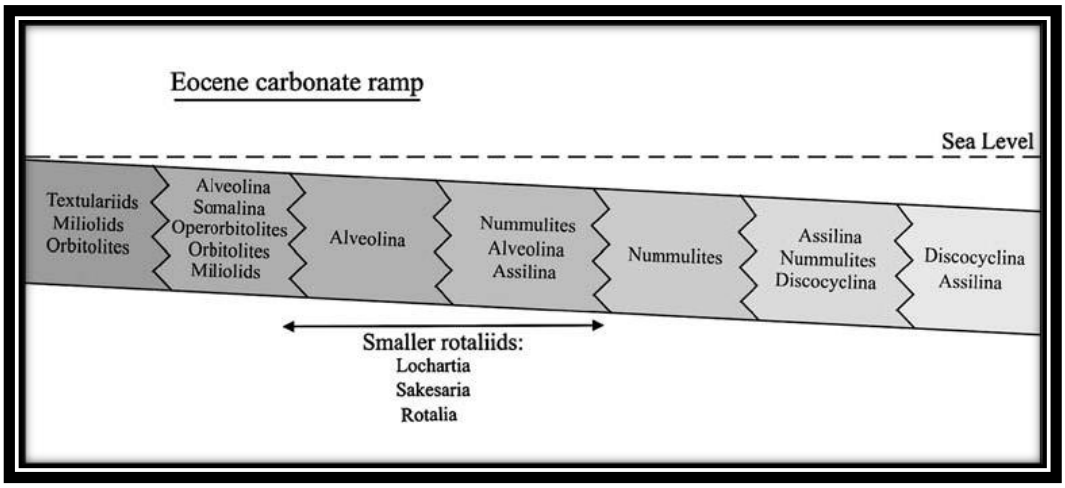

Figure. 27 Summary of the key faunal associations on idealized carbonate ramps during the Eocene (not to scale, after Racey, 1994). Taxa listed in order of decreasing abundance.

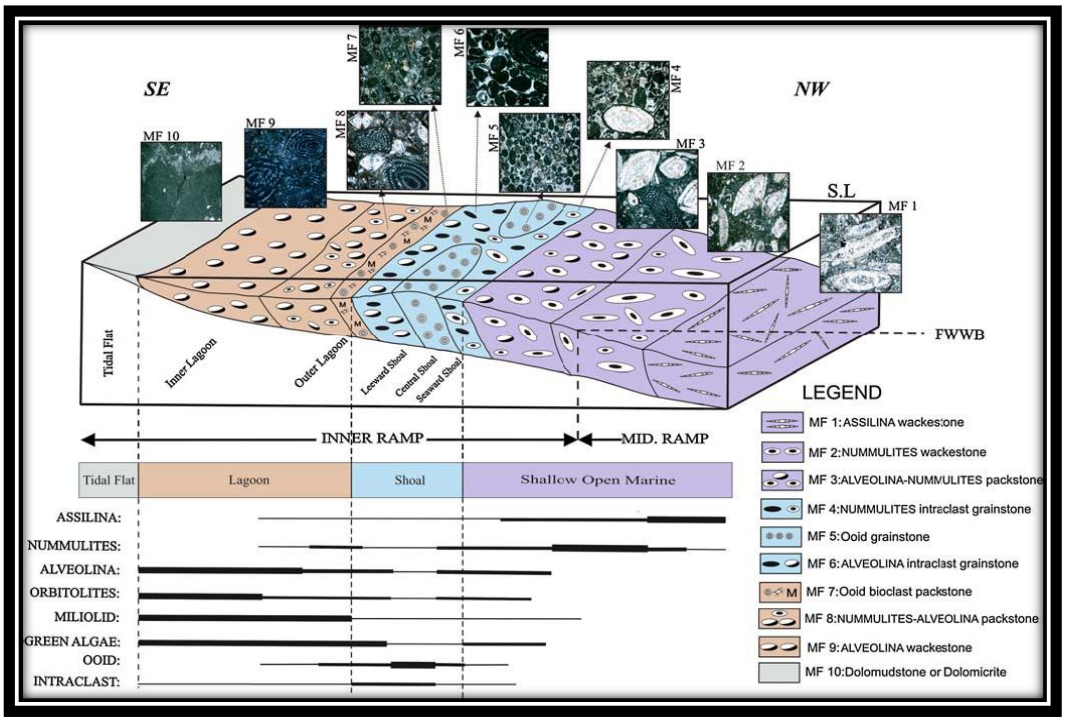

Figure 28. Depositional model for the platform carbonates of the Tale-Zang Formation at the type section and Kialo section, Zagros Basin, SW Iran (Adabi *et al.*, 2008).

In the composite depositional model, three major facies associations were distinguished, from deepest to shallowest, as: shallow open marine, shoal and lagoon, by distribution of *Discocyclina*, *Assilina*, *Nummulites*, *Alveolina* and other benthic foraminifera and microfacies describtions mainly based on these foraminifera. These three environments are represented by ten microfacies. The shallow open marine part is reperesented by bioclastic, discocyclinid, nummulitid packstone with red algae microfacies (MF 10), bioclastic, discocyclinid, nummulitid packstone microfacies (MF 9) and bioclastic, assilinid, nummulitid packstone (MF 8). The shoal part is associated with bioclastic nummulitid packstone with abundant small and large benthic foraminifera (MF 7), bioclastic, assilinid, nummulitid wacke to packstone with abundant small and large benthic foraminifera (MF 6), bioclastic, alveolinid, nummulitid wackestone with abundant small and large benthic foraminifera (MF 5) bioclastic, alveolinid, nummulitid wacke to packstone with abundant small and large benthic foraminifera (MF 4), and the lagoon part is characterized with and bioclastic, alveolinid, nummulitid packstone with abundant small and large benthic foraminifera (MF 3), benthic foraminiferal wackestone (MF 2) and mudstone to wackestone with small benthic foraminifera (MF 1).

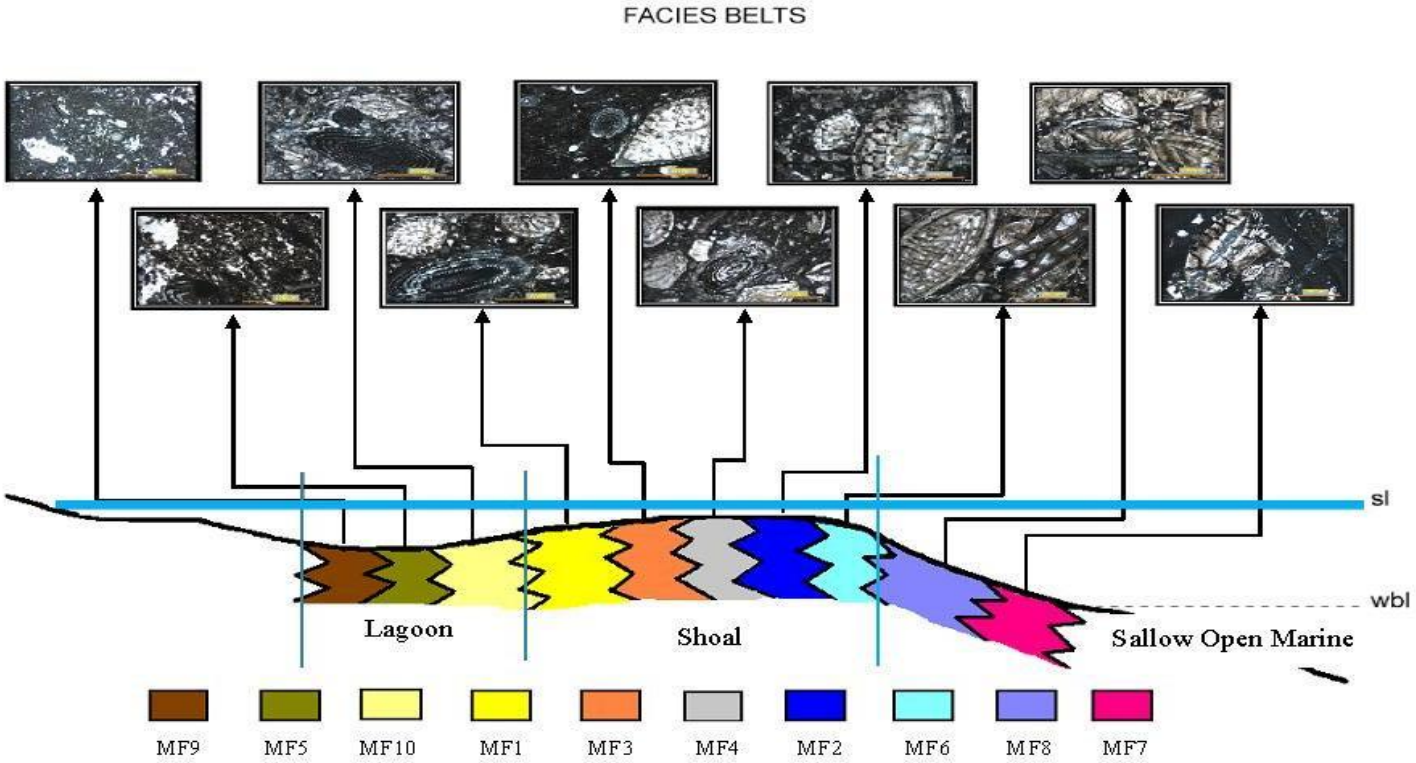

Figure 29. Composite depositional model of the studied area.

3.5. Types of meter-scale cycles

In this study meter-scale cycles were defined firstly based on detailed vertical lithofacies association which were carried out and documented in the field and secondly based on the microfacies analyses which were identified strictly based on the biofacies. Result of this study eleven cycles were recognized in the measured sections. Section 1 is represented by five cycles (Figure 30) and section 2 (Figure 31) is represented by six cycles. Lithostratigraphic and microfacies details of these cycles are given in the following sections.

3.5.1. Meter-scale cycles in Section 1

Cycle 1

Cycle 1 of the first cycle in the section 1 (Figure 30) and measures 5,4 m. This cycle includes the samples number ÇBG 1, ÇBG 2 and ÇBG 3 and is represented by limestones with *Nummulites* and *Discocyclina*. This cycle consists of bioclastic, discocyclinid, nummulitid packstone with red algae microfacies (MF 10) (Figure 32). It is composed of the pile of shallow open marine facies.

Cycle 2

Cycle 2 is the second cycle of the section 1 (Figure 30) and measures 9,4 m. It covers the interval with sample number ÇBG 4 and ÇBG 9. Cycle 2 begins with clayey limestones with *Nummulites* and *Discocyclina* in the lower part and continues with limestones with *Nummulites* and *Discocyclina* in the middle and upper parts. This cycle is composed of bioclastic, discocyclinid, nummulitid packstone with red algae microfacies (MF 10) at the bottom. Bioclastic, discocyclinid, nummulitid packstone microfacies (MF 9) follow the bottom facies and the cycle is capped by bioclastic, discocyclinid, nummulitid packstone with red algae microfacies (MF 10) (Figure 33). This cycle also represents a shallow open marine facies variation.

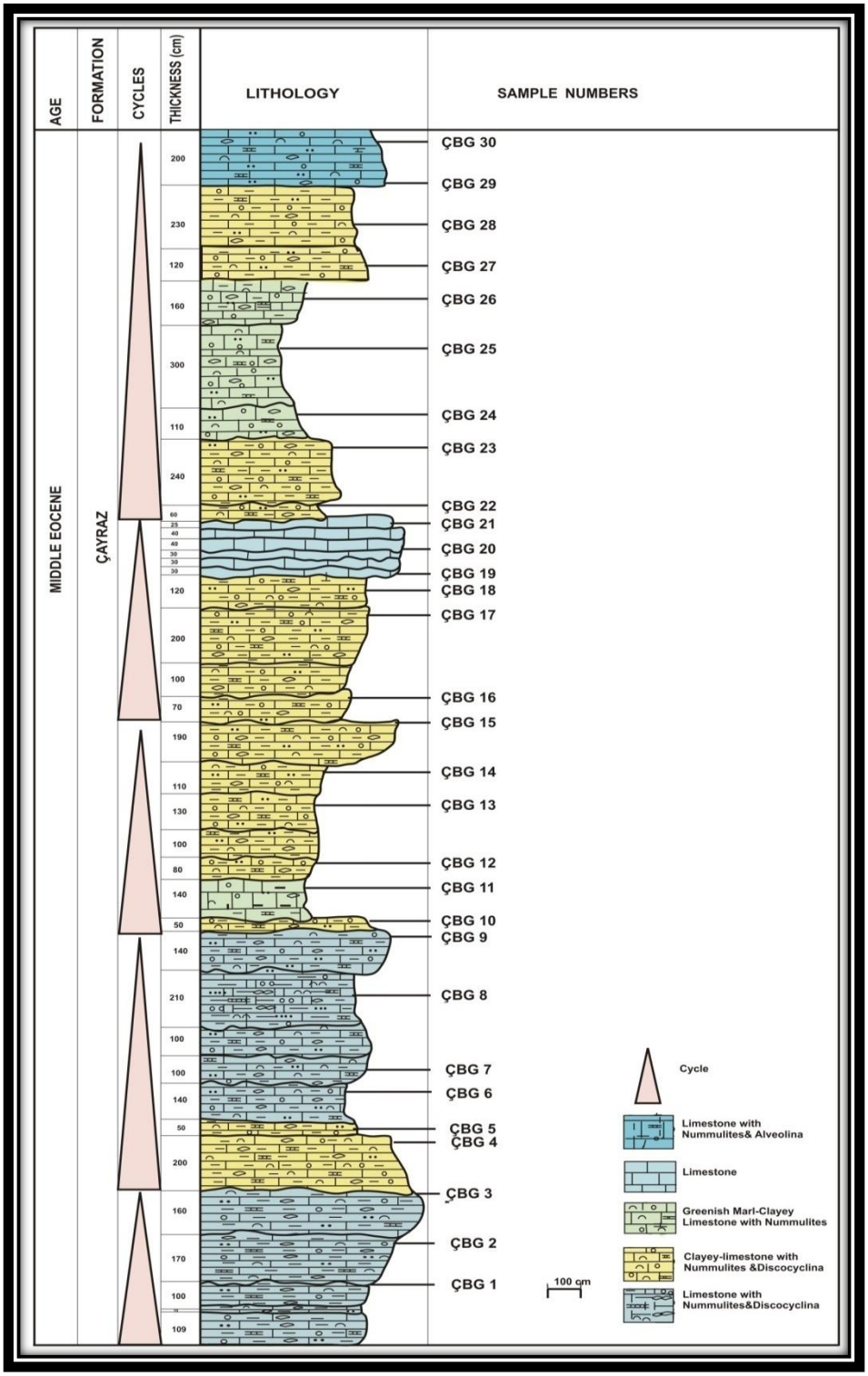

Figure 30. Meter scale cycles in Section 1.

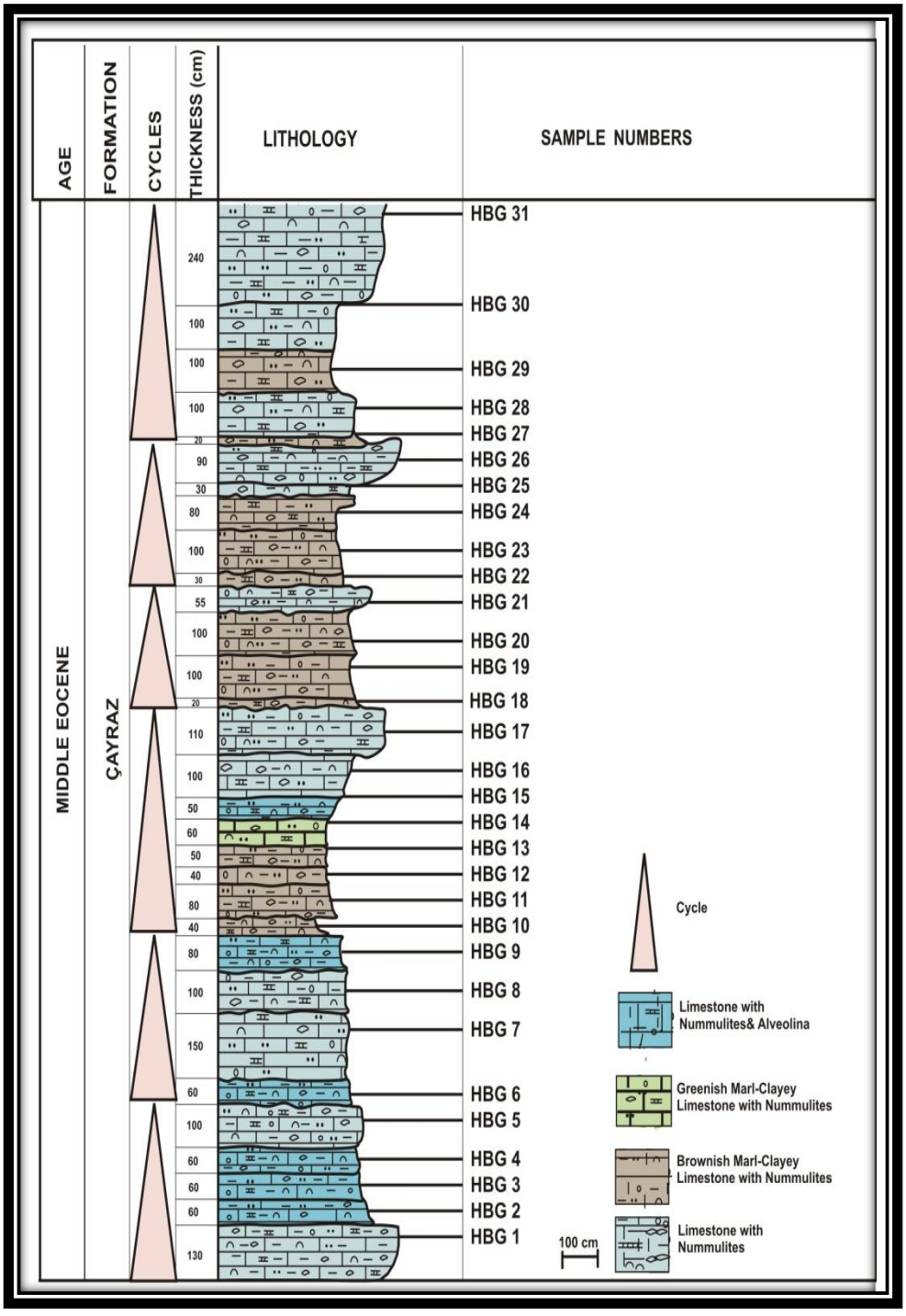

Figure 31. Meter scale cycles in Section 2.

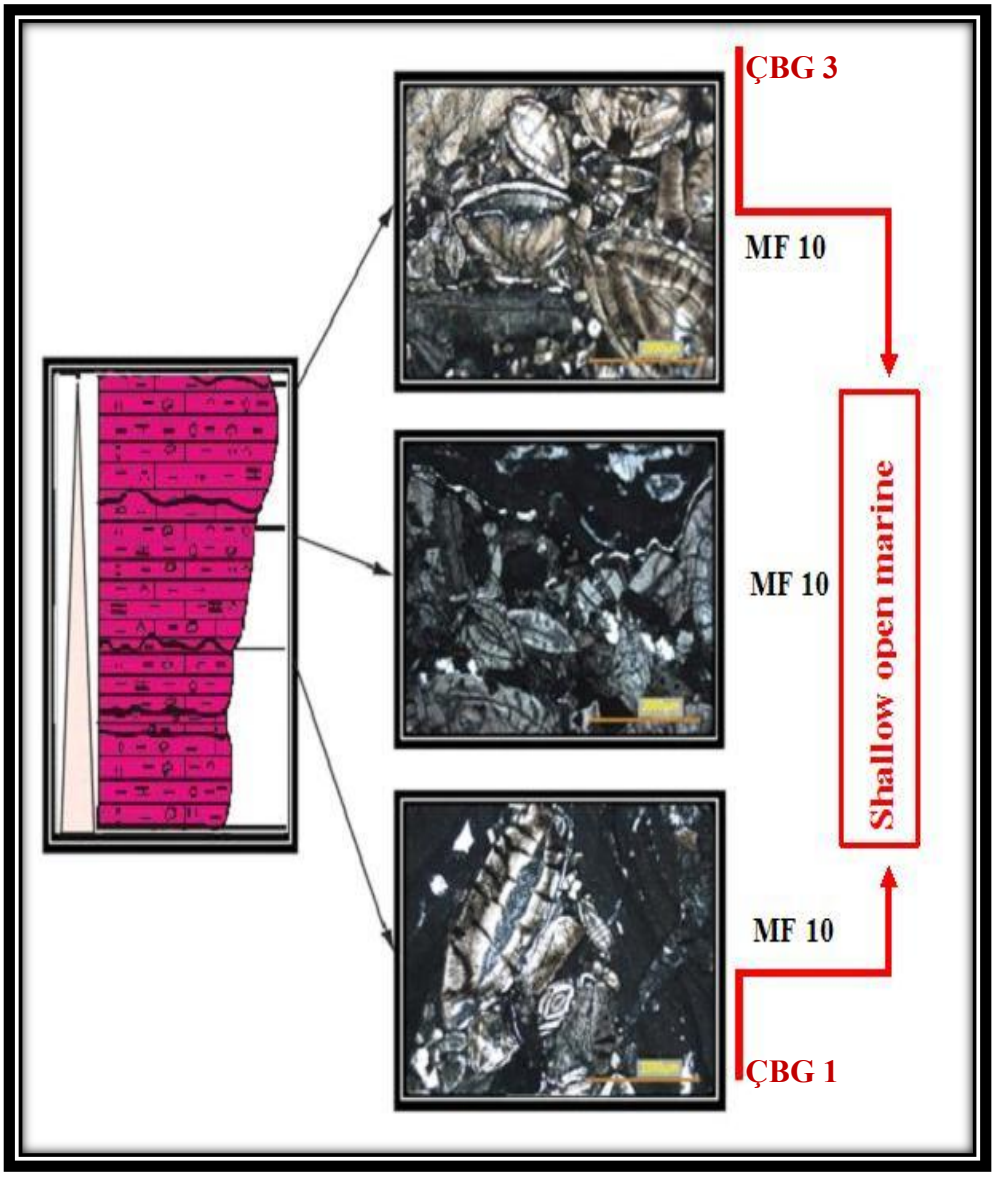

Figure 32. Cycle 1 of the Section 1 and photomicrographs of microfacies deposited within this cycle.

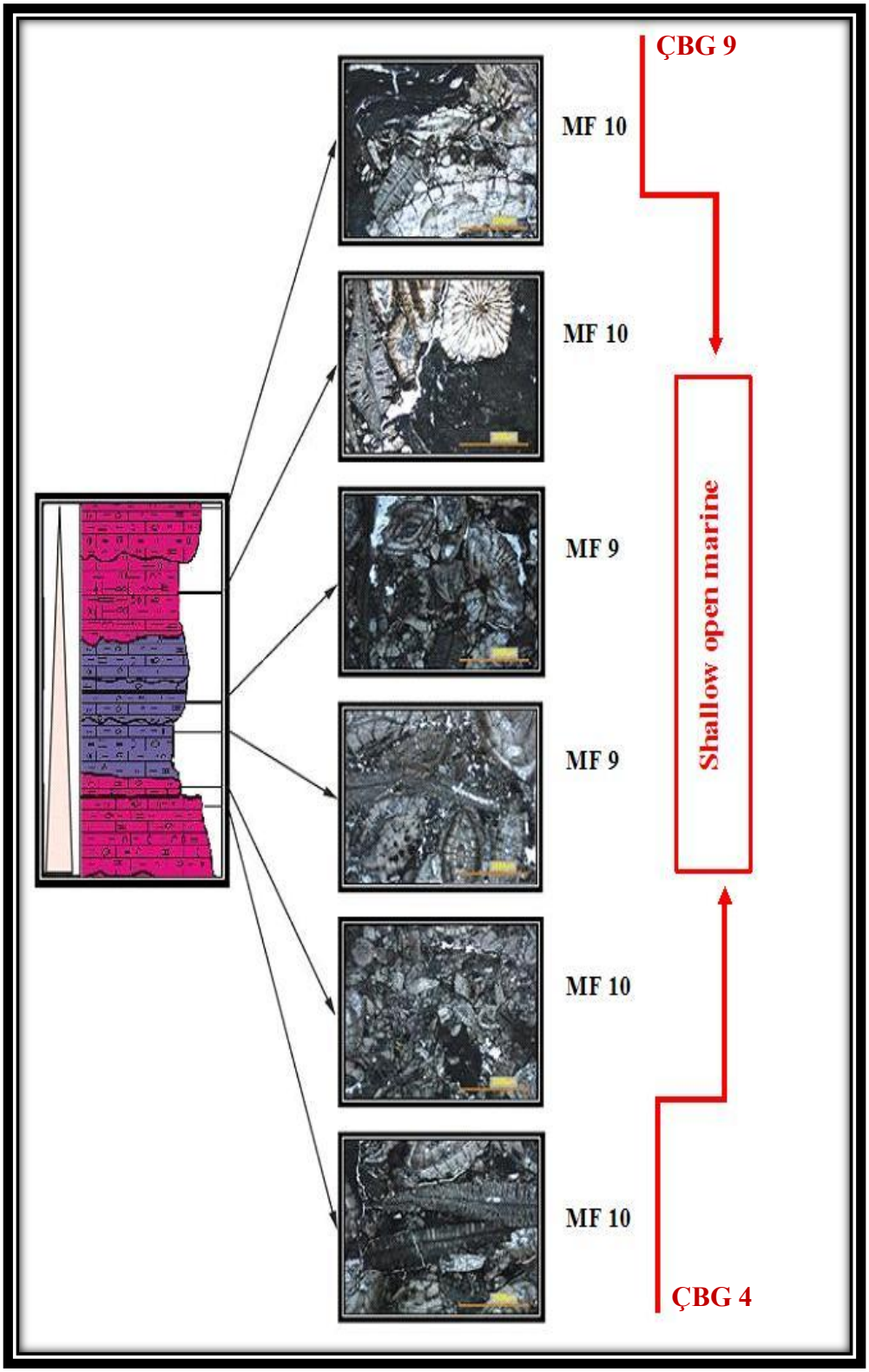

Figure 33. Cycle 2 of the Section 1 and photomicrographs of microfacies deposited within this cycle.

Cycle 3

The third cycle of the measured section 1 (Figure 30) is cycle the 3 and measures 8 m. It is between the samples number ÇBG 10 and ÇBG 15 and represented by clayey limestones with *Nummulites* and *Discocyclina* and greenish marl-clayey limestones with *Nummulites.* The cycle begins with the bioclastic, discocyclinid, nummulitid packstone with red algae microfacies (MF 10) and continues with the bioclastic, discocyclinid, nummulitid packstone microfacies (MF 9). The bioclastic, discocyclinid, nummulitid packstone with red algae microfacies (MF 10) follow these facies and the cycle finally finishes with bioclastic, discocyclinid, nummulitid packstone microfacies (MF 9) (Figure 34). Characterized totally by the variation of shallow open marine facies this cycle also represents one of the open marine cycle of the section 1.

Cycle 4

Cycle 4 is the fourth cycle of the section 1 (Figure 30) and includes the interval with samples ÇBG 16 and ÇBG 21. The thickness of the cycle is 6,85 m. It starts and continues with clayey limestones with *Nummulites* and *Discocyclina* and finishes with a limestone which contains few fossils. Cycle 4 is represented by the clayey limestone with *Nummulites* and *Discocyclina* (MF 9) at the bottom, the bioclastic, discocyclinid, nummulitid packstone with red algae (MF 10) in the middle and the mudstone to wackestone with small benthic foraminifera (MF 1) at the top (Figure 35). This cycle shows a drastic return from shallow open marine conditions to lagoonal depositional conditions. This change may be explained by the relative sea level fall at that time.

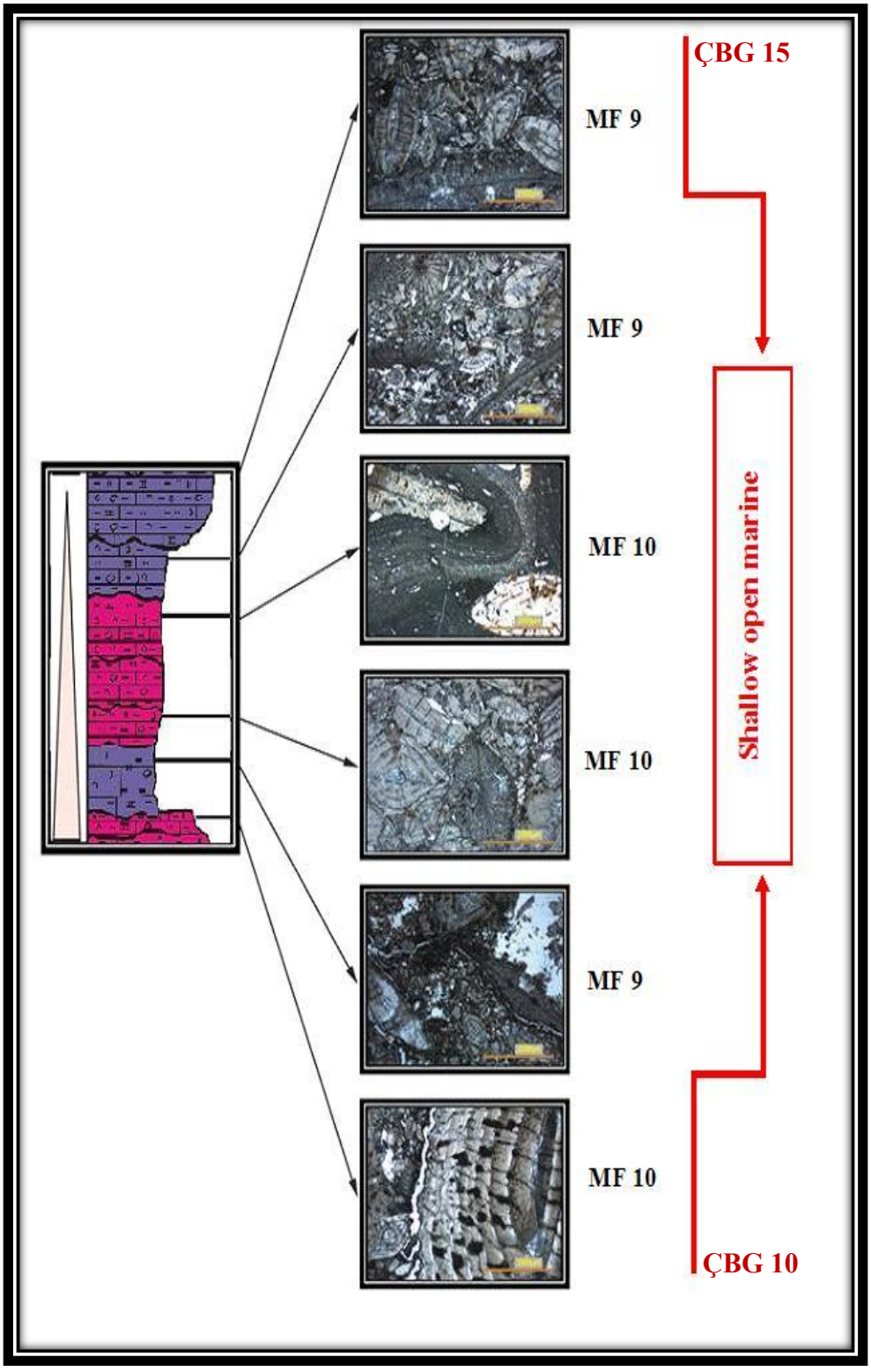

Figure 34. Cycle 3 of the Section 1 and photomicrographs of microfacies deposited within this cycle.

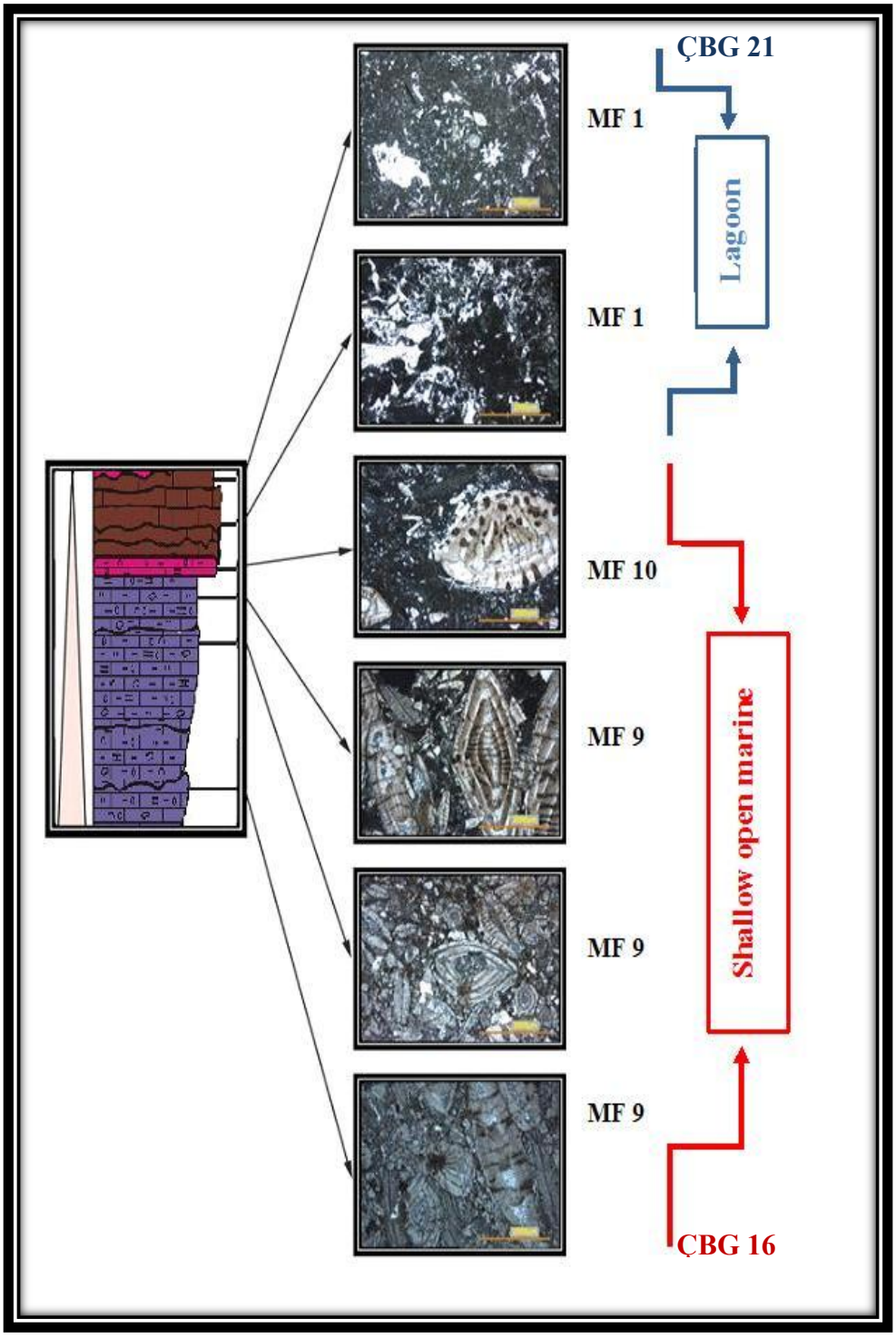

Figure 35. Cycle 4 of the Section 1 and photomicrographs of microfacies deposited within this cycle.

Cycle 5

The last cycle of the measured section 1 (Figure 31) is the cycle 5. It is from the sample number ÇBG 22 to ÇBG 30 and is 12,6 m thick. Cycle 5 is composed of clayey limestones with *Nummulites* and *Discocyclina* at the bottom, greenish marl-clayey limestones with *Nummulites* and clayey limestones with *Nummulites* and *Discocyclina* in the middle and limestones with *Nummulites* and *Alveolina* at the top. The cycle begins with the bioclastic, discocyclinid, nummulitid packstone with red algae microfacies (MF 10) and continues with the clayey limestone with *Nummulites* and *Discocyclina* microfacies (MF 9). The cycle is capped by the bioclastic, alveolinid, nummulitid packstone with abundant small and large benthic foraminifera microfacies (MF 3) (Figure 36). This cycle also indicates a drastic return from shallow open marine conditions to lagoonal depositional conditions like cycle 4.

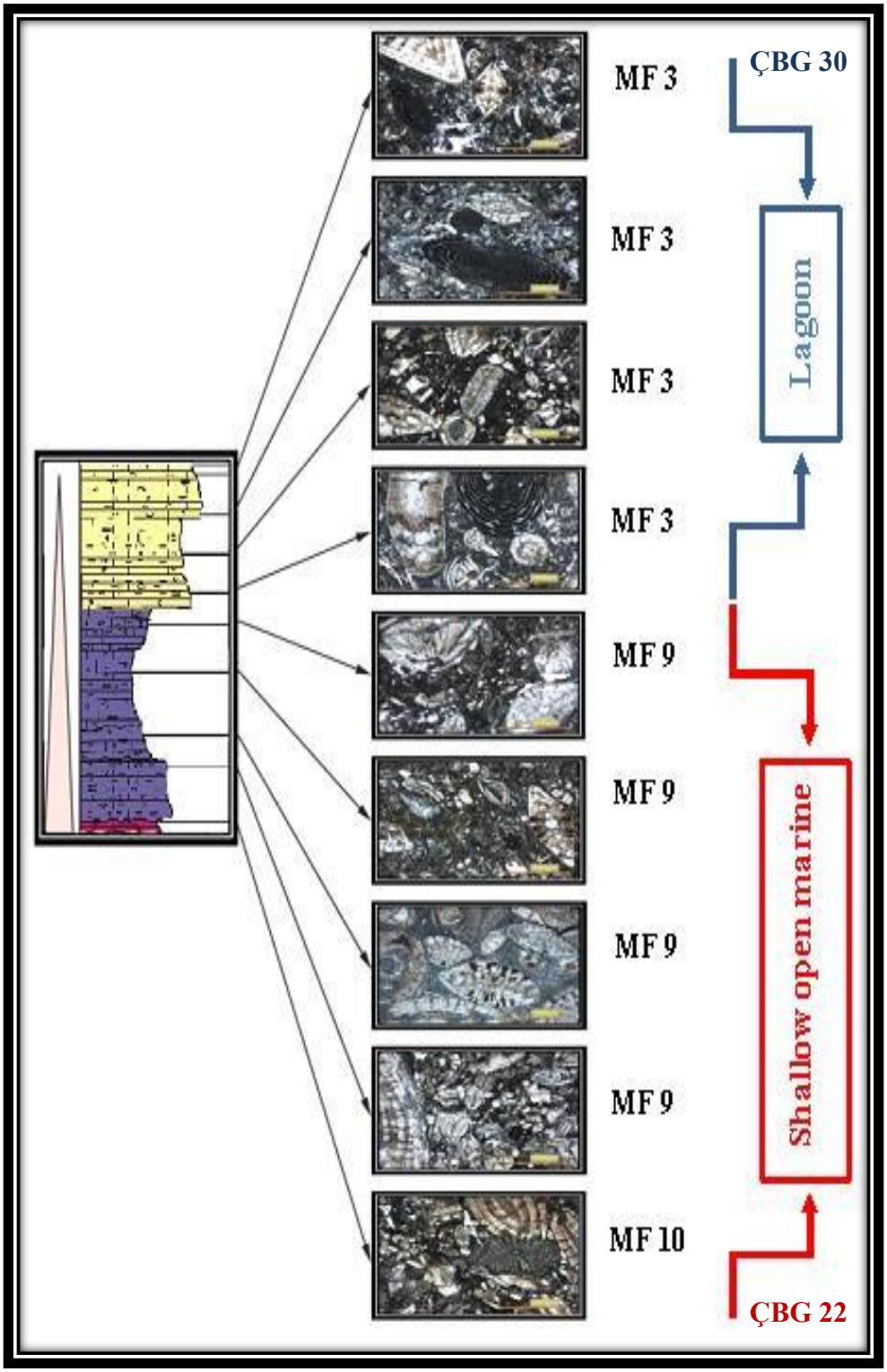

Figure 36. Cycle 5 of the Section 1 and photomicrographs of microfacies deposited within this cycle.

5.2. Meter scale cycles in Section 2

Cycle 1

Cycle 1 is the first cycle of the measured section 2 (Figure 31) and covers the interval from the sample number HBG 1 to the sample number HBG 5. Total thickness of the cycle is 4,1 m. The succession is characterized by limestones with *Nummulites* and limestones with *Nummulites* and *Alveolina*. This cycle begins with the bioclastic, alveolinid, nummulitid wacke to packstone with abundant small and large benthic foraminifera microfacies (MF 4); grades into the bioclastic nummulitid packstone with abundant small and large benthic foraminifera microfacies (MF 7) and ends with the bioclastic, alveolinid, nummulitid wackestone with abundant small and large benthic foraminifera microfacies (MF 5) (Figure 37). According to our composit deposional model (Figure 29) this cycle begins with lagoonal deposits after a flooding episode and shoals upward into the shoal facies.

Cycle 2

Cycle 2 is the second cycle of the measured section 2 (Figure 31) and it starts with the sample number HBG 6 and finishes with the sample number HBG 9. Total thickness of this cycle is 3,9 m. This cycle like cycle 1 is represented by limestones with *Nummulites* and limestones with *Nummulites* and *Alveolina*. It begins with bioclastic, alveolinid, nummulitid wackestone with abundant small and large benthic foraminifera microfacies (MF 5) and is followed and capped by bioclastic, assilinid, nummulitid wacke to packstone with abundant small and large benthic foraminifera microfacies (MF 6) (Figure 38). Apperantly this cycle is characterized by the oscillations with the shoal environment.

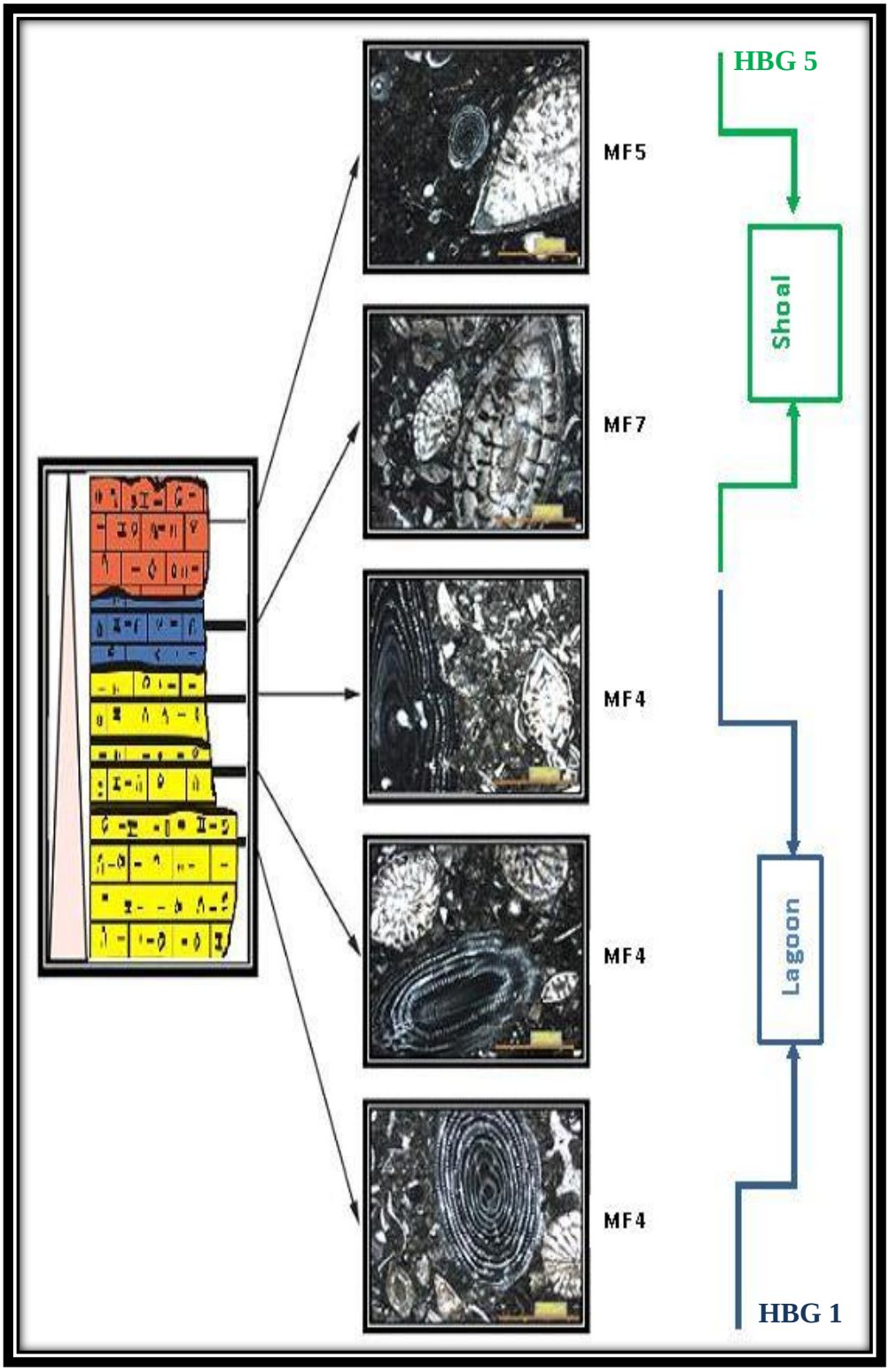

Figure 37. Cycle 1 of the Section 2 and photomicrographs of microfacies deposited within this cycle.

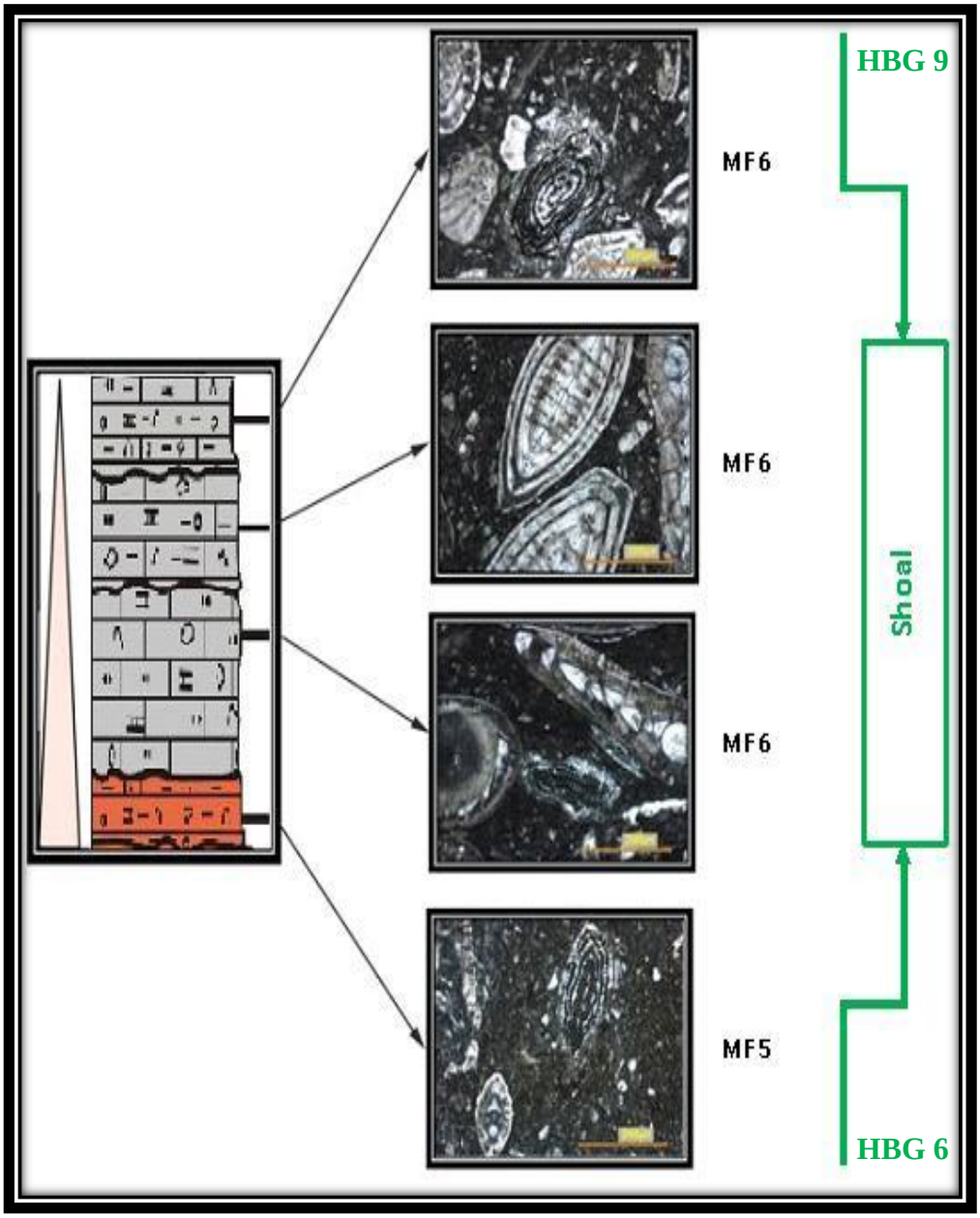

Figure 38. Cycle 2 of the Section 2 and photomicrographs of microfacies deposited within this cycle.

Cycle 3

Cycle 3 is the third cycle of the measured section 2 (Figure 31) and it covers the interval from the sample number HBG 10 to HBG17. This cycle is 5,3 m thick. It is defined in the field with brownish marl- clayey limestones at its base, grading upwards into greenish marl-clayey limestones and limestones with *Nummulites* and *Alveolina*. The succession is capped by limestones with *Nummulites*. The microfacies descriptions indicate a three fold subdivision in depositional environment. The lower part of the section is characterized by benthic foraminiferal wackestone (MF 2) indicating the lagoonal setting. The middle part consists of bioclastic, alveolinid, nummulitid wackestone with abundant small and large benthic foraminifera microfacies (MF 5) and bioclastic, assilinid, nummulitid wacke to packstone with abundant small and large benthic foraminifera microfacies (MF 1) characterizing the shoal environment. The bioclastic, assilinid, nummulitid packstone (MF 8) caps the cycle representing shallow open marine setting. The nature of the cycle is deepening upward (Figure 39).

Cycle 4

The fourth cycle of the measured section 2 (Figure 31) is the cycle 4 with a thickness of 2,75 m. It covers the interval from the sample number HBG 18 to HBG 21. This cycle is represented by brownish marl- clayey limestones and limestones with *Nummulites* in the field. Microfacies description of this cycle is bioclastic, assilinid, nummulitid packstone (MF 8) (Figure 40). This cycle is characterized by the oscillations within the shallow open environment.

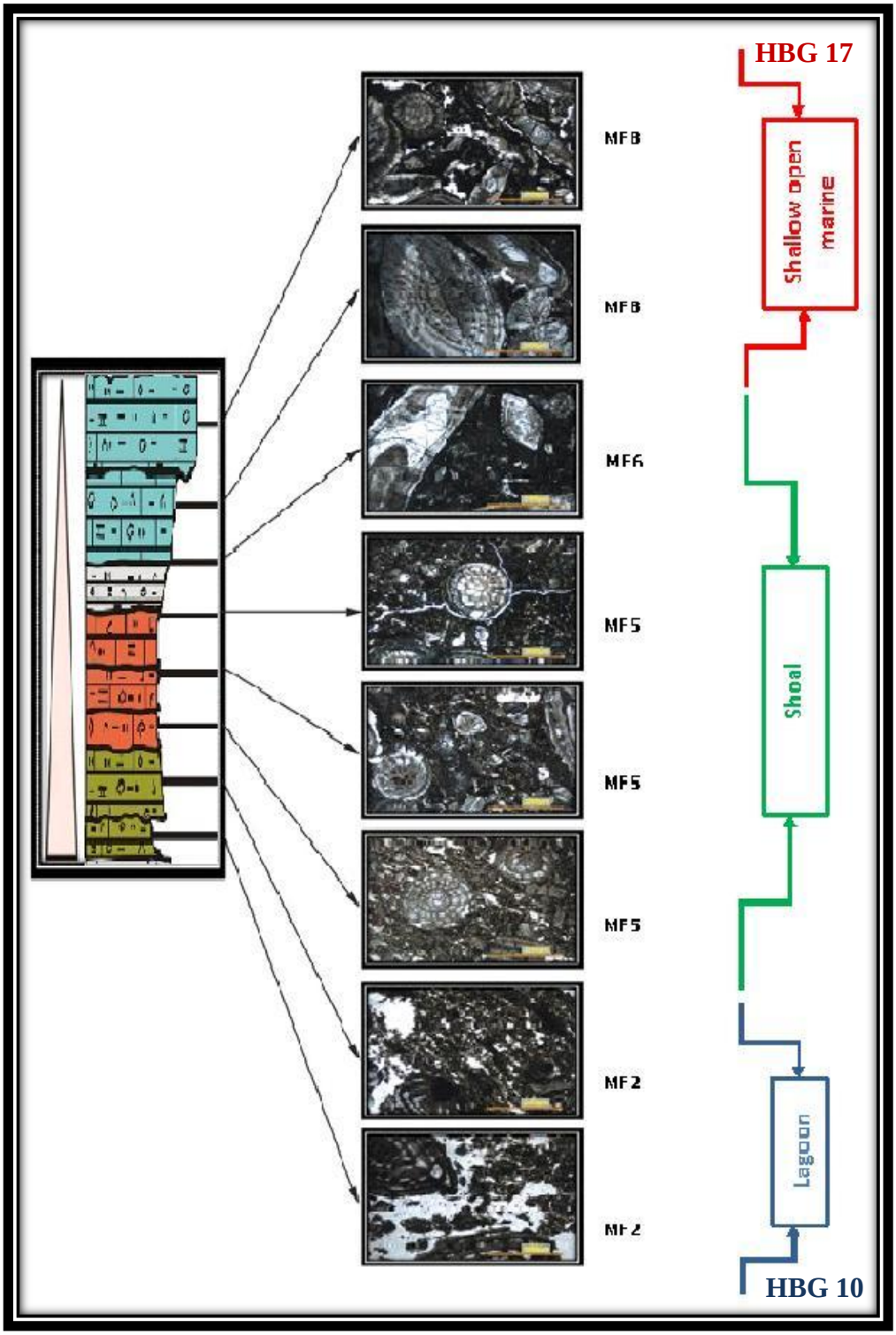

Figure 39. Cycle 3 of the Section 2 and photomicrographs of microfacies deposited within this cycle.

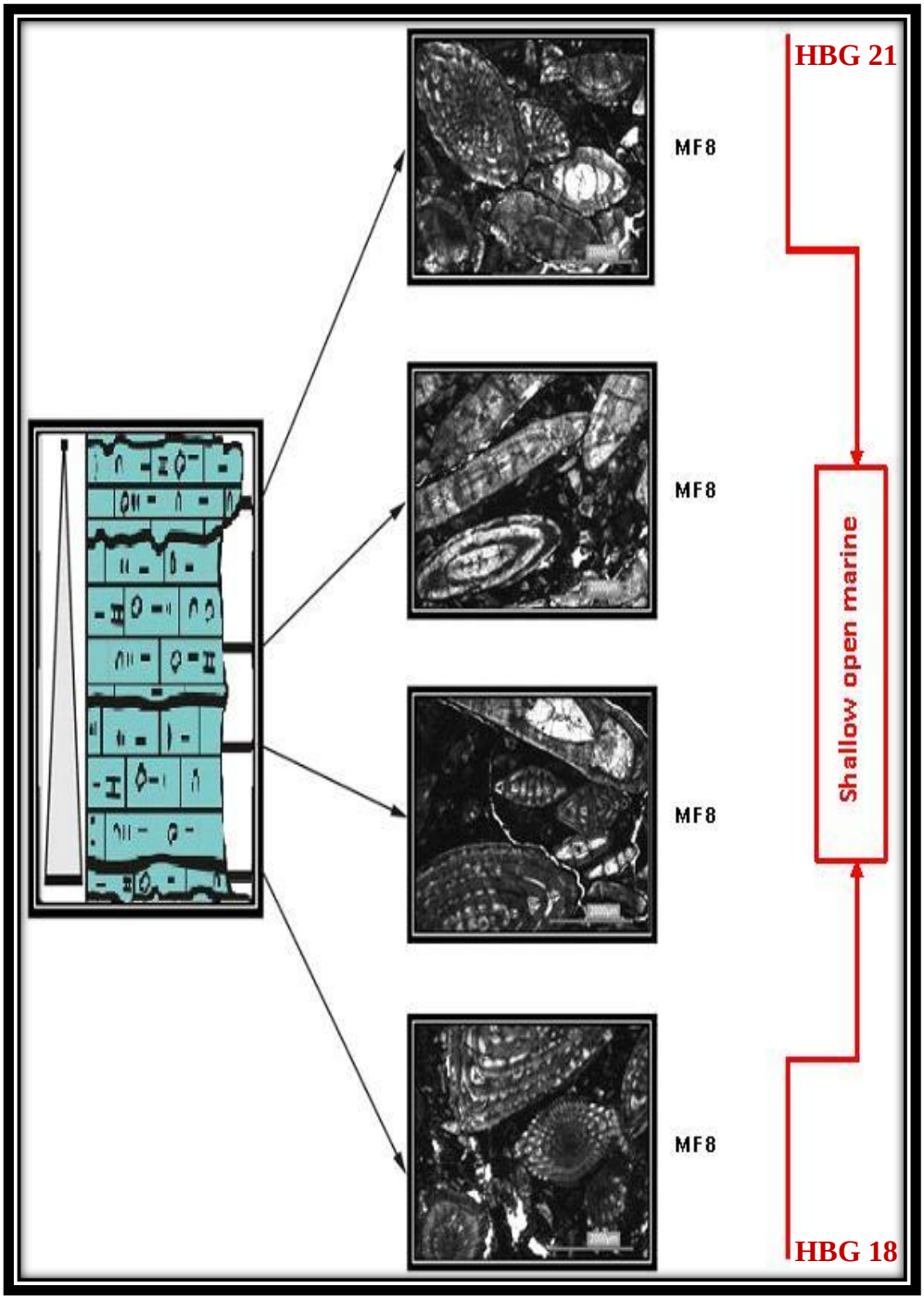

Figure 40. Cycle 4 of the Section 2 and photomicrographs of microfacies deposited within this cycle.

Cycle 5

The fifth cycle of the section 2 (Figure 31) is cycle 5 and it is from the sample number HBG22 to HBG 26. The thickness is 3,3 m. This cycle is composed of brownish marl-clayey limestones and limestones with *Nummulites* and is mainly represented by bioclastic, assilinid, nummulitid packstone microfacies (MF 6) (Figure 41) like cycle 4. This cycle also is characterized by the oscillations within the shallow open environment.

Cycle 6

Cycle 6 is the last cycle of the section 2 (Figure 31). It is 5,5 m thick and the thickest cycle of the section 2. It is from the sample number HBG 27 to HBG 31. Lithology of the cycle is composed of brownish marl-clayey limestones and limestones with *Nummulites* alternations. Cycle 6 is also represented by the bioclastic, assilinid, nummulitid packstone microfacies (MF 8) (Figure 42) like cycle 4 and 5. The characteristic of the cycle is the gradual increase of the fossil content and dense packing. This cycle also characterized by shallow open marine deposits. Clay content is clearly decreases at the top of the cycle.

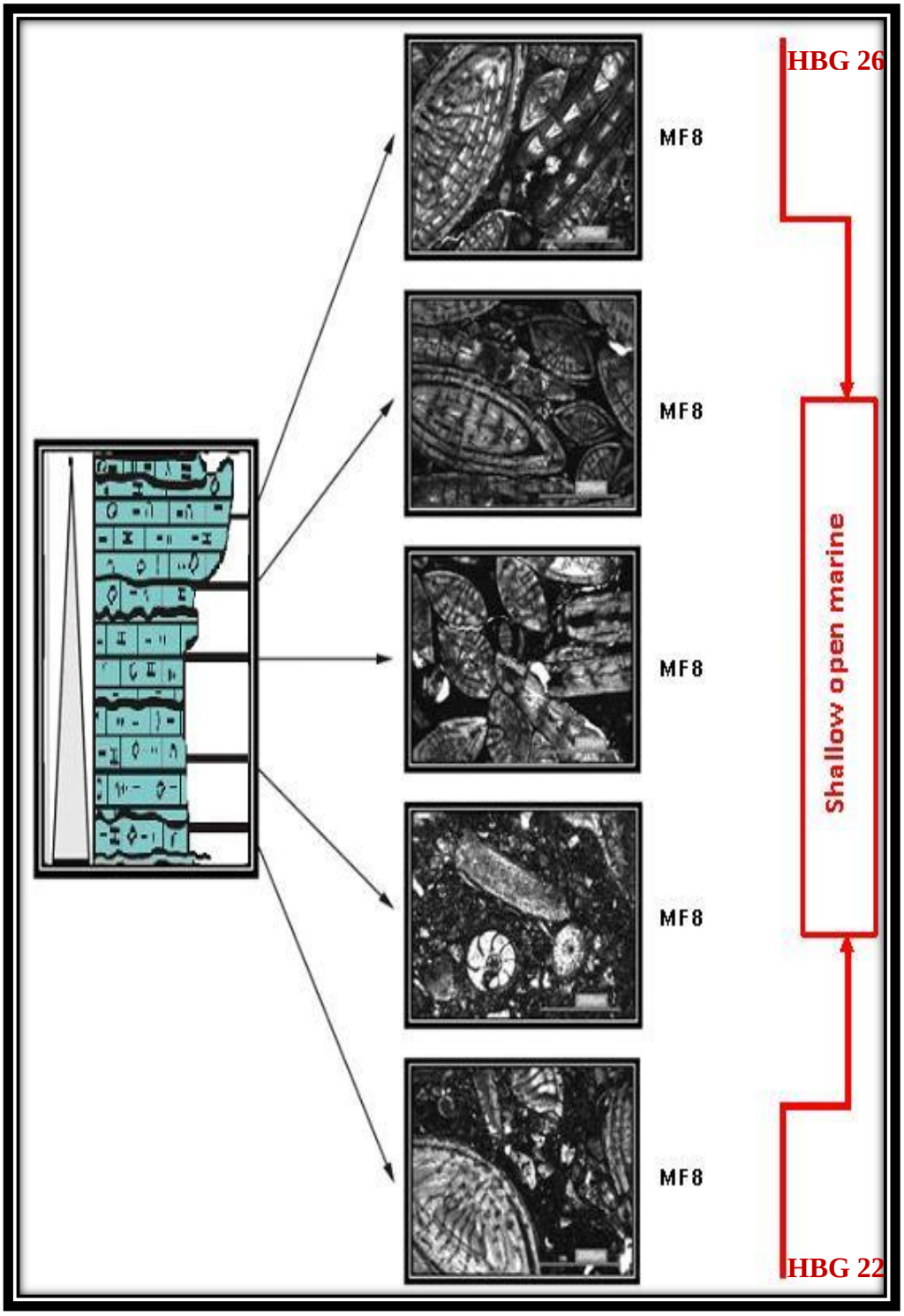

Figure 41. Cycle 5 of the Section 2 and photomicrographs of microfacies deposited within this cycle.

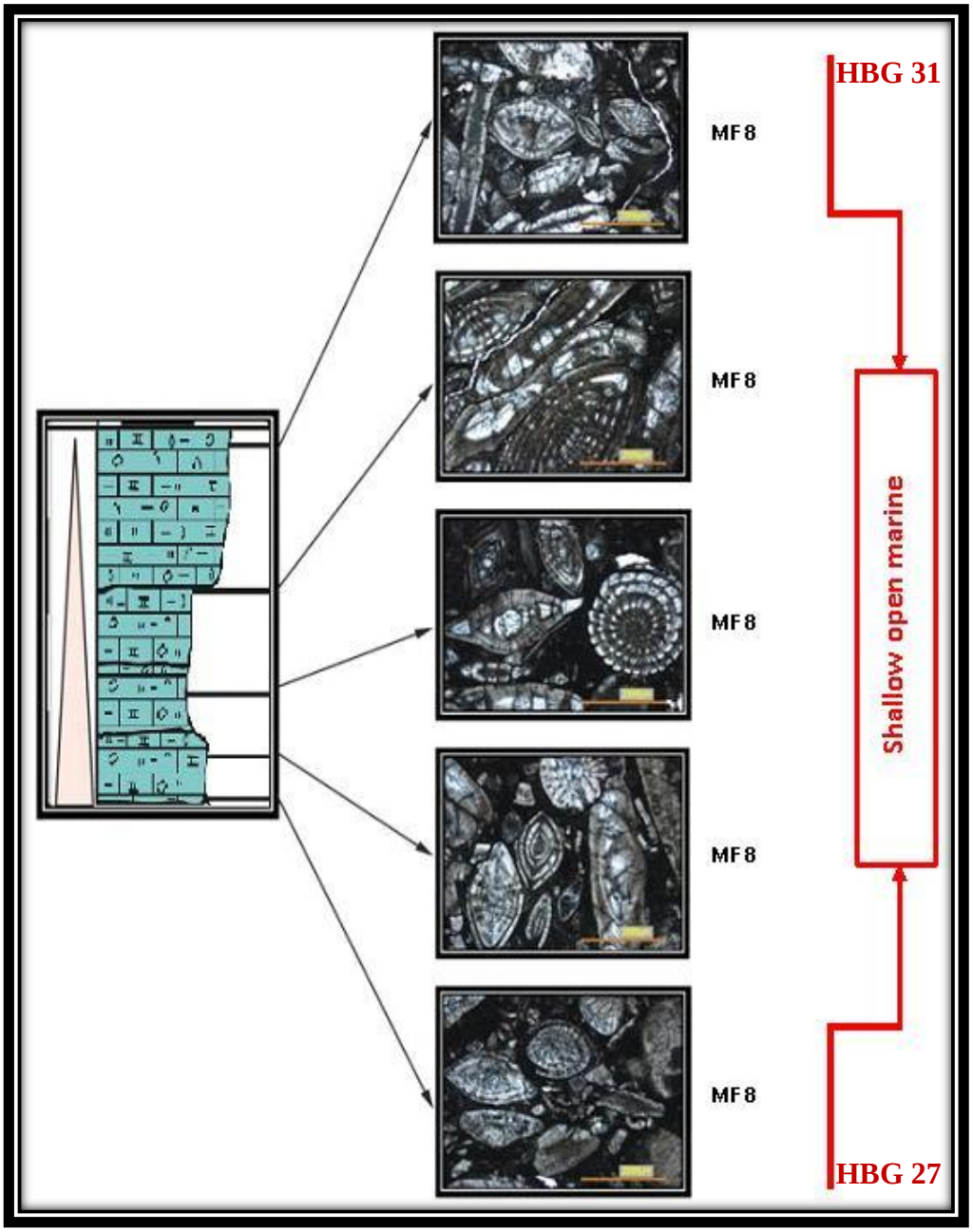

Figure 42. Cycle 6 of the Section 2 and photomicrographs of microfacies deposited within this cycle.

3.6. Sequence stratigraphic interpretation

For sequence stratigraphic interpretation, the concepts developed by many investigators (Sarg, 1988; Van Wagoner *et al.* 1988, 1990; Read and Horbury 1993; Read 1995; Emery and Myers, 1996; Catuneanu, 2006) were used. In marine shallow shelf environments, it is sometimes difficult to distinguish the different system tracts of a depositional sequence (Vail *et al.*, 1984; Posamentier and Vail, 1988; Sarg 1988). This is particularly true when dealing with homogeneous lithology. Therefore, it is most helpful to use the various markers of high and low sea-level phases within strata to support sequence stratigraphic interpretations (Vaziri-Moghadam *et al.*, 2006). The functional morphology and life style of foraminifers can be used to determine their former position on the platform and to detect upwards shallowing and deepening trends in sedimentary sequences (Geel, 2000). Additionally, variations in both abundance patterns and specific fossil content can be used to characterize depositional systems tracts (Armentrout *et al.*, 1990). This is what we did in this study because our microfacies definitions are strictly based on biofacies, that means the method directly dealing with the identification of depositional environment.

According Çiner *et al*. 1993, the Çayraz Formation is represented by a repetition of four types of basic units embedded in three types of basic sequences based on the field observations data. Each basic unit or basic sequences shows two distinct facies calcareous mudstones and nummulite banks, that implies a deepening-shallowing or transgressive regressive character.

In this study, distribution of foraminifers and facies data of meter scale cycles (parasequences) were used for the sequence stratigraphic interpretation. Based on the vertical evolution of microfacies and the stacking pattern of meter scale-cycle types within the sections two systems tracts were recognized, each belonging to one of the measured sections.

Cycles of section 1 are represented by shallow open marine depositional setting and lagoonal depositional setting. Cycle 1 of the section 1 is composed of the pile of shallow open marine facies and cycle 2 of the section 1 represents a shallow open marine facies variation. Cycle 3 which is characterized totally by the variation of shallow open marine facies and also represents one of the shallow open marine cycle of the section 1. Then by cycle 4 and cycle 5 the section shows a drastic return from shallow open marine conditions to lagoonal depositional conditions. Since the early highstand commonly consists of an aggradational parasequence set, cycle 1 and cycle 2 are aggradational and deposited in early highstand and cycle 4,5 and 6 are progradational and deposited in the late highstand because the late highstand is composed of one or more progradational parasequence sets. According to these section 1 is represented by a high stand systems tract (HST) (Figure 43) deposits, which is composed of mainly of lagoonal microfacies and shallow open marine microfacies.

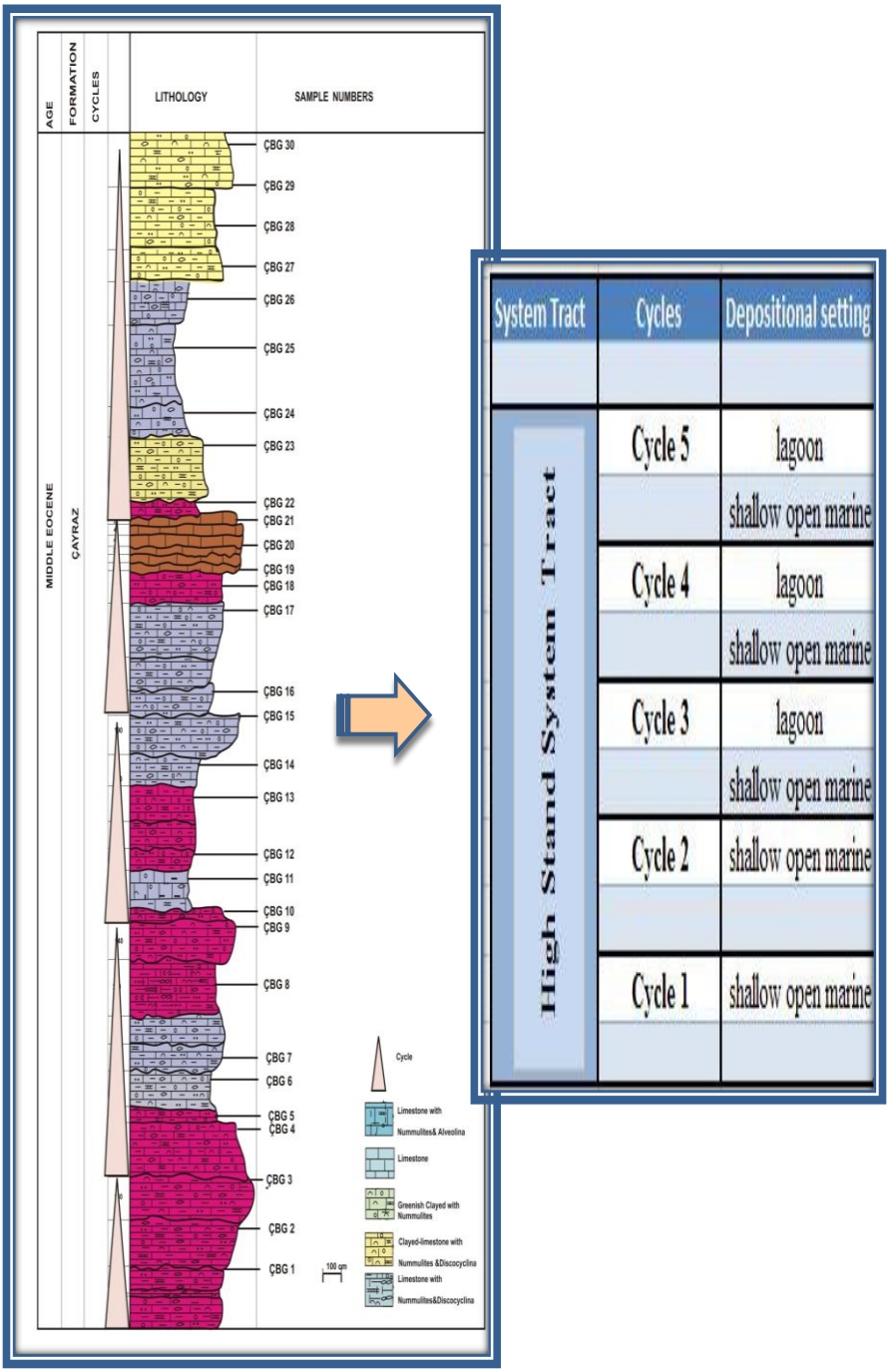

Figure 43. Cycle distribution and sequence stratigraphic interpretation of Section 1.

Parasequences within the transgressive systems tract backstep in a retrogradational parasequence set and the systems tract progressively deepens upward as successively younger parasequences step farther landward like. Cycles of the section 2 are represented by shoal, lagoonal and shallow open marine microfacies. Biofacies tend to be shallow below and deepening above in the TST as recognized in the cycles of section 2. Cycle 1 of the section 2 begins with lagoonal deposits after a flooding episode and shoals upward into the shoal facies and cycle 2 of section 2 is characterized by the oscillations with the shoal environment. Cycle 3 indicates the lagoonal setting in the lower part, the shoal environment in the middle part and shallow open marine setting the upper part. This cycle shows the transition from lagoonal conditions to shoal conditions and from shoal conditions to shallow open marine conditions with a deepening upward trend. Cycle 4 and 5 are characterized by the oscillations within the shallow open marine environment. Cycle 6 is also characterized by shallow open marine deposits. As described general trend of the cycles of section 2 are deepening upward and represent the TST. According to this section 2 is represented by TST (Figure 44) deposits, which is composed of shoal, lagoonal and shallow open marine microfacies.

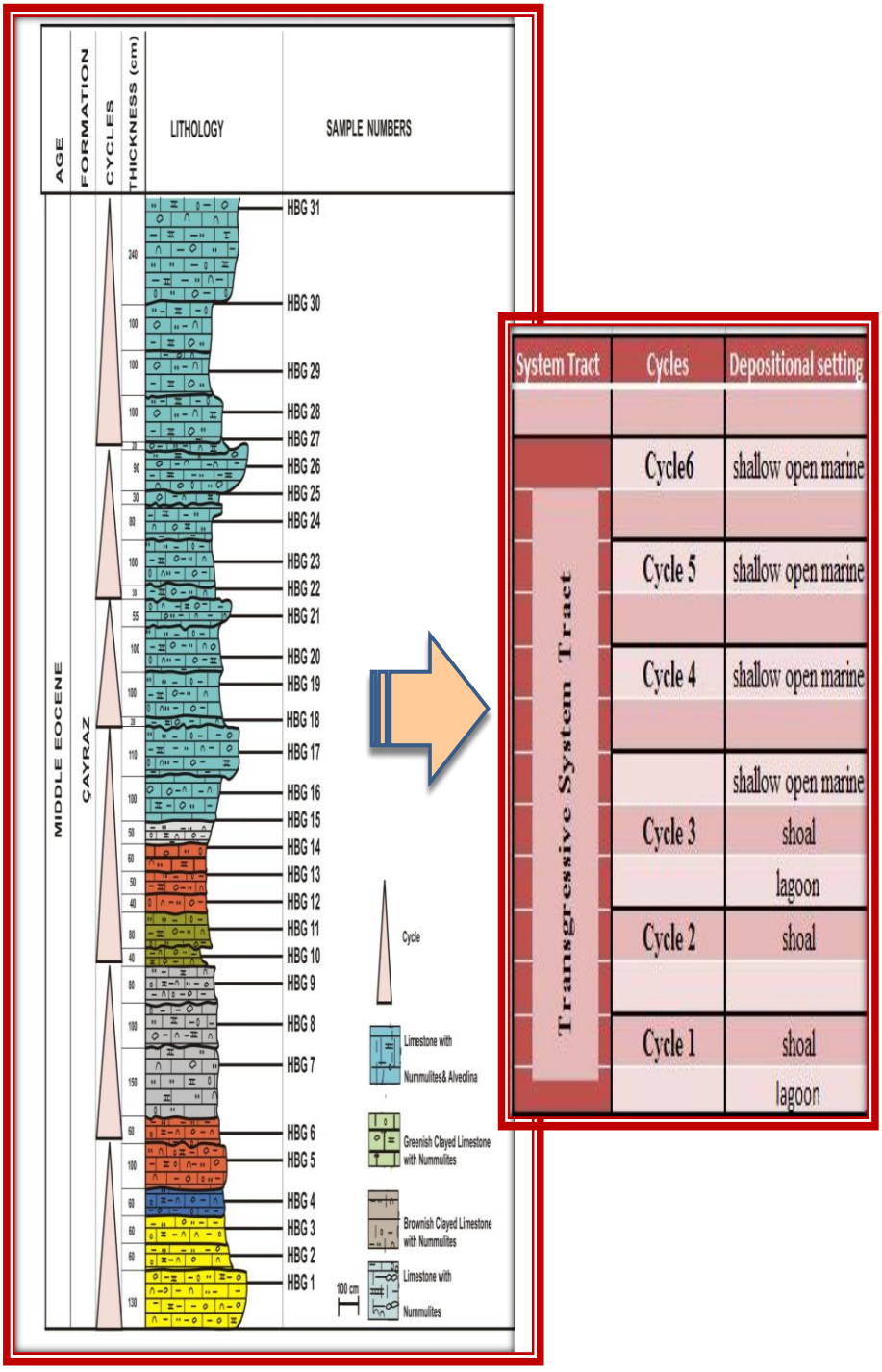

Figure 44. Cycle distribution and sequence stratigraphic interpretation of Section 2.

CHAPTER 4

RESPONSE OF FORAMINIFERAL ASSEMBLAGES TO CYCLICITY

4.1. Foraminiferal Assemblages used in the detection of cyclicity

Microfossils are useful and an important tool for studying their response to cyclic deposits and larger benthic foraminifera (LBF) are considered to be good indicators of shallow marine carbonate cycles in fossil series. Because LBF occur abundantly in many carbonate platforms they can be easily identified in thin section or in the field, with the aid of a hand lens. Although they cover a wide range of platform environments, these biotas are influenced by global and local factors such as ecology (e.g. temperature, water chemistry and trophic resources), geology (e.g. sea level, plate tectonics) and phylogeny (e.g. radiation, extinction). Variation of these parameters affects the biotic composition and the abundance of biota (Chaproniere, 1975; Hottinger, 1983, 1997; Reiss and Hottinger, 1984; Hallock and Glenn, 1986) and the abundance of them is an important criteria for determining shallowing upward cycles. Therefore, in this study, a quantitative analysis is carried out to determine the biological response to the cyclicity. The predominant forms are larger benthic foraminifera in the facies and therefore, mainly larger benthic foraminifera were used for this study. LBF are milimeter to centimeter in size with complex endoskeletal structures which must be studied in oriented thin sections. But in this study we did not study in oriented sections because the aim of this study is to show foraminiferal response to cyclicity by classifiying them into family and generic level. Their axial sections show whorls, the character and dimensions of the chambers and distribution of pillars and their

equatorial sections display growth character of whorls, the number and the shape of septa and character of initial chambers.

In order to perform this study benthic foraminiferal taxa were classified into twenty one different groups and for the taxonomic subdivision we have followed Loeblich and Tappan (1988) (Figure 45). The foraminifera groups used in the point counting are *Nummulites* sp., *Discocyclina* sp., *Assilina* sp., *Operculina* sp., *Alveolina* sp., *Sphaerogypsina* sp., miliolid, *Pygro* sp., *Triloculina* sp., *Spiroloculina* sp, *Coskinolina* sp., *Orbitolite*s sp., *Lockhartia* sp., biserialy to uniserialy coiled forms, *Medocia?* sp., *Valvulina* sp., *Textularia* sp., *Valvulina* sp. or *Textularia* sp., *Rotalia* sp., Verneulinidae and others (unidentified textularid, miliolid and rotalid forms) (Figure 45).

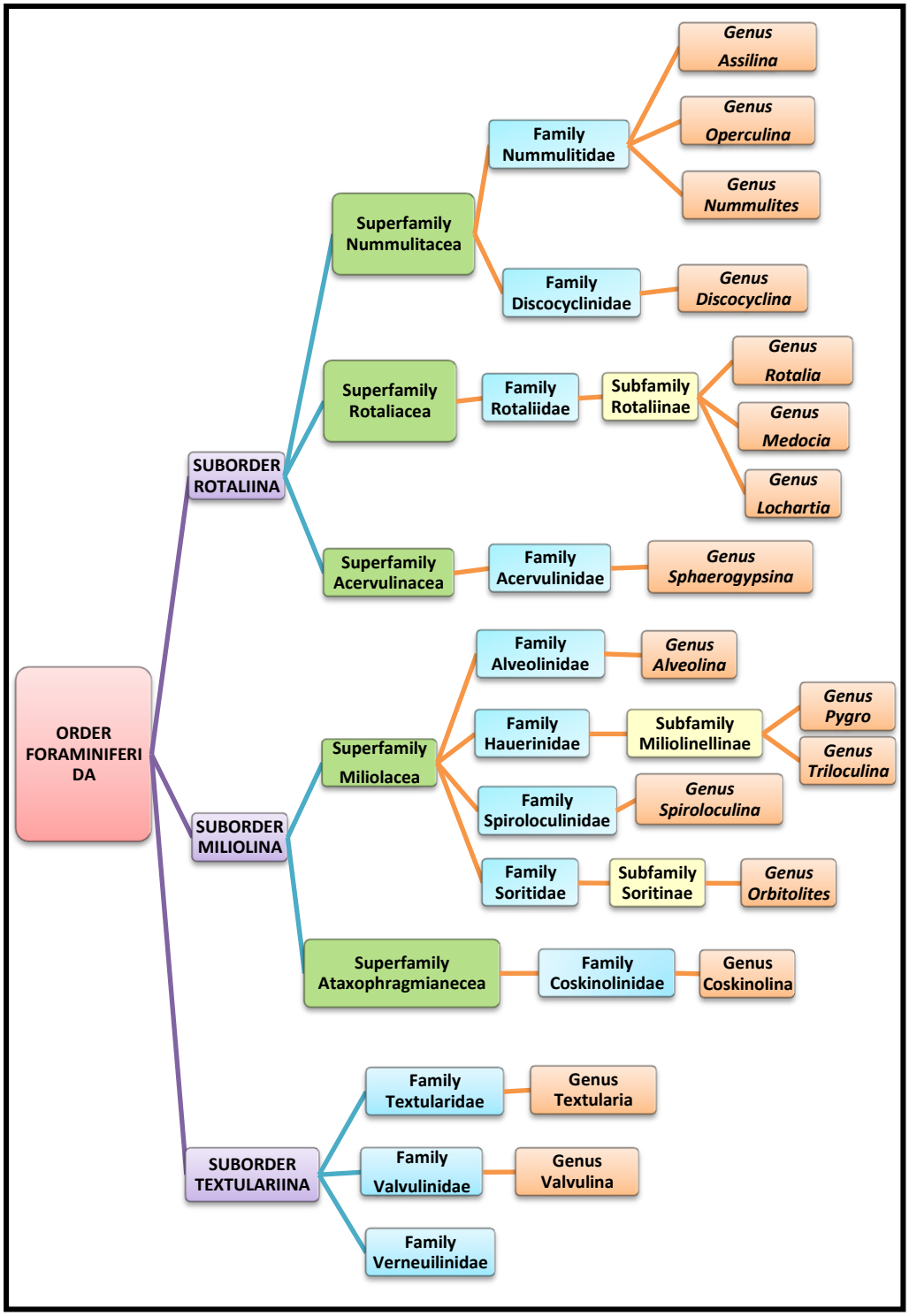

Figure 45. Hierachy of foraminiferal groups.

4.1.1. *Nummulites* sp.

Nummulites sp. is the larger benthic foraminifera, which was unique in their rock forming potential amongst the early Cenozoic LBF. It is abundant in Palaeocene to Upper Eocene sediments (e.g. Loucks *et al.*, 1998; Sinclair *et al.*, 1998; Allen *et al.*, 2001; Pomar, 2001). In this study this genus is also abundant in all samples except sample number ÇBG 20 and ÇBG 21. It is characterized by radial hyaline and perforate tests with septa. Its tests are globular, lenticular or discoidal in shape. It is biconvex planispirally enrolled and commonly involute but may be evolute in the later stage. Chambers may be simple or differentiated into median and lateral layers (Appendix B, plate 1, figure 1-6; plate 2, figure 1-6; plate 3, figure 1-6).

4.1.2. *Assilina* sp.

Assilina sp. is also characterized by radial hyaline and perforate tests with septa like *Nummulites* sp. It has large flattened evolute tests with rapidly enlarging whorls and numerous numerous chambers per whorl (Appendix B, plate 7, figure 1-5).

4.1.3. *Operculina* sp.

Operculina sp. is defined by hyaline and perforate tests with septa like *Nummulites* sp. and *Assilina* sp. Its coiling is planisipiral. It has flattened test and its wall is calcareous, lamellar and finely perforate. It is evolute (Appendix B, Plate 7, figure 5-6).

4.1.4. *Discocyclina* sp.

Discocyclina sp. has radial hyaline and perforate tests. A median layer of chambers is differentiated from lateral chambers. It has radiating pillars and these pillars give rise to granules of the outer surface (Appendix B, plate 6, figure 1-5).

4.1.5. *Rotalia* sp.

This form has a trochospiral, biconvex test. All chambers of the form are visible on the strongly convex spiral side, only those of the final whorl visible on the umbilical side simple interiomarginal aperture. It has radial hyaline wall (Appendix B, plate 14, figure 1-5).

4.1.6. *Medocia?* sp.

Medocia? sp. has lenticular, trochospiral test. Its spiral side is strongly convex. Its wall is calcareous, perforate and laminated, with thick lamellar wall on the spiral side as in *Rotalia.* The aperture of the form is interiomarginal, which is extending from the umbilical mass nearly to the periphery (Appendix B, plate 14, figure 6-7).

4.1.7. *Lockhartia* sp.

This form is characterized by a conical to lenticular test. It is trochospirally enrolled. Numerous chambers are visible on the strongly convex spiral side. The septa are double. It has intraseptal canals and its umbilicus filled with numerous pillars that arise at the umbilical end of the chambers. The wall of the form is calcareous, lamellar, radially fibrous, coarsely perforate and punctate on the spiral side (Appendix B, plate 13, figure 3-6).

4.1.8. *Sphaerogypsina* sp.

Sphaerogypsina sp. has a large test , up to 2 mm in diameter. The shape of the test is globular to somewhat irregular and constructed of numerous layers of small and closely packed chambers (Appendix B, plate 9, figure 1-7).

4.1.9. *Alveolina* s.l.

Alveolina s.l. has imperforate calcareous tests of porcelaneous appearance. Its coiling is fusiform to ovate planispiral. Chambers are divided by septulae into numerous chamberlets arranged in one or more rows and several inner whorls may have extreme basal thickening of the wall that fills

most of the chamber lumen. The form is characterized by the presence of preseptal and postseptal passages. Its aperture consists of two rows of openings in the apertural face and alternating in position (Appendix B, plate 8, figure 1-6).

4.1.10. Miliolid

Miliolids have calcareous porcellanous tests. They are characterized by miliolid coiling (Appendix B, plate 10, figure 1-8, 10,12). The aperture is terminal and simple

4.1.11. *Pygro* sp.

The test of this form is ovate in outline and compressed through the midpoint of the opposing chambers. Its chambers have one half coil in length and have in the microspheric stage early quinqueloculine later cryptoquinqueloculine arrangement. The adult stage is biloculine. The wall of the form is calcareous, imperforate and porcelaneous. Its aperture is present at the end of the final chamber (Appendix B, plate 10, figure 9, 11; plate 11, figure 1-7).

4.1.12. *Triloculina* sp.

The test of the *Triloculina* sp. is ovate in outline and equilaterally triangular or subtriangular in thin sections. Its chambers are one half coil in length, at the early stage cryptoquinqueloculine at least in its microspheric generation, but this stage may be lacking in the megalospheric generation. The form is later pseudotriloculine or triloculine enrolled. Only three chambers are visible from the exterior. The wall of the form is calcareous, imperforate and porcelaneous. Its aperture is rounded and is present at the end of the final chamber (Appendix B, plate 11, figure 8-10).

4.1.13. *Spiroloculina* sp.

Spiroloculina sp. has an ovate to fusiform test. The proloculus of the form is followed by a planispirally enrolled tubular second chamber of one whorl in length. The wall of the form is calcareous, imperforate and porcelaneous. The aperture is at the open end of the final chamber (Appendix B, plate 11, figure 11-12; plate12, figure 1-3).

4.1.14. *Orbitolite*s sp.

The test of the form is large, discoidal and very slightly biconcave. It has large proloculus and cyclic chambers are subdivided into many chamberlets, those of successive cycles alternating in position. The chamberlets of a single cycle is not interconnected but these cycles are connected by a crosswise oblique stolon system. Annular chambers are less defined in the later stage and chamberlets separated by thickened oblique walls. The aperture of the form has numerous rounded openings in transverse rows crossing the peripheral margin (Appendix B, plate 12, figure 5-6; plate 13, figure 1-2).

4.1.15. *Coskinolina* sp.

Coskinolina sp. has a high cone test and porcelaneous wall. Its wall consists of imperforate granular calcite with keriothecal structure. It is trochospirally enrolled in the early stage and uniserially enrolled at the later stages. Its numerous low chambers are rapidly enlarging in diameter and consists of vertical interseptal pillars. Its aperture is composed of pores scattered over the surface of the gently convex apertural face (Appendix B, plate 12, figure 4).

4.1.16. *Textularia* sp.

Textularia sp. is characterized by a simple agglutinated wall and biserially arranged numerous chambers. Its test is free and elongate. It has a

single aperture at the base of the last chamber face (Appendix B, plate 4, figure 8-9).

4.1.17. *Valvulina* sp.

Valvulina sp. has agglutinated wall and its test is free, elongated. The chambers are arranged triserially (Appendix B, plate 4, figure 3-5).

.

4.1.18. *Valvulina* sp. or *Textularia* sp.

This group consists of forms which could be assigned either *Valvulina* sp. or *Textularia* sp. Because it is sometimes difficult to decide whether the forms are biserially or triserially enrolled in thin section views (Appendix B, plate 4, figure 1-2, 6-7).

4.1.19. Verneulinidae

Family Verneulinidae has a free, elongate test. Its wall is agglutinated, finely perforate. The coiling of chambers is initially triserial and triangular in cross section, then the coiling of chambers become biserial and slightly inflated. The sutures are indistinct in triserial section and become depressed in biserial portion. The aperture of the form is located at base of the final chamber (Appendix B, plate 5, figure 5-6).

4.1.20. Biserialy to uniserialy coiled forms

These forms are characterized by small, bilocular to unilocular tests. The wall of the forms is agglutinated. The shape of the test is globular, spherical or slightly irregular (Appendix B, plate 14, figure 8-9).

4.1.21. Others

This group consists of unidentified textularid (Appendix B, plate 5, figure 1, 3), miliolid (Appendix B, plate 16, figure 1-5) and rotalid forms

(Appendix B, plate 15, figure 1-10). These forms are defined according to their wall structure. Unidentified textularid forms have agglutinated wall, unidentified miliolid forms have porcelaneous wall and unidentified rotalid forms have hyaline wall.

After classifying benthic foraminifera, quantitative analysis were carried out for understanding foraminiferal responses to the sedimentary cyclicity of the Middle Eocene Çayraz Formation. The Quantitative analysis of benthic foraminifera were carried out in 4 cm^2 area of each thin section and approximately 200 to 300 specimens were counted in most thin sections to find out the abundance of these benthic foraminiferal groups. The results of this countings are listed in appendix C.

4.2. Distribution and interpretation of the Foraminiferal Assemblages in the cycles

Data obtained from the fossil record may provide key information on depositional environments critical to the interpretation of marine sedimentary cycles and, thereby, to the recognition of ancient cycles and sequences. Because paleoecological changes are closely correlated with fluctuations in sea level and sedimentation, one may predict many genetic relationships between fossil distributional patterns and depositional sequences. In this study diversity of the foraminifera is high and abundance of them provides a good response to sedimentary cyclicity. After obtaining counting results of the foraminiferal assemblages, excell graphs were prepared in order to see the distribution of the foraminiferal assemblages in to cycles. These distributions are given in the following figures (Figure 46-49).

The total distribution of counted foraminifera in the studied section 1 is given in figures 46-47 and section 2 is given in figures 48-49. According to the

obtained data from the figures 42-44 studied groups have different distribution patterns within the the section 1.

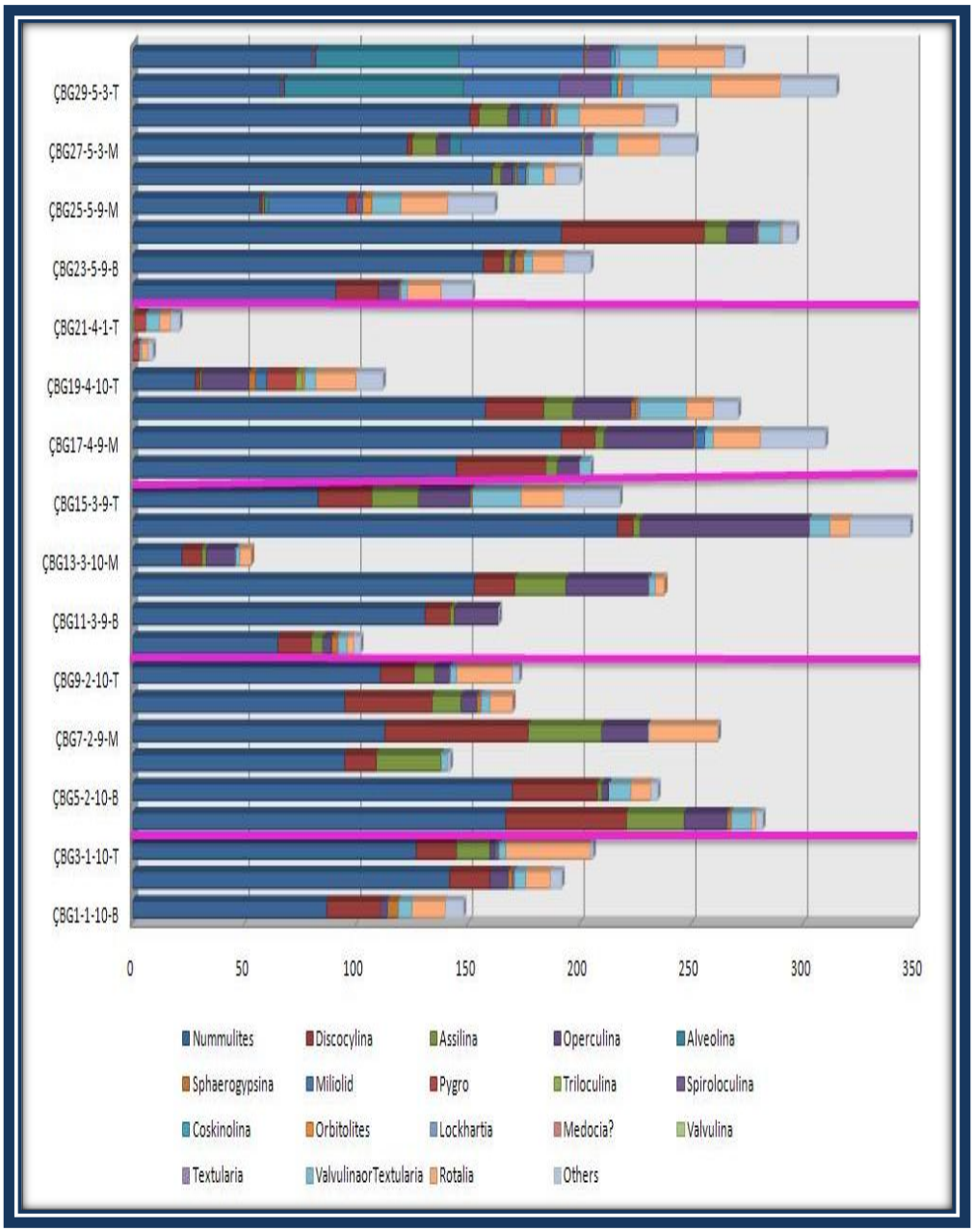

Figure 46. Distribution of the foraminiferal assemblages sample by sample in the section 1 (ÇBG1-1-10-B, 1: cycle number, 10: microfacies (MF 10), B: bottom of the cycle. Other symbols, M: middle part of the cycle; T: top of the cycle). Pink horizontal lines indicate meter scale cycle boundaries.

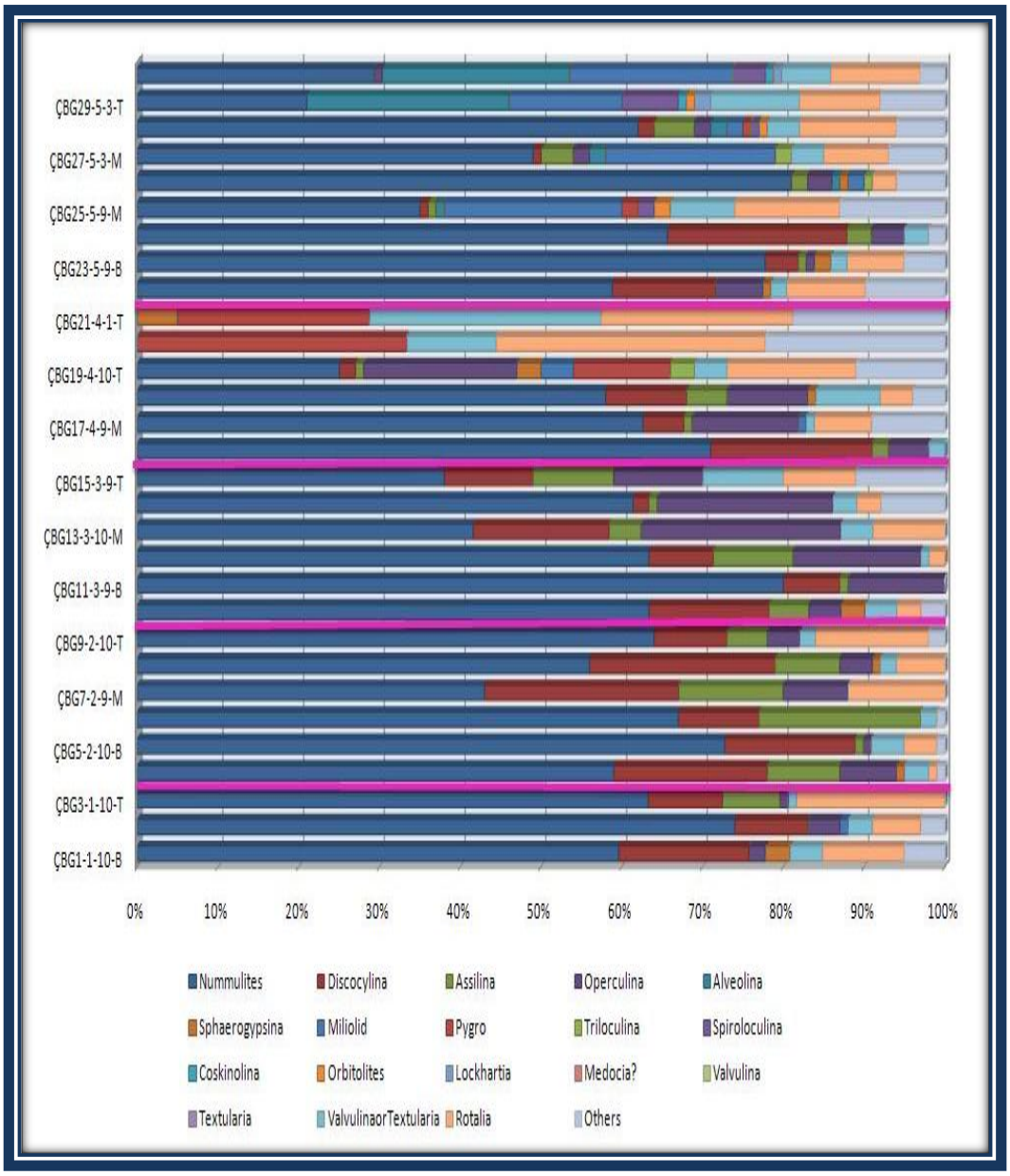

Figure 47. Percentage distribution of the foraminiferal assemblages sample by sample in the section 1 (ÇBG1-1-10-B, 1: cycle number, 10: microfacies (MF 10), B: bottom of the cycle. Other symbols, M: middle part of the cycle; T: top of the cycle). Pink horizontal lines indicate meter scale cycle boundaries.

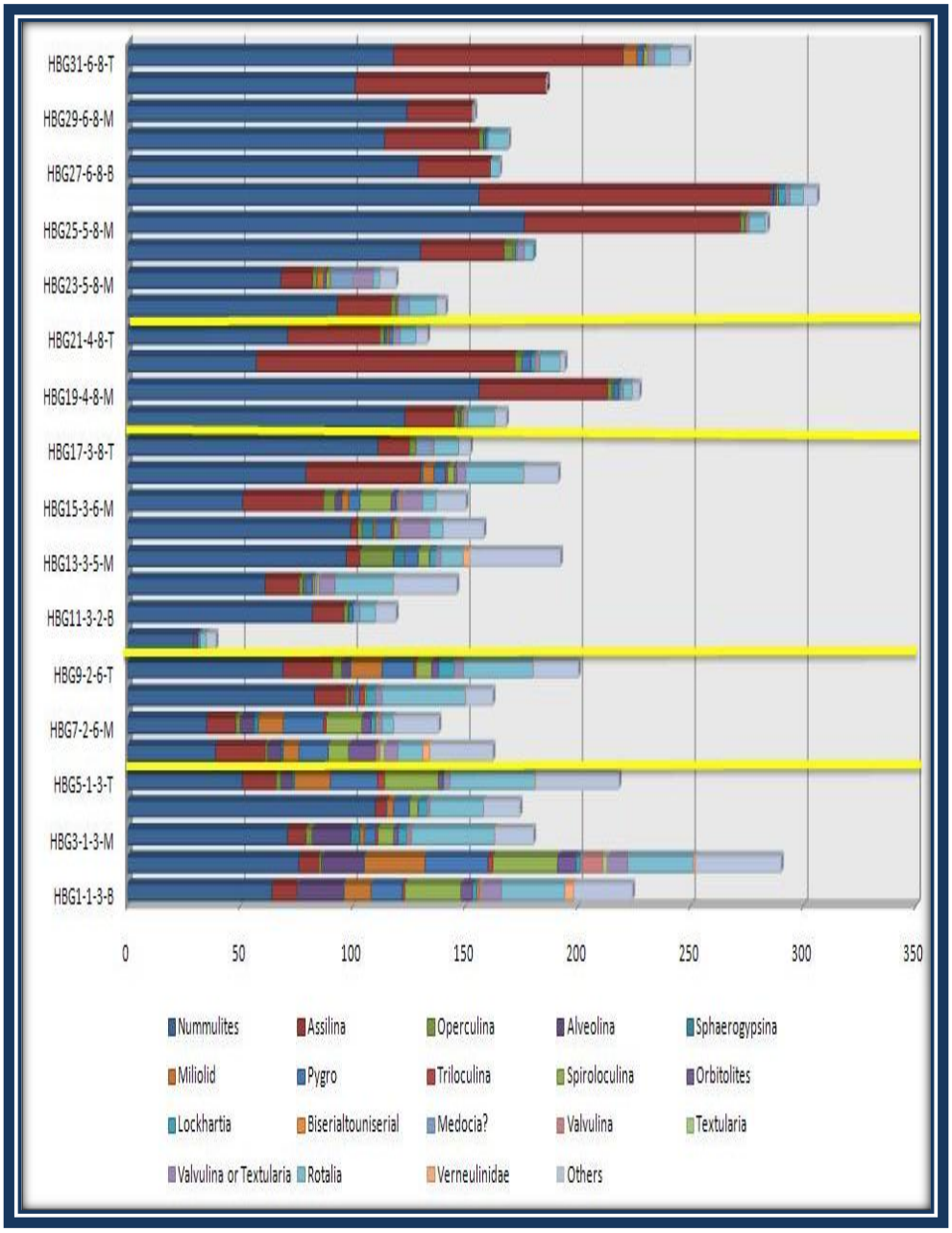

Figure 48. Distribution of the foraminiferal assemblages sample by sample in the section 2 (HBG1-1-3-B, 1: cycle number, 1: microfacies (MF 3), B: bottom of the cycle. Other symbols, M: middle part of the cycle; T: top of the cycle). Yellow horizontal lines indicate meter scale cycle boundaries.

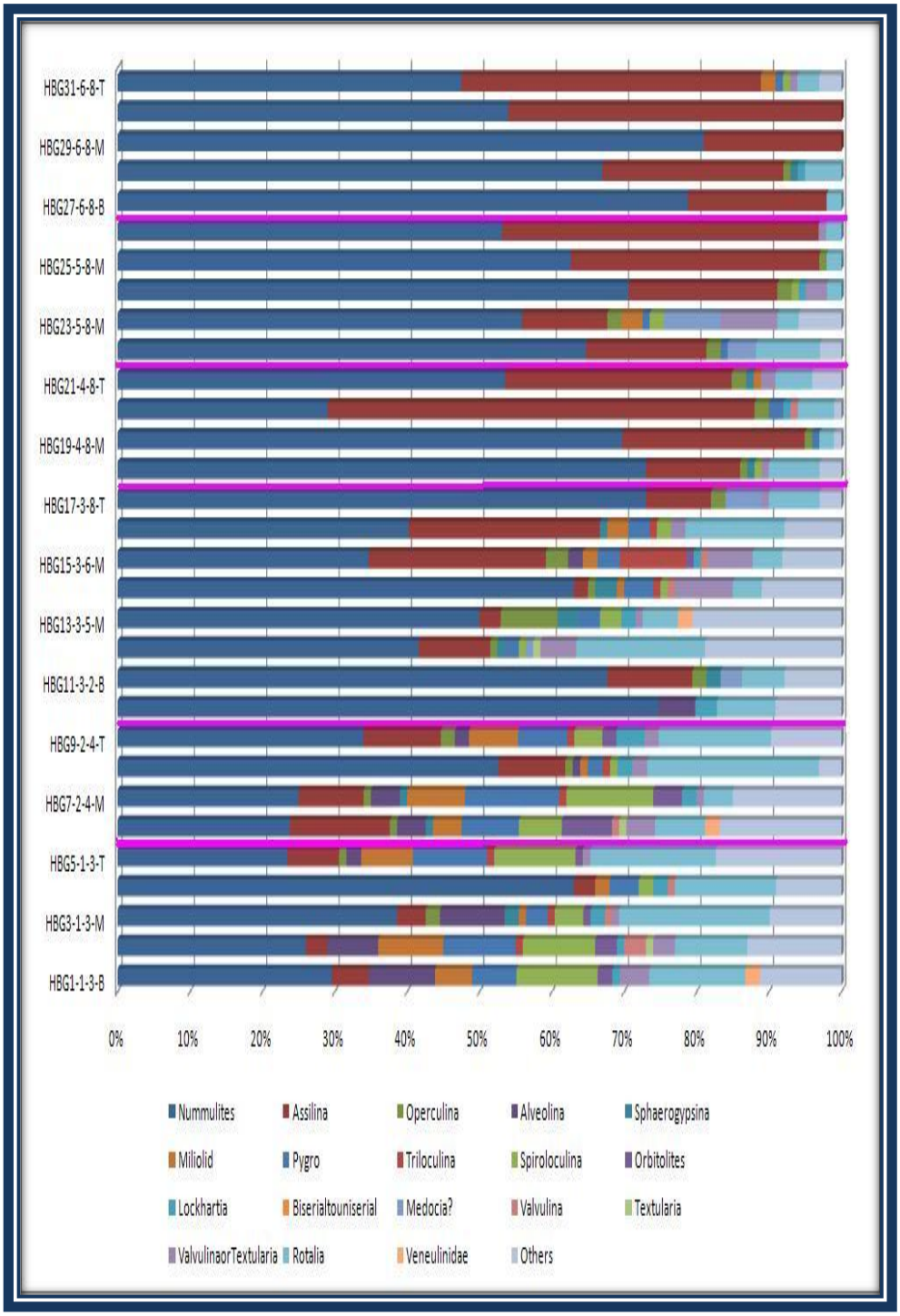

Figure 49. Pecentage distribution of the foraminiferal assemblages sample by sample in the section 2 (HBG1-1-3-B, 1: cycle number, 1: microfacies (MF 3), B: bottom of the cycle. Other symbols, M: middle part of the cycle; T: top of the cycle). Pink horizontal lines indicate meter scale cycle boundaries.

Nummulites is the most abundant foraminiferal group in both sedimentary cycles than the other groups in the measured sections (Figure 46-47). In most of the cycles in the section 1, the relative abundance of *Nummulites* displays good response to the cyclicity (Figure 50). The relative abundance increases towards the upper part of the cycle 1 and cycle 2, which are characterized by shallow open marine facies. In cycle 3, which is characterized totally by the variation of shallow open marine facies, the relative amount of *Nummulites* shows variations and decreasing trend toward the top of the cycle 3. The relative amount of *Nummulites* decreases towards the upper part of the cycle 4 and 5 which show a drastic return from shallow open marine conditions to lagoonal depositional conditions and *Nummulites* disappears in the top of the cycle 4 in the samples ÇBG 20 and 21. This can be explained by a sudden facies change from shallow open marine facies to lagoonal facies.

Nummulites is again the dominant group within the section 2 (Figure 48-49). In most cycles, there are some variations within the cycles but the relative abundance is less at the top of the cycles (cycle 1, 4, 5, 6) except cycle 2 and 3 (Figure 51). According to this the counted results *Nummulites* has different response to shallowing and deepening cycles (Figure 51). Within the cycle 1 that begins with lagoonal deposits after a flooding episode and shoals upward into the shoal facies, the relative abundance of *Nummulites* is decreasesing towards the top. Within the cycle 3 which represents logoon, shoal and shallow open marine setting and deepening upward trend, relative abundance of *Nummulites* is increasing towards the top of the cycle. The relative amount of *Nummulites* decreases towards the upper part of cycles 4, 5 and 6 that are characterized by the oscillations within the shallow open environment.

Figure 50. Distribution (in %) of *Nummulites* in the meter scale cycles of the section 1.

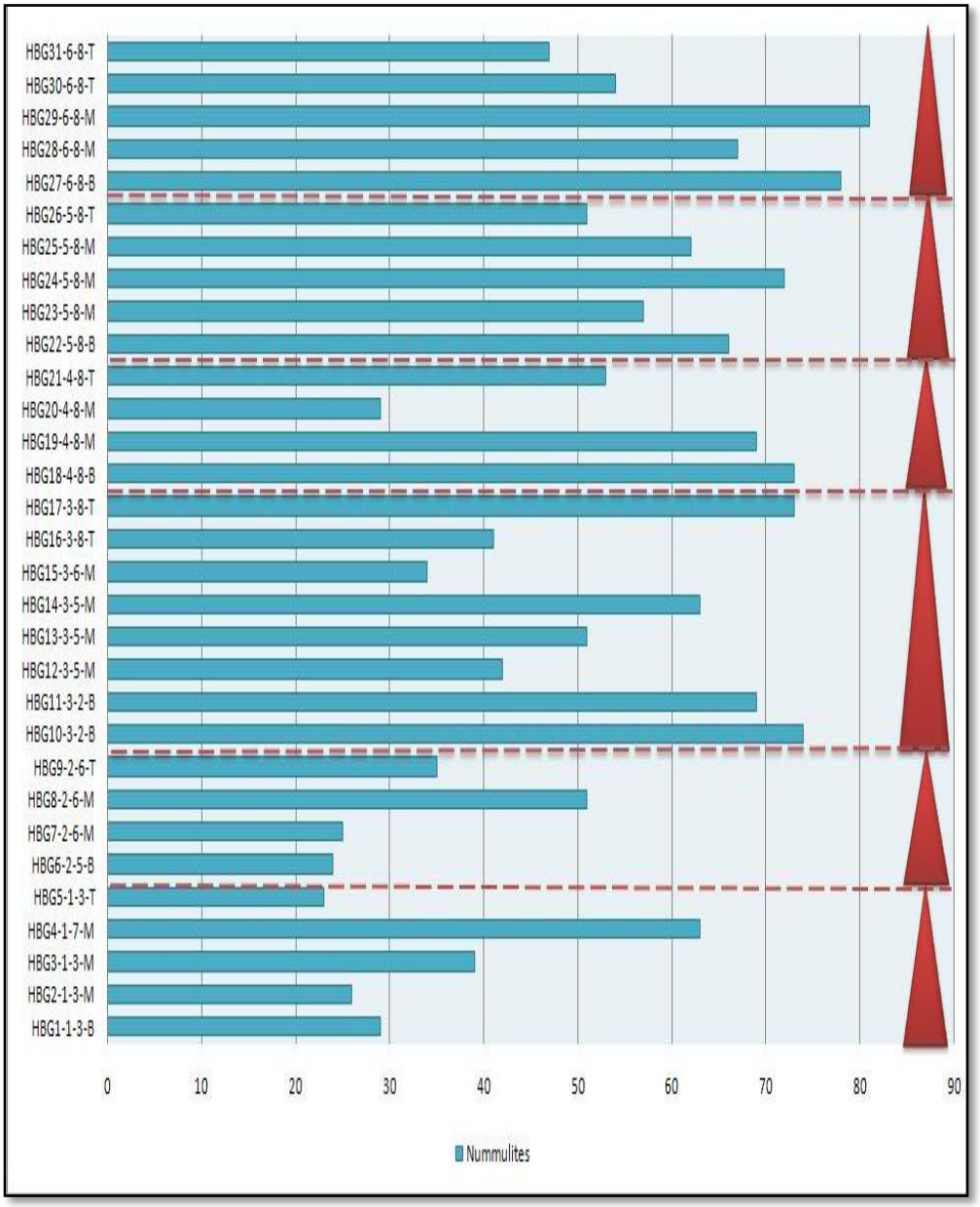

Figure 51. Distribution (in %) of *Nummulites* in the meter scale cycles of the section 2.

The responses of *Assilina* in cycles of the section 1 (Figure 52) exhibits variations. It is not present in all cycles and it displays different abundance curve in different cycles. But the relative amount of *Assilina in cycles* (1-3) which are characterized by shallow open marine facies is more than cycles (4-5) that return from shallow open marine conditions to lagoonal depositional conditions. This indicates that *Assilina* is most abundant in relatively deep-water environments.

Assilina is the second dominant group within the section 2 (Figure 48-49). The responses of *Assilina* (Figure 53) and *Nummulites* is incompatible in section 2. The relative abundance of *Assilina* is more at the top of the cycles (cycle 1, 4, 5, 6) except cycle 2 and 3 (Figure 51). According to this the counted results *Assilina* like *Nummulites* has different response to shallowing and deepening cycles (Figure 53). In the cycle 1 which begins with lagoonal deposits after a flooding episode and shoals upward into the shoal facies, the relative abundance of *Assilina* is increasesing towards the top. Within the cycle 3 which is deepening upward, relative abundance of *Assilina* is decreasing towards the top of the cycle and The relative amount of *Assilina* increases towards the upper part of the shallow open environment cycles (Cycle 4-6).

The relative abundance of *Discocyclina* in section 1 cycles exhibits variations like *Assilina* (Figure 54). *Discocyclina* is present only in section 1 and it is characterized by shallow open marine. Therefore the presence of it indicates deposition environment of cycles within the section 1 is more deeper than cycles in section 2. *Discocyclina* is abundant in the shallow open environment cycles and the relative amoun of *Discocyclina* is decreasing towards the lagoonal depositional conditions and it disappears in the top of the cycle 4 in the samples ÇBG 20 and 21 and in the middle to top parts of the cycle 5 (ÇBG 26, 29-30), which indicates the facies change from shallow open marine to lagoonal settings.

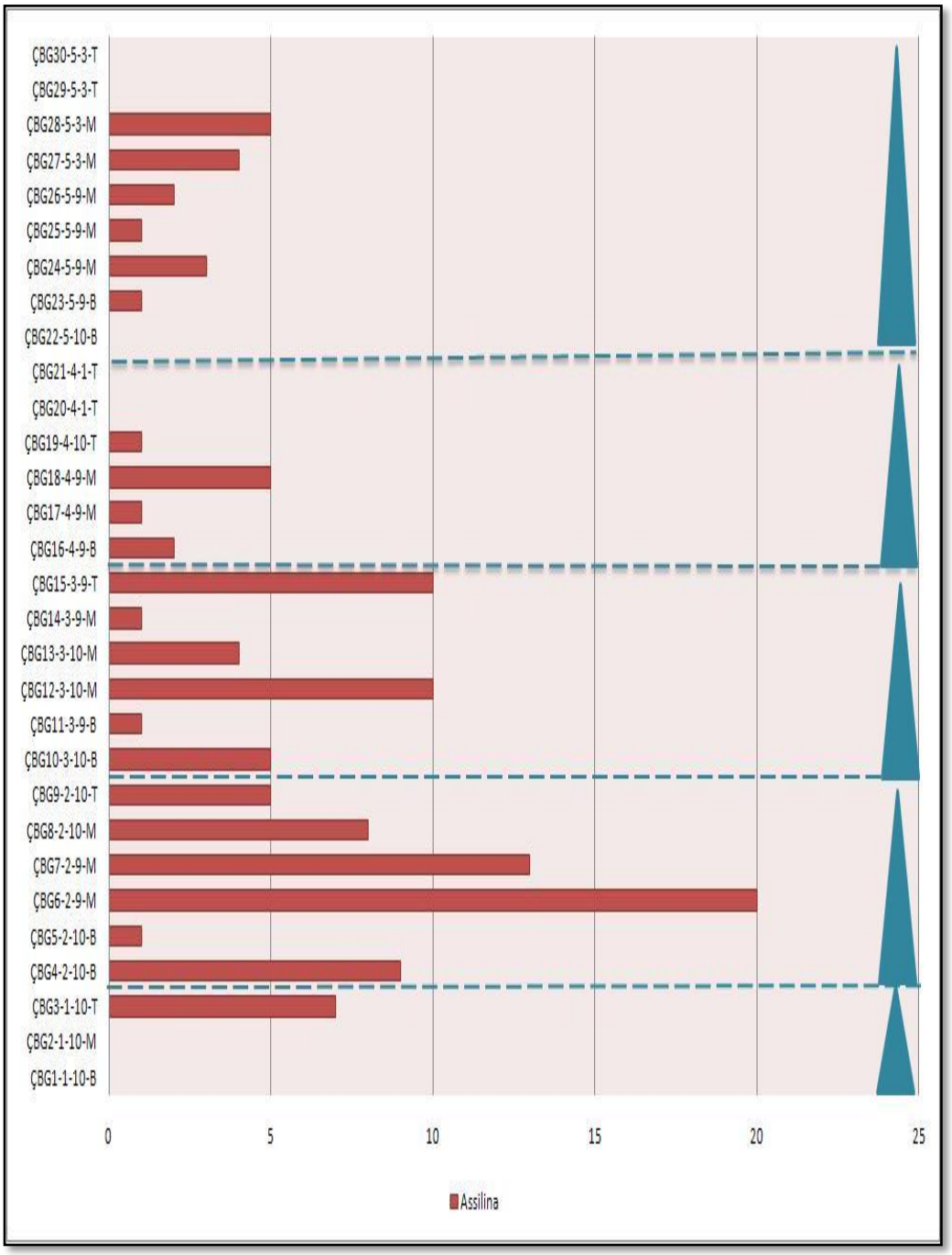

Figure 52. Distribution (in %) of *Assilina* in the meter scale cycles of the section 1.

Figure 53. Distribution (in %) of *Assilina* in the meter scale cycles of the section 2.

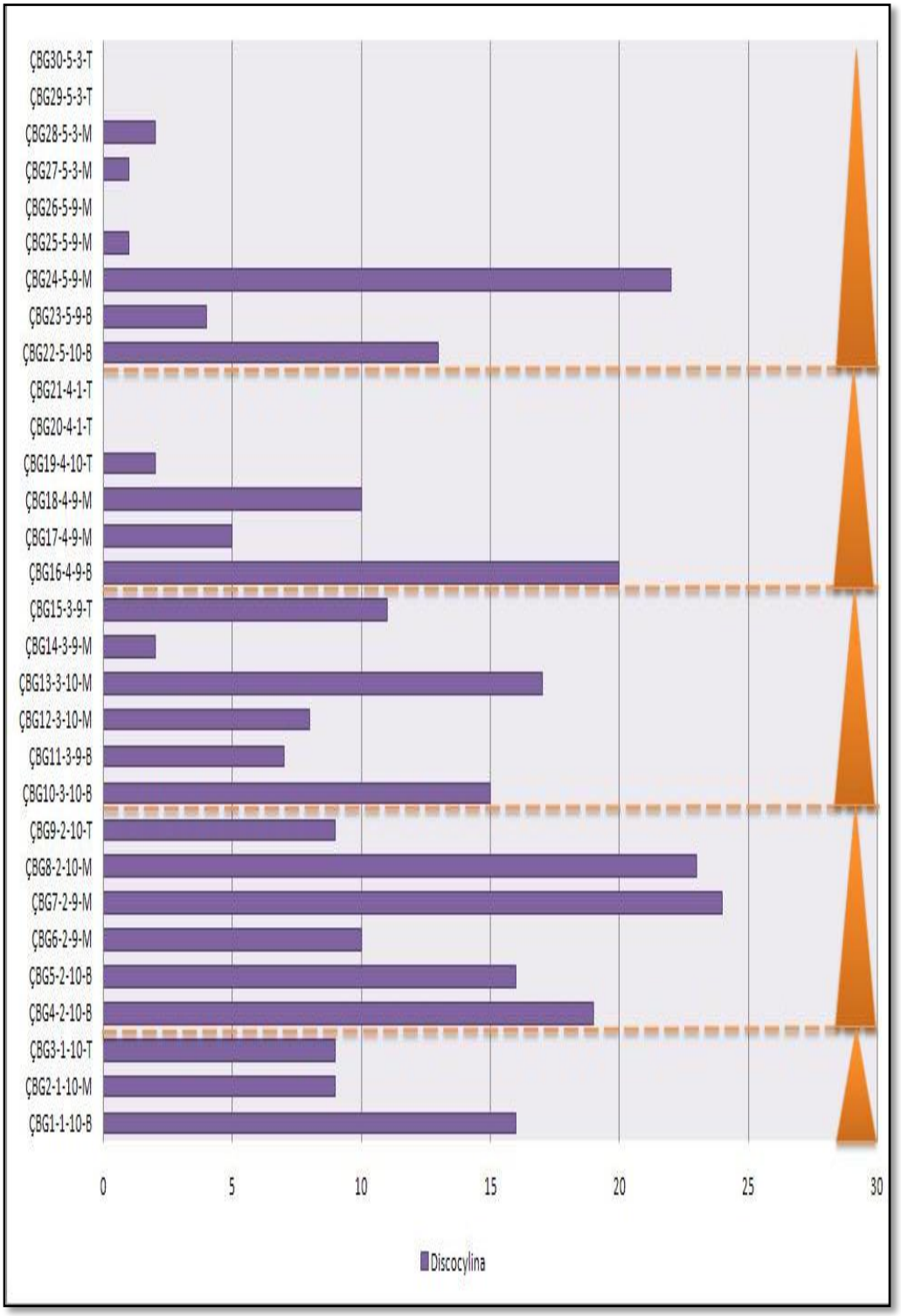

Figure 54. Distribution (in %) of *Discocyclina* in the meter scale cycles of the section 1.

According to the counting results of the *Alveolina* s.l. in section 1 (Figure 55), it is present just at the top and middle part of the last cycle of the section 2. It is is characterized by shallow water environment and it indicates that the last cycle of the section 1 is shallowing upward.

The response of *Alveolina* s.l. (Figure 56) and *Orbitolites* (Figure 57) are not present in all cycles but the disappearance of them after sample number HBG 15 towards top of the cycle 3 indicates that cycles after cycle 3 are deposited relatively in a deeper environment.

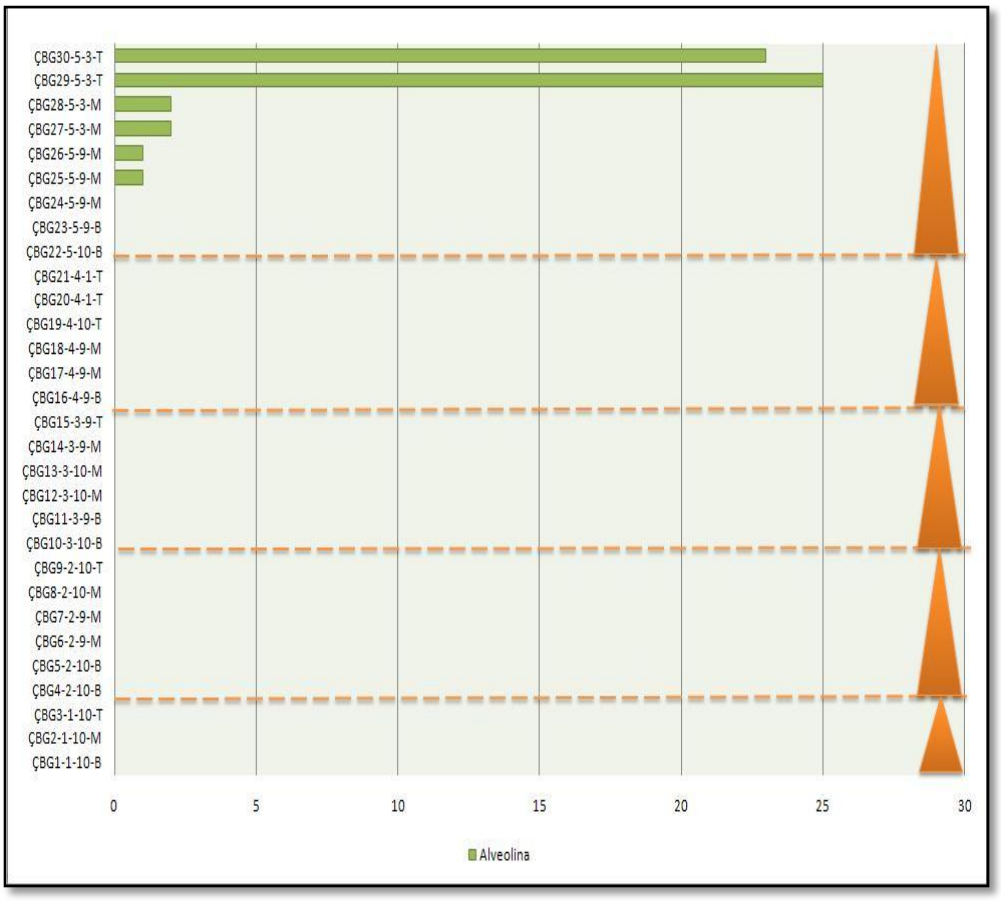

Figure 55. Distribution (in %) of *Alveolina* s.l. in the meter scale cycles of the section 1.

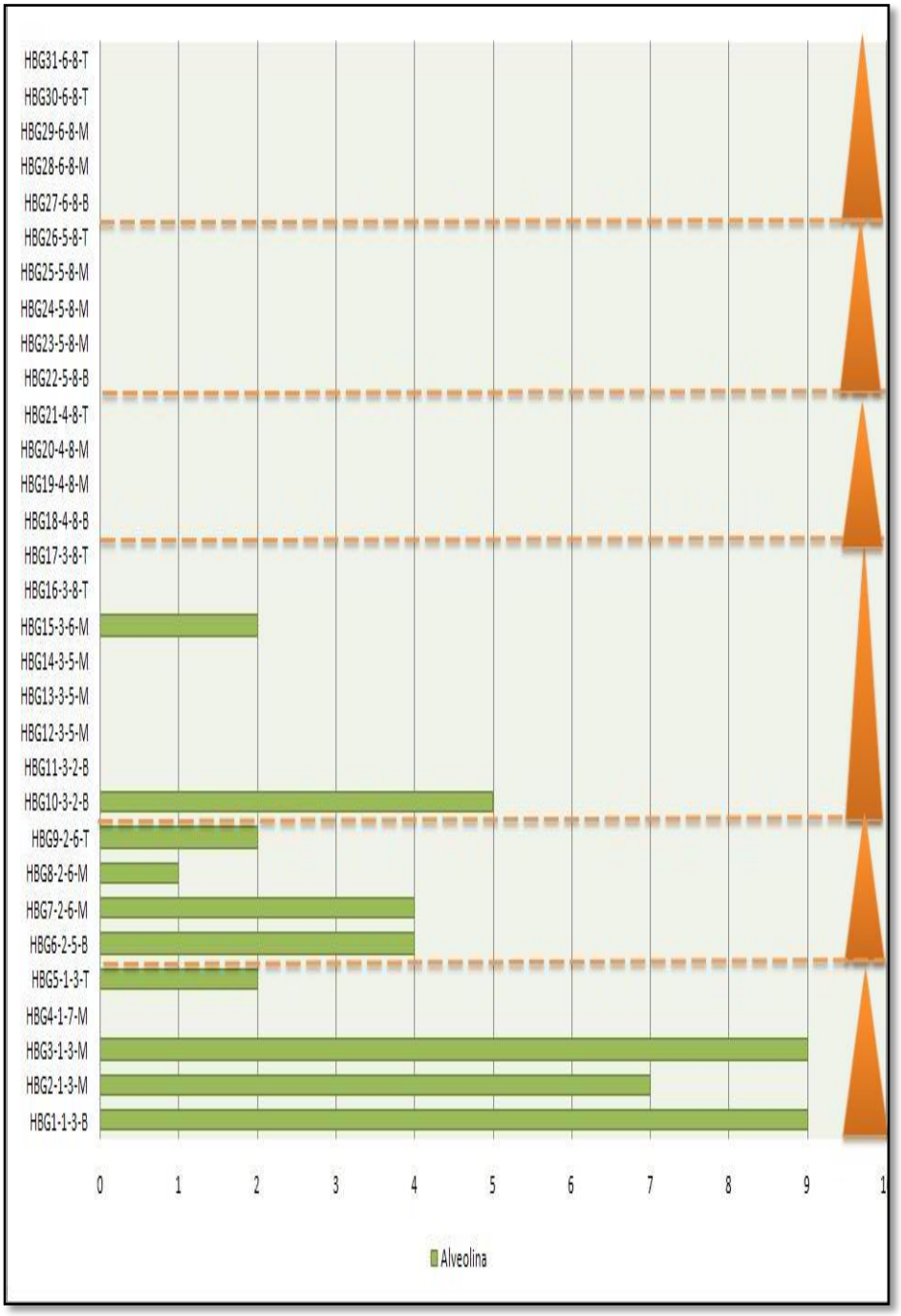

Figure 56. Distribution (in %) of *Alveolina* s.l. in the meter scale cycles of the section 2.

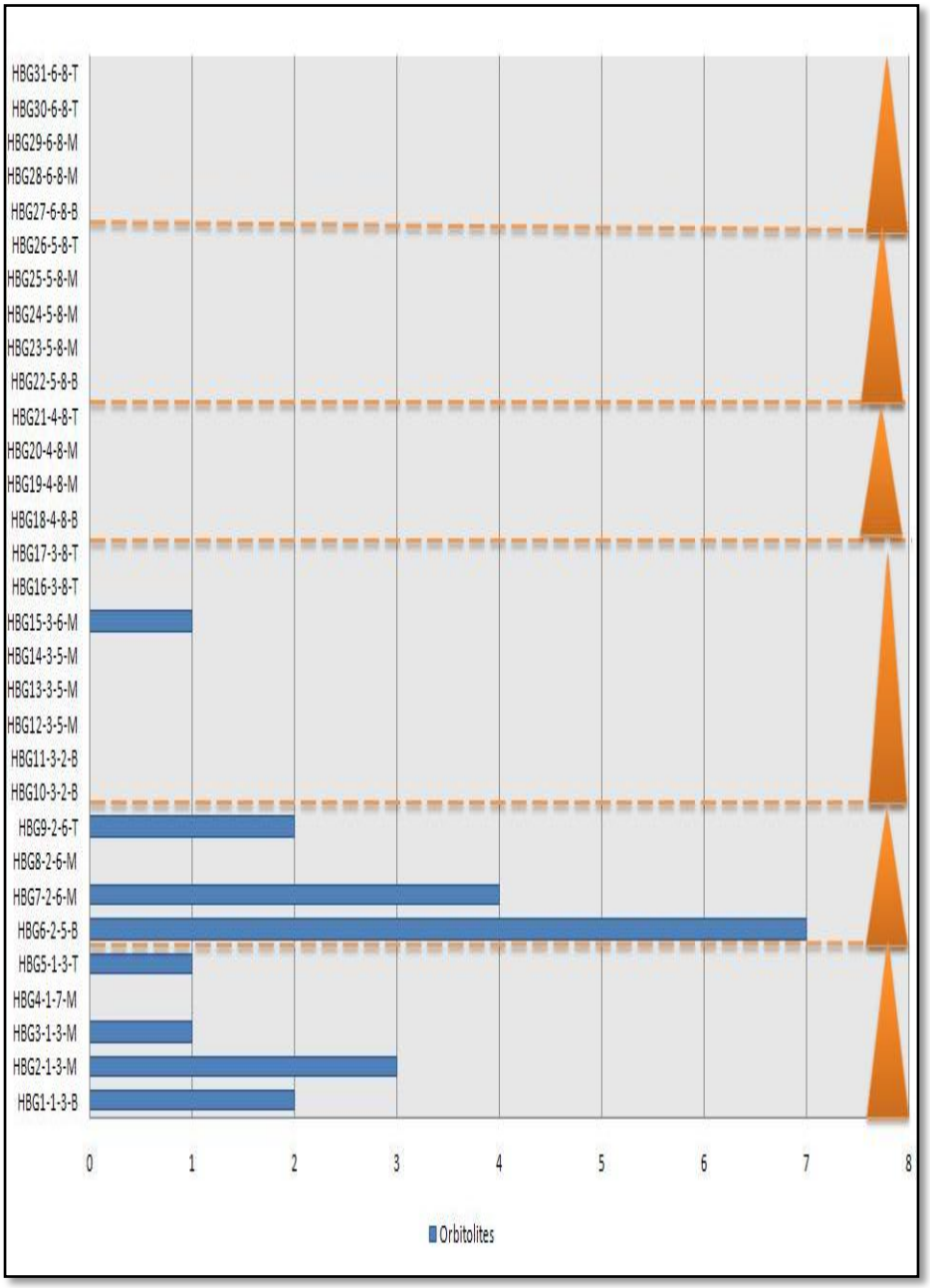

Figure 57. Distribution (in %) of *Orbitolites* in the meter scale cycles of the section 2.

The other groups do not give any remarkable response. Due to the dominance of *Nummulites* they are not abundant in all cycles. However they display a good role in the component analysis by determining paleoenvironmental distribution of the cycles.

4.3. Statistical Applications

In the twenty first century paleontology becomes a quantitative science and there is a need to know both statistical procedures and analytical methods for paleontological problems. Therefore, in this study cluster analyses were done by using the multi varied statistical package program. Cluster Analysis is a classification method that is used to arrange a set of cases into clusters. The aim in this analysis is to establish a set of clusters such that cases within a cluster are more similar to each other than they are to cases in other clusters. It should be emphasized that cluster analysis, unlike a formal statistical technique, is a typical method for data exploration and visualization. It is based on a given distance or similarity measure. Selection of a distance or similarity measure depends on type of data and other considerations (Hammer and Harper, 2006).

Cluster analysis is much more common than other methods and it is followed by principal coordinate analysis, principal components analysis and non-metric multidimensional scaling, all of that give two dimensional distribution of samples and species.

Because the purpose of cluster analysis is to assemble observations into relatively homogenous groups or clusters, the members of which are at once alike and at the same time unlike members of other groups, in this study, Q mode cluster analysis, which is grouping of variables and R mode cluster analysis, which is grouping of taxa, have been applied to counted forms in order to see the response of foraminifera to cylicity (Figure 58-61). Correspondance analysis which is a useful statistical technique that has found

application in fields such as face recognition and image compression, and is a common technique for finding patterns in data of high dimension, has been also applied to the counted forms for detecting paleoenvironmental controls on the distribution of the forms (Figure 62-63).

In figure 58, which is prepared based on the Q-mode cluster analysis of section 1, we obtained two clusters and three subclusters. According to cluster 1 and subcluster 1, which is shown in purble colour, indicates that MF 1 is the most different microfacies. This microfacies is characterized by apsence of *Nummulites,* within the whole section. The second cluster has two subclusters. First subcluster, which is shown in red colour, indicates the second different microfacies MF 3. MF 3 is deposited relatively shallower environment than the others since in section 1 MF 1 and MF 3 are represented by lagoonal setting and MF 10 and MF 9 are represented by shallow open marine setting. The other subcluster which is in green colour indicates relatively deeper depositional environment for section 1.

The R-mode cluster analysis of the section 1 (Figure 59) shows two clusters and three subclusters according to the depositional environments (deep and shallow) of the foraminiferal associations. First cluster reflect the forms (*Nummulites, Operculina, Assilina* and *Discocyclina*) that lived relatively in deeper environment than the other foraminiferal groups and *Operculina, Assilina* and *Discocyclina* lived relatively deeper environment than *Nummulites* ,which is shown in green and orange coloured subclusters. The environmental differences of the orher forms from *Nummulites, Operculina, Assilina* and *Discocyclina* are determined by red coloured subcluster and cluster. These forms lived relatively shallower than *Nummulites*, *Operculina*, *Assilina* and *Discocyclina*.

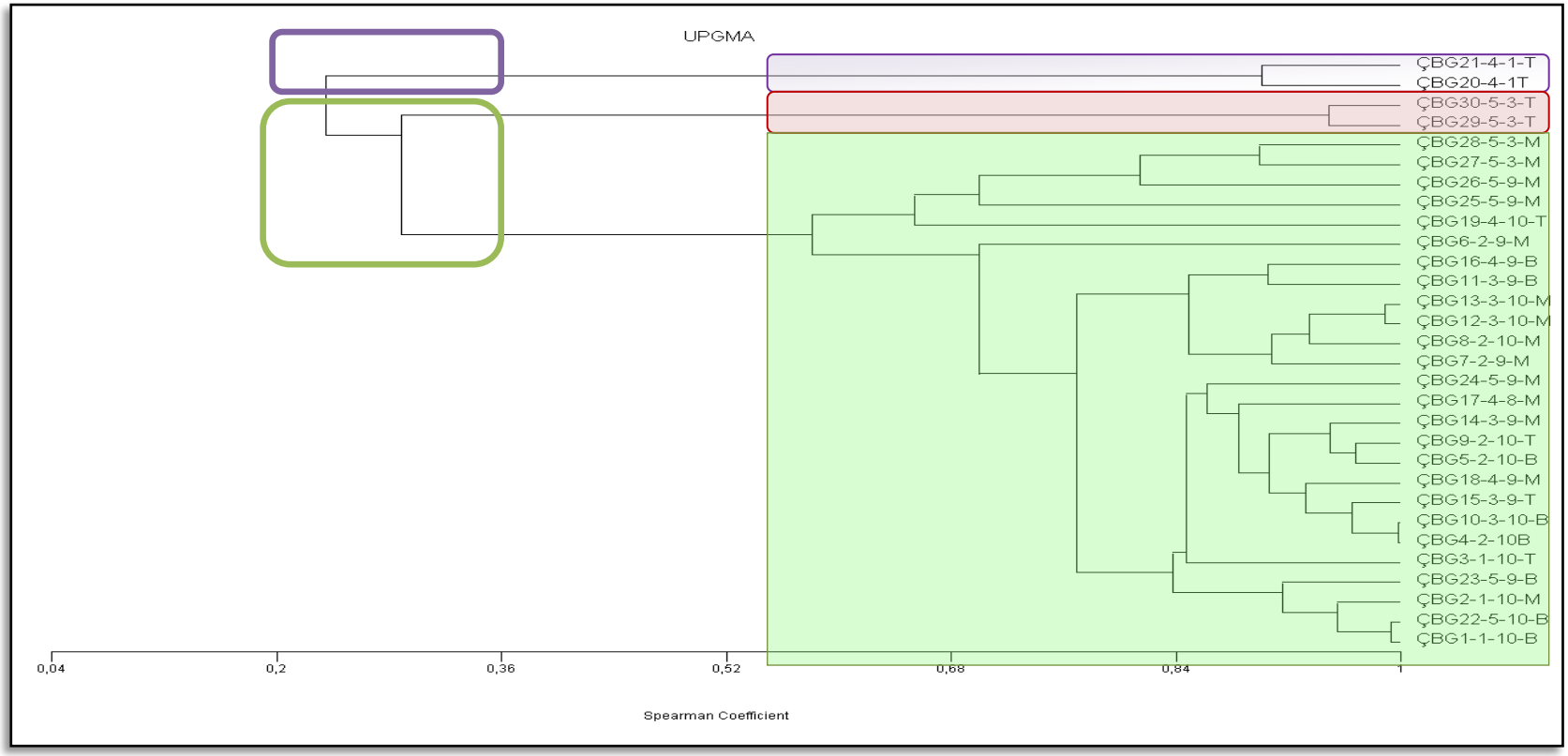

Figure 58. Dendrogram resulting from a Q-mode cluster analysis based on the relative abundance of the most frequent taxa in 30 variables (samples) from section 1, using the Spearman Coefficient method for agglomeration.

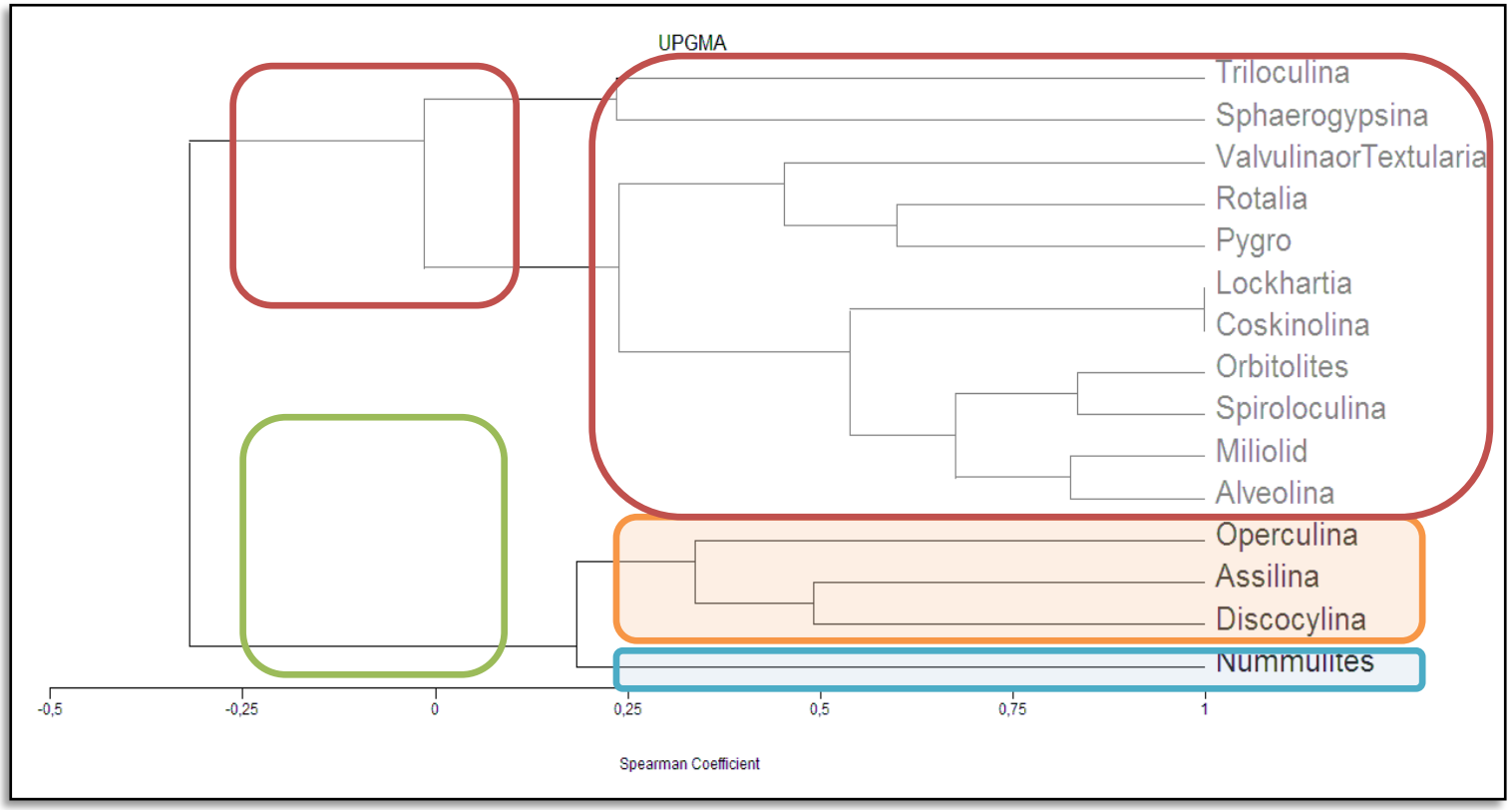

Figure 59. Dendrogram resulting from a R-mode cluster analysis based on the relative abundance of the most frequent taxa in 30 variables (samples) from section 1, using the Spearman Coefficient method for agglomeration.

The Q-mode cluster analysis of section 2 shows a grouping into two clusters, cluster A and cluster B (Figure 60) based on the microfacies data. According to cluster A, MF 8 should be deposited different environment than the other microfacies and the defininition such a microfacies is necessary. It means that MF 8 represents relatively deeper depositional facies than the other microfacies in Cluster B which consists of MF 4, MF 7, MF 5, MF 6 and MF 2, which are deposited relatively shallower environment. This analysis support the composite depositional model suggested for the studied area in Figure 29 interms of vertical facies distribution.

The R-mode cluster analysis of section 2, which is clustering data with respect to genera distribution (Figure 61) indicates that *Nummulites* (red coloured subcluster) is the dominant group within the cycles, *Assilina* (blue coloured subcluster) is second dominant group and the third dominant group is *Rotalia* (orange coloured subcluster). The distribution of other groups is almost the same (green coloured subcluster).

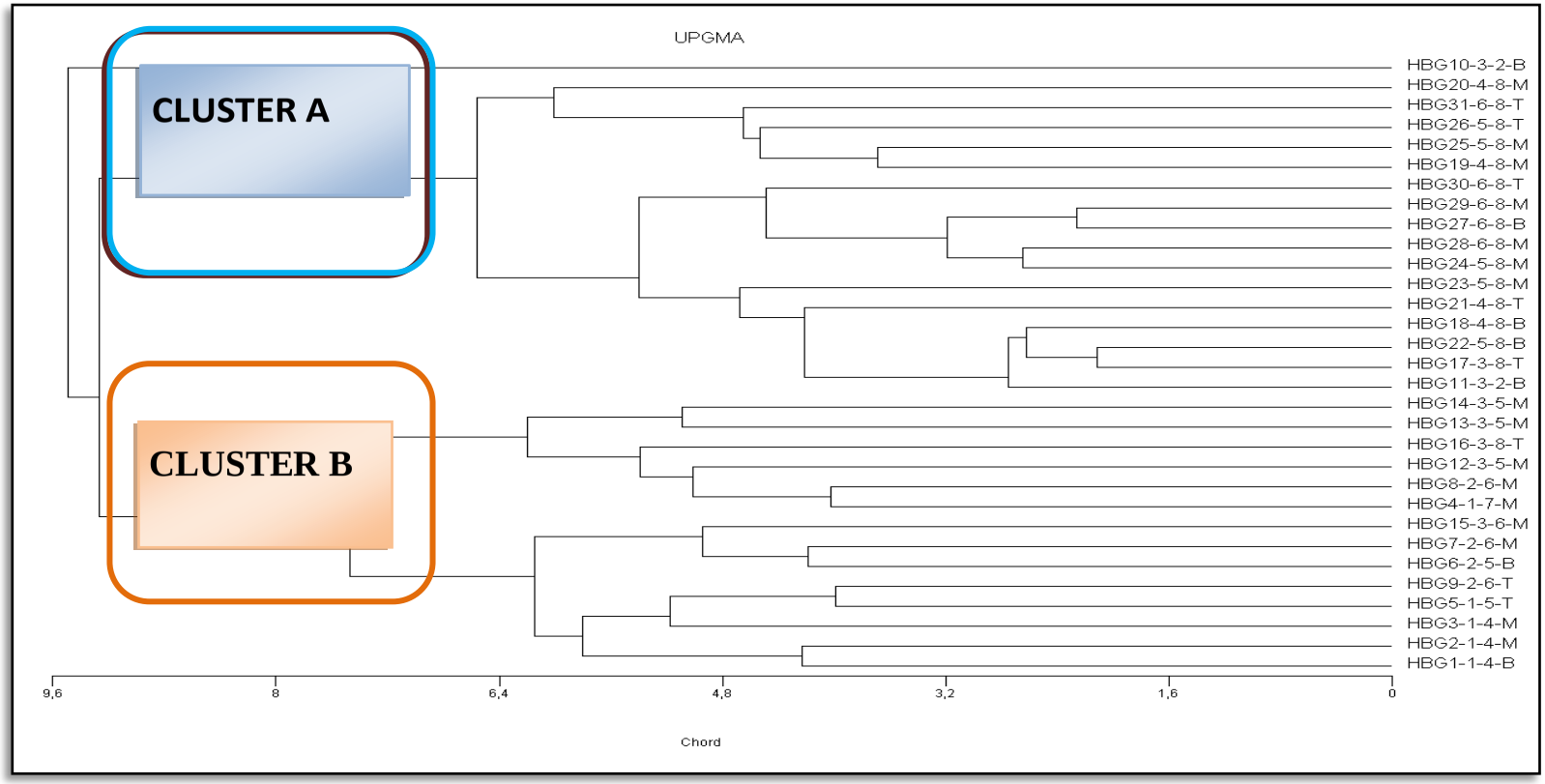

Figure 60. Dendrogram resulting from a Q-mode cluster analysis based on the relative abundance of the most frequent taxa in 31 variables (samples) from section 2, using the Chord method for agglomeration.

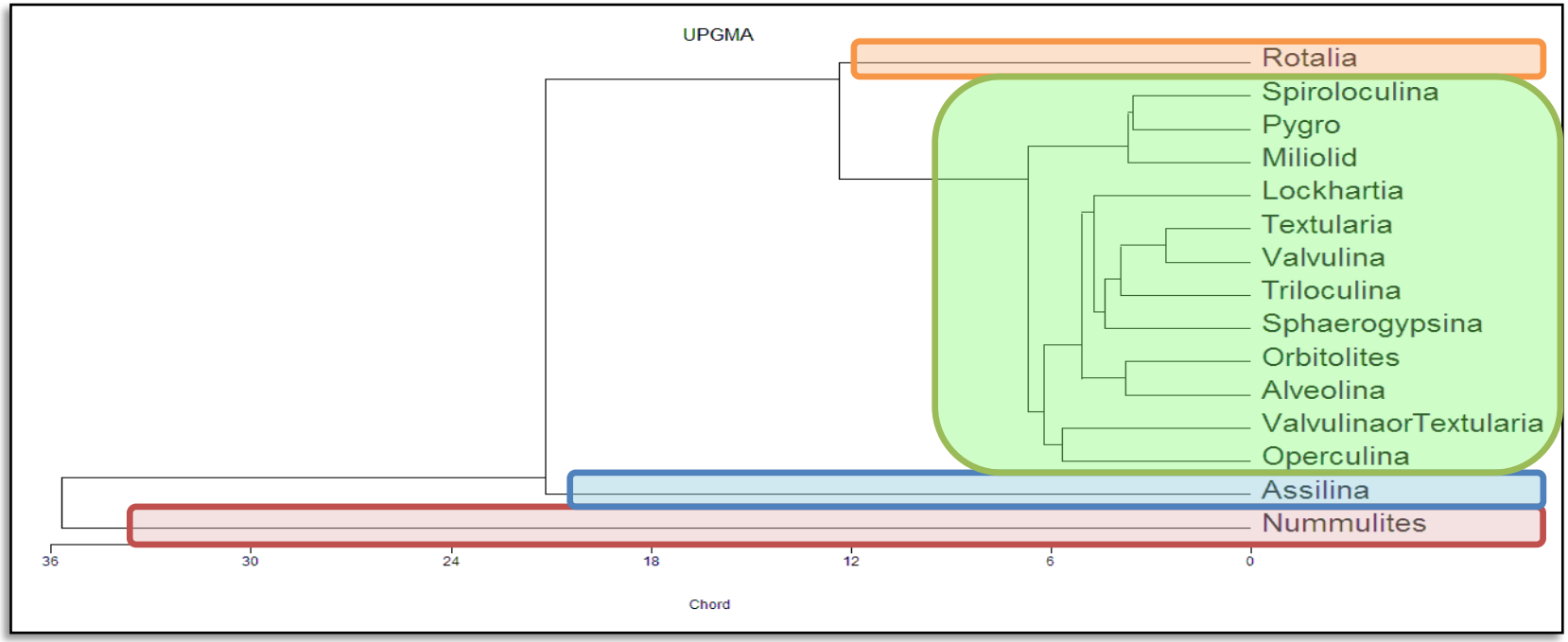

Figure 61. Dendrogram resulting from a R-mode cluster analysis based on the relative abundance of the most frequent taxa in 31 variables (samples) from section 2, using the Chord method for agglomeration.

Correspondance analysis, which is a method of factoring categorical variables and displaying them in aproperty space, groups values that are close together. In this study, correspondance analysis based on case scores and variable scores, which indicates the paleoenvironmental distribution of the forms and also cycles (Figure 62-63) are used. In figure 62, there are three groups. First and second group red and green coloured reflect shallower environmental microfacies and third group blue colored reclect relatively deeper environment.

In figure 63 we obtained four group of forms. First group *Coskinolina* as in figure 26, which indicates the idealized foraminiferal environmental distribution in early-middle Eocene by classifying foraminifera into 5 groups: *Coskinolina* and miliolids distributed in the inner shelf platform, *Alveolina* distributed in the inner shelf platform near edge *Nummulites* distributed in the edge, planktonic and benthic foraminifera distributed in the slope and planktonic foraminifera distributed in the basin, in the previous chapter characterizes the shallowest depositional environment and fourth group *Discocyclina* represents the deepest depositional environment. The other groups represent forms deposited in between these two environments.

To sum up, the foraminiferal assemblages display good response to sedimentary cyclicity and benthic foraminiferal associations provide useful information for paleoenvironmental reconstructions. Detailed examination of benthic foraminifera, counting and identification of different foraminiferal associations, provide an excellent data for the recognition of different paleoenvironments. Moreover, changes in frequency and distribution of benthic foraminifera are useful in reconstructing the sea level changes and sequence stratigraphy of a given area.

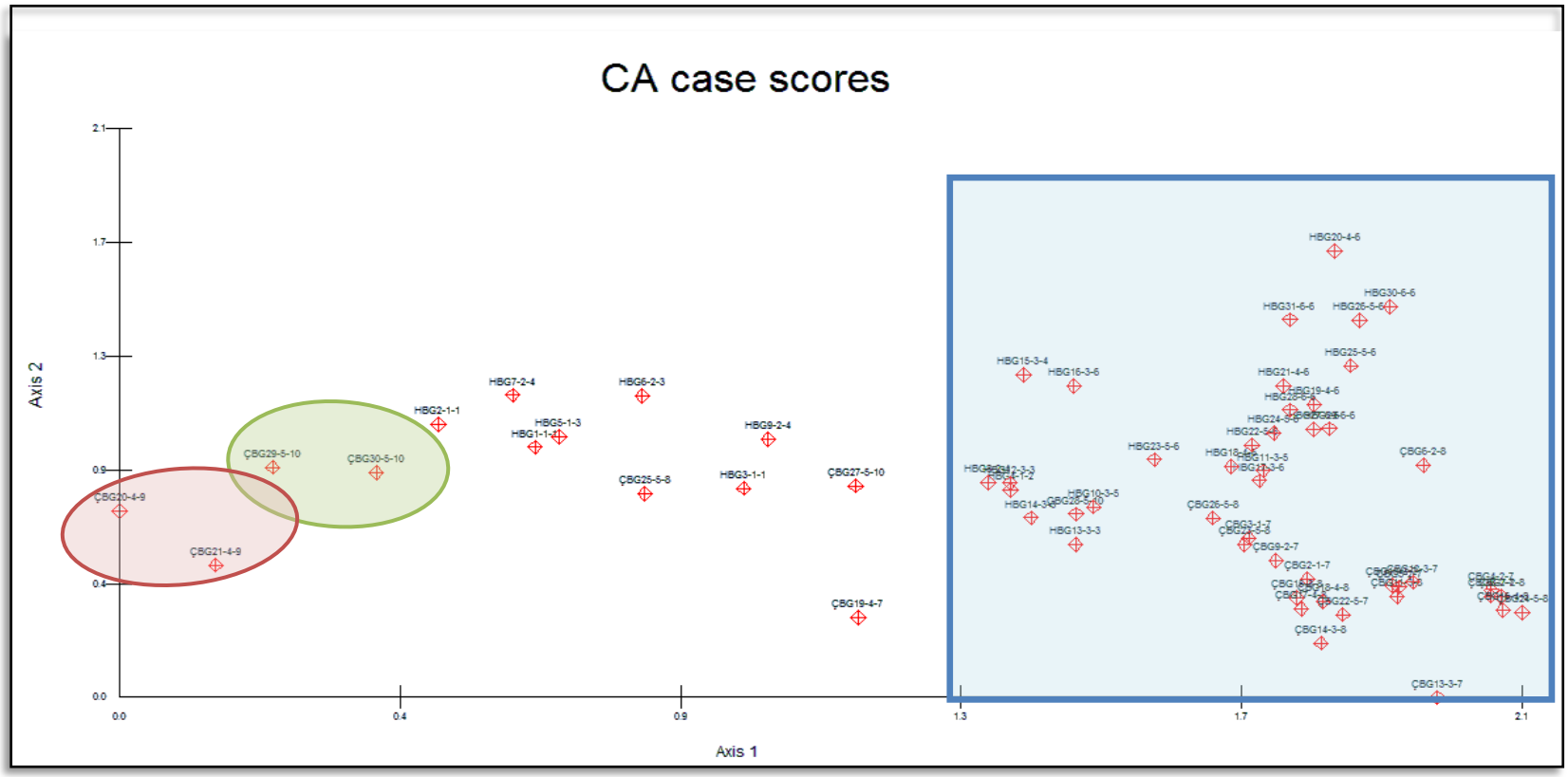

Figure 62. CA plot showing the distribution of 61 samples in axes 1 and 2 in relation to the paleoenvironmental parameters.

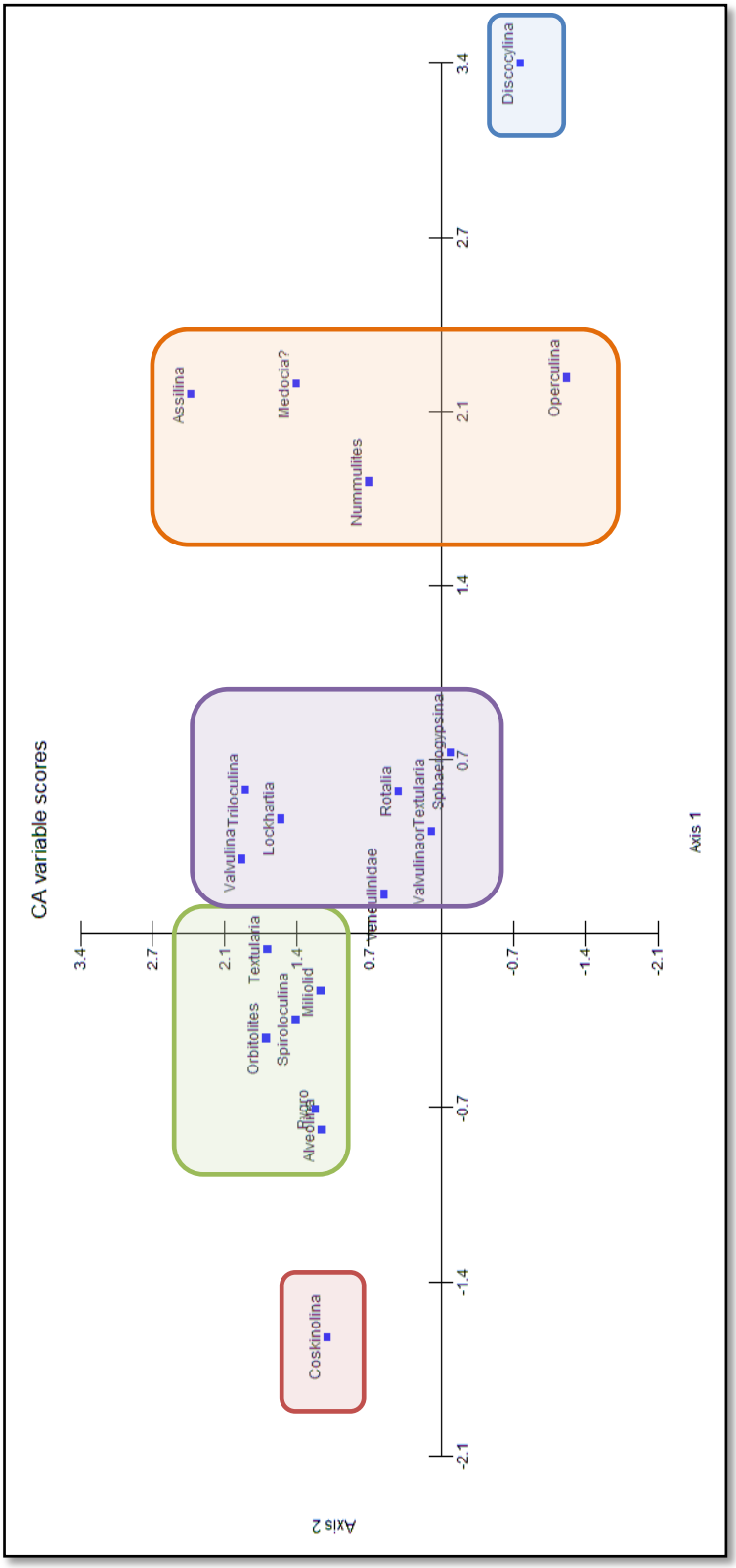

Figure 63. CA plot showing the distribution of 61 samples in axes 1 and 2 in relation to the paleoenvironmental parameter.

CHAPTER 5

DISCUSSIONS AND CONCLUSIONS

In the Haymana Basin, two stratigraphic sections, which are 44,55 m and 25,95 m in thickness, were measured within the Middle Eocene Çayraz Formation, mainly composed of carbonates and siliciclastics. The aim of this study is to investigate the nature of the shallowing upward meter-scale cycles and to study the response of foraminifera to the cyclicity.

The measured sections are within the two shelf systems, lower and upper shelf systems of the formation (Çiner 1993). Section 1 is measured in the uppermost part of the lower shelf system and begins with limestones with *Nummulites* and *Discocyclina* and continues with clayey limestones with *Nummulites* and *Discocyclina* and greenish marl-clayey limestones with *Nummulites* alternations and finishes with limestones with *Nummulites* and *Alveolina*. Section 2 is measured within the upper shelf system and is composed of limestones with *Nummulites* and *Alveolina* and continues upward with marl-clayey limestones with *Nummulites* alternations and with limestones with *Nummulites*.

Detailed microfacies analyses were carried out on the samples collected from studied sections in order to define the nature of meter scale cycles of the Çayraz Formation. Ten different microfacies types defined strictly based on the biofacies are mudstone to wackestone with small benthic foraminifera (MF 1); benthic foraminiferal wackestone (MF 2); bioclastic, alveolinid, nummulitid packstone with abundant small and large benthic foraminifera (MF 3); bioclastic, alveolinid, nummulitid wacke to packstone with abundant small and large benthic foraminifera (MF 4); bioclastic, alveolinid, nummulitid wackestone with abundant small and large benthic foraminifera (MF 5);

bioclastic, assilinid, nummulitid wacke to packstone with abundant small and large benthic foraminifera (MF 6); bioclastic nummulitid packstone with abundant small and large benthic foraminifera (MF 7); bioclastic, assilinid, nummulitid packstone (MF 8); bioclastic, discocyclinid, nummulitid packstone (MF 9) and bioclastic, discocyclinid, nummulitid packstone with red algae (MF 10).

Based on detailed microfacies analyses and the vertical distribution of the microfacies a composite depositional model is suggested. According to this model, three major facies associations were distinguished, from deepest to shallowest, as: shallow open marine, shoal and lagoon. These three environments are represented by ten microfacies. The shallow open marine part is reperesented by bioclastic, discocyclinid, nummulitid packstone with red algae microfacies (MF 10) and bioclastic, discocyclinid, nummulitid packstone microfacies (MF 9). The shoal part is associated with bioclastic, assilinid, nummulitid packstone (MF 8), bioclastic nummulitid packstone with abundant small and large benthic foraminifera (MF 7), bioclastic, assilinid, nummulitid wacke to packstone with abundant small and large benthic foraminifera (MF 6), bioclastic, alveolinid, nummulitid wackestone with abundant small and large benthic foraminifera (MF 5), bioclastic, alveolinid, nummulitid wacke to packstone with abundant small and large benthic foraminifera (MF 4), at the lagoon part is characterized by bioclastic, alveolinid, nummulitid packstone with abundant small and large benthic foraminifera (MF 3), benthic foraminiferal wackestone (MF 2), mud to wackestone with small benthic foraminifera (MF 1).

In this study, distribution of foraminifers and facies data of shallowing upward cycles (parasequences) were used for sequence stratigraphic interpretation. Based on the vertical evolution of microfacies and the stacking pattern of meter-scale cycle types within the sections two system tracts were recognized, each belonging to one of the measured sections. According to this,

section 1 is represented by a high stand systems tract (HST) deposits whereas the section 2 is represented by a transgressive systems tract (TST) deposit.

Quantitative and statistical analyses are carried out to determine the biological response to the cyclicity. In order to perform this study benthic foraminiferal taxa were classified into twenty one different groups and for the generic subdivision the classification of Loeblich and Tappan (1988) was followed. The foraminifera groups used in the countings are *Nummulites* sp., *Discocyclina* sp., *Assilina* sp., *Operculina* sp., *Alveolina* sp., *Sphaerogypsina* sp., miliolid, *Pygro* sp., *Triloculina* sp., *Spiroloculina* sp, *Coskinolina* sp., *Orbitolite*s sp., *Lockhartia* sp., biserialy to uniserialy coiled forms, *Medocia?* sp., *Valvulina* sp., *Textularia* sp., *Valvulina* sp. or *Textularia* sp., *Rotalia* sp., Verneulinidae and others (unidentified textularid, miliolid and rotalid forms). *Nummulites* is the most abundant foraminiferal group in both sedimentary cycles than the other groups in the measured sections and displays good response to the cyclicity. According to this the counted results *Nummulites* has different response to shallowing and deepening cycles. *Nummulites* shows increasing trend toward the top of the cycle in the deepening cycles and decreasing trend toward the top of the cycle in the shallowing cycles. According to counted results, *Assilina* like *Nummulites* has different response to shallowing and deepening cycles. But the responses of *Assilina* and *Nummulites* is incompatible. *Discocyclina* is present only in section 1 and it is characterized by shallow open marine. Therefore the presence of it indicates deposition environment of cycles within the section 1 is more deeper than cycles in section 2. *Alveolina* s.l. and *Orbitolites* are not present in all cycles and the disappearance of them indicates that cycles are deposited relatively in a deeper environment.The other groups do not give any remarkable response. Due to the dominance of *Nummulites* they are not abundant in all cycles. However they display a good role in the component analysis by determining paleoenvironmental distribution of the cycles. In addition, Q mode cluster analysis and R mode cluster analysis were applied to counted forms in order to

see the response of foraminifera to cylicity. Component analysis were also applied to the counted forms for detecting paleoenvironmental controls on the distribution of them. These statistical analysis support the composit depositional model suggested for the studied area.

As a recomendation for further studies, it can be suggested to examine the whole part of the Çayraz Formation by measuring additional stratigraphic sections in order to construct the sequence stratigraphic framework of the formation.

REFERENCES

Adabi M. H., Zohdi A., Ghabeishavi A., Amiri-Bakhtiyar H., 2008. Applications of nummulitids and other larger benthic foraminifera in depositional environment and sequence stratigraphy: an example from the Eocene deposits in Zagros Basin, SW Iran. Facies 2008, Volume 54, P: 499–512.

Acar A., Sarı A., Sonel N and Aliyev S., 2007. Source Rock Characterization and Depositional Environment of the Late Cretaceous Haymana Formation in the Salt Lake Basin of Turkey. Energy Sources, Part A: Recovery, Utilization, and Environmental Effects, 29: 3, 277 – 291.

Akarsu İ., 1971. II. Bölge AR/TPO/747 nolu sahanın terk raporu. Pet. İş. Gen. Md., Ankara. Dergisi, 85, 17-38.

Allen J., G. Ferguson and A. Stent, "An Architecture for More Realistic Conversational Systems", Proc. of Intelligent User Interfaces *(IUI-01)*, Santa Fe, NM 2001.

Arıkan Y., 1975. Tuzgölü havzasının jeolojisi ve petrol imkanları. MTA Dergisi, 85, 17-38.

Armentrout, J. M., 1987. Integration of Biostratigraphy and Seismic Stratigraphy, Gulf of Mexico. Society of Economic Paleontologists and Minerologists, 8. Anual Research Conferance, 6-14.

Bailey E. B. and Mccallien W. J. 1953. Ankara me1ange and the Anatolian Thrust. Trans. Roy. Soc. Edinburgh. 62, 403-42.

Beavington-Penney S., Wright V., Racey A., 2006. The Middle Eocene Seeb Formation on Oman: an investigation of a cyclicity, stratigraphic completeness, and accumulation rates in shallow marine carbonate setting. Journal of Sediment Res. 76:1137–1161.

Borer J.M. and Haris P.M., 1991. Depositional facies and cyclicity in the Yates Formation, Permian Basin- Implications for reservoir heterogeneity, American Association of Petroleum Geologists Bulletin,v.75,p.726-779.

Burollet P. F., 1956. Contribution à l' étude stratigraphique de la Tunisie Centrale : Annales Mines Géologie, v. 18, 345 p.

Buxton M., Pedley H. 1989. Short paper: a standardised model for Tethyan Tertiary carbonate ramps. J Geol Soc 146:746–748.

Bush R.M. and West, R.R., 1987. Hierarchal genetic stratigraphy: a framework for paleoceanography. Paleoceanography, 2: 141-164.

Chaproniere G., 1975. Palaeoecology of Oligo-Miocene larger foraminiferida, Australia. Alcheringa 1:37–58.

Chaput E., 1932. Observations géologiques en Asie Mineure: Le Crétacé supérieur dans l'Anatolie Centrale. C. R. A. S., 194, 1960-1961.

Chaput E., 1935a. L'Eocene du plateau de Galatie (Anatolie Centrale). C. R. A. S.,200, 767-768.

Chaput E., 1935b. Les plissements Tertiare de l'Anatolie Centrale. C. R. A. S., 201, 1404-1405.

Chaput E., 1936. Voyages d'études géologiques et géomorphologiques en Turquie. Mém. Inst. Françaiş D'Archaéo. İstanbul, II, 312 p.

Catuneanu O., 2002. Sequence stratigraphy of clastic systems: concepts, merits, and pitfalls. Journal of African Earth Sciences., 35, 1, 1-43.

Catuneanu O (2006) Principles of sequence stratigraphy. Elsevier, New York, p 386.

Catuneanu O. *et al.*, 2008. Towards the standardization of Sequence stratigraphy. Earth Science Reviews (2008).

Çiner A., 1992. Sediméntologie et stratigraphie séquentielle du bassin.d'Haymana à l'Eocene moyen Turquie. Doktora Tezi, l'Univ. Louis Pasteur, Fransa, 190 s.

Çiner A., 1993. Geology of Haymana Basin (U. Cretaceous – M. Eocene); Central Anatolia, Turkey. 6th International Meeting and Training School on IGCP Project 269, Middle East Technical University, Field Trip Guide Book, 21 s.

Çiner A., 1996. Distribution of small scale sedimentary cycles throughout several selected Basins, Tr. J. of Earth Sciences, 5, 25-37.

Çiner A., Deynoux M., Koşun E. ve Gündoğdu N., 1993. Yamak türbidit karmaşığının (YTK) sekansiyel stratigrafik analizi: Haymana Baseni (Orta Eosen). Sekans Stratigrafisi, Sedimantoloji Çalışma Grubu Özel Yayını, 1, 53-70.

Çiner A., Deynoux M., Koşun E. ve Gündoğdu N., 1993. Beldede örgülü-delta karmaşığının (BÖDK) sekans stratigrafik analizi: Polatlı-Haymana baseni (Orta Eosen) Orta Anadolu. Yerbilimleri, 16, 67-92.

Çiner A., Deynoux M., Ricou S. ve Koşun E., 1993. Cyclicity in the middle Eocene Çayraz Carbonate Formation, Haymana Basin, Central Anatolia.Palaeogeography, Palaeoclimatology, Palaeoecology, 121, 313-329.

Çiner A., Deynoux M. ve Koşun E., 1996. Cyclicity in the Middle Eocene Yamak turbidite complex of the Haymana basin, Central Anatolia, Turkey. Geol. Rundschau., 85, 669-682.

Crevello, P.D. 1001, High-frequency carbonate cycles and stacking patterns:interplay of orbital forcing and subsidence of Lower Jurassic rift platforms, High Atlas, Morocco in Franseen E. K., Watney W. L., Kendall C. G. St. C., and Ross W., eds., Sedimentary modeling: computer simulations and methods for improved parameter definition:Kansas Geological Survey Bulletin 233, p.207-230.

Dağer Z., Öztümer E., Sirel E. ve Yazlak Ö., 1963. Ankara civarında birkaç stratigrafik kesit. TJK Bülteni, 8/1-2, 84-95.

Dickinson, S.R. and Selly, D.R., 1979. Structure and stratigraphy of forearc regions. AAPG Bull., 63: 67-94.

Dizer A., 1964. Sur quelques alveolines de l'Eocene de Turquie. Revue de Micropaléontologie, 7, 265-279.

Dizer A., 1968. Etude micropaléntologique du nummulitique de Haymana (Turquie). Revue de Micropaléontologie, 11, 13-21.

Druitt C. E. ve Reckamp J. U., 1959. Çaldağ columnar section. TPAO Arşivi, Ankara.

Dunham R.J., 1962. Classification of carbonate rocks accor ding to depositional texture. In: Ham, W.E. (eds.): Classification of carbonate rocks. A symposium. Amer. Ass. Petrol. Geol. Mem., 1, 108-171.

Egeran N. ve Lahn E., 1951. Kuzey ve Orta Anadolu'nun tektonik durumu hakkında not. MTA Bülteni, 41, 23-28.

Einsele G., Ricken W. and Seilacher, A., 1991. Cycles and Events in Stratigraphy - basic concepts and terms. In: W. R. G. Einsele, W. Ricken & A. Seilacher (eds.), Cycles and Events in Stratigraphy, Berlin, Heidelberg, New York, Springer Verlag, 1-19.

Emery D., Myers K (1996) Sequence stratigraphy. Blackwell, Oxford, p 297.

Erol O., 1954. Ankara civarının jeolojisi hakkında rapor. MTA Ensitüsü, Rapor no 2491, Ankara.

Erol O., 1961. Ankara bölgesinin tektonik gelişmesi. TJK Bülteni, 7/1, 57-85.

Fisher A.G., 1964. The Lofer cyclothems of the Alpine Triassic. Kans. State Geol. Surv. Bull., 169: 107-149.

Flügel E., 2004. Microfacies of carbonate rocks: analysis, interpretation and application. Springer, 976 p.

Fourquin C., 1975. L'Anatolie du Nord Ouest, marge méridionale du continent Européen, histoire paléogéographique, technique et magmatique Durant le Secondaire et Tertiaire. Bull. Soc. Géol. Fr., (7) 2: 1058-1070.

Geel T., 2000. Recognition of stratigraphic sequences in carbonate platform and slope deposits: empirical models based on microfacies analysis of Palaeogene deposits in southeastern Spain. Palaeogeogr. Palaeoclimatol. Palaeoecol. 155:211–238.

Gez S., 1957. Dereköy-Haymana-Elifköy stratigrafik profilleri hakkında. MTA Enstitüsü, Rapor no. 2748, Ankara.

Gilham R., Bristow C., 1998. Facies architecture and geometry of a prograding carbonate ramp during the early stages of foreland basin evolution: lower Eocene sequences, Sierra del CadÌ, SE Pyrenees, Spain. Geol Soc Lond Spec Publ 149:181–203.

Ghose B., 1977. Palaeoecology of the Cenozoic reefal foraminifers and algae, brief review. Palaeogeogr Palaeoclimatol. Palaeoecol. 22:231–256.

Goldhammer R. K., Dunn, P. A. and Hardie, L. A., 1987. High frequency glacio-eustatic sea-level oscillations with Milankovitch characteristics recorded in Middle Triassic platform carbonates in northern Italy. Am. J. Sci., 287, 853-892.

Goldhammer R. K., Oswald E. J., and Dunn P. A., 1991. Hierarchy of stratigraphic forcing: Example from Middle Pennsylvanian shelf carbonates of Paradox Basin, in E. K. Franseen W.L., Watney, C.G., Kendall and W. Ross, eds., Sedimentary Modeling:Computer Simulations and Methods for Improved Parameter Definition,Kansas Geological Survey Bulletin 233,p.361-413.

Görür N. ve Derman A. S. (1978) – Stratigraphic and tectonic analysis of the Tuzgölü-Haymana basins. TPAO rap. 1514, 60 s.

Görür N., Oktay F.Y., Seymen, I., Sengör, A.M.C., 1984. Paleotectonic evolution of the Tuzgölü basin complex, Central Turkey: sedimentary record of a Neo – Tethyan closure. In: Dixon, J.E., Robertson, A.H.F., (eds) The geological evolution of the eastern Mediterranean. Geol Soc Lond, 467 - 482.

Görür N., Tüysüz O. ve Şengör A. M. C. (1998) – Tectonic evolution of the central Anatolian basins. International Geology Review, 40, 831-850.

Graubau A. W., 1936, Ossilation or pulsation: International Geological Congress, Report of the 16th Session, v. 1, p. 539-553.

Grotzinger J.P., 1986. Upward shallowing platform cycles: a response to 2.2 billion years of low-amplitude, high-frequency (Milankovitch band) sea-level oscillations. Paleoceanography 1, 403–416.

Grove W.K., Silverman, R.M., Rasmussen, R.D., Penfield, T.G., Gurnert, R.W., Grateral, V., 2000. AAPG Regional international conference, Istanbul Turkey.

Goldhammer R. K., Dunn, P. A. and Hardie, L. A., 1990. Depositional cycles, composite sea-level changes, cycle stacking patterns, and their hierarchy of stratigraphic forcing: examples from Alpine Triassic platform carbonates. Geol. Soc. of Am. Bull., 102, 663.

Goodwin P.W. and Anderson, E.J., 1985. Punctuated aggradational cycles: A general hypothesis of episodic stratigraphic accumulation. J. Geol., 93: 515-533.

Grotzinger J.P., 1986. Cyclicity and Paleoenvironmental Dynamics, Rocknest Platform, northwest Canada. Geol. Soc. Am. Bull. 97: 1208-1231.

Hallock P., Glenn E., 1986. Larger foraminifera: a tool for paleoenvironmental analysis of Cenozoic depositional facies. Palaios 1:55–64.

Hanford C. R. and Loucks R. G., 1993. Carbonate depositional sequences and systems tracts-responses of carbonate platforms to relative sea level changes in Loucks, R.G., and Sarg, J. F., (eds) Carbonate Sequence Stratigraphy Recent Developments and Applications, American Association of Petroleum Geologists, Memoir 57, p 3-41.

Haq, B. U., Hardenbol, J. and Vail, P. R., 1987. Chronology of fluctuating sea – level since the Triassic (250 million years to present). Science. Volume 235, 1156 – 1167.

Hammer, Ø., and Harper, D.A.T., 2006, Paleontological Data Analysis, Blackwell, 351 pp.

Hardie L.A., Bosellini A., Goldhammer R.K., 1986. Repeated subaerial exposure of subtidal carbonate platforms, Triassic, Northern Italy: evidence for high frequency sea-level oscillations on a 104 year-scale. Paleoceanography 1, 447–457.

Hottinger L., 1983. Processes determining the distribution of larger foraminifera in space and time. Utrecht Micropaleontol Bull 30:239–253.

Hottinger L., 1997. Shallow benthic foraminiferal assemblages as signals for depth of their deposition and their limitations. Bull Soc Geol Fr 168:491–505.

Hottinger L., 1998. Shallow benthic foraminifera at the Paleocene–Eocene boundary. Strata 9:61–64.

Hohenegger J., 2000. Coenoclines of larger foraminifera. Micro-paleontology 46:127–151.

Hüseyinov A., 2007. Sedimantary Cyclicity in the upper Cretaceous Successions of the Haymana Basin (Turkey): Depositional sequences as response to relative sea level changes. MS thesis, University of METU.

James N. P., 1979, Shallowing-upward sequences in carbonates, in Walker, R. G., ed., Facies Models: Geoscience Canada Reprint Series 1,Toronto, p.109-119.

James N.P., 1984. Shollowing-upward sequences in carbonates. In: RG.Walker (Editor), Facies Models. Geosci. Can. Repr. Ser., 1(2nd Ed.): 213-228.

Koçyiğit A., 1991. An example of an accretionary fore –arc basin from northern Central Anatolia and its implications for the history of subduction of Neo–Tethys in Turkey. Geol Soc Am Bull, 103, 22 - 36.

Koçyiğit A., Özkan S., Rojay F.B., 1988. Examples from the fore-arc basin remnants at the active margin of northern Neo –Tethys; development and emplacement ages of the Anatolian nappe, Turkey. J Pure Appl Sci Ankara, 21, 183 - 210.

Koçyiğit A. ve Lünel A. T. (1987) – Geology and tectonic setting of Alcı region, Ankara. METU Journal of Pure and Applied Sciences, 20, 1, 35-57.

Koershner W. F., and Read J. F., 1989. Field and modelling studies of Cambrian carbonate cycles, Virginia Appalachians, Journal of Sedimentary Petrology, v.59,p.654-687.

Lahn E., 1949. Orta Anadolu'nun jeolojisi hakkında, TJK Bülteni, 1, 1.

Lemoine P., 1911, Géologie du basin de Paris, Librairie SCI. Hermann ET FI.

Lokman K. ve Lahn D., 1946. Haymana bölgesi jeolojisi. MTA Dergisi, 36, 292-300.

Leutenegger S., 1984. Symbiosis in benthic foraminifera: specificity and host adaptations. J Foraminiferal Res 14:16–35.

Loucks RG, Moody RTJ, Bellis JK, Brown AA (1998) Regional depositional setting and pore network systems of the El Garia Formation (Metlaoui Group, Lower Eocene), offshore Tunisia. In: MacGregor DS, Moody RTJ, Clark-Lowes DD (eds) Petroleum Geology of North Africa. Geol Soc Lond Spec Pub 132:355–374.

Loeblich A.R., Jr., Tappan H., 1988. Foraminiferal Genera and Their Classification. Van Nostrand Reinhold, New York.

Luterbacher H., 1998. Sequence stratigraphy and the limitations of biostratigraphy in the marine Paleogene strata of the Tremp Basin (central part of the southern Pyrenean foreland basin, Spain. SEPM Spec Publ 60:303–309.

Maillet B. DE, 1748. Telliamed, ou Entreties d'un philosophe indien avec un missionaire français sur la diminution de la mer, la formation de la tere, l' origine de l' homme. Et Mise en ordre sur les mémoires de feu M. de Maillet, par J. A. G.: Amsterdam, Chez l' Honoré et Fils, v. 1, 208 p. and v. 2, 231 p.

Meriç E. ve Görür N., 1979-80. Haymana-Polatlı havzasındaki Çaldağ kireçtaşının kireçtaşının yaş konağı. MTA Dergisi, 93/94, 137-142.

Mithchum R. M., Vail P. R. and Thomson, S., 1977. Seismic stratigraphy and global changes of sea level, part 2: The depositional sequences as a basic unit of for stratigraphic analysis. Applications to Hydrocarbon Exploration: Association of Petroleum Geologist Memoir, 26, 53-62.

Norman T., Gökçen S. L. ve Şenalp M., 1980. Sedimentation pattern in Central Anatolia at the Cretaceous-Tertiary boundary. Cretaceous Research, 1, 61-84.

Norman T., 1973. Ankara Yahşıhan bölgesinde Üst Kretase-Alt Tersiyer sedimantasyonu. TJK Bülteni, 16, 41-66.

Osleger D.A., Read J.F., 1992. Relation of eustasy to stacking patterns of meter scale carbonate cycles, Late Cambrian, USA. Special Issue on Orbital Forcing and Sedimentary Sequences, Journal of Sedimentary Petrology 61, 1225–1252.

Özcan E., Özkan, S.A., 1997. Late Campanian – Maastrichtian evolution of orbitoidal foraminifera in Haymana Basin successions (Ankara, Central Turkey). Revue Paleobiol., Geneve, 16, (1), 271 – 290.

Özcan E., Özkan, S.A., 1999. The genera *Lepidorbitoides* and *Orbitoides:*evolution and stratigraphic significance in some Anatolian basins. GeologicalJournal, 34, 275 – 286.

Özcan E., Özkan, S.A., 1999. The Genus Lepidorbitoides: Evolution and Stratigraphic Significance in some Anatolian Basins (Turkey). Revue de Micropaleontologie, 42, 111-131.

Özkan S.A., Özcan, E., 1999. Upper Cretaceous planktonic foraminiferal biostratigraphy from NW Turkey: calibration of the stratigraphic ranges of larger benthonic foraminifera Geological Journal, 34, 287 – 301.

Özcan E., Özkan, S.A., 2001. Description of an early ontogenetic evolutionary step in Lepidorbitoides: Lepidorbitoides bisambergensis asymmetrica subsp. n., Early Maastrichtian (central Turkey) Rivista Italiana di Paleontologia e Stratigrafia, 107, 137-144.

Özcan E., Sirel E., Özkan S.A. and Çolakoğlu S., 2001. Late Paleocene Orthophragminae (foraminifera) from the Haymana – Polatli Basin, (central Turkey) and description of a new taxon, *Orbitoclypeus haymanaenis* Micropaleontology, 47, 339 - 357.

Özcan E., 2002. Cuisian orthophragminid assemblages (*Discocyclina*, *Orbitoclypeus* and *Nemkovella*) from the Haymana-Polatlı Basin (central Turkey): biometry and description of two new taxa. Eclogae geol. Helv., 95, 75-97.

Özcan E., Gyorgy L. and Botond K., 2007. Late Ypresian to Middle Lutetian Orthophragminid Record From Central and Northern Turkey: Taxonomy and Remarks on Zonal Scheme. Turkish Journal of Earth Sciences (Turkish J. Earth Sci.), Vol. 16, pp. 281−318.

Pomar L., 2001. Ecological control of sedimentary accommodation: evolution from a carbonate ramp to rimmed shelf, Upper Miocene, Balearic Islands. Palaeogeography, Palaeoclimatology, Palaeoecology, 175: 249-272.

Posamentier H. W., Jervey M. T. and Vail P. R. 1988. Eustatic controls on clastic Deposition I-Conceptual framework. Sea-Level Changes-An Integrated Approach. The Society of Economic Paleontologist and Minaralogist, Special Publication , 42, 109-124.

Pratt B. R., James N. P., and Cowan C. A., 1992. Peritidal Carbonates, in Walker R. G., and James N. P. eds., Facies Models, Response to Sea Level Change, Geological Association of Canada, in press.

Racey A., 1988. Nummulitid biostratigraphy and Palaeogene palaeoenvironments, Sultanate of Oman. PhD thesis, University of London, 510pp.

Racey A., 1994. Biostratigraphy and palaeobiogeographic significance of Tertiary nummulitids (Foraminifera) from northern Oman. In: Simmons MD (ed) Micropalaeontology and hydrocarbon exploration in the Middle East. Chapman and Hall, London, pp 343–370

Racey A., 1995. Palaeoenvironmental significance of larger foraminiferal biofabrics from the Middle Eocene Seeb Limestone Formation of Oman: Implications for petroleum exploration. In: Al-Husseini, M.I. (Ed.) GE0’94 The Middle East Petroleum Geosciences, Volume II selected Middle East papers from the Middle East geoscience conference, published by Gulf-Petrolink, Bahrain, pp. 793-8 10.

Racey A., 2001. A review of Eocene nummulite accumulations: structure, formation and reservoir potential. J Pet Geol 24:79–100.

Rasser M., Scheibner C., Mutti M., 2005. A paleoenvironmental standard section for Early Ilerdian tropical carbonate factories (Corbieres, France; Pyrenees, Spain). Facies 51:217–232.

Read JF, Horbury AD (1993) Diagenesis and porosity evolution associated with metre-scale disconformities and sequence bounding unconformities. In: Horbury AD, Robinson AG (eds) Diagenesis and basin development, vol 36. Am Assoc Pet Geol Studies in Geol, pp 155–19.

Read JF (1995) Overview of carbonate platform sequences, cycle stratigraphy and reservoirs in greenhouse and icehouse worlds. SEPM Short Course 35:1–102

Reckamp J. U. and Özbey S., 1960. Petroleum geology of Temelli and Kuştepe structures, Polatlı area. Pet. İş. Gen. Md., Ankara.

Reiss Z., Hottinger L., 1984. The Gulf of Aqaba; ecological micropaleontology. Springer, New York, p 354.

Ricken, W., 1985. Epicontinental marl-limestone alternation: event deposition and diagenetic bedding (Upper Jurassic southwest Germany). In: U. Bayer and A. Seilacher (Editors), Sedimentary and Evolutionary Cycles. Springer, Berlin, PP. 122-162.

Rigo de Righi M. ve Cortesini A., 1959. Regional studies in central Anatolian basin. Progress Report 1, Turkish Gulf Oil Co., Pet. İş. Gen. Md., Ankara.

Sarg J. F., 1988. Carbonate sequence stratigraphy. SEPM Spec Publ 42:155–188.

Sartorio S., and Venturini S., 1988. Southern Tethys Biofacies. AGIP Milan.

Schlager W., 1992. Sedimentology and sequence stratigraphy of reefs and carbonate platforms: AAPG Continuing Education Course Note Series, no.34, p. 71.

Schmidt G. C., 1960. AR/MEM/365-266-367 sahalarının nihai terk raporu. Pet. İş. Gen. Md., Ankara.

Sinclair H. D., Sayer Z.R., Tucker M.E., 1998. Carbonate sedimentation during early foreland basin subsidence: the Eocene succession of the French Alps. In: Wright VP, Burchette TP (eds) Carbonate ramps, vol 149. Geol Soc London Spec Publ, pp 205–227.

Sirel E., 1975. Polatlı (GB Ankara) güneyinin stratigrafisi. TJK Bülteni, 18, 2, 181-192.

Sirel E., Gündüz, H., 1976. Description and stratigraphical distrubition of the some species of the genera Nummulites, Assilina and Alveolina from the Ilerdian, Cuisian and Lutetian of the Haymana region. Bull Geol Soc Turkey 19, 31 - 44 (in Turkish).

Sirel E., 1999. Four new genera (*Haymanella, Kayseriella, Elazigella and Orduella*) and one new species of *Hottingerina* from the Paleocene of Turkey Micropaleontology, 42, 113 – 137.

Sloss L. L., 1962, Stratigraphic models in exploration. Journal of Sedimentary Petrography, v. 32, p. 415-422.

Steno N., 1669/1916, The Prodomus of Nocolau Steno's Dissertation: Newyork, University of Michigan Studies, Humanistic Series, v. 11. (translated by: J. G., Winter).

Strasser A., 1988. Shallowing-upward sequence in Purbeckian peritidal carbonates (Lowermost Creataceous, Swiss and French Jura mountains). *Sedimentology*, 35, 369-383.

Strasser A., Pittet, B., Hillga¨rtner, H., Pasquier, Jean-Bruno., 1999. Depositional sequences in shallow water carbonate-dominated sedimentary systems : concepts for a high-resolution analysis. Sedimentary Geology 128, 201–221.

Suess E., 1888, Das Antlitz der Erde: Praque, Tempsky-Freytag, v. 2, 703 p.

Şenalp M., Gökçen L.S., 1978. Sedimentological Studies of the Oil-Saturated Sandstones of the Haymana Region. Bull Geol Soc Turkey, 21,87 – 94 (in Turkish).

Şengör A. M. C. ve Yılmaz Y., 1981. Tethyan evolution of Turkey: a plate tectonic approach. Tectonophysics, 75, 181-241.

Toker V., 1979. Upper Cretaceous Planktonic Foraminifera and the biostratig-raphic investgations of the Haymana area. Bulliten of the Geological Society of Turkey, 22, 121 – 132.

Tucker M.E., Calvet F., Hunt D., 1993. Sequence stratigraphy of carbonate ramps: systems tracts, models and application to the Muschelkalk carbonate platforms of Eastern Spain. In: Posamentier, H.W., Summerhayes, C.P., Haq, B.U., Allen, G.P. (Eds.), Sequence stratigraphy and facies associations. Special Publication, International Association of Sedimentologists 18, pp. 397–419.

Ünalan G., Yüksel V., Tekeli T., Gonenç O., Seyirt Z., Hüseyn S., 1976. Upper Cretaceous – Lower Tertiary stratigraphy and paleogeographic evolution of Haymana – Polatli region (SW Ankara). Turkish Geol Soc Bull19,159 – 176 (in Turkish).

Ünalan G. ve Yüksel V., 1985. Haymana-Polatlı havzasının jeolojisi ve petrol olanakları. MTA Petrol ve Jeotermal Enerji Dairesi Raporu.

Vail P. R., and Mitchum J. R., 1977. Seismic stratigraphy and global changes of sea level, Part 1: Overview-Applications to Hydrocarbon Exploration. Am.Association of Petroleum Geologists. Memoir, 26, 63-81.

Vail P. R., Mitchum R. M. and Thompson S., 1977. Seismic stratigraphy and global changes of sea level, Part 4: Global cycles of relative changes of the sea level, in payton, C. E., eds., seismic stratigraphy. Application to Hydrocarbon Exploration. Am. Association of Petroleum Geologist Memoir, 26, 83-97.

Vail P. R., Hardenbol J, Todd R. G., 1984. Jurassic unconformities, chronostratigraphy and sea level changes from seismic stratigraphy. In: Schlee JS (ed) Interregional unconformities and hydrocarbon exploration, vol 33. Am Assoc Pet Geol Mem, pp 129–144.

Vail P. R., 1987. Seismic stratigraphy interpretation using sequence stratigraphy in Bally, A. W., ed., Atlas of seismic stratigraphy, American Association of Petroleum Geologists Studies in Geology, no. 27,v. 1, p.1-10.

Van Wagoner, J. C., Posamentier H. W., Mithchum R. M., Vail, P. R., Sarg J. F. Loutit, T. S. and Hardenbol, J. 1988. An overview of the Fundamentals of sequence stratigraphy and key definitions. Sea-Level Changes-An Integrated Approach, The Society of Economic Paleontologist and Mineralogist. Special Publication, 42, 40-44.

Van Wagoner J. C., Mitchum R. M., Campion K. M., Rahmanian V. D., 1990. Siliciclastic sequence stratigraphy in well logs, cores and outcrop: concepts for high resolution correlation of time and facies. Am Assoc Pet Geol Methods Explor Ser 7:55.

Vaziri-Moghadam H, Kimiagari M, Taheri A (2006) Depositional environment and sequence stratigraphy of the Oligo-Miocene Asmari Formation in SW Iran. Facies 52:41–51.

Weber M. E., Fenner J., Thies A. and Cepek P. 2001. Biological response to Milankovitch forcing during the Late Albian (Kirchrode I borehole, northwest Germany). Paleogeography, Paleoclimatology, Palaeoecology, 174, 269-286.

Wilson J. L., 1975. Carbonate facies in geologic history. Springer-Verlag, New York, 469 p.

Wray J. L., 1977. Calcareous algae. Amsterdam, Elsevier, p 185.

Wright V. P., 1986. Facies sequences on a carbonate ramp: the Carboniferous Limestone of South Wales. Sedimentology, 33: 221-241.

Yang W., Kominz, M.A., Major, R.P. 1998. Distinguishing the roles of autogenic versus allogenic processes in cyclic sedimentation, Cisco Group (Virgilian and Wolfcampanian), north-central Texas. *GSA Bulletin*, 110, 10,p.1333-1353.

Yüksel, S., 1970. Etude geologique de la region d'Haymana (Turquie Centrale). These Univ Nancy, 1 - 179.

APPENDIX A

BULK MINERALOGICAL ANALYSES (XRD) RESULT

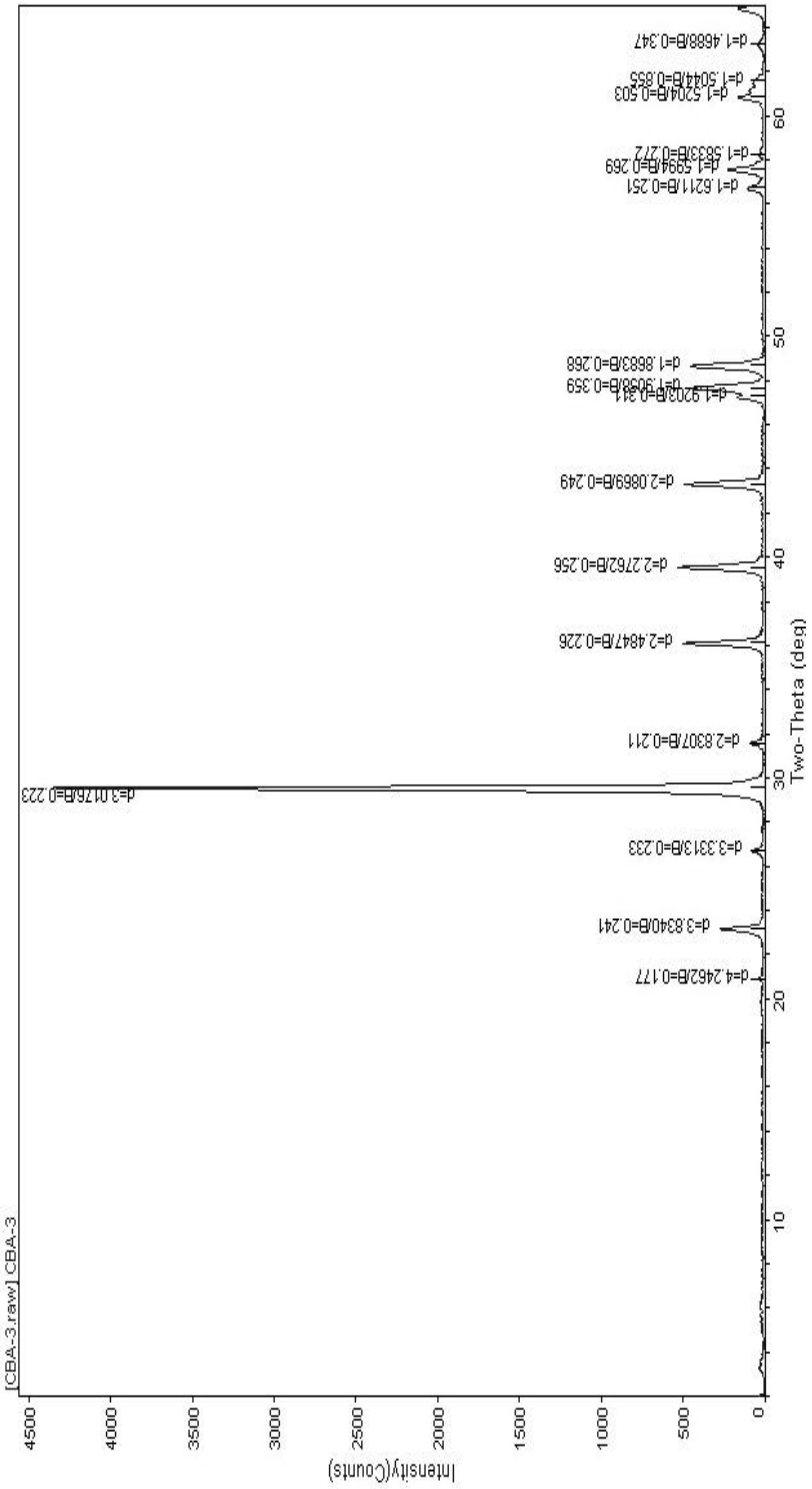

Figure A1. Bulk Minerological Analysis (XRD) result of sample ÇBG 3.

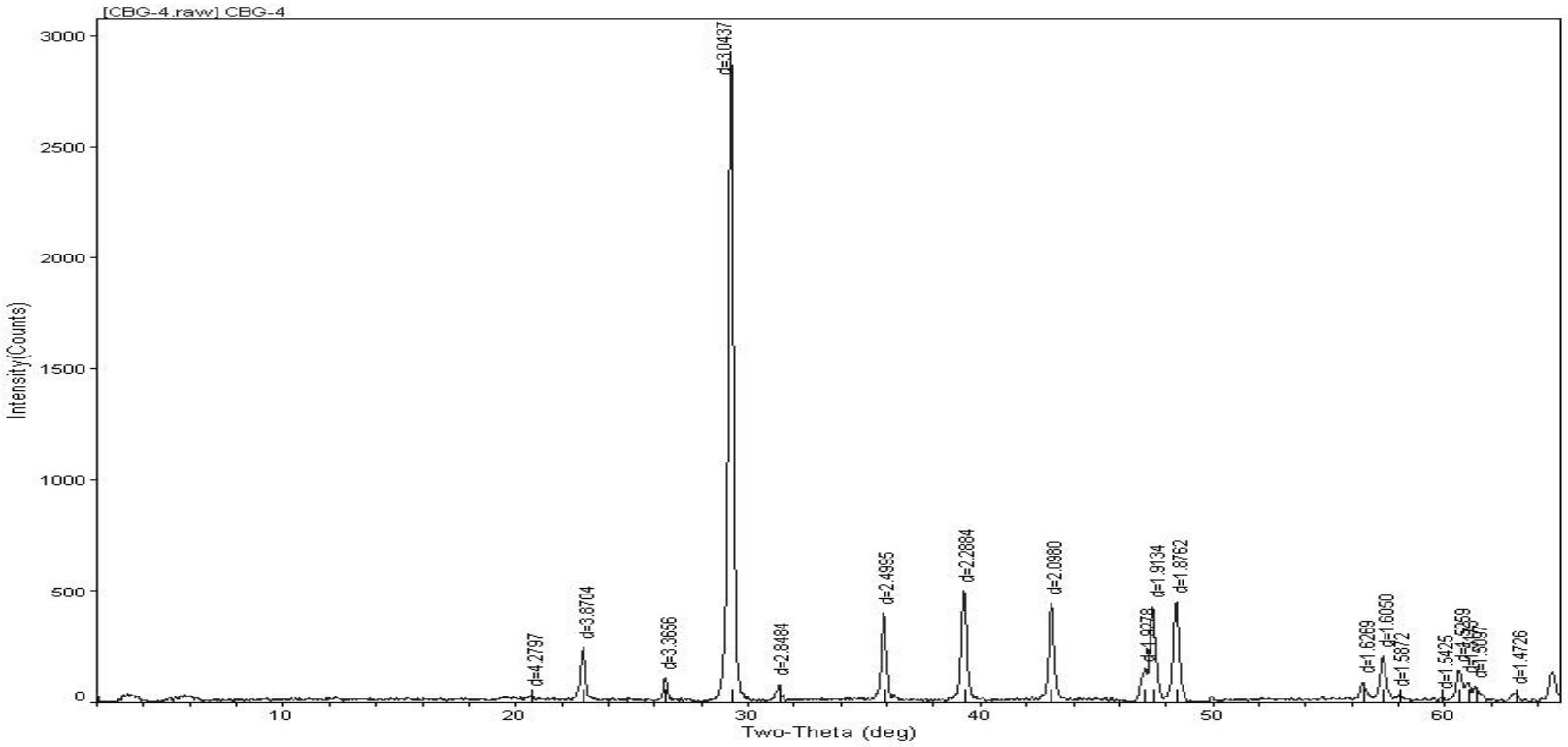

Figure A2. Bulk Minerological Analysis (XRD) result of sample ÇBG 4.

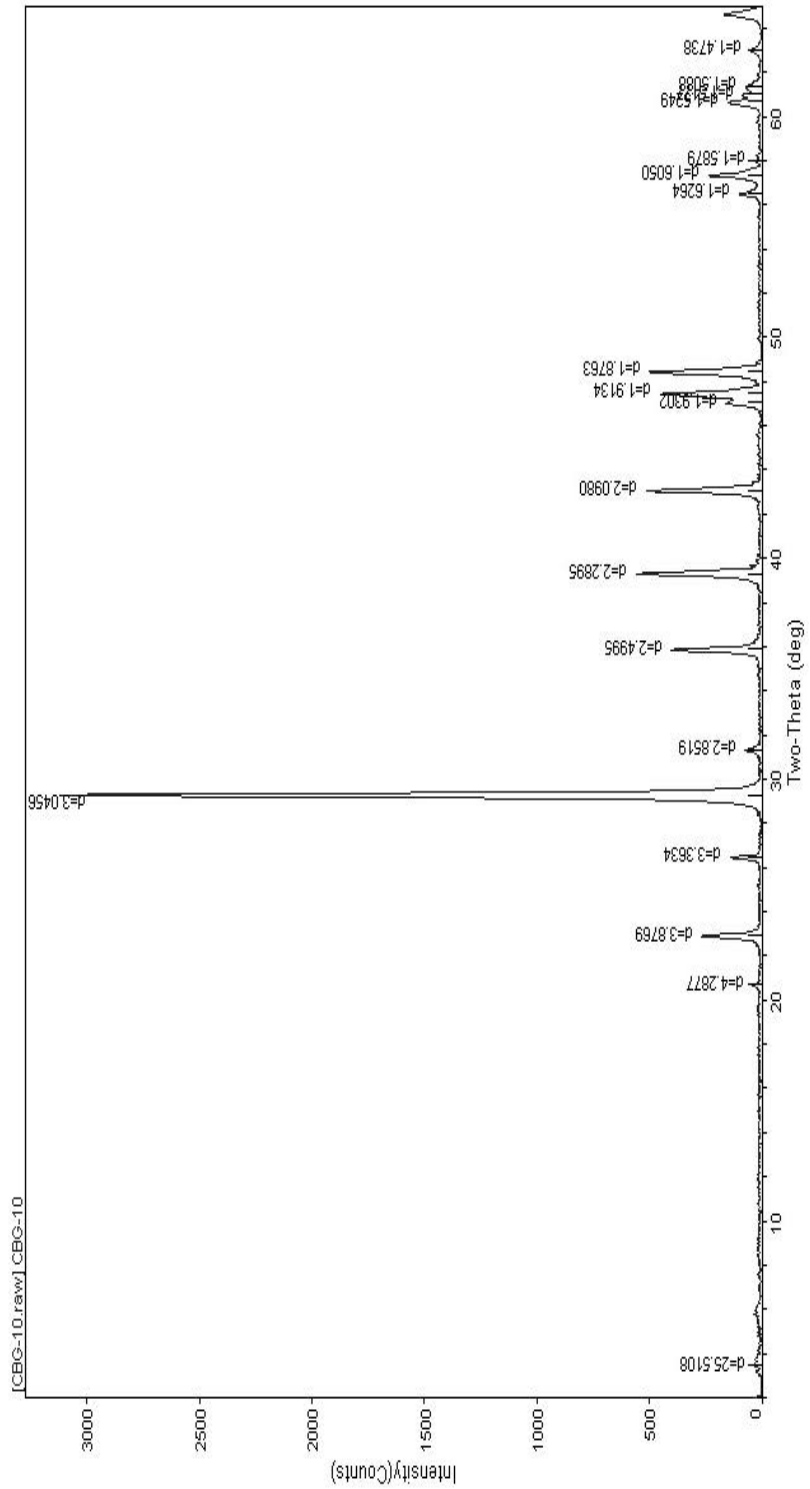

Figure A3. Bulk Minerological Analysis (XRD) result of sample ÇBG 10.

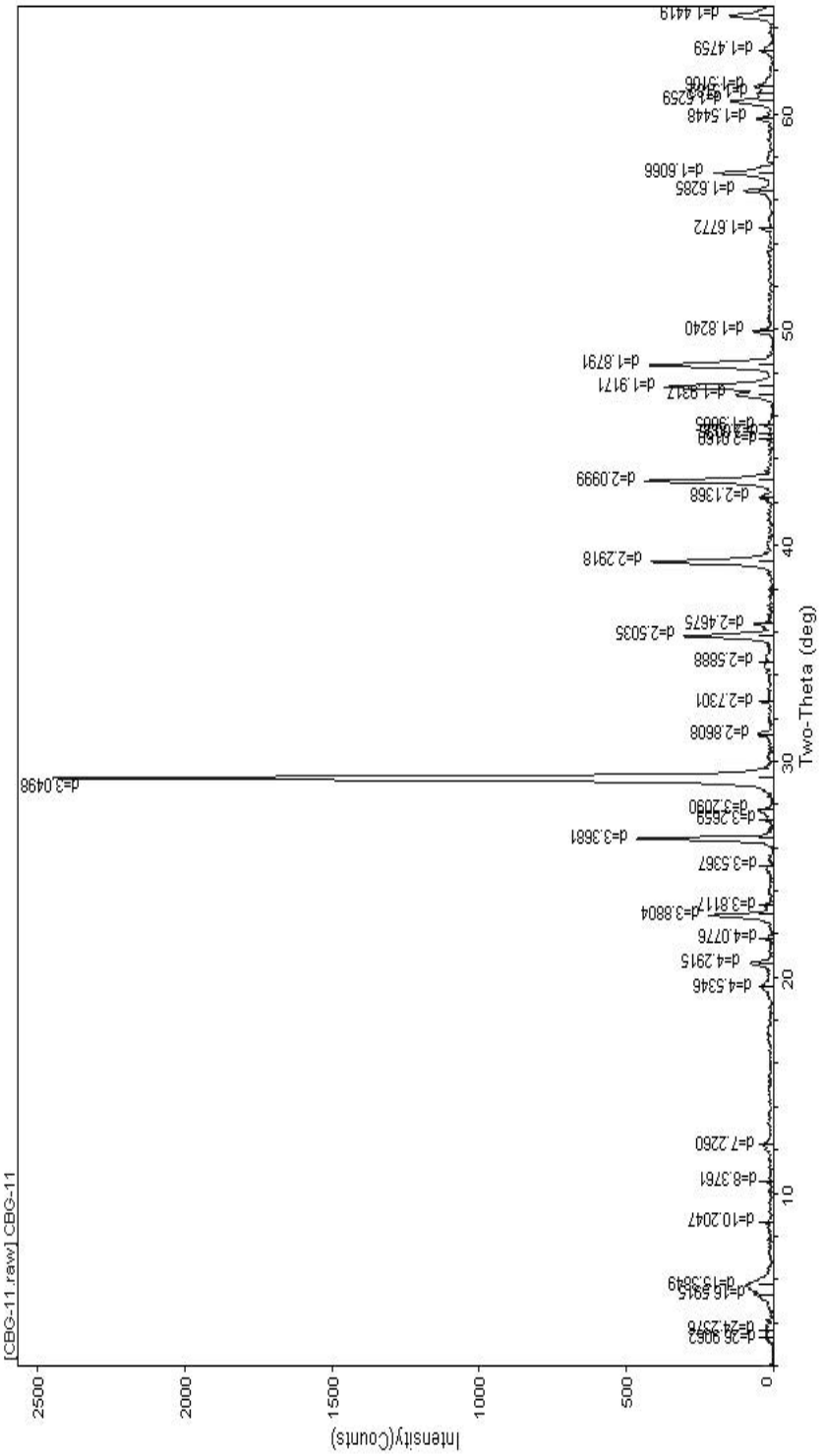

Figure A4. Bulk Minerological Analysis (XRD) result of sample ÇBG 11.

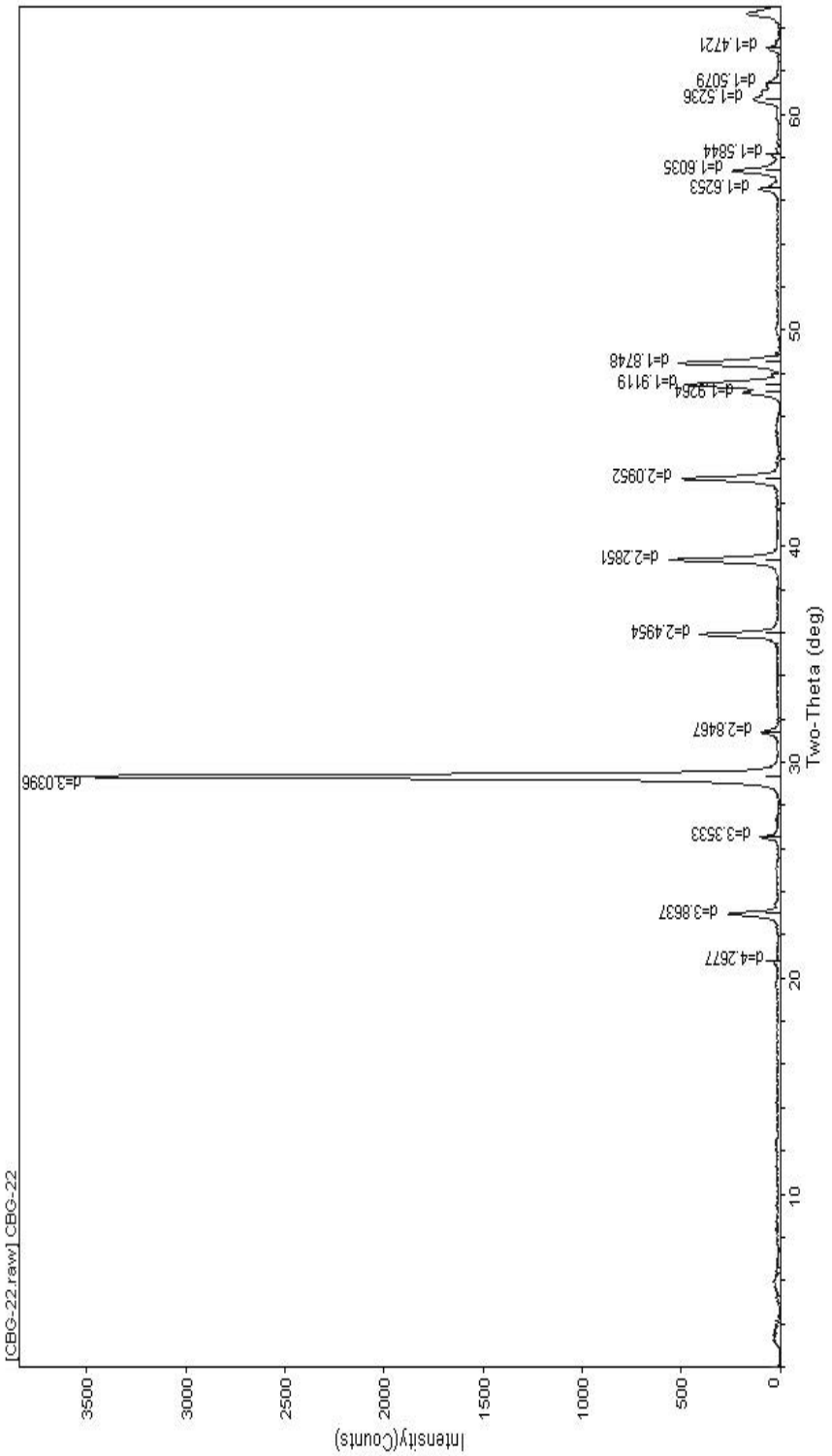

Figure A5. Bulk Minerological Analysis (XRD) result of sample ÇBG 22.

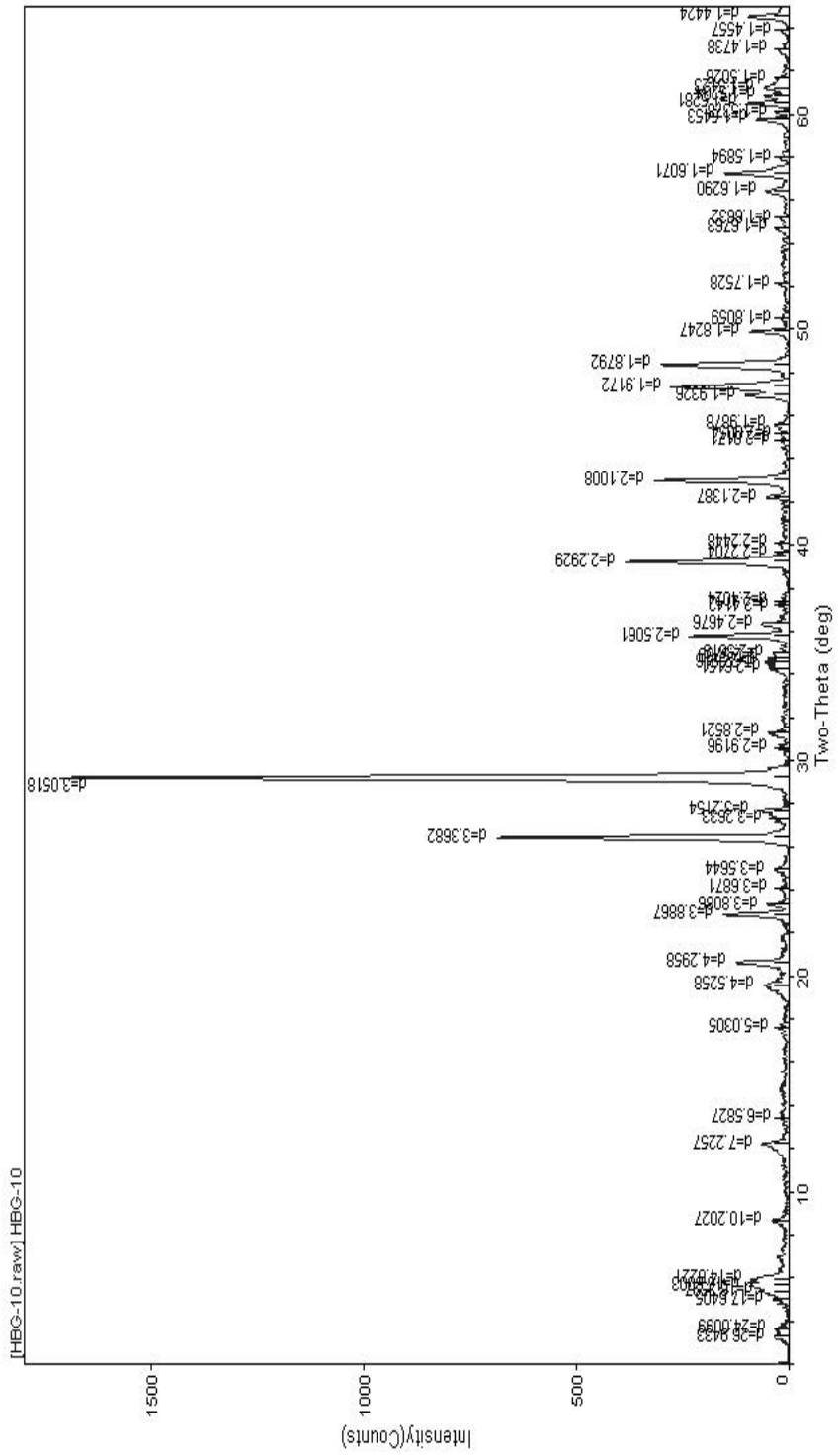

Figure A6. Bulk Minerological Analysis (XRD) result of sample HBG 10.

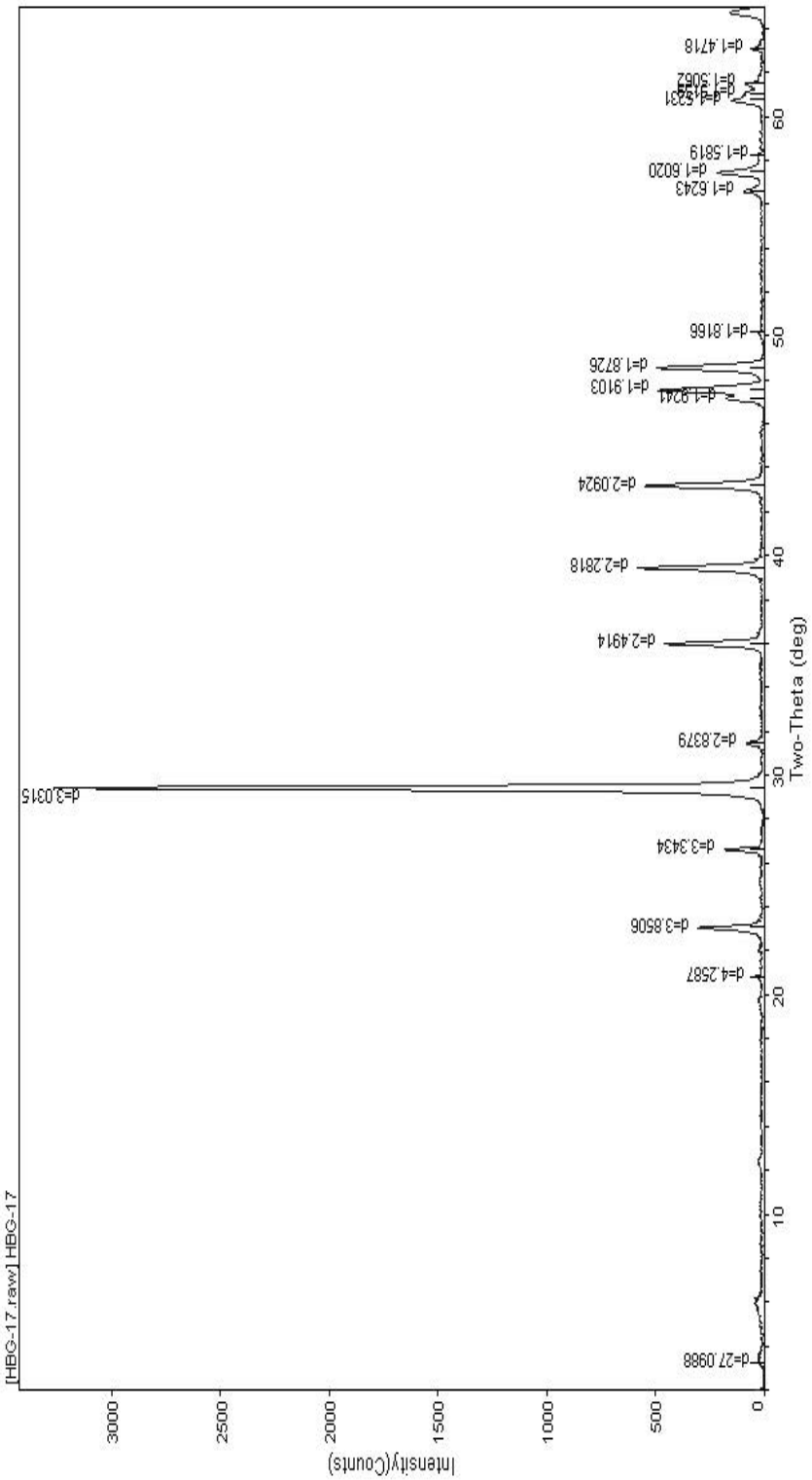

Figure A7. Bulk Minerological Analysis (XRD) result of sample HBG 17.

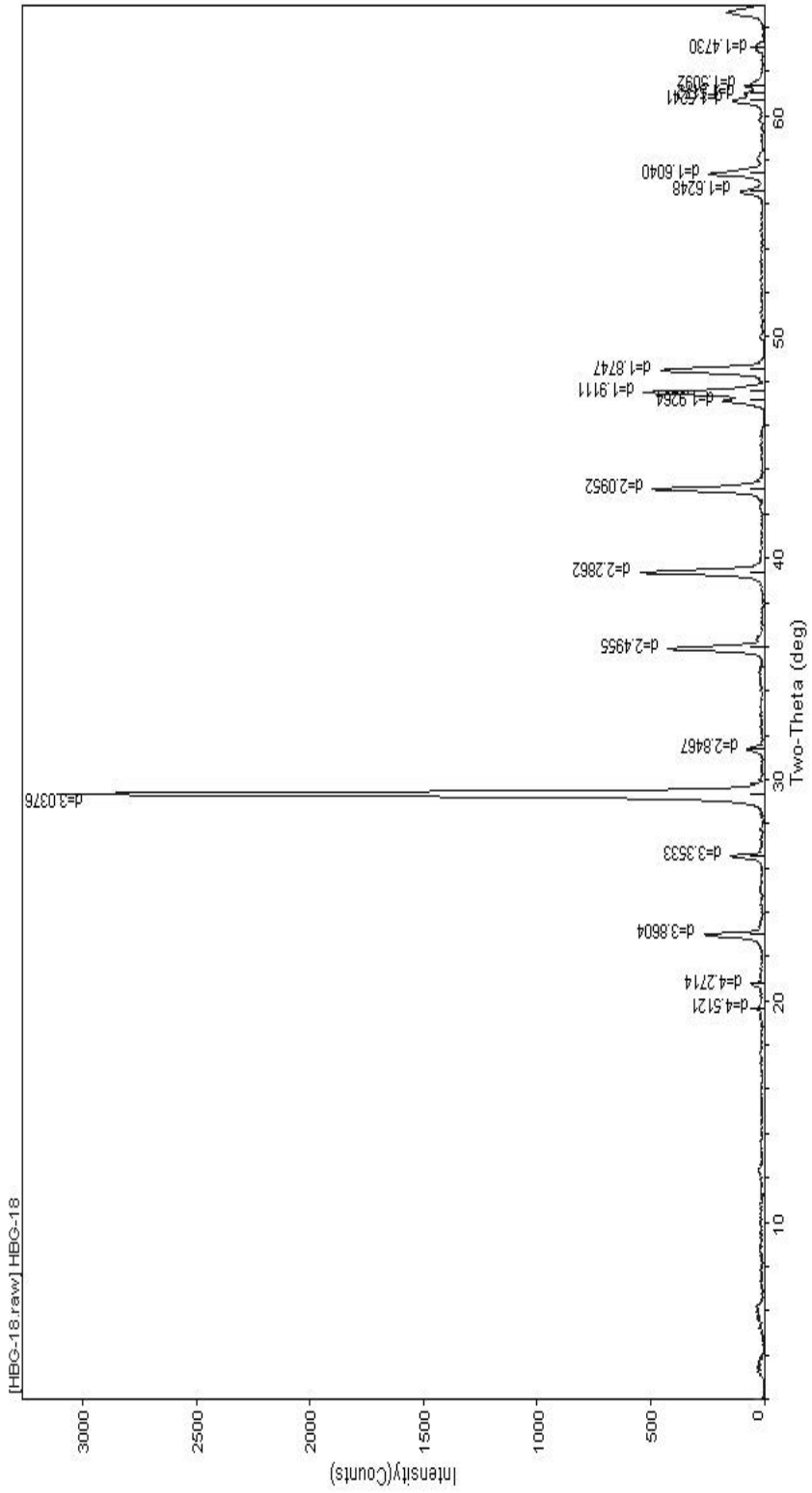

Figure A8. Bulk Minerological Analysis (XRD) result of sample HBG 18.

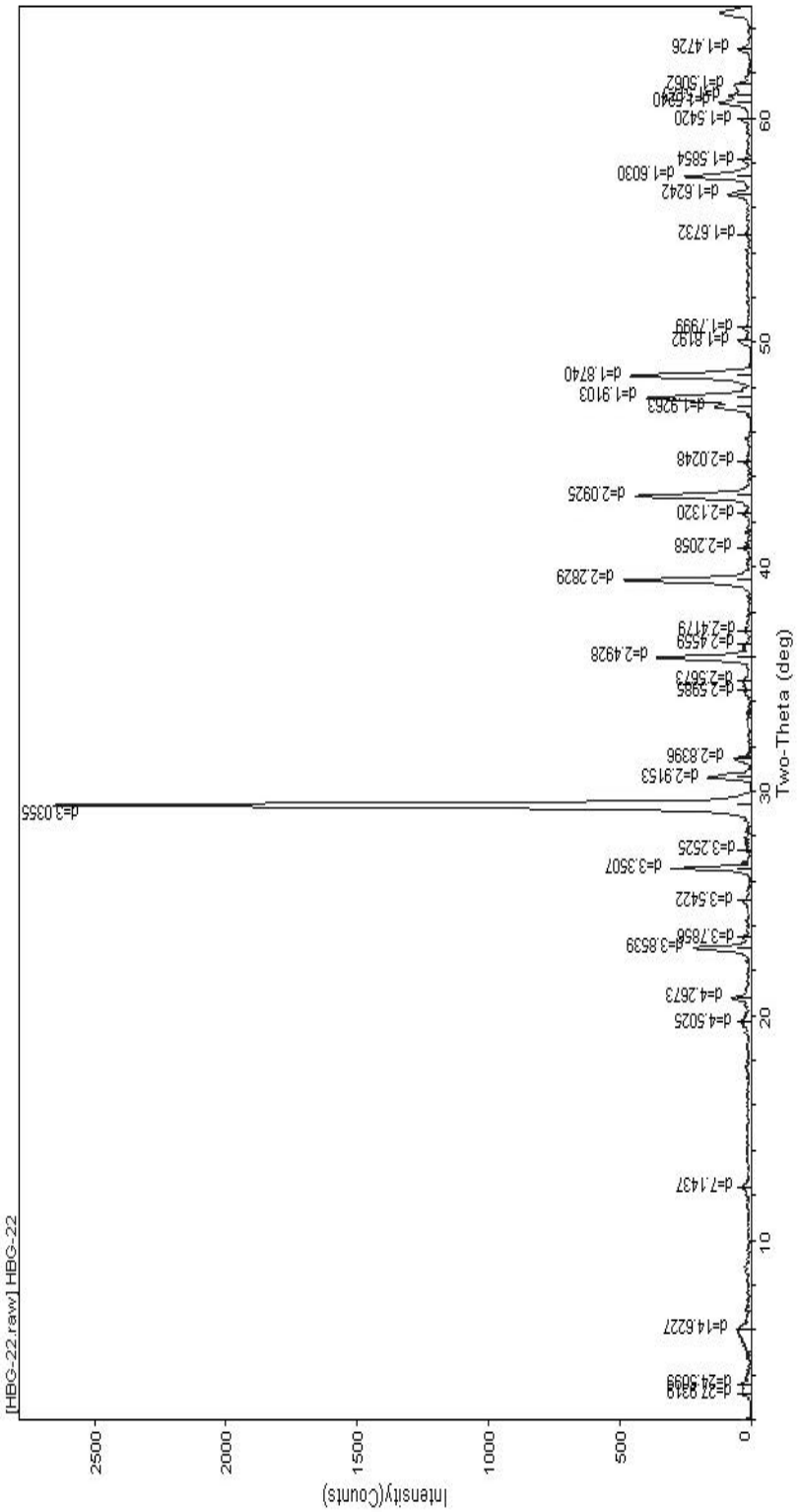

Figure A9. Bulk Minerological Analysis (XRD) result of sample HBG 22.

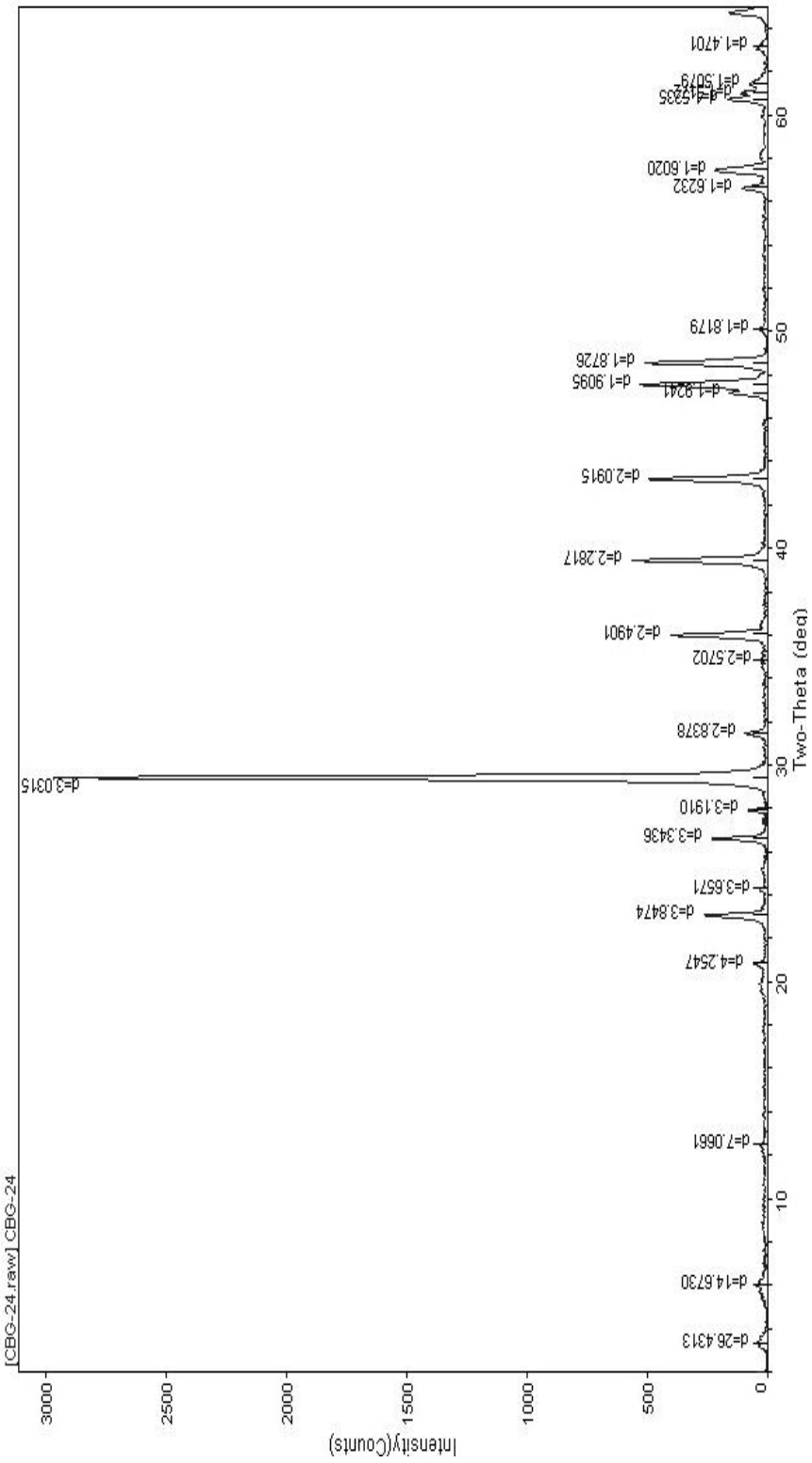

Figure A10. Bulk Minerological Analysis (XRD) result of sample ÇBG 24.

APPENDIX B

EXPLANATION OF PLATES

PLATE 1

Figure 1*: Nummulites* sp., sample no: ÇBG 1

Figure 2: *Nummulites* sp., sample no: ÇBG 1

Figure 3: *Nummulites* sp., sample no: ÇBG 1

Figure 4: *Nummulites* sp., sample no: ÇBG 1

Figure 5: *Nummulites* sp., sample no: ÇBG 1

Figure 6: *Nummulites* sp., sample no: ÇBG 1

PLATE 1

1

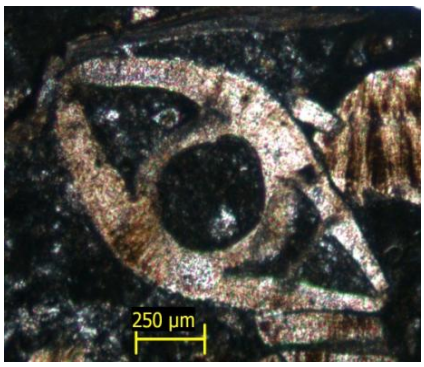

2

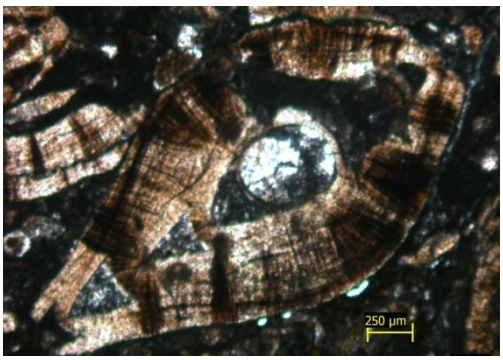

3

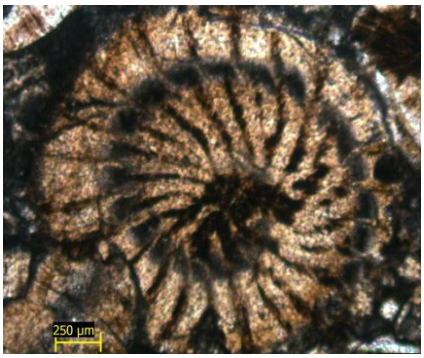

4

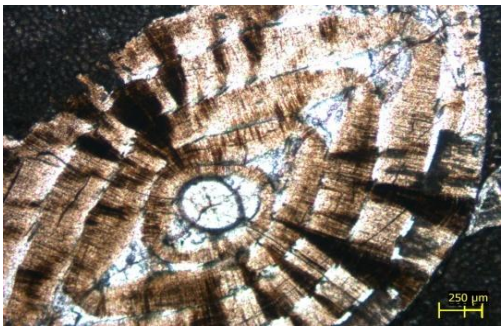

5

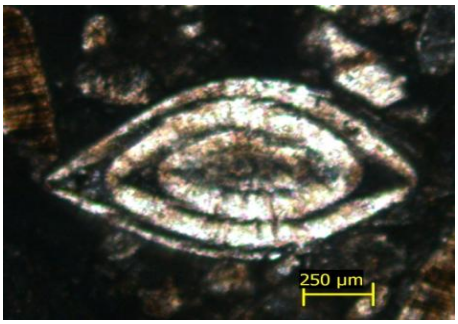

6

PLATE 2

Figure 1: *Nummulites* sp., sample no: ÇBG 2

Figure 2: *Nummulites* sp., sample no: ÇBG 2

Figure 3: *Nummulites* sp., sample no: ÇBG 2

Figure 4: *Nummulites* sp., sample no: ÇBG 2

Figure 5: *Nummulites* sp., sample no: ÇBG 3

Figure 6: *Nummulites* sp., sample no: ÇBG 3

PLATE 2

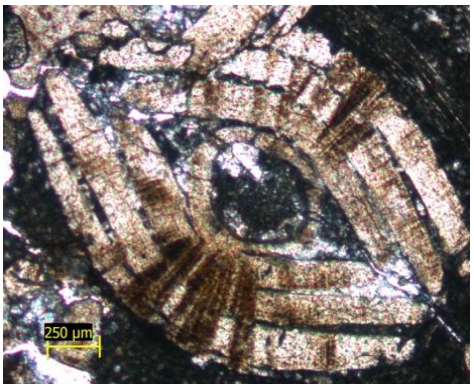

1

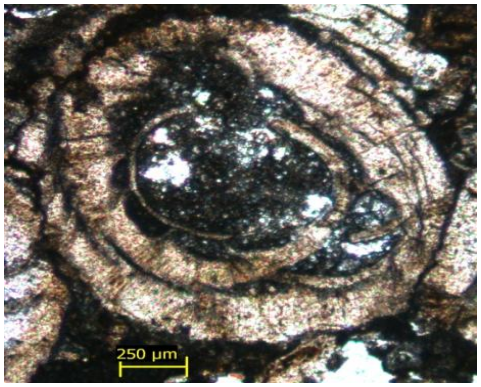

2

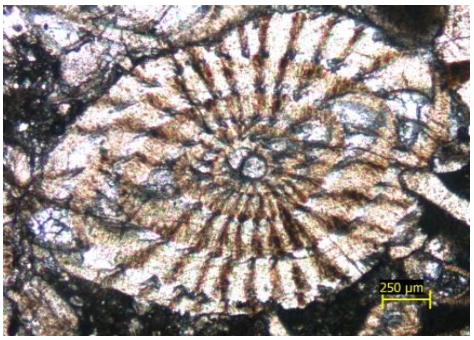

3

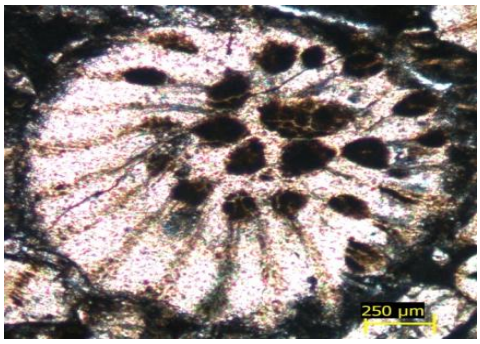

4

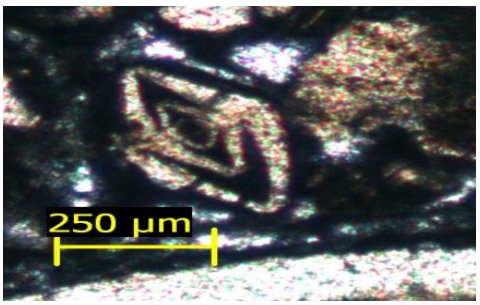

5

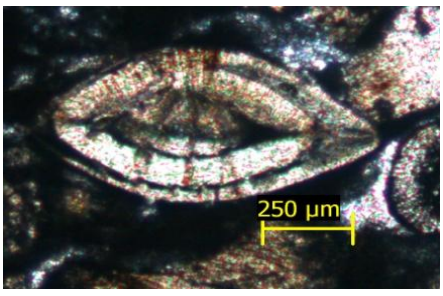

6

PLATE 3

Figure 1: *Nummulites* sp., sample no: ÇBG 4

Figure 2: *Nummulites* sp., sample no: ÇBG 4

Figure 3: *Nummulites* sp., sample no: ÇBG 3

Figure 4: *Nummulites* sp., sample no: ÇBG 3

Figure 5: *Nummulites* sp., sample no: ÇBG 3

Figure 6: *Nummulites* sp., sample no: ÇBG 4

PLATE 3

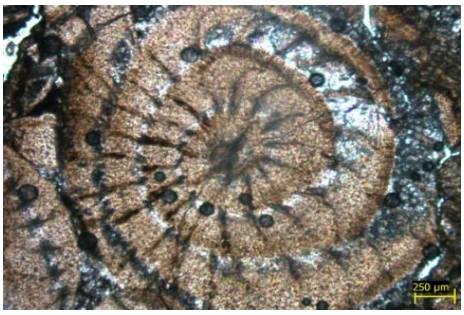

1

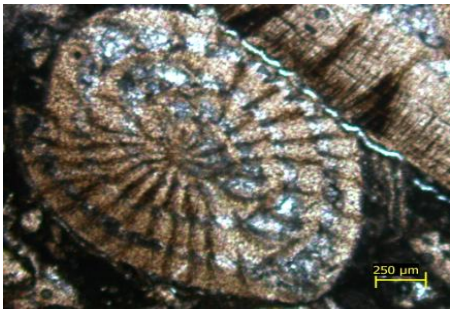

2

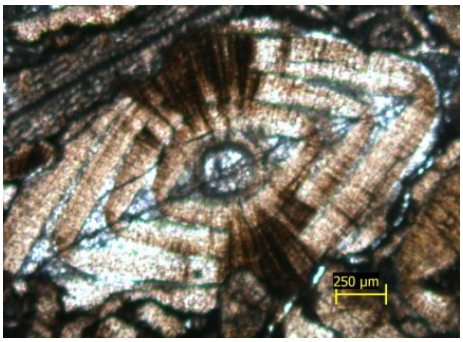

3

4

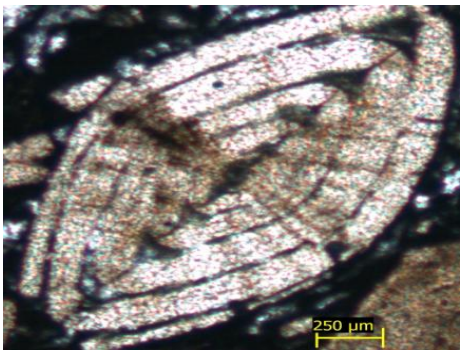

5

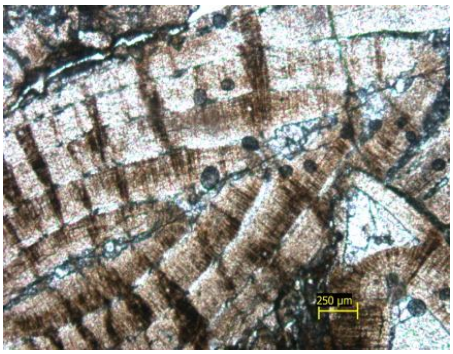

6

PLATE 4

Figure 1: *Textularia* sp. or *Valvulina* sp., sample no: HBG 1

Figure 2: *Textularia* sp. or *Valvulina* sp., sample no: HBG 2

Figure 3: *Valvulina* sp., sample no: HBG 2

Figure 4: *Valvulina* sp., sample no: HBG 2

Figure 5: *Valvulina* sp., sample no: HBG 2

Figure 6: *Textularia* sp. or *Valvulina* sp., sample no: HBG 2

Figure 7: *Textularia* sp. or *Valvulina* sp., sample no: HBG 2

Figure 8: *Textularia* sp., sample no: HBG 6

Figure 9: *Textularia* sp., sample no: HBG 8

PLATE 4

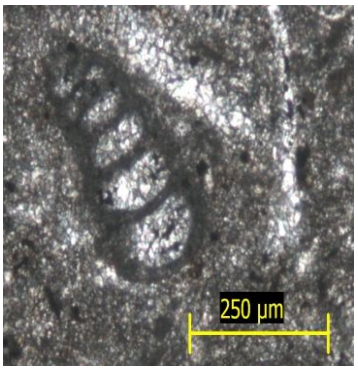

1

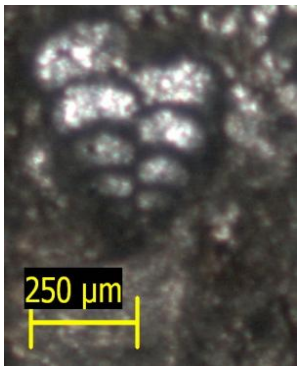

2

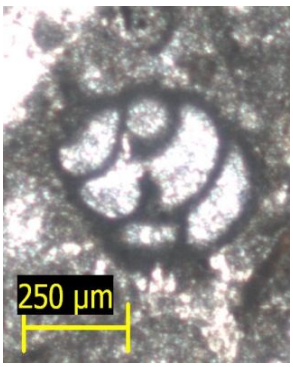

3

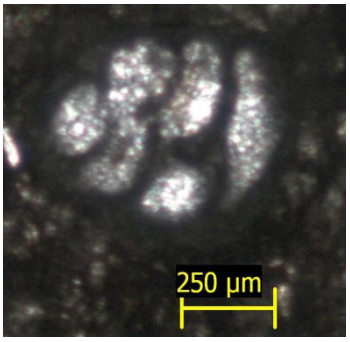

4

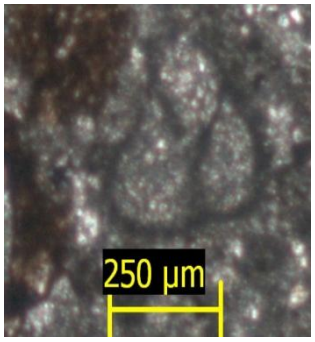

5

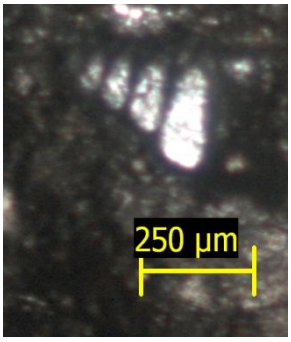

6

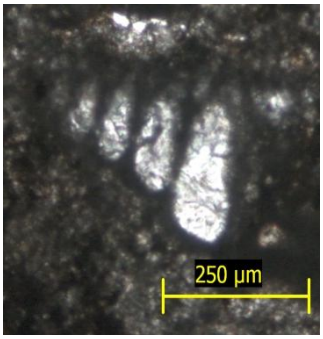

7

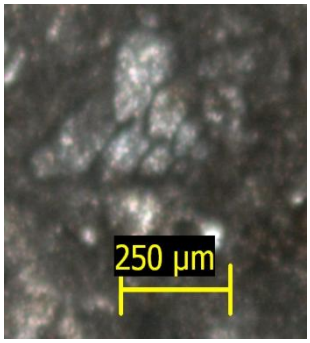

8

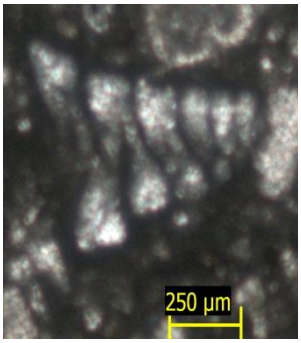

9

PLATE 5

Figure 1: Unidentified textularid form, sample no: HBG 13

Figure 2: Unidentified rotalid form, sample no: HBG 11

Figure 3: Unidentified textularid form, sample no: HBG 2

Figure 4: Unidentified rotalid form, sample no: HBG 5

Figure 5: Veneulinidae, sample no: HBG 13

Figure 6: Veneulinidae, sample no: ÇBG 30

PLATE 5

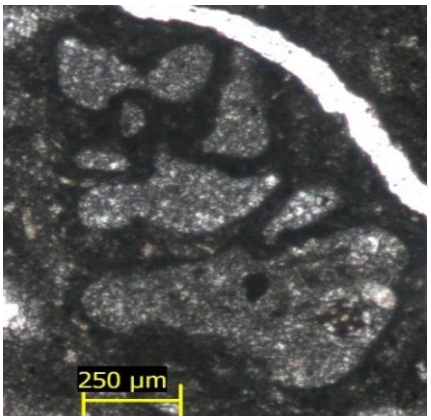

1

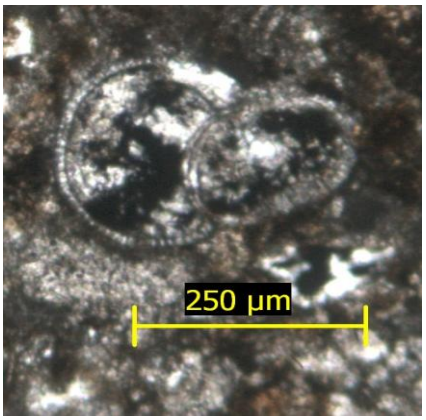

2

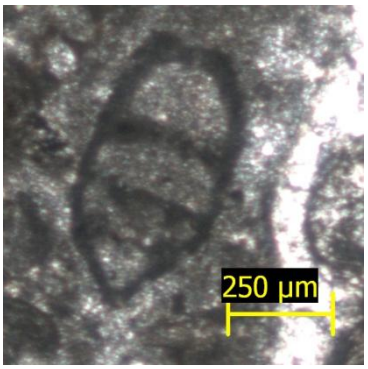

3

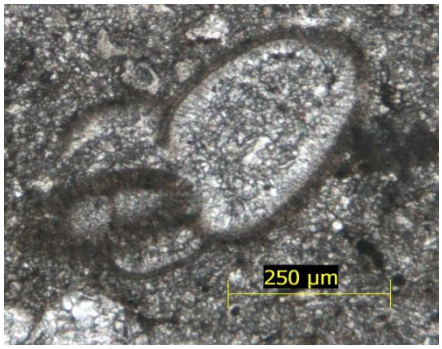

4

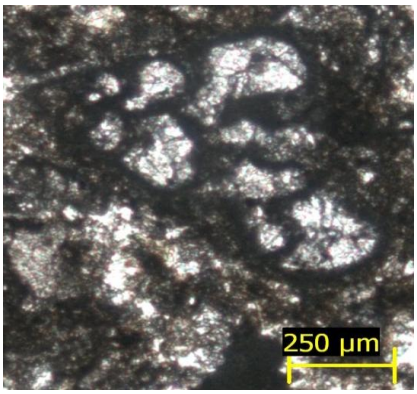

5

6

PLATE 6

Figure 1: *Discocyclina* sp., sample no: ÇBG 1, X25

Figure 2: *Discocyclina* sp., sample no: ÇBG 2, X25

Figure 3: *Discocyclina* sp., sample no: ÇBG 3, X25

Figure 4: *Discocyclina* sp., sample no: ÇBG 4, X25

Figure 5: *Discocyclina* sp., sample no: ÇBG 4, X25

PLATE 6

1

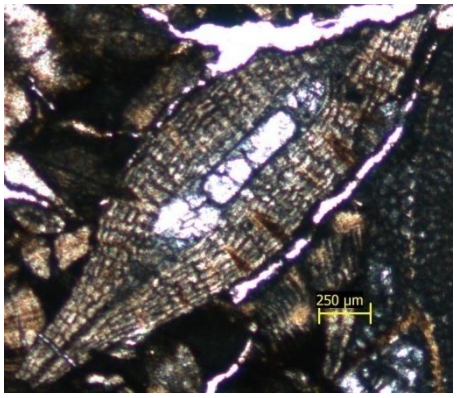

2

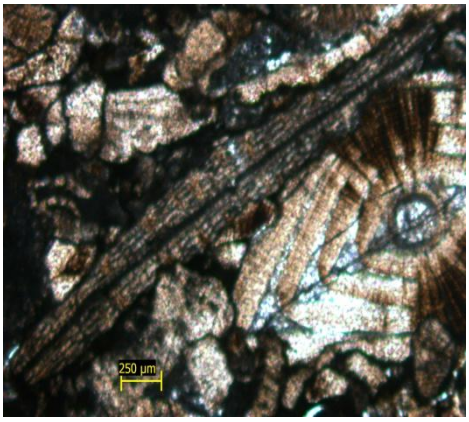

3

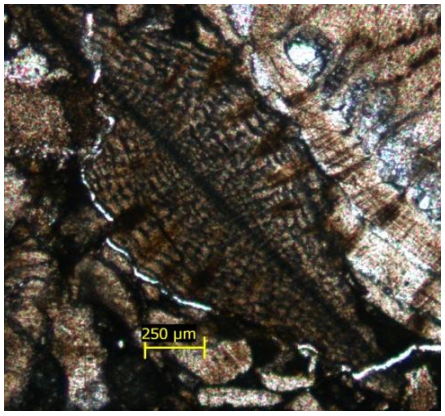

4

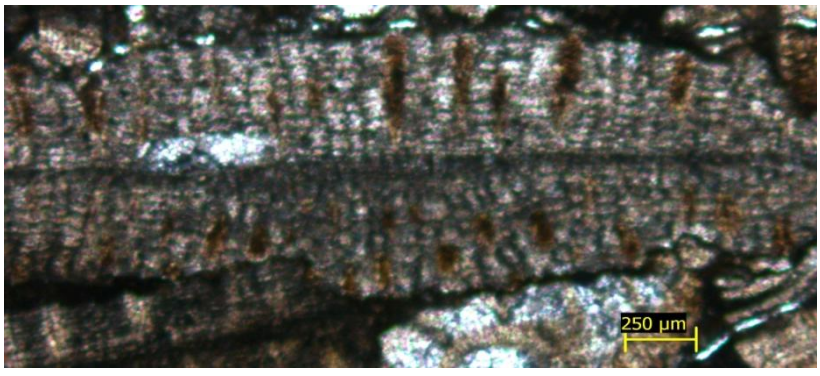

5

PLATE 7

Figure 1: *Assilina* sp., sample no: HBG 8

Figure 2: *Assilina* sp., sample no: HBG 20

Figure 3: *Assilina* sp., sample no: HBG 25

Figure 4: *Assilina* sp., sample no: HBG 26

Figure 5: *Assilina* sp., *Operculina*, sample no: HBG 26

Figure 6: *Operculina* sp., sample no: HBG 26

PLATE 7

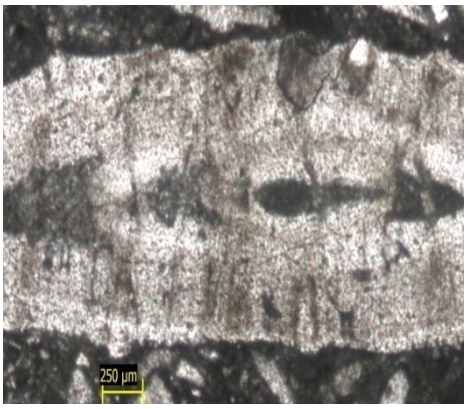

1

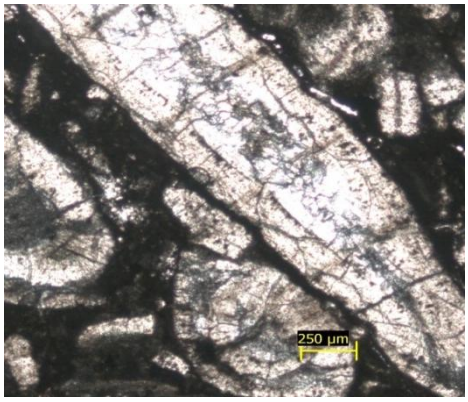

2

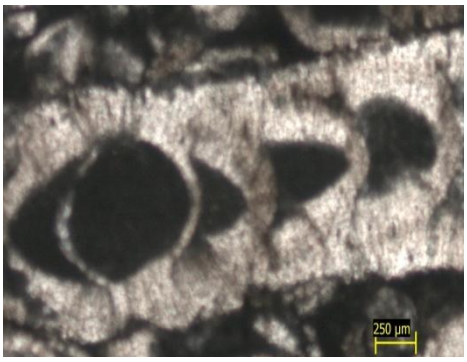

3

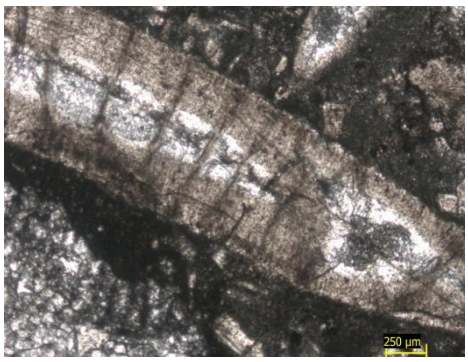

4

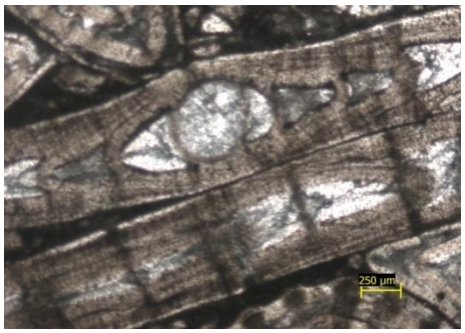

5

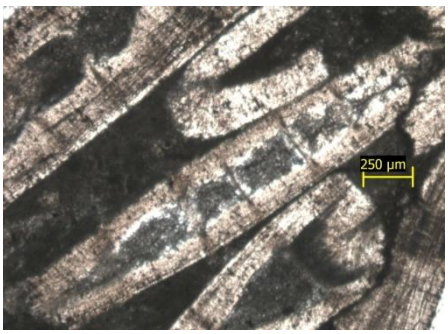

6

PLATE 8

Figure 1: *Alveolina* sl., sample no: HBG 1

Figure 2: *Alveolina* sl., sample no: ÇBG 27

Figure 3: *Alveolina* sl., sample no: ÇBG 29

Figure 4: *Alveolina* sl., sample no: ÇBG 29

Figure 5: *Alveolina* sl., sample no: ÇBG 29

Figure 6: *Alveolina* sl., sample no: ÇBG 29

PLATE 8

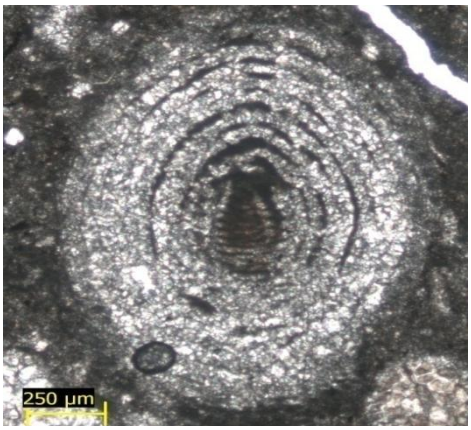

1

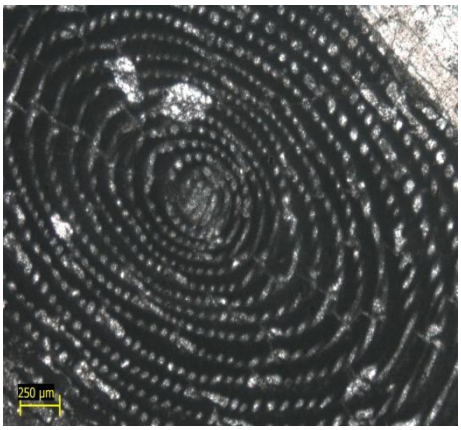

2

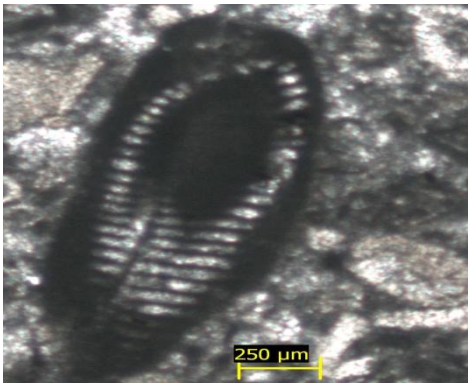

3

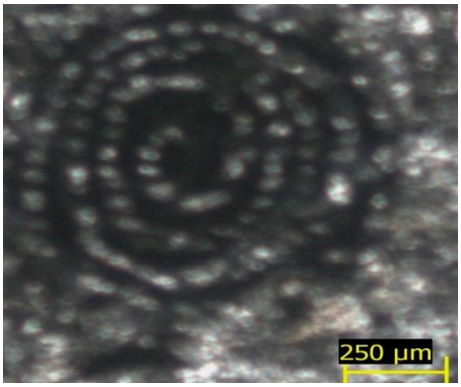

4

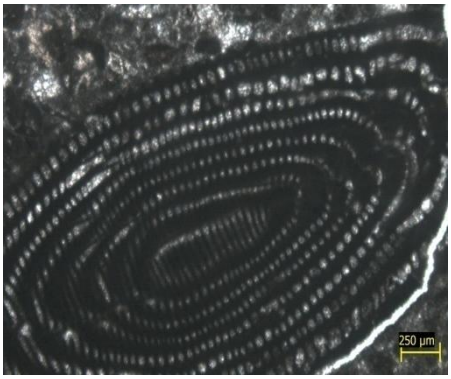

5

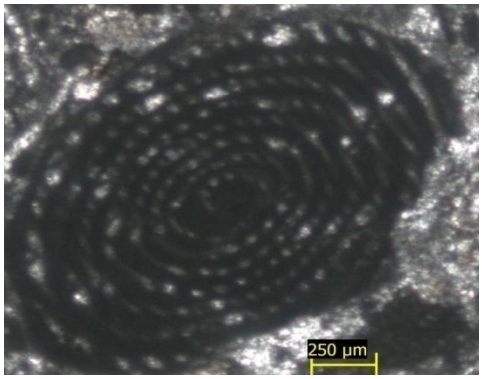

6

PLATE 9

Figure 1: *Sphaerogypsina* sp., sample no: ÇBG 1

Figure 2: *Sphaerogypsina* sp., sample no: ÇBG 23

Figure 3: *Sphaerogypsina* sp., sample no: ÇBG 21

Figure 4: *Sphaerogypsina* sp., sample no: ÇBG 19

Figure 5: *Sphaerogypsina* sp., sample no: HBG 21

Figure 6: *Sphaerogypsina* sp., sample no: HBG 18

Figure 7: *Sphaerogypsina* sp., sample no: HBG 11

PLATE 9

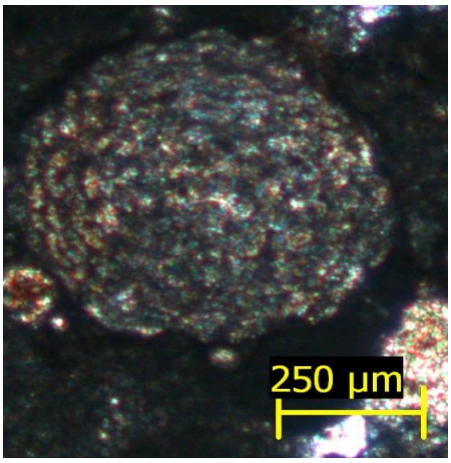

1

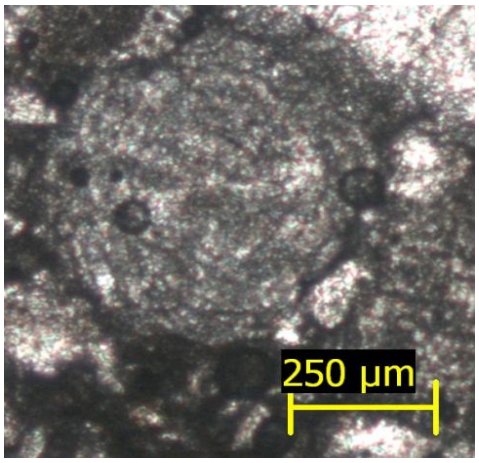

2

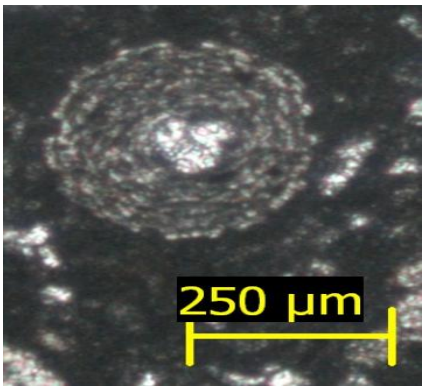

3

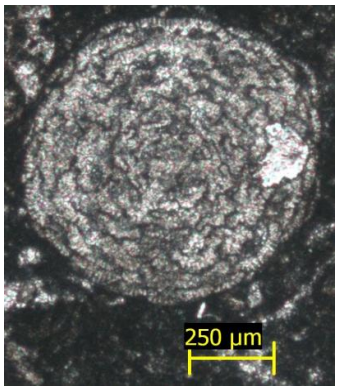

4

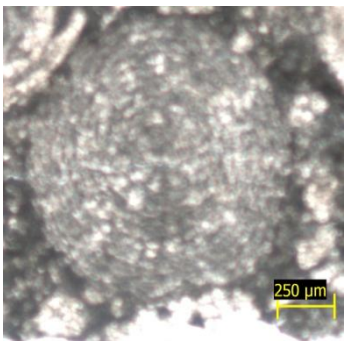

5

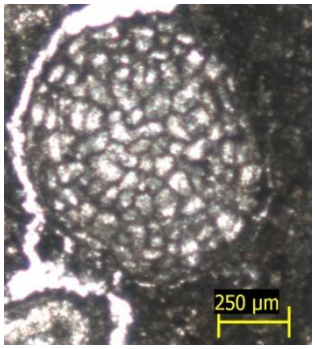

6

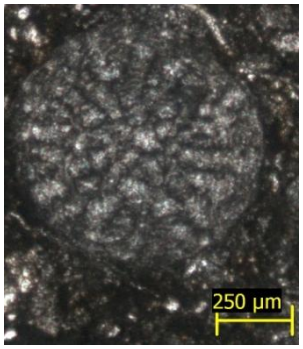

7

PLATE 10

Figure 1: Miliolids., sample no: HBG 2

Figure 2: Miliolids., sample no: HBG 5

Figure 3: Miliolids., sample no: HBG 16

Figure 4: Miliolids., sample no: ÇBG 25

Figure 5: Miliolids., sample no: ÇBG 25

Figure 6: Miliolids., sample no: ÇBG 27

Figure 7: Miliolids., sample no: ÇBG 29

Figure 8: Miliolids., sample no: ÇBG 29

Figure 9: *Pyrgo* sp., sample no: HBG 1

Figure 10: Miliolids., sample no: HBG 1

Figure 11: *Pyrgo* sp., sample no: HBG 1

Figure 12: Miliolids., sample no: HBG 1

PLATE 10

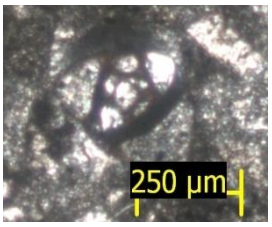

1

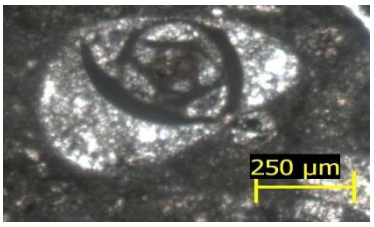

2

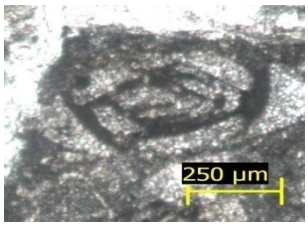

3

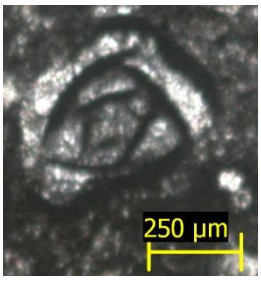

4

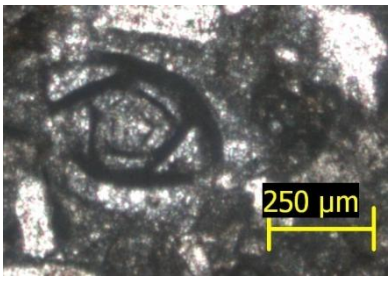

5

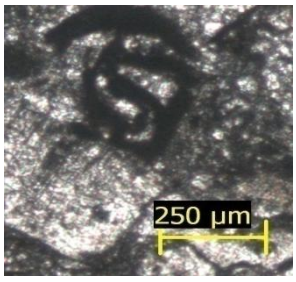

6

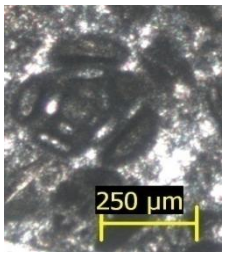

7

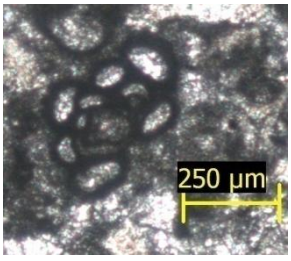

8

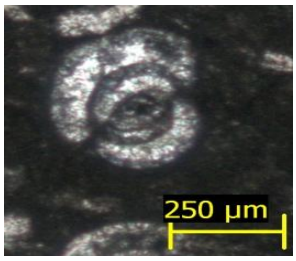

9

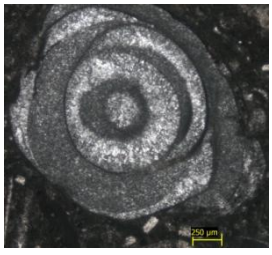

10

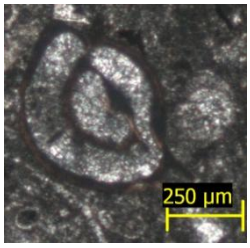

11

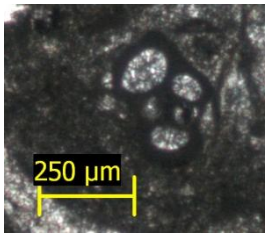

12

PLATE 11

Figure 1: *Pyrgo* sp., sample no: HBG 7

Figure 2: *Pyrgo* sp., sample no: HBG 7

Figure 3: *Pyrgo* sp., sample no: HBG 8

Figure 4: *Pyrgo* sp., sample no: HBG 19

Figure 5: *Pyrgo* sp., sample no: ÇBG 19

Figure 6: *Pyrgo* sp., sample no: ÇBG 20

Figure 7: *Pyrgo* sp., sample no: ÇBG 25

Figure 8: *Triloculina* sp., sample no: HBG 5

Figure 9: *Triloculina* sp., sample no: HBG 8

Figure 10: *Triloculina* sp., sample no: ÇBG 19

Figure 11: *Spiroloculina* sp., sample no: HBG 7

Figure 12: *Spiroloculina* sp., sample no: HBG 13

PLATE 11

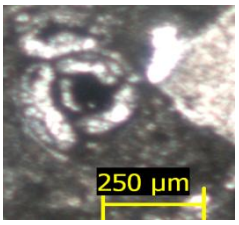

1

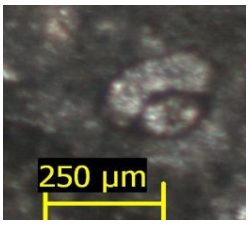

2

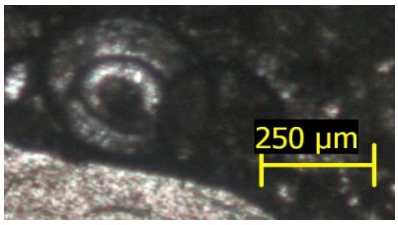

3

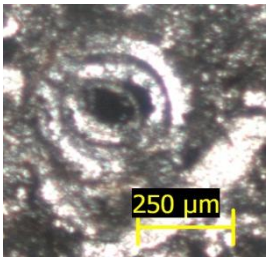

4

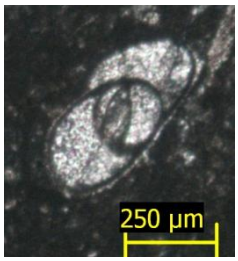

5

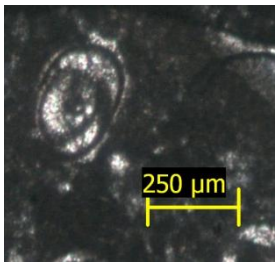

6

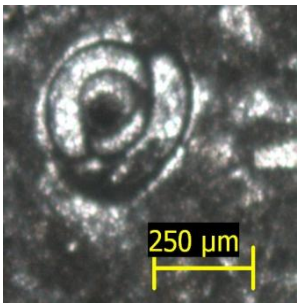

7

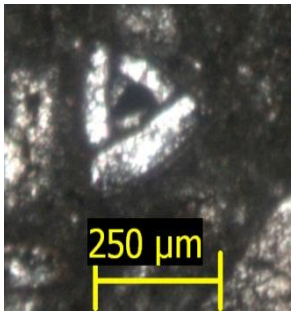

8

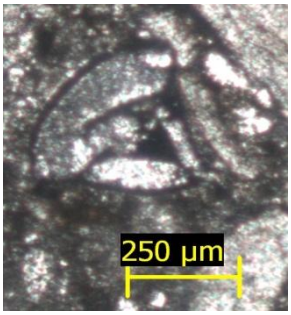

9

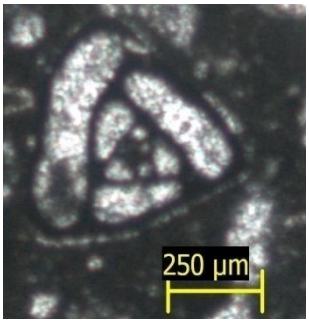

10

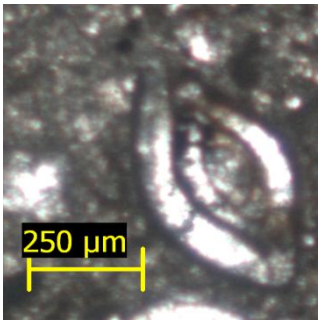

11

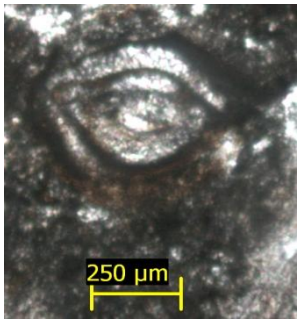

12

PLATE 12

Figure 1: *Spiroloculina* sp., sample no: HBG 13

Figure 2: *Spiroloculina* sp., sample no: ÇBG 19

Figure 3: *Spiroloculina* sp., sample no: ÇBG 30

Figure 4: *Coskinolina* sp., sample no: ÇBG 29

Figure 5: *Orbitolites* sp., sample no: HBG 2

Figure 6: *Orbitolites* sp., sample no: HBG 2

PLATE 12

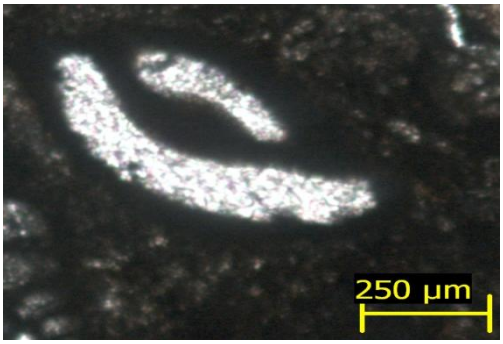

1

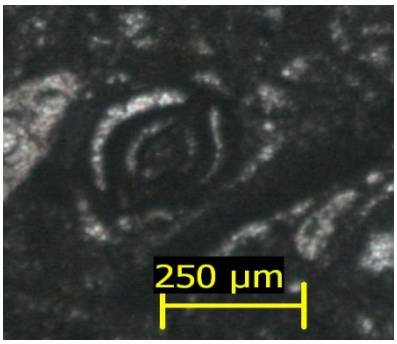

2

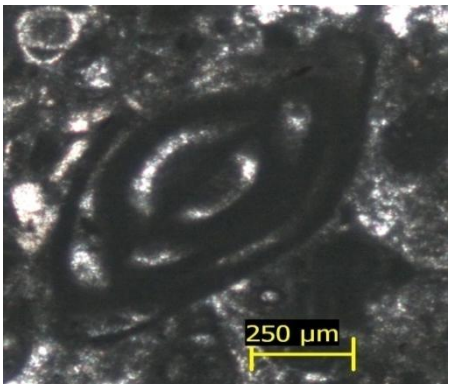

3

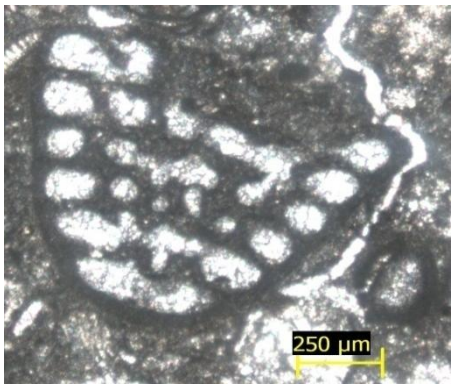

4

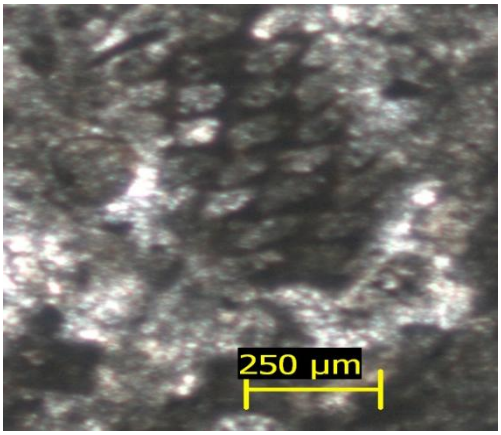

5

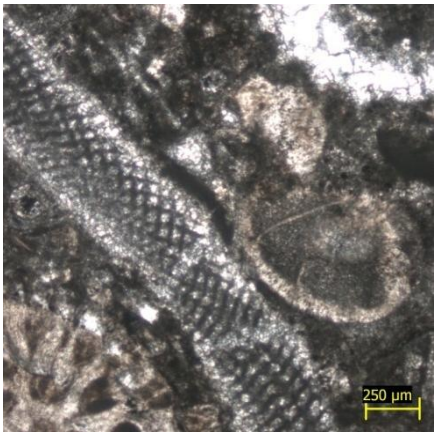

6

PLATE 13

Figure 1: *Orbitolites* sp., sample no: HBG 9

Figure 2: *Orbitolites* sp., sample no: HBG 9

Figure 3: *Lockhartia* sp., sample no: HBG 20

Figure 4: *Lockhartia* sp., sample no: HBG 19

Figure 5: *Lockhartia* sp., sample no: HBG 29

Figure 6: *Lockhartia* sp., sample no: HBG 15

PLATE 13

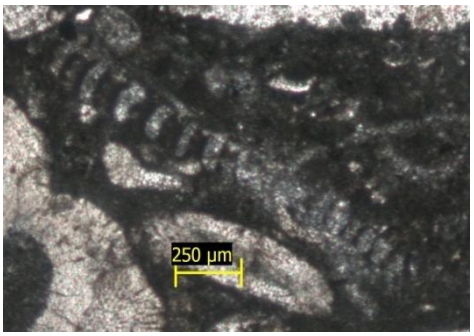

1

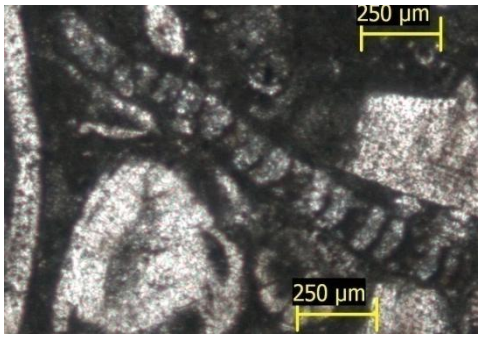

2

3

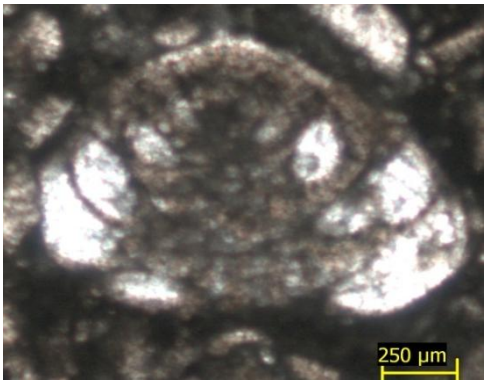

4

5

6

PLATE 14

Figure 1: *Rotalia* sp., sample no: ÇBG 30

Figure 2: *Rotalia* sp., sample no: ÇBG 27

Figure 3: *Rotalia* sp., sample no: HBG 9

Figure 4: *Rotalia* sp., sample no: ÇBG 29

Figure 5: *Rotalia* sp., sample no: ÇBG 29

Figure 6: Medocia? sp., sample no: HBG 23,

Figure 7: Medocia? sp., sample no: HBG 23

Figure 8: Biserially to uniserialy coiled forms., sample no: HBG 12

Figure 9: Biserially to uniserialy coiled forms., sample no: HBG 1

PLATE 14

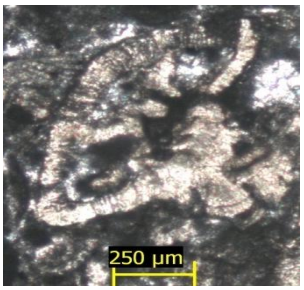

1

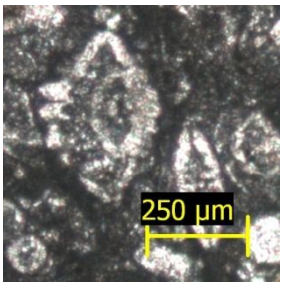

2

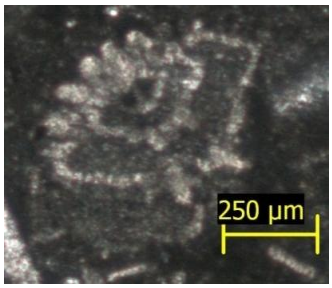

3

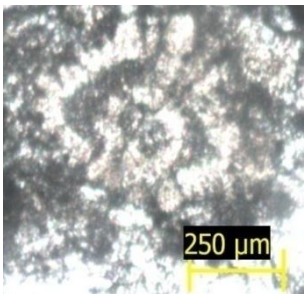

4

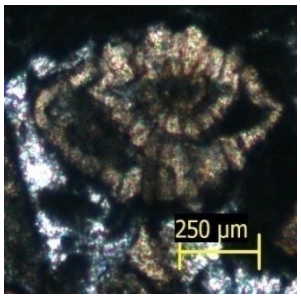

5

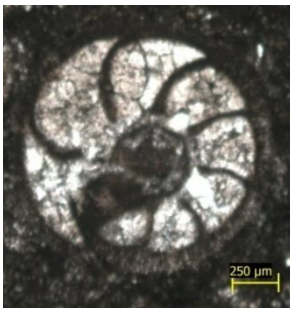

6

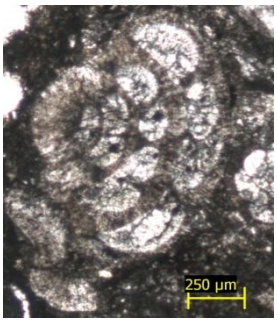

7

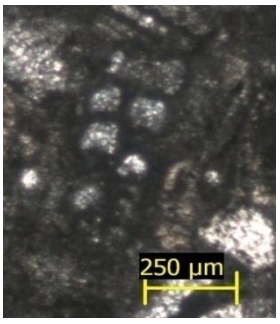

8

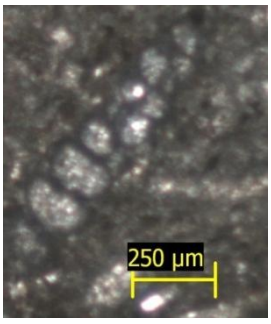

9

PLATE 15

Figure 1: Unidentified rotalid form, sample no: ÇBG 23

Figure 2: Unidentified rotalid form, sample no: ÇBG 23

Figure 3: Unidentified rotalid form, sample no: ÇBG 24

Figure 4: Unidentified rotalid form, sample no: ÇBG 27

Figure 5: Unidentified rotalid form, sample no: ÇBG 25

Figure 6: Unidentified rotalid form, sample no: ÇBG 15

Figure 7: Unidentified rotalid form, sample no: ÇBG 29

Figure 8: Unidentified rotalid form, sample no: ÇBG 29

Figure 9: Unidentified rotalid form, sample no: ÇBG 29

Figure 10: Unidentified rotalid form, sample no: ÇBG 30

PLATE 15

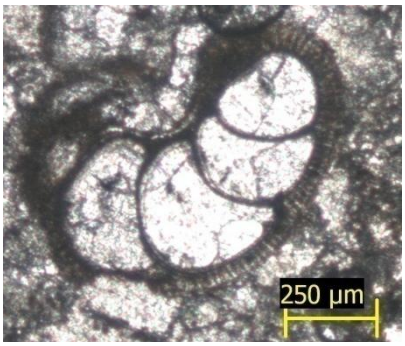

1

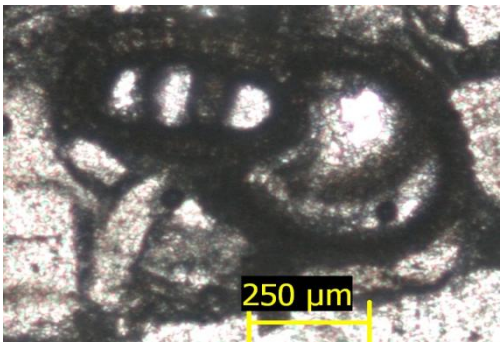

2

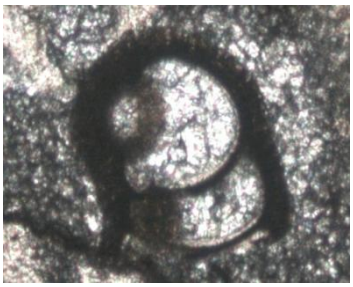

3

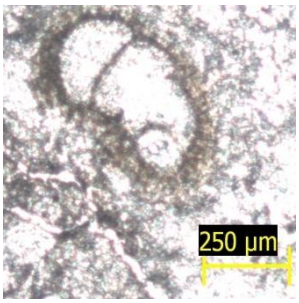

4

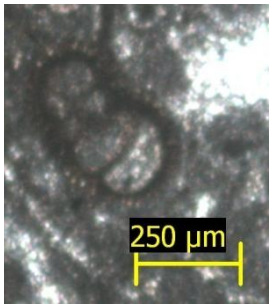

5

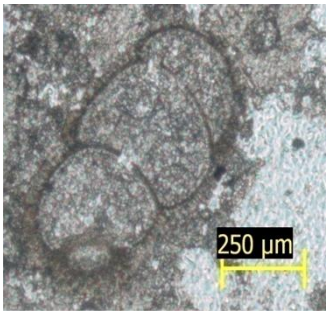

6

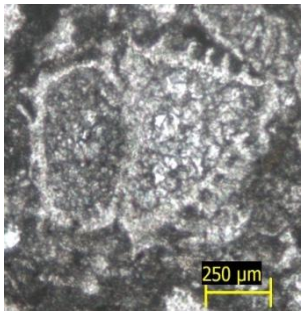

7

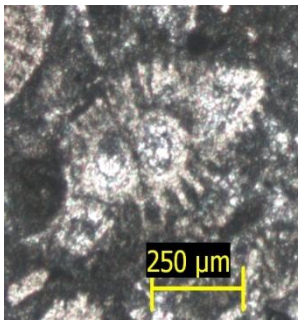

8

PLATE 16

Figure 1: Unidentified miliolid , sample no: ÇBG 21

Figure 2: Unidentified miliolid, sample no: ÇBG 21

Figure 3: Unidentified miliolid, sample no: ÇBG 19

Figure 4: Unidentified miliolid, sample no: HBG 1

Figure 5: Unidentified miliolid, sample no: HBG 13

PLATE 16

1

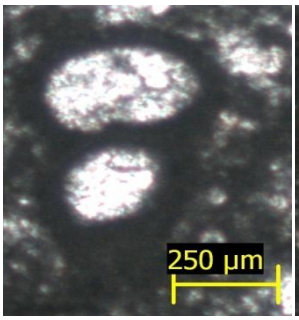

2

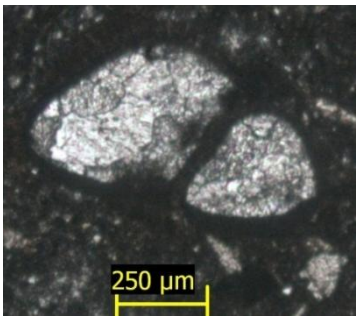

3

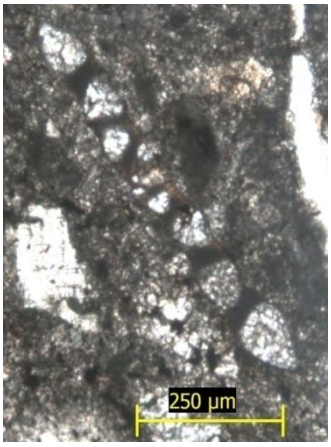

4

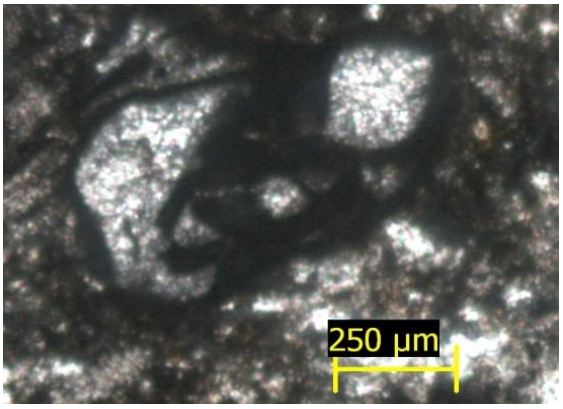

5

APPENDIX C

COUNTING RESULTS OF FORAMINIFER

	ÇBG																													
	1	2	3	4	5	6	7	8	9	10	11	12	13	14	15	16	17	18	19	20	21	22	23	24	25	26	27	28	29	30
Nummulites	87	142	127	167	170	95	113	95	111	65	131	153	22	217	83	145	192	158	28	0	0	91	157	192	57	161	123	151	66	80
Discocylina	24	18	18	54	38	14	64	39	15	15	11	18	9	7	24	40	15	26	2	0	0	19	9	64	1	0	2	4	0	0
Assilina	0		15	26	2	29	33	13	9	5	2	23	2	3	21	5	4	13	1	0	0	0	3	10	1	4	11	13	0	0
Operculina	3	8	2	19	3		21	7	7	4	20	37	13	76	23	10	40	26	21	0	0	9	2	12	0	5	6	5	2	2
Alveolina	0	0	0	0	0	0	0	0	0	0	0	0	0	0	0	0	0	0	0	0	0	0	0	0	2	1	5	4	80	64
Sphaerogypsina	5	2	0	2	0	0	0	2	0	3	0	0	0	0	1	0	1	2	3	0	1	1	4	0	0	1	0	0	0	0
Miliolid	0	1	1	0	0	0	0	0	0	0	0	0	0	0	0	0	4	0	5	0	0	0	0	1	35	4	54	6	43	56
Pygro	0	0	0	0	0	0	0	0	0	0	0	0	0	0	0	0	0	0	13	3	5	0	0	1	4	0	0	2	0	1
Triloculina	0	0	0	0	0	0	0	0	0	0	0	0	0	0	0	0	0	0	3	0	0	0	0	0	0	1	1	0	0	0
Spiroloculina	0	0	1	0	0	0	0	0	0	0	0	0	0	0	0	0	0	0	0	0	0	0	0	0	3	0	4	2	23	11
Coskinolina	0	0	0	0	0	0	0	0	0	0	0	0	0	0	0	0	0	0	0	0	0	0	0	0	0	0	0	0	3	2
Orbitolites	0	0	0	0	0	0	0	0	0	0	0	0	0	0	0	0	0	1	1	0	0	0	0	0	4	0	0	2	2	0
Lockhartia	0	0	0	0	0	0	0	0	0	0	0	0	0	0	0	0	0	1		0	0	0	0	0	0	0	0	0	5	2
Medocia?	0	0	0	0	0	0	0	0	0	0	0	0	0	0	0	0	0	0	0	0	0	0	0	0	0	0	0	1	0	0
Valvulina	0	0	0	0	0	0	0	0	0	0	0	0	0	0	0	0	0	0	0	0	0	0	0	0	0	0	0	0	0	0
Textularia	0	0	0	0	0	0	0	0	0	0	0	0	0	0	0	0	0	0	0	0	0	0	0	0	0	0	0	0	0	0
ValvulinaorTextularia	6	5	3	9	10	3	0	4	3	4	0	3	2	9	22	5	4	21	5	1	6	3	4	10	13	7	11	10	35	17
Rotalia	15	11	38	2	9		31	10	25	3	0	4	5	9	19	0	21	12	18	3	5	15	14	1	21	5	19	29	31	30
Others	8	5	1	3	3	1	0	0	3	3	0	0	0	27	25	0	29	11	12	2	4	14	12	6	21	11	16	14	25	8
Total	156	197	207	285	238	143	262	170	176	105	164	238	53	375	243	205	339	282	121	11	25	165	214	303	181	211	266	257	340	28

Figure C1. Counting results of section 1.

	ÇBG																													
	1	2	3	4	5	6	7	8	9	10	11	12	13	14	15	16	17	18	19	20	21	22	23	24	25	26	27	28	29	30
Nummulites	59	74	62	59	72	67	43	56	64	64	80	64	42	62	38	71	62	58	25	0	0	60	77	65	35	81	49	62	21	29
Discocylina	16	9	9	19	16	10	24	23	9	15	7	8	17	2	11	20	5	10	2	0	0	13	4	22	1	0	1	2	0	0
Assilina	0	0	7	9	1	20	13	8	5	5	1	10	4	1	10	2	1	5	1	0	0	0	1	3	1	2	4	5	0	0
Operculina	2	4	1	7	1	0	8	4	4	4	12	16	25	22	11	5	13	10	19	0	0	6	1	4	0	3	2	2	0	1
Alveolina	0	0	0	0	0	0	0	0	0	0	0	0	0	0	0	0	0	0	0	0	0	0	0	0	1	1	2	2	25	23
Sphaerogypsina	3	0	0	1	0	0	0	1	0	3	0	0	0	0	0	0	0	1	3	0	5	1	2	0	0	1	0	0	0	0
Miliolid	0	1	0	0	0	0	0	0	0	0	0	0	0	0	0	0	1	0	4	0	0	0	0	0	22	2	21	2	14	20
Pygro	0	0	0	0	0	0	0	0	0	0	0	0	0	0	0	0	0	0	12	33	24	0	0	0	2	0	0	1	0	0
Triloculina	0	0	0	0	0	0	0	0	0	0	0	0	0	0	0	0	0	0	3	0	0	0	0	0	0	1	2	0	0	0
Spiroloculina	0	0	0	0	0	0	0	0	0	0	0	0	0	0	0	0	0	0	0	0	0	0	0	0	2	0	0	1	7	4
Coskinolina	0	0	0	0	0	0	0	0	0	0	0	0	0	0	0	0	0	0	0	0	0	0	0	0	0	0	0	0	1	1
Orbitolites	0	0	0	0	0	0	0	0	0	0	0	0	0	0	0	0	0	0	0	0	0	0	0	0	2	0	0	1	1	0
Lockhartia	0	0	0	0	0	0	0	0	0	0	0	0	0	0	0	0	0	0	0	0	0	0	0	0	0	0	0	0	2	1
Medocia?	0	0	0	0	0	0	0	0	0	0	0	0	0	0	0	0	0	0	0	0	0	0	0	0	0	0	0	0	0	0
Valvulina	0	0	0	0	0	0	0	0	0	0	0	0	0	0	0	0	0	0	0	0	0	0	0	0	0	0	0	0	0	0
Textularia	0	0	0	0	0	0	0	0	0	0	0	0	0	0	0	0	0	0	0	0	0	0	0	0	0	0	0	0	0	0
Valvulina or Textularia	4	3	1	3	4	2	0	2	2	4	0	1	4	3	10	2	1	8	4	11	29	2	2	3	8	0	4	4	11	6
Rotalia	10	6	18	1	4	0	12	6	14	3	0	2	9	3	9	0	7	4	16	33	24	10	7	0	13	3	8	12	10	11
Others	5	3	0	1	1	1	0	0	2	3	0	0	0	8	11	0	9	4	11	22	19	10	5	2	13	6	7	6	8	3

Figure C2. Counting results (%) of section 1 .

	HBG																														
	1	2	3	4	5	6	7	8	9	10	11	12	13	14	15	16	17	18	19	20	21	22	23	24	25	26	27	28	29	30	31
Nummulites	64	76	71	110	51	39	35	83	69	29	82	61	97	99	51	79	111	123	156	57	71	93	68	130	176	156	129	114	124	101	118
Assilina	11	9	8	5	15	22	13	14	22	0	14	15	6	3	36	51	14	22	57	115	41	24	14	37	96	129	32	42	29	85	102
Operculina	0	1	3	0	2	1	2	1	4	0	2	2	15	2	5	0	3	2	2	3	2	2	2	4	2	0	0	2	0	0	0
Alveolina	21	19	17	0	5	6	6	1	4	2	0	0	0	0	3	0	0	0	0	0	0	0	0	0	0	2	0	0	0	0	0
Sphaerogypsir	0	0	4	0	1	1	2	0	0	0	2	1	5	5	0	1	0	1	1	0	1	0	0	0	0	1	0	1	0	0	0
Miliolid	12	27	2	3	16	7	11	1	14	0	0	0	0	1	3	5	0	0	0	0	1	0	3	0	1	0	0	0	0	0	6
Pygro	14	28	5	7	21	13	18	3	14	0	0	3	6	7	5	5	0	0	2	4	2	1	1	0	0	0	0	0	0	0	3
Triloculina	1	2	1	0	3	0	1	2	1	0	0	0	0	1	0	1	0	0	0	0	0	0	0	0	0	0	0	0	0	0	0
Spiroloculina	25	29	7	4	24	9	16	1	7	0	0	1	5	2	14	3	0	1	0	0	0	0	2	1	0	1	0	0	0	0	2
Orbitolites	5	8	2	0	2	12	4	0	3	0	0	0	0	0	2	1	0	0	0	0	0	0	0	0	0	0	0	0	0	0	0
Lockhartia	2	2	4	4	1	0	2	4	7	1	0	0	3	0	1	0	0	0	1	2	0	0	0	1	0	3	0	1	0	0	0
Biserialtounis	1	0	0	0	0	1	1	0	0	0	0	0	0	0	0	0	0	0	0	0	0	0	0	0	0	0	0	0	0	0	0
Medocia?	0	1	0	0	0	0	0	0	0	0	3	1	0	0	0	0	7	1	0	0	0	5	10	0	0	0	0	0	0	0	0
Valvulina	1	9	1	1	0	1	0	0	0	0	0	0	0	1	2	0	0	0	0	1	0	0	0	0	1	0	0	0	0	0	1
Textularia	0	2	0	0	0	2	0	0	0	0	0	1	0	0	0	0	0	0	0	0	0	0	0	0	0	0	0	0	0	0	0
ValvulinaorTe	9	9	1	0	2	6	2	3	4	0	0	7	2	13	9	4	1	1	1	1	3	0	9	3	0	2	0	0	1	0	2
Rotalia	28	29	37	24	38	11	5	37	31	3	7	26	10	6	6	26	11	12	4	9	7	12	3	4	7	6	4	9	0	0	7
Veneulinidae	4	1	0	0	0	3	0	0	0	0	0	0	3	0	0	0	0	0	0	0	0	0	0	0	0	0	0	0	0	0	0
Others	26	38	17	16	37	28	20	12	20	4	9	28	40	18	13	15	5	5	3	2	5	4	7	0	1	6	0	0	0	0	8
Total	224	290	180	174	218	162	138	162	200	39	119	146	192	158	158	206	157	173	230	196	138	145	126	180	285	312	165	169	154	186	257

Figure C3. Counting results of section 2.

	HBG																														
	1	2	3	4	5	6	7	8	9	10	11	12	13	14	15	16	17	18	19	20	21	22	23	24	25	26	27	28	29	30	31
Nummulites	29	26	39	63	23	24	25	51	35	74	69	42	51	63	34	41	73	73	69	29	53	66	57	72	62	51	78	67	81	54	47
Assilina	5	3	4	3	7	14	9	9	11	0	12	10	3	2	24	27	9	13	25	59	31	17	12	21	34	42	19	25	19	46	41
Operculina	0	0	2	0	1	1	1	1	2	0	2	1	8	1	3	0	2	1	1	2	2	2	2	2	1	0	0	1	0	0	0
Alveolina	9	7	9	0	2	4	4	1	2	5	0	0	0	0	2	0	0	0	0	0	0	0	0	0	0	0	0	0	0	0	0
Sphaerogypsina	0	0	2	0	0	1	1	0	0	0	2	1	3	3	0	1	0	1	0	0	1	0	0	0	0	0	0	1	0	0	0
Miliolid	5	9	1	2	7	4	8	1	7	0	0	0	0	1	2	3	0	0	0	0	1	0	3	0	0	0	0	0	0	0	2
Pygro	6	10	3	4	10	8	13	2	7	0	0	2	3	4	3	3	0	0	1	2	0	1	1	0	0	0	0	0	0	0	1
Triloculina	0	1	1	0	1	0	1	1	1	0	0	0	0	1	9	1	0	0	0	0	0	0	0	0	0	0	0	0	0	0	0
Spiroloculina	11	10	4	2	11	6	12	1	4	0	0	1	3	1	0	2	0	1	0	0	0	0	2	1	0	0	0	0	0	0	1
Orbitolites	2	3	1	0	1	7	4	0	2	0	0	0	0	0	1	0	0	0	0	0	0	0	0	0	0	0	0	0	0	0	0
Lockhartia	1	1	2	2	0	0	2	2	4	3	0	0	2	0	1	0	0	0	0	1	0	0	0	1	0	0	0	1	0	0	0
Biserial to uniserial	0	0	0	0	0	0	0	0	0	0	0	0	0	0	0	0	0	0	0	0	0	0	0	0	0	0	0	0	0	0	0
Medocia?	0	0	0	0	0	0	0	0	0	0	3	1	0	0	0	0	5	0	0	0	0	4	8	0	0	0	0	0	0	0	0
Valvulina	0	3	1	1	0	1	0	0	0	0	0	0	0	1	1	0	0	0	0	1	0	0	0	0	0	0	0	0	0	0	0
Textularia	0	1	0	0	0	1	0	0	0	0	0	1	0	0	0	0	0	0	0	0	0	0	0	0	0	0	0	0	0	0	0
Valvulina or Textularia	4	3	1	0	1	4	1	2	2	0	0	5	1	8	6	2	1	1	0	0	2	0	8	3	0	1	0	0	0	0	1
Rotalia	13	10	21	14	17	7	4	23	16	8	6	18	5	4	4	14	7	7	2	5	5	9	3	2	2	2	2	5	0	0	3
Veneulinidae	2	0	0	0	0	2	0	0	0	0	0	0	2	0	0	0	0	0	0	0	0	0	0	0	0	0	0	0	0	0	0
Others	11	13	10	9	17	17	15	3	10	9	8	19	21	11	8	8	3	3	1	1	4	3	6	0	0	0	0	0	0	0	3

Figure C4. Counting results (%) of section 2 .